CHOLINERGIC MODULATION OF CARDIAC

FUNCTION: SELECTIVE DISRUPTION BY

ORGANOPHOSPHORUS ANTICHOLINESTERASES

By

NIKITA SHRIRAM MIRAJKAR

Bachelor of Veterinary Sciences and Animal Husbandry

Bombay Veterinary College, Mumbai 400012

Maharashtra Animal and Fishery Sciences University

Seminary Hills, Nagpur, India

2002

Submitted to the Faculty of the
Graduate College of the
Oklahoma State University
in partial fulfillment of
the requirements for
the Degree of
DOCTOR OF PHILOSOPHY
July, 2008

CHOLINERGIC MODULATION OF CARDIAC

FUNCTION: SELECTIVE DISRUPTION BY

ORGANOPHSPHORUS ANTICHOLINESTERASES

Dissertation Approved:

Dr. Carey N. Pope
_____
Dissertation Adviser

Dr. Lara Maxwell
_____

Dr. David Wallace
_____

Dr. Guangping Chen
_____

Dr. A. Gordon Emslie
_____
Dean of the Graduate College

ACKNOWLEDGEMENTS

during the credit seminar series. To this day, I still use some of her tips while giving presentations.

Finally, I would like to thank the Department of Physiological Sciences, Center for Veterinary Health Sciences for providing me the resources and generous financial support in the form of Teaching Assistantship for the past five years.

TABLE OF CONTENTS

LIST OF TABLES

LIST OF FIGURES

Figure

Page

Figure   Page

LIST OF ABBREVIATIONS

ACh	Acetylcholine
AC	Adenylyl cyclase
AChE	Acetylcholinesterase
Acetyl CoA	Acetyl coenzyme A
AD	Alzheimers Disease
AE	A-esterase
ANOVA	Analysis of Variance
ATP	Adenosine triphosphate
BCh	Butyrylcholine
BChE	Butyrylcholinesterase
BSA	Bovine serum albumin
BW	BW 284C51
cAMP	Cyclic adenosine 5'-monophosphate
CarbE	Carboxylesterase
ChAT	Choline acetyltransferase
ChE	Cholinesterase
CPF	Chlorpyrifos
Cpm	Counts per minute
CD	cis-dioxolane

CNS	Central nervous system
CO_2	Carbon dioxide
CPO	Chlorpyrifos oxon
cc	Cubic centimeter
ChAT	Choline acetyl transferase
DFP	Diisopropylfluorophosphate
DAG	Diacyl glycerol
4-DAMP	4-diphenylacetoxy-N-methylpiperadine methiodide
ECG	Electrocardiogram
EDTA	Ethylene diamine tetraacetic acid
EEG	Electroencephalogram
EMG	Electromyogram
FQPA	Food Quality Protection Act
GDP	Guanosine diphosphate
GTP	Guanosine triphosphate
HACU	High affinity choline uptake
IC_{50}	Concentration of chemical that inhibits 50% of activity
IM	Involuntary movement
IP_3	Inositol triphosphate
i.p.	Intraperitoneal
IQR	Interquartile range
Iso-OMPA	Tetraisopropylpyrophosphoramide
Kg	Kilogram

LD_{50}	Dose that causes 50% lethality
mAChR	Muscarinic acetylcholine receptor
MANOVA	Multivariate Analysis of Variance
MePS	Methyl parathion
MePO	Methyl paraoxon
mg	Milligram
ml	Milliliter
mm	Millimeter
mM	Millimolar
mRNA	Messenger ribonucleic acid
MTD	Maximum Tolerated Dose
nAChR	Nicotinic acetylcholine receptor
OP	Organophosphorus
OC	Organochlorine
OXO	Oxotremorine
PKC	Protein kinase C
p-NPA	p-nitrophenyl acetate
PS	Parathion
PO	Paraoxon
p.o.	Perioral
QNB	Quinuclidinyl benzilate
sc	Subcutaneous
SE	Standard error

SLUD	Salivation, lacrimation, urination, defecation
TEPP	Tetraethylpyrophosphate
μM	Micromolar
USEPA	United States Environmental Protection Agency
VAChT	Vesicular acetylcholine transporter

CHAPTER 1

INTRODUCTION

Organophosphorus Insecticides and Their Mechanism of Action

According to the U.S. Environmental Protection Agency (USEPA), a pesticide is "any substance or a mixture of substances intended for preventing, destroying, repelling or mitigating any pest". What makes these compounds uniquely different from other toxicants or contaminants is that they are intentionally released into the environment to elicit toxicity in certain pests. Pesticides include insecticides, herbicides, fumigants, fungicides, repellants, rodenticides and disinfectants. The total expenditure on pesticides in 2000 and 2001 exceeded $32.5 billion/year globally and $11 billion/year in the US, which accounted for 5 billion pounds of pesticides used worldwide and ~ 1.2 billion pounds used in the US annually, respectively (Kiely et al, 2005).

Unfortunately, a lack of selectivity of pesticides leads to toxicity in non-target species. The American Association of Poison Control Centers received 2,155,952 cases of human poisoning in the US in 1996, of which, 86,912 cases, comprising 4% of the total poisoning cases, occurred as a result of exposure to pesticides (Litovitz et al, 1997). According to the World Health Organization, around 3 million people worldwide suffer from acute pesticide poisoning annually (Walker and Nidiry, 2002). These pesticide-related poisonings can occur through occupational exposures, accidental exposure, or intentional exposure (i.e., suicide attempts).

Organophosphorus (OP) insecticides are one of the major chemical classes of insecticides used in the world today. The first synthetic OP compound, tetraethylpyrophosphate (TEPP) was synthesized in 1854 by Philip de Clermount, but its insecticidal properties were not realized until much later (see review by Pope et al, 2005a). In 1937, a group of German chemists led by Gerhard Schrader at Farbenfabriken Bayer AG synthesized the first organophosphorus insecticides. Unfortunately, during this World War II era, nerve agents such as tabun, soman and sarin were also synthesized as potential chemical warfare agents. The OP insecticides in use today are the fourth generation derivatives of these compounds. The first commercially used OP insecticide was TEPP (used in the 1930's). Although effective, TEPP had high non-target species toxicity and was chemically unstable in the presence of moisture. This led to the development of the prototype OP insecticide parathion (PS) in 1944 and its highly potent oxygen analog, paraoxon at a later date. Although both these chemicals possessed properties that were considered desirable in an insecticide, such as low volatility, environmental persistence and chemical stability in the presence of sunlight and water, they showed evidence of marked mammalian toxicity, with a lack of target species selectivity. The organochlorine (OC) pesticides of the 1950's were largely replaced with OPs, which was associated with a large number of poisonings of pesticide applicators due to the lack of selectivity of the highly toxic OPs compared to the relatively non-toxic and more familiar OCs. This led to the search for analogs that had greater selectivity for target species and were less toxic to non-target species. Chlorpyrifos (CPF) is one of the most extensively used and studied OP insecticides due to the fact that it has relatively low mammalian toxicity (Ecobichon, 2001).

OP insecticides are among the most commonly used insecticides in the US and throughout the rest of the world. OP insecticide use in the US in 2001 totaled approximately 73 million pounds and represented 70% of the total insecticides used (Kiely et al, 2005). OPs have been used in both human and veterinary medicine, in agriculture as well as in industry (Ehrich, 1998). Currently, there exist 38 OP anticholinesterases under 10 different chemical classifications that are registered and approved for use by the USEPA (Pope, 1999). OP compounds are generally lipophilic and can be readily absorbed through the gastrointestinal tract, skin and respiratory tract (Atkinson, 1976; Kecik et al, 1993, Fuortes, 2000; Peter and Cherian, 2000). Due to the lipophilic nature of these compounds, bioaccumulation occurs in fatty tissues (Kecik et al, 1993).

OP insecticides elicit toxicity by disrupting normal cholinergic neurotransmission, which has been diagrammatically represented in Figure 1. Acetylcholine (ACh) is the primary neurotransmitter present in the central and peripheral nervous systems of cholinergic neurons. Acetylcholine is synthesized in the presynaptic nerve terminal by the action of choline acetyltransferase (ChAT; E.C. 2.3.1.6) by utilizing choline and acetyl coenzyme A (CoA) as substrates (Lefkowitz et al, 1996). A vesicular acetylcholine transporter (VAChT) transports the newly synthesized ACh into secretory vesicles. Action potential-induced depolarization of the pre-synaptic nerve terminal results in the release of ACh by exocytosis into the synapse from central nervous system (CNS) neurons, all preganglionic autonomic and postganglionic parasympathetic neurons, somatic motor neurons and a few postganglionic sympathetic neurons (Moffett et al, 1993; Nicoll 1995; Lefkowitz et al 1996). Acetylcholine then interacts with the

postsynaptic receptors and thereby influences the postsynaptic cell's function. The ACh that is released into the synapse is degraded almost immediately, thereby terminating receptor activation, by means of the enzyme acetylcholinesterase (AChE, E.C. 3.1.1.7). AChE is one of the most active and efficient of enzymes and is capable of hydrolyzing up to 10^5 molecules of ACh per second/enzyme molecule (Hoskins and Ho, 1992; Sultatos 1994). Acetylcholinesterase hydrolytically cleaves the ester bond of acetylcholine, forming choline and acetic acid. The choline that is released is then once again taken back into the presynpatic nerve terminal via a high-affinity choline uptake process (Happe and Murrin, 1993).

Cholinergic neurotransmission plays an important role in the normal functioning of the heart. Heart rate, contractile force and conduction are controlled by the intrinsic cardiac nervous system (Batulevicius et al, 2004). The intrinsic cardiac ganglia, comprised of parasympathetic efferent postganglionic neurons, local circuit neurons and afferent neurons, are under the control of cholinergic neurotransmission (Darvesh et al, 1998). Acetylcholine (ACh) activates K^+ channels via G-protein-coupled muscarinic receptors, culminating in decreased heart rate. Acetylcholine also produces a decrease in the pacemaker current in the cells of the sinoatrial node via muscarinic M2 receptor activation. The net result of ACh acting directly on the heart is therefore inhibitory (Sauviat, 1999). As in other synapses, hydrolysis of ACh is mediated by acetylcholinesterase.

OP insecticides alter cholinergic neurotransmission by inhibiting acetylcholinesterase. OPs phosphylate the hydroxyl moiety of a serine residue at the active site of the enzyme, thus inactivating its catalytic activity. Interaction between an OP compound and the

active site of the AChE enzyme leads to the formation of a transient intermediate complex that partially hydrolyzes, resulting in the loss of the "leaving group" and the formation of a stable, phosphylated enzyme that (under normal circumstances) is reactivated at a very slow rate. Due to the slow rate of spontaneous reactivation, de novo synthesis of new enzyme molecules may be required for catalytic recovery, a process that can take up to 20-30 days to complete with some OP pesticides. Thus, it is typically stated that AChE is "irreversibly" inhibited by OP insecticides. More accurately, the phosphylated enzyme can be reactivated, although at a very slow rate (Ecobichon, 2001). However, if "aging" of AChE occurs, spontaneous reactivation cannot occur and true irreversible inhibition of that enzyme molecule is the result. During the "aging" process, dealkylation of the intermediate dialkylphosphylated enzyme occurs by nonenzymatic cleavage of one alkyl side-chain of the OP molecule. Recovery of enzyme activity in this case relies on synthesis of new enzyme molecules (Sultatos, 1994; Ecobichon, 2001).

Due to extensive inhibition of AChE by OP insecticides, acetylcholine accumulates in the synapse and causes overstimulation of muscarinic and nicotinic cholinergic receptors in the central and peripheral nervous systems (Silver, 1974; Sultatos, 1994; Pope, 1999). Signs of the ensuing cholinergic toxicity can include excessive secretions such as salivation, lacrimation, urination and defecation (SLUD, signs of autonomic dysfunction), involuntary movements (e.g., muscle fasciculations, tremors, and seizures), bradycardia, miosis, nausea, vomiting, restlessness, ataxia, loss of memory, generalized weakness, slurred speech, hypothermia, loss of body weight and respiratory dysfunction. Death from OP-induced cholinergic toxicity generally occurs as a result of depressed respiratory control centers in the brain, paralysis of the diaphragm
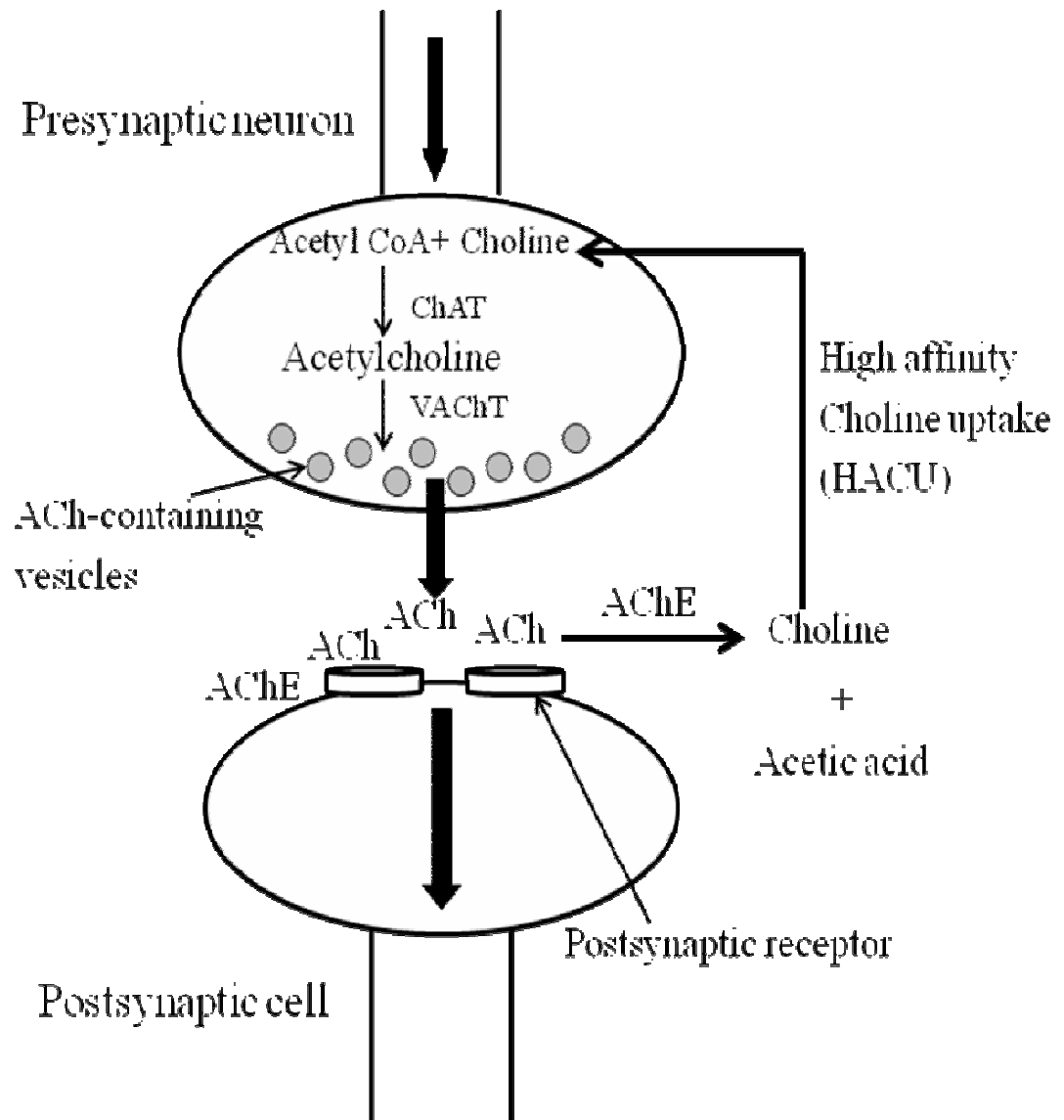
Figure 1: A general description of the primary components of and events occurring at the cholinergic synapse

and excessive airway secretions (Ecobichon, 2001; Saunders and Harper, 1994; Gupta 1998; Gordon et al, 1997; Pope et al, 1991; Pope 1999).

In addition, electrocardiographical (ECG) abnormalities have been found to occur in humans with severe OP intoxication, the most common of which are prolongation of the Q-Tc interval and ST/T changes (elevated ST segment and inverted T waves) (Karki et al, 2004). Another common ECG abnormality that has been found to occur in OP poisoning is the *torsade de pointes* type of polymorphic ventricular tachycardia, which has been attributed to the prolonged Q-Tc interval (Saadeh et al, 1997; Ludomirsky et al, 1982). Although the exact mechanism of cardiotoxicity is still unkown, there have been some proposed mechanisms. Peter and Cherian (2000) suggested that OP-induced cardiotoxicity may be due to a 1) direct toxic effect on the myocardium, 2) overactivity of muscarinic or nicotinic receptors leading to haemodynamic alterations, and 3) complications that might arise as a result of high dose atropine therapy. Abraham et al (2001) implicated several factors in OP-induced cardiotoxicity, including catecholamine overflow, neurogenic effects and direct myocardial damage. Saadeh et al (1997) suggested possible mechanisms of cadiotoxicity included sympathetic and parasympathetic over-activity, hypoxemia, acidosis, electrolyte imbalance and a direct toxic effect of the OP compounds on the myocardium.

Three primary types of OP insecticides compounds exist, namely, phosphates (absence of a sulfur atom), phosphorothioates (containing one sulfur atom) and phosphorodithioates (containing 2 sulfur atoms) (WHO, 1986). All OP insecticides that are currently in use have four atoms directly attached to the phosphorus atom by three single bonds and one double (or coordinate covalent) bond (Chambers, 1992).

Chlorpyrifos (CPF) and Parathion (PS), whose structures are depicted in Figures 2 and 3 respectively, are phosphorothioates. Both CPF and PS are referred to as parent compounds in that they both require bioactivation by cytochrome P450 enyzmes to their active metabolites, paraoxon (PO) and chlorpyrifos oxon (CPO), respectively. The activation step, referred to as oxidative desulfuration, involves enzymatic replacement of the double-bonded sulfur by oxygen. The active metabolites (oxons) are about 1,000 times more potent inhibitors of acetylcholinesterase compared to the parent insecticides (Holmstedt, 1963). The structures of CPO and PO are shown in Figures 2 and 3, respectively.

CPF is a broad spectrum OP insecticide which is moderately toxic (oral LD_{50} ~ 82-155 mg/kg in rats) (Gaines, 1969), and is widely used, in spite of recent restrictions on its use. It is the second most commonly used insecticide in the US (behind malathion), with 11-16 million pounds of the active ingredient being used annually in 2001, the latest year of use data available (Kiely et al, 2005). Parathion (PS) is a prototype OP that is highly toxic (oral LD_{50} 13 mg/kg in rats). Although not used in the US, it is commonly used in numerous other countries throughout the world. Most OPs in use today are potent inhibitors of AChE and thus can elicit classic signs of cholinergic toxicity as listed above.
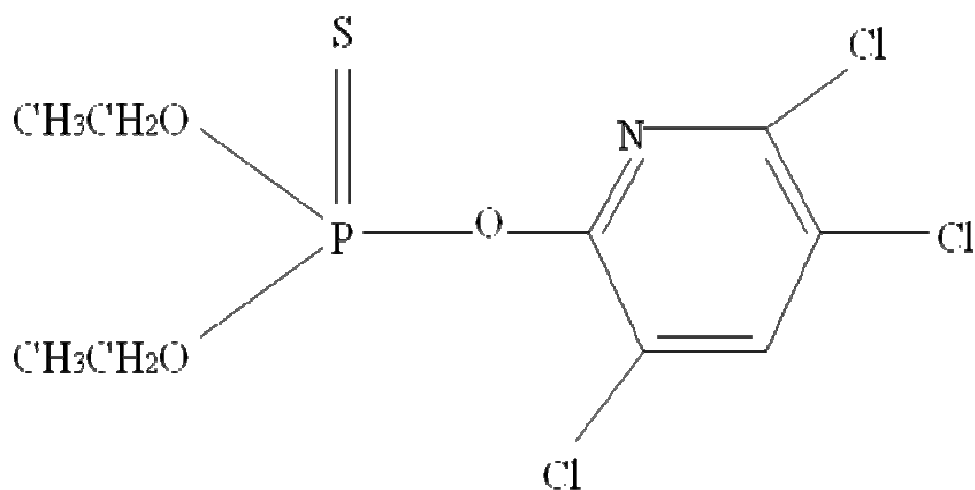
Chlorpyrifos
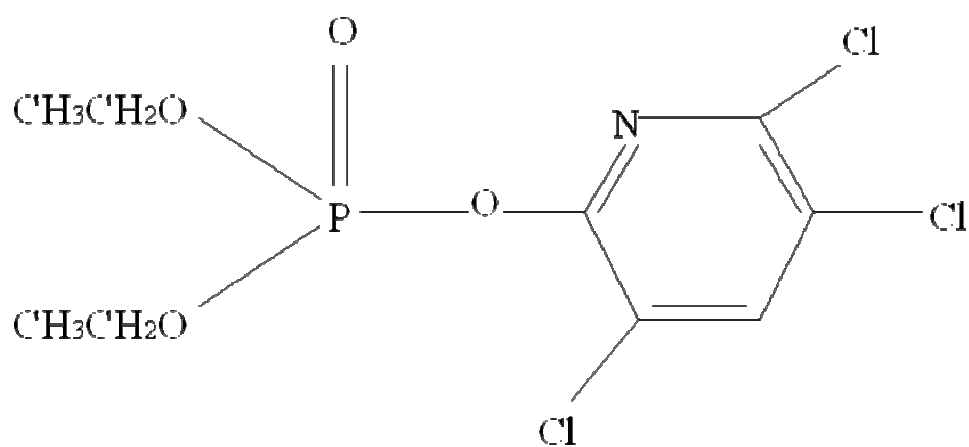
Chlorpyrifos oxon

Figure 2: Chemical structures of chlorpyrifos (CPF, O,O'-diethyl-O-(3,5,6-trichloro-2-pyridyl) phosphorothioate) and chlorpyrifos oxon (CPO, O,O'-diethyl-O-(3,5,6-trichloro-2-pyridyl) phosphate).
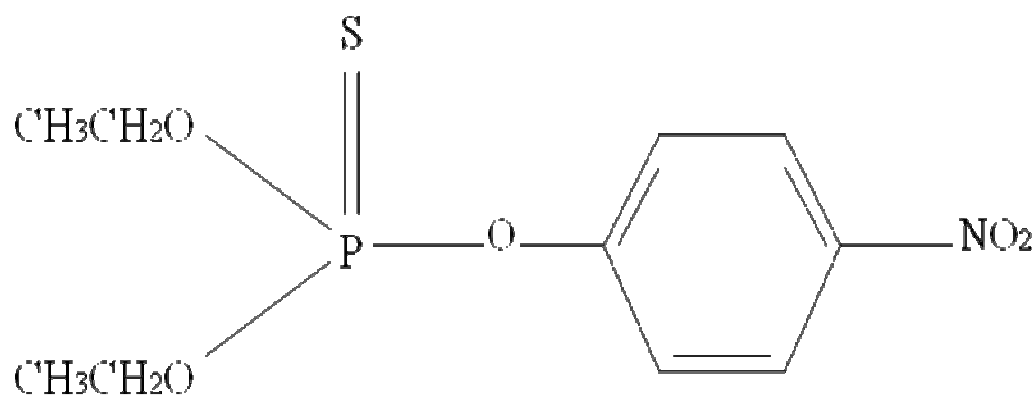
Parathion
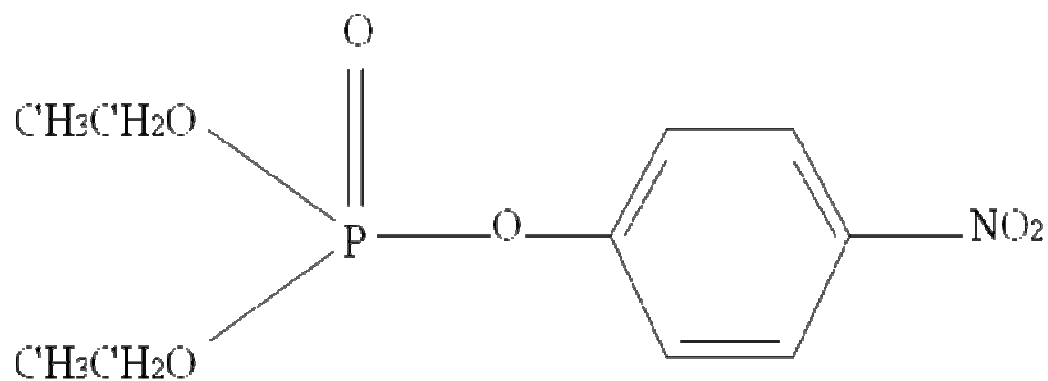
Paraoxon

Figure 3: Chemical structures of parathion (PS, O,O'-diethyl-(4-nitrophenyl) phosphorothioate)and paraoxon (PO, O,O'-diethyl-(4-nitrophenyl) phosphate)

Acetylcholinesterase and Butyrylcholinesterase

Aldridge and Reiner (1972) operationally classified all esterases into three subsets based on their interaction with OP compounds, namely A-esterases, B-esterases and C-esterases. A-esterases (AE) such as paraoxonase (E.C. 3.1.1.2) can catalyze the hydrolysis and detoxification of OPs without being inhibited themselves and are rapidly reactivated (Furlong et al 1989; Pond et al, 1996). B-esterases, which include acetylcholinesterase (AChE, E.C. 3.1.1.7), butyrylcholinesterase (BChE, E.C. 3.1.1.8) and carboxylesterase (CarbE, E.C. 3.1.1.1) stoichiometrically and covalently bind to OPs and in the process, become inhibited due to their very slow dephosphylation (Chambers et al, 1990). C-esterases (e.g., acetylesterase) do not interact with OP compounds.

There are two types of cholinesterases in vertebrates, i.e., acetylcholinesterase (AChE, acetylcholine acetyl-hydrolase) and butyrylcholinesterase (BChE, acylcholine acyl-hydrolase) (Patocka et al, 2004; Dave and Katyare, 2002). These enzymes are protein products of two distinct genes (on human chromosomes 7 and 3, respectively). The AChE gene is G-C rich, while the BChE gene is A-T rich (Schwarz et al, 1995). AChE can exist in multiple forms. The membrane bound is thought to play a prominent role in cholinergic synapses throughout the nervous system in regulating cholinergic neurotransmission. Soluble forms, as well as monomeric vs. tetrameric, globular and assymetric forms of AChE are found in different sites and thought to play different roles.

AChE, also referred to as "true" cholinesterase, is the main enzyme involved in the hydrolysis of the neurotransmitter acetylcholine, and its critical role in cholinergic neurotransmission is well understood. In addition to the critical role it plays in cholinergic neurotransmission, AChE appears to participate in non-classical functions,

which include synaptic development and maintenance, and neurodevelopment via neurite outgrowth (Silman and Sussman 2005).

On the other hand, BChE, also referred to as "pseudo" cholinesterase based on its ability to hydrolyze several choline esters, has long been thought to be a vestigial enzyme with no known physiological function (Silver, 1974). Since the synthetic substrate of BChE, i.e., butyrylcholine (BCh), is not found in living systems, the function of BChE has been difficult to determine. For a long time, BChE was of great interest in the field of anaesthesiology, wherein its metabolism of the muscle relaxant succinylcholine ensured that people receiving this drug did not experience prolonged, life-threatening apnoea (Darvesh et al, 2003). This enzyme also gained interest as a scavenger of anti-cholinesterases such as organophosphates and carbamates. A physiological role for BChE, if any, has not been determined. In a 2003 review, Darvesh et al ascribed several functions to BChE, including co-regulation of cholinergic neurotransmission, neurodevelopment, metabolism of drugs such as heroin, cocaine and succinylcholine, and scavenging for natural and synthetic anti-cholinesterases. Additionally, Patocka et al (2004) suggested that BChE may also play a role in lipoprotein metabolism, myelin maintenance and in the processing of the amyloid precursor protein, thought to play an important role in the formation of senile placques. Along with AChE, BChE is found in the neurofibrillary plaques and tangles of the Alzheimer's brain.

AChE and BChE exhibit 51-54% amino acid identity. In both AChE and BChE, the catalytic triad is comprised of serine, histidine and glutamate and is found at the bottom of a 20 Å gorge. This gorge is lined by 6 aromatic amino acids in the case of BChE, and 14 aromatic amino acids in AChE. AChE also contains a peripheral anionic

binding site which is distinct from its catalytic site. Interaction with this peripheral site may influence both substrate and inhibitor binding to the active site. This peripheral anionic binding site is absent in BChE. The active site gorge also contains an acyl pocket that holds the acyl group of choline esters in place during catalysis. This acyl pocket is larger in BChE than in AChE, thus explaining the larger (synthetic) substrates that can be hydrolyzed by BChE compared to AChE (Darvesh et al, 2003; Jbilo et al, 1994a; Harel et al, 1992).

While AChE is capable of hydrolyzing only ACh, BChE can hydrolyze both ACh (albeit less efficiently than AChE) as well as its own synthetic substrate butyrylcholine (4 times more rapidly than ACh) (Patocka et al, 2004). Another point of distinction between the two enzymes is that AChE displays substrate inhibition, whereas BChE displays substrate activation at high concentrations of ACh. As noted before, these differences may be based on the presence or absence of the peripheral binding site in the two enzymes (Jbilo et al, 1994a). The cumulative evidence suggests that AChE is the primary enzyme responsible for hydrolysis of the neurotransmitter ACh, while BChE plays a supportive role at high ACh concentrations. ACh levels have been predicted to reach high micromolar levels in the vicinity of the synaptic cleft, and the close proximity of glial BChE with normal synaptic AChE (which may be inhibited by substrate at high concentrations) may facilitate hydrolysis of ACh (Giacobini, 2001). The contribution of BChE to cholinergic neurotransmission remains unclear, however.

AChE and BChE exist in two molecular forms, namely globular (G1, G2 and G4) and asymmetric. The globular forms G1 (monomeric), G2 (dimeric) and G4 (tetrameric), are comprised of 1, 2 and 4 catalytic subunits respectively, held together by

intermolecular disulfide bonds, and are symmetrical, hydrophilic and soluble. Globular forms of AChE and BChE can also exist in asymmetric, amphiphilic membrane-bound forms. G2 and G4 globular dimers and tetramers are anchored to the cell membrane by a protein anchor known as the proline-rich membrane anchor (PRiMA). Another asymmetric collagen-tailed form of AChE and BChE consists of tetramers of catalytic subunits that are attached to membranes by a triple helical, non-catalytic collagen anchor called collagen Q. One such tetramer is called the A4 form, two such tetramers make up the A8 form and three such tetramers comprise the A12 form (Chatonnet and Lockridge, 1989; Darvesh et al, 2003). Approximately 95% of the cholinesterase activity in human plasma is made up of the soluble G4 tetramer of BChE. G1 and G2 forms of BChE in the plasma are believed to be degradation products of the G4 form. AChE has also been found to exist as a G4 water soluble form in adrenal gland secretions. The asymmetric, immobilized A12 collagen-tailed forms of AChE and BChE are localized in synapses and motor end plates of skeletal muscles in birds and mammals. Membrane-bound amphiphilic globular G2 forms of AChE are found in the plasma membrane of erythrocytes. Mammalian brain contains the G4 amphiphilic membrane-bound globular forms of AChE and BChE. The heart of some species contains G2 and G4 membrane-bound amphiphilic globular forms of BChE (Chatonnet and Lockridge, 1989). In adult rats, globular G1 and G4 and asymmetric A12 were the major isoforms of AChE in the heart, with small amounts of G2 and A8. A certain percentage of the globular isoforms of AChE were found to be membrane-bound (Nyquist-Battie et al, 1987).

The distribution of AChE and BChE is tissue-dependent. AChE and BChE are typically both found in blood. In most species, BChE is the predominant cholinesterase in

the plasma, while erythrocyte membranes exclusively contain AChE. The liver and heart generally contain a high concentration of BChE, while the brain and sketelal muscles predominantly express AChE (Jbilo et al, 1994a). The adult rat brain contains ~80% AChE and 20% BChE, whereas in humans, ~95% of the total ChE in the brain is AChE, with only 5% BChE. AChE in the brain is predominantly located in neurons and axons, while BChE is of primarily glial origin, but can be associated with neurons in specific nuclei (Ballard et al, 2005; Giacobini, 2004).

The total ChE of adult hearts of higher vertebrates is made up of around 85% BChE and around 15% AChE (Chatonnet and Lockridge, 1989). Although present in small amounts, AChE is concentrated in the conducting system of the heart (sinus node, atrio-ventricular node and the ventricular conduction tissues), while BChE is concentrated in the contractile portions of the atria and ventricles (Chow et al, 2001). The relative proportions of AChE and BChE have been found to vary in the heart during post-natal development. Slavikova and Tucek found that the amount of AChE relative to the total ChE in rat heart atrium increased from 6% on postnatal day 1 to 12-15 % in the adult (Slavikova and Tucek, 1986). Additionally, it has been observed that in the human heart the conducting system predominantly contains BChE in the infant, but mainly AChE in the adult (Chow et al, 2001).

Previous studies suggest discreet association of these two different cholinesterases with separate populations of intrinsic cardiac neurons, and their possible selective involvement in neurotransmission in the intrinsic cardiac ganglia (Darvesh et al, 1998). In the canine right atrial neurons, 4 neuronal populations were present: those containing only 1) AChE, 2) only BChE, 3) both AChE and BChE and 4) those containing neither

enzyme. The local application of acetylcholine was found to increase the activity of intrinsic cardiac neurons, with an even greater increase being observed by local application of the non-physiological substrate butyrylcholine. These two substrates were found to preferentially affect different populations of intrinsic cardiac neurons, which agreed with enzyme kinetic studies showing that canine AChE preferentially hydrolyzed ACh, while canine BChE preferentially hydrolyzed BCh. Using AChE-specific and BChE-specific inhibitors, and cholinesterase inhibitors inhibiting both enzymes, it was found that the activity of neurons in the intrinsic cardiac ganglia were only affected when both cholinesterases were inhibited, leading to the conclusion that AChE and BChE containing intrinsic cardiac neurons act synergistically to influence the overall tonic activity of the intrinsic cardiac ganglia. In a subsequent study using porcine intrinsic cardiac neurons which contained AChE and/or BChE, acetylcholine and butyrylcholine increased or decreased spontaneous activity of the intrinsic cardiac neurons. Moreover, various cholinesterase inhibitors which were used in the study were also found to change spontaneous neuronal activity. It was concluded from these studies that inhibition of AChE and BChE by cholinesterase inhibitors indirectly affects the porcine intrinsic cardiac nervous system (Darvesh et al, 2004).

Commonly used specific inhibitors of AChE are 1,5-bis [allyldimethylammoniumphenyl] pentane-3-dibromide (BW284C51) and Huperzine A, while specific inhibitors of BChE include tetraisopropylpyrophosphoramide (*iso*-OMPA), bambuterol and ethopropazine. *Iso*-OMPA (see Figure 4) is an organophosphorus compound that has mainly been used for experimental purposes due to its highly selective

16

inhibition of BChE relative to AChE (Girard et al, 2005; Minic et al, 2003). *Iso*-OMPA is a direct-acting esterase inhibitor, i.e., it does not require metabolic activation.

Recent studies have evaluated the role of BChE in cholinergic neurotransmission *in vivo*. Studies on the physiological role of BChE have been stimulated by the cholinergic hypothesis of Alzheimer's disease (AD), wherein deficits in learning, memory and behavior are believed to be caused in part by decreased levels of acetylcholine in selected brain areas. Researchers have suggested that AChE inhibitors may be used to intensify the effects of the remaining ACh, thus diminishing the effects of cholinergic deficiency, since this was the only enzyme believed to be responsible for the hydrolysis of ACh. More recently, however, it was found that BChE did, in fact, play a role in the hydrolysis of ACh. Perfusion of a selective BChE inhibitor into the rat brain was found to increase extracellular ACh by around 15-fold (Giacobini, 2004). As an additional complicating factor, BChE levels in the brain were found to increase in AD (for review, see Ballard et al, 2005). These findings increased research into butyrylcholinesterase and its possible role in normal physiological as well as pathophysiological functions.

One approach to evaluate the role of BChE was through generation of an AChE-knockout (-/-, -/+) mouse model. AChE-knockout (-/-) mice expressing normal levels of BChE were found to live into adulthood, even though they had weak muscles, could not eat solid food and died early from seizures. Three mechanisms were indentified that ensured the survival of AChE-knockouts, including 1) a reduction in muscarinic and nicotinic receptors, 2) morphological remodeling of the endplate and 3) enhanced hydrolysis of ACh by BChE (Li et al, 2003; Adler et al, 2004). AChE (-/-) mice

demonstrated a heightened sensitivity to BChE-specific inhibitors such as *iso*-OMPA and bambuterol, suggesting that it was the BChE activity in the knockout mice that facilitated their survival, and that a role of BChE (in this model) was to compensate for the function of AChE (i.e., hydrolysis of ACh) (Xie et al, 2000; Li et al, 2000). BChE is present in all parts of the brain receiving cholinergic signaling in wild types and knockouts. Moreover, it was suggested that BChE plays a constitutive rather than a back-up role in the hydrolysis of acetylcholine in the normal brain (Mesulam et al, 2002a). Further support for this came from the fact that in the absence of AChE, BChE controls the levels of extracellular ACh as evidenced by increased hippocampal ACh levels in AChE-knock-out mice and their regulation by BChE (Hartmann et al, 2007a).

Measurements of contractility on phrenic nerve-hemidiaphragm preparations from AChE (-/-) mice further support the conclusion that BChE functions to hydrolyze acetylcholine in these mice (Adler et al, 2004). In a separate study of nerve-evoked quantal transmitter release from the hemidiaphragm muscle of the AChE-knockout (-/-) mouse, however, it was reported that BChE was not involved in hydrolysis of ACh in the AChE-knockout (-/-) mice, since BChE inhibitors did not affect the time course of synaptic potentials (Minic et al, 2003). These inhibitors did however, decrease evoked-quantal transmitter release, suggesting that BChE might be involved in a presynaptic modulation of synaptic transmission at mature neuromuscular junctions (Minic et al, 2003). These investigators hypothesized that BChE inhibition led to diminished rather than elevated acetylcholine in the neuromuscular junction (Girard et al, 2005; Girard et al, 2007), and measurements of respiratory activity in AChE (-/-) mice agreed with this hypothesis (Chatonnet et al, 2003).

Recently, BChE homozygous (-/-) and heterozygous (-/+) knockout mice have been developed (Li et al, 2006a). BChE (-/-, -/+) knockout, AChE (-/-) knockout and wild type mice were treated with AChE-specific inihibitors Huperzine A and donepezil, as well as with the OP inhibitors, ecothiophate and chlorpyrifos oxon. After treatment with Huperzine A and donepezil, BChE homozygous knockout mice exhibited severe signs of toxicity and subsequently died. The BChE heterozygous knockouts exhibited intermediate signs of toxicity and survived for a longer time, while the wild type mice showed very minor signs of toxicity and recovered after 24 hours. Plasma AChE activity was inhibited to the same extent in all 3 groups, whereas plasma BChE activity was unaffected. In contrast, AChE (-/-) mice were unaffected by huperzine A and donepezil, thereby confirming their specificity for this enzyme. Together, these results suggested that the protective effect of BChE in AChE knockouts was not due to inhibitor scavenging but transmitter catalysis. When AChE (-/-) mice were treated with chlorpryifos oxon, they lost all BChE activity, developed severe signs of cholinergic toxicity and died of convulsions, thus demonstrating once again that BChE activity was essential for the survival of the AChE (-/-) mouse. From this study, Duysen et al (2007) concluded that BChE exerted its protective effect by hydrolyzing excess ACh in physiologically relevant regions such as the diaphragm, cardiac muscle and the brain, and that BChE functions in cholinergic neurotransmission.
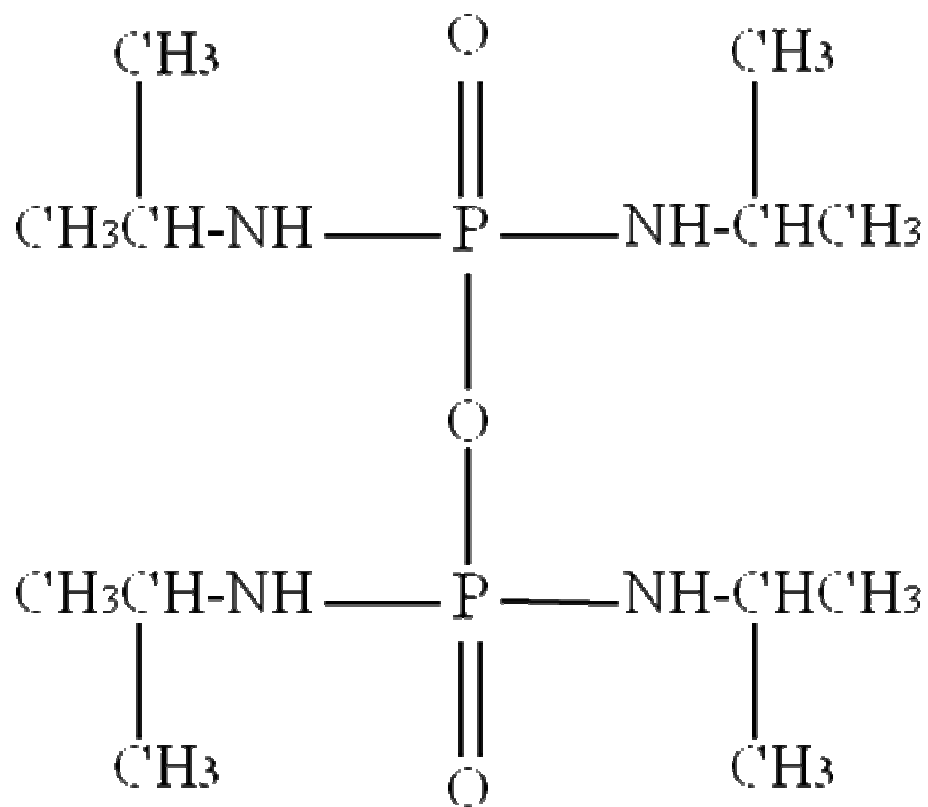
Figure 4: Chemical structure of *iso*-OMPA (tetraisopropylpyrophosphoramide)

Muscarinic Cholinergic Receptors

There are two major subtypes of cholinergic receptors, i.e., nicotinic receptors (nAChR) and muscarinic receptors (mAChR). Our studies focused on muscarinic receptors. Muscarinic receptors, which are located in both the central and peripheral cholinergic nervous systems, mediate the effects of acetylcholine in both locations. Four muscarinic receptor subtypes (M_1, M_2, M_3 and M_4) have been pharmacologically identified (Brown and Taylor, 1996), whereas, using molecular biological techniques, five subtypes, designated as M1, M2, M3, M4 and M5 have been identified (Alberts et al, 1994). These five muscarinic receptors are encoded by 5 distinct genes (Caulfield and Birdsall, 1998; Hamilton et al 1998; Eglen et al, 1994). Subtype-specific muscarinic receptor antagonists include pirenzipine (M_1 receptor selective; Caulfield, 1993; Eglen et al, 1994), methoctramine or AF-DX 116 (M_2 receptor selective; Eglen et al, 1994), 4-diphenylacetoxy-N-methylpiperidine methiodide (4-DAMP; M_3 receptor selective; Lazareno et al, 1990; Eglen et al, 1994) and himbacine (M_4 receptor selective; Caulfield and Brown, 1991; Eglen et al, 1994). Until now, there are no reports on M5-selective antagonists or agonists.

Muscarinic receptors are glycoproteins and belong to the largest superfamily of cell-surface receptors, the G protein-coupled receptors. Muscarinic receptors contain 7 hydrophobic segments that span the phospholipid bilayer and are connected by 3 extracellular and 3 intracellular loops (Alberts et al, 1994). G proteins, which are located on the cytoplasmic face of the plasma membrane, mediate the interaction between the receptor and second messenger systems or ion channels. G proteins are so named due to their interaction with guanine nucleotides, and are heterotrimeric molecules consisting of

α, β and γ subunits (Alberts et al, 1994; Brody, 1994). G proteins, which exist in multiple forms, are classified according to their α subunits. There are various subtypes of the α subunit (G_α), including $G_{\alpha s}$, $G_{\alpha i}$, $G_{\alpha q/11}$ and $G_{\alpha 12}$, and these are coupled to various second messenger systems (Bourne and Roberts, 1995; Nestler and Duman, 1999). $G_{\alpha s}$ is typically coupled to the stimulation of adenylyl cyclase, $G_{\alpha i}$ to the inhibition of adenylyl cylclase, $G_{\alpha q}$ to the activation of phospholipase C, and $G_{\alpha 12}$ to ion channels (Brody, 1994). The G protein heterotrimer has guanosine 5'-diphosphate (GDP) bound to the G_α subunit in the inactive state, i.e., in the absence of a receptor agonist. When an agonsist binds to the receptor, guanosine 5'-triphosphate (GTP) displaces GDP from the G_α subunit, leading to dissociation of the trimer into G_α and $G_{\beta\gamma}$ subunits. Depending on the subtype of the released G_α subunit, selective signaling effects are produced. Once the agonist dissociates from the receptor, second messenger signaling mechanism is terminated. The activity of the G_α subunit is terminated by its intrinsic GTPase activity, which hydrolyses the GTP to GDP, consequently allowing the G_α subunit to re-combine with the $G_{\beta\gamma}$ subunits, leading to the re-formation of the heterotrimeric complex (Alberts et al, 1994). More recently, cellular signaling roles for the $G_{\beta\gamma}$ subunits $G_{\beta\gamma}$ subunits have been identified.

Stimulation or inhibition of the membrane-bound adenylyl cyclase modulates the formation of the second messenger cyclic AMP (cAMP). Cyclic AMP-dependent protein kinases (PKA) which are activated by cAMP, and in turn phosphorylate regulatory proteins leading to a cascade of downstream signaling events. The effect of cAMP is

terminated by the action of phosphodiesterase, which hydrolyzes it to adenosine 5'-monophosphate. Inhibition of adenylyl cyclase by activation of M_2 or M_4 receptors (coupled to $G_{\alpha i/o}$) leads to a decreased production of cAMP and decreased activity of PKA, thus altering numerous cellular processes. In some cases, the $G_{\beta\gamma}$ subunit activates the inwardly rectifying potassium channel, influencing membrane polarity. Muscarinic receptors can be located both presynaptically and postsynaptically. Stimulation of presynaptic M_2 and M_4 muscarinic receptors leads to a decrease in neurotransmitter release, thus functioning as autoreceptors (Wessler, 1992; O'Neill and Doukas, 1994). Activation of M_1, M_3 and M_5 receptors typically leads to stimulation of phospholipase C via $G_{\alpha q/11}$. Phospholipase C hydrolyzes phosphotidylinositol bis-phosphate (PIP2) to inositol triphosphate (IP3) and diacylglycerol (DAG). DAG activates protein kinase C (PKC), while IP3 releases Ca^{2+} from the endoplasmic reticulum, which in turn activates calmodulin. Protein kinase C and calmodulin lead to a series of downstream cellular events (Alberts et al, 1994). Through these two basic second messenger pathways, i.e., cAMP and IP3/DAG, the muscarinic receptors regulate a diverse range of physiological functions.

Under physiological ionic conditions, muscarinic agonist binding is heterogeneous, while antagonist binding is homogeneous (Berrie et al, 1979; Vickroy et al, 1984). Cardiac and brain muscarinic receptors exist in multiple agonist binding affinity states: super high, high and low (Galper and Smith, 1978; Watson et al, 1986). Guanine nucleotides are capable of modulating agonist binding to muscarinic receptors. It has been reported that divalent cations such as magnesium are capable of increasing the potency of guanine nucleotides, as well as increasing agonist binding in the absence of

23

guanine nucleotides (Wei and Sulakhe, 1980; Sulakhe et al, 1990). The most common muscarinic antagonist and agonist used in radioligand binding studies are [^{3}H]quinuclidinyl benzilate (QNB) and [^{3}H]oxotremorine methiodide (OXO), respectively.

In the presence of continuous and excessive stimulation of muscarinic receptors by an agonist (acetylcholine), the tissue develops tolerance via modulation of receptor density. Reduction in receptor numbers (down-regulation) is a prominent adaptation to prolonged agonist exposure. Regulation of G protein-coupled receptors including muscarinic receptors involves three steps: desensitization, internalization and down-regulation. Agonist-bound muscarinic receptors are rapidly phosphorylated by G protein coupled receptor kinases: this is the first committed step in receptor desensitization (Schlador and Nathanson, 1997; Hamilton et al, 1998). Beta arrestin, a cytoplasmic protein, binds to the phosphorylated receptor thus preventing further receptor-G protein interaction (Haddad and Rousell, 1998; Lee et al, 2000). These β-arrestins in some manner direct phosphorylated receptors to clatharin-coated pits or caveolae, and the receptors are subsequently internalized by endocytosis. The internalized receptors can return to the surface of the cell membrane after dephosphorylation by receptor phosphatases or can be degraded in lysosomes to mediate down-regulation (Logsdon, 1999).

While the M_1, M_2 and M_3 subytpes of muscarinic receptors are found in the heart of several species including humans, the most predominant is the M_2 receptor subtype (Dhein et al, 2001; Wang et al, 1999; Sharma et al, 1996). Nishimaru and colleagues (2000) suggested that the presence of M_2 and M_3 receptors in the mouse atrium led to a

biphasic response with increasing concentrations of acetylcholine, i.e., a transient negative inotropic response (mediated by M_2 receptors) followed by a positive inotropic response (mediated by M_3 receptors), both of which were blocked by atropine. Obserhauser et al (2001) demonstrated that in human right atrial appendages, presynaptic muscarinic autoreceptors are of the M_2 subtype. Other investigators showed that in several other species including chicken, rat, rabbit and guinea-pig, the cardiac presynaptic muscarinic autoreceptor belonged to either the M_1 or M_2 subtype (Jeck et al 1988; Bognar et al, 1990; Habermeier-Muth et al, 1990). Muscarinic receptors are present in higher concentrations in the atria as compared to the ventricles in several species, including rat, rabbit, frog and man (Hartzell, 1980; Hancock et al, 1987; Deighton et al, 1990), whereas similar densities of muscarinic receptors were found in the two regions in guinea-pig and dog (Wei and Sulakhe, 1978). Roskoski Jr. et al (1985) observed regional differences in down-regulation in the rat heart, wherein, agonist-induced down-regulation only occurred in the right atria, left atria and left ventricle, but not in the right ventricle.

In the brain, all five subtypes of muscarinic receptors have been found in the cortex, hippocampus, thalamus, hypothalamus, striatum, pons and cerebellum. In these regions, muscarinic receptors play an important role in such processes as learning and memory, body temperature, emotions and involuntary processes such as respiration and metabolism (Caulfield, 1993; Stillman et al, 1996). A greater distribution and concentration of muscarinic receptor subtypes is present in the brain regions compared to peripheral regions such as glands, heart, lung and vasculature (Caulfield, 1993). Tice et al (1996), using subtype specific antibodies showed that all five muscarinic receptor subtypes were found in all the brain regions examined in the adult rat, but the percentage

making up the total was different among regions. The most abundant subtype was m4 in the cortex (m4>m1~m2>m3>m5), m2 in the cerebellum (m2>m3>m4=m1=m5), m1 in the hippocampus (m1>m4>m2>m3>m5) and m4 in the striatum (m4>m1>m2>m3>m5).

Additional Macro-molecular Targets of Organophosphorus Insecticides

Although the common mechanism of action for all OPs is through inhibition of AChE, there have been reports of differential expression of cholinergic toxicity in the presence of similar degrees of AChE inhibition (Chaudhuri et al, 1993; Pope et al., 1995; Liu and Pope, 1998). This led to the suggestion that in addition to AChE inhibition, OPs produce toxicity by direct or indirect interaction with other macromolecular targets (Pope, 1999; Silveira et al, 1990; Ward et al, 1993). Numerous studies indicate that inhibit the enzyme BChE, due to which, this enzyme is often used as a biomarker for exposure to these pesticides (Thiermann et al, 2007; Casida and Quistad, 2005; Amitai et al, 1998). While ~90% of brain cholinesterase (ChE) consists of AChE (Silver, 1974; Li et al, 2000; Mortensen et al, 1998), several studies have shown proportionately higher levels of BChE in some organs including heart, where BChE makes up about 90% of the total cholinesterase activity (Silver, 1974; Li et al, 2000; Slavikova et al, 1982). Due to the high density of BChE in the heart, we hypothesized that OPs with selectivity at inhibiting this enzyme may have preferential effects on cardiac regulation.

There have also been several reports indicating that OPs may directly interact with muscarinic receptors (Silveira et al, 1990; Ward and Mundy, 1996; Bomser and Casida, 2001). Paraoxon, dichlorvos and tetraethylpyrophosphate inhibited QNB binding

26

in bovine caudate membranes at low nanomolar concentrations (Volpe et al, 1985). Katz and Marquis (1989) reported that paraoxon, at concentrations as low as 10^{-15} M, was capable of blocking radioligand binding to M_2 and M_3 receptors. Bakry et al (1988) showed that the organophosphorus compounds echothiophate and VX potently blocked the binding of tritiated cis-dioxolane (CD), a high affinity M2-selective agonist, to muscarinic receptors. Subsequently, paraoxon, echothiophate and the nerve agents VX, soman and tabun were shown to block the *in vitro* binding of CD to rat cardiac tissues at high nanomolar concentrations (Silveira et al, 1990). Jett and colleagues (1991) reported that in rat striatal cells, paraoxon displaced CD binding and inhibited the formation of cAMP in an atropine-sensitive manner, while the parent insecticide parathion was 180-fold less potent. Ward et al (1993) observed that paraoxon and malaoxon were more potent at blocking CD binding to rat hippocampal and cortical membranes than their parent compounds, parathion and malathion.

Chlopyrifos oxon was a potent displacer of CD binding and inhibited adenylyl cylcase in the rat striatum (Huff et al, 1994). The abilities of paraoxon, malaoxon and chlorpyrifos oxon to alter muscarinic receptor-mediated phosphoinositide turnover and cAMP formation in rat cortex were examined by Ward and Mundy (1996). All three oxons displaced CD binding and inhibited cAMP formation in a concentration-dependent manner, with chlorpyrifos oxon being most potent and malaoxon being least potent. All of these studies (Jett et al, 1991; Huff et al, 1994; Ward and Mundy, 1996) indicate that some OPs can bind directly to M2 receptors and act as agonists in various tissues. The binding of the muscarinic agonist [3H]oxotremorine-M was also found to be sensitive to low concentrations of some OPs. Paraoxon was a more potent displacer of radiolabeled

oxotremorine-M binding to rat brain membranes compared to parathion (Van Den Beukel et al, 1997).

Howard and Pope (2002) compared the *in vitro* effects of selected OPs (chlorpyrifos, parathion, methyl parathion, and their oxons) on cardiac muscarinic receptor binding in neonatal and adult rats. Although all three oxons displaced [^{3}H]oxotremorine-M binding from neonatal and adult cardiac muscarinic receptors in a concentration-dependent manner, CPO was the most potent and efficacious of the three. Surprisingly, MePS displaced [^{3}H]oxotremorine-M from adult but not neonatal cardiac muscarinic receptors. While the interaction between CPO and cardiac muscarinic receptors appeared to be irreversible, that between MePS and adult cardiac muscarinic receptors was not. This finding was similar to the studies by Bomser and Casida (2001), who found that CPO bound covalently and irreversibly to the rat cardiac M2 receptor, as evidenced by the diethylphosphorylation of the receptors in vitro. All these studies suggest that muscarinic receptors, particularly the M2 subtype may be additional sites of action for certain OP compounds. Since the heart predominantly contains M2 receptors, this organ could be particularly sensitive to these direct receptor effects of OPs. Together, all of these studies suggest that the heart may be sensitive to the effects of certain OPs, based on high densities of both BChE and M2 receptors in this organ.

Age-related Differences in Sensitivity to Organophosphorus Insecticides

A topic of major concern for over a decade has been age-related differences in sensitivity to pesticides in general, and OPs in particular. A number of studies have demonstrated marked differences in sensitivity to OPs during maturation (Atterberry et al, 1997; Moser et al, 1998; Pope et al, 1991). In general, immature animals are more sensitive than adults to the acute toxicity of OP pesticides. Uncertainty in determination of safe exposure levels to pesticides (including OP insecticides) by the USEPA has been influenced by the possibility of age-related differences in sensitivity. The Food Quality Protection Act of 1996 was passed unanimously by the US Congress, partially based on the potential for higher sensitivity of children to pesticides. This Act included the requirement of an additional safety factor (up to 10-fold if necessary) to account for uncertainty in data relative to childrens protection, as well as an explicit determination that tolerances were safe for children (FQPA, 1996).

Several toxicokinetic and toxicodynamic factors were suggested to play an important role in age-related OP toxicity, including nature of the exposure (i.e. acute vs. repeated, high level vs. low level), timing of exposure during development relative to critical developmental processes and time available for exposure to occur or toxicity to develop (Pope, 2001). While several studies have demonstrated marked age-related differences in sensitivity to OPs such as chlorpyrifos, parathion and methyl parathion (Atterberry et al, 1997; Moser et al, 1998; Pope et al, 1991), most of these studies have focused on maturational differences, and very little is known regarding possible sensitivity differences with aging.

Karanth and Pope (2000) found that while aged (24 month) Sprague Dawley rats exhibited relatively similar acute sensitivity to CPF as compared to adults (3 month) based on lethality, they were about 3-fold more sensitive to the acute effects of parathion. In the same study, they also evaluated the activity of carboxylesterases (CarbE) and A-esterases (AE) in the liver, plasma and lung, as well as the *in vitro* sensitivity of CarbE to CPO and PO in different age groups. While aged rats demonstrated similar levels of AE in all tissues compared to adults, CarbE levels were similar between adult and aged rats only in the liver and lung. In the plasma, however, CarbE levels in aged rats were 50% lower than in adults. Moreover, no significant age-related differences were observed in the in vitro sensitivity of CarbE to either CPO or PO in any tissue. The acute sensitivity to CPF was highly correlated with age-related differences in CarbE and AE activities across all three tissues, whereas, only plasma CarbE activity was highly correlated with acute sensitivity to PS. Thus, the authors concluded that although both CarbE and AE activities were correlated with acute sensitivity to CPF and PS, age-related differences in CarbE activity were of more importance in differential toxicity, and that plasma CarbE played a crucial role in differential sensitivity to PS between adult and aged rats. Padilla et al (2000) arrived at a similar conclusion when they observed that chlorpyrifos elicited a toxic response at a 5-fold lower dose in the pre-weanling rat than in the adult rat, whereas methamidophos had the same oral maximum tolerated dose in both age-groups of rats. Since CPF is detoxified by both CarbE and AE, while methamidophos is not significantly detoxified by either enzyme, the authors hypothesized that OP pesticides like CPF, which are effectively detoxified by CarbE and/or AE, are more likely to exhibit age-related differences in toxicity than OPs that are not detoxified by these enzymes.

Age-related differences in muscarinic receptor density and/or affinity, as well as acetylcholinesterase and butyrylcholinesterase activities have been reported in a variety of species. These variations in muscarinic receptors or AChE/BChE activity could potentially contribute to age-related differences in OP insecticide toxicity. There are several conflicting reports on aging-related changes in the functionality and density of muscarinic receptors in rats (Dhein et al, 2001). Narayanan and Derby (1983) reported that while muscarinic receptor density was higher in the atria of aged rats compared to adults, ventricles from both age-groups had similar densities of muscarinic receptors. However, they did not observe any age-related change in agonist or antagonist binding affinities of atrial or ventricular muscarinic receptors. In contrast, Baker et al (1985) reported that with increasing age, the ability of the cardiac muscarinic receptor to form a high affinity agonist binding state was reduced. Chevalier et al (1991) reported a reduction in cardiac muscarinic receptor density in aged as compared to adult rats. Several investigators have reported a reduction in cardiac parasympathetic activity with increasing age in humans. This reduced activity has been ascribed to a decrease in the density (Brodde et al, 1998) as well as functionality (Brodde et al, 1998; Oberhauser et al, 2001; Poller et al, 1997) of cardiac muscarinic receptors in the heart of older individuals.

A decrease in the densities of muscarinic receptors in the brain of aged as compared to adult animals have been reported by several investigators (Tayebati et al, 2006; Yufu et al, 1994; Araujo et al, 1990; Kadar et al, 1990) using a variety of experimental approaches, including radioligand binding methods (Yufu et al, 1994; Araujo et al, 1990; Schwarz et al, 1990; Amenta et al, 2006; Amenta et al, 1995), in vitro quantitative receptor autoradiography (Tayebati et al, 2006; Kadar et al, 1990) and

31

assessing subtype specific mRNA expression (Lee et al, 1994; Blake et al, 1991). Using the radial arm maze, Kadar et al (1990) correlated working memory deficits in 3, 12, 17 and 24 month-old Wistar rats with an age-related decrease muscarinic receptor density in various brain regions.

Several reports indicate that basal parasympathetic tone decreases during aging. Meyer et al (1985), using a rat atrial mince preparation, reported that choline uptake, acetylcholine synthesis and acetyhlcholine release were all decreased in aged rats. Kelliher and Conahan (1980) found that the positive inotropic response that is normally observed following vagotomy in adult rats was abolished in aged rats. The authors also reported that the heart rate response to the muscarinic agonist methacholine was reduced in aged compared to adult rats. Kennedy and Seifen (1990) reported that right atrial preparations from aged rats were more sensitive to the negative chronotropic action of acetylcholine compared to adult rats. However, no age-related difference in sensitivity was observed with carbachol, a muscarinic agonist that is resistant to degradation by cholinesterases. When the right atrial preparations were pre-treated with diisopropylfluorophosphate (DFP), an irreversible OP cholinesterase inhibitor, age-related differences in responsiveness to acetylcholine were abolished. The authors concluded that the increased sensitivity of atria from aged rats to acetylcholine as compared to adults occurred as a result of decreased acetylcholinesterase activity. These findings agreed with those of Su and Narayanan (1992), who, using isolated, perfused, spontaneously-beating rat hearts, found that the greater sensitivity of aged rats to the negative chronotropic effects of acetylcholine as compared to adults was diminished in the presence of a maximally effective concentration of eserine, a cholinesterase inhibitor.

The negative chronotropic and inotropic response to carbachol was also greater in aged than in adult rats. Moreover, acetylcholinesterase activities were found to be decreased by 50-60% in aged atria and ventricles; however, no age-related differences were observed in binding of the muscarinic antagonist [^{3}H]QNB in either the atria or ventricles. These authors concluded that the enhanced responsiveness of the aging heart to cholinergic agonists was at least partly due to an age-related reduction in cardiac acetylcholinesterase activity and/or muscarinic receptors.

Age-related changes in AChE and/or BChE activities and molecular isoforms have been reported in brain of several species including man. Skau and Triplett (1998) observed a significant reduction (20-50%) of AChE activity in different brain regions of aged (24 months) as compared to adult (6 months) Fischer 344 rats. When the ratio of G4/G1 isoforms was evaluated in different brain regions, it was found to be unaltered in aged rats, thus indicating that although aged rats exhibit decreased brain AChE levels, there does not appear to be any selective reduction of a particular isoform. In contrast, Das et al (2001), who evaluated AChE activity in different brain regions of adult (3 months) and aged (18-22 months) male and female Sprague-Dawley rats, found a significant decrease (40-55%) in G4 but not G1 AChE in brain regions of aged male rats. Relatively similar differences were observed in adult and aged female rats. Interestingly, higher levels of the G4 isoform were observed in female compared to male rats in both age-groups. From these studies, the authors concluded that age-related differences in AChE were predominantly due to changes in the G4 isoform, and gender-dependent differences occur. Atack et al (1986) compared the activities and molecular forms of AChE and BChE in different regions of the aged human CNS. AChE activity varied

extensively (~50-fold) while BChE activity varied only slightly (3-fold) among the different regions studied. Although G4 was the predominant isoform, G1 and G2 isoforms were also detected in various brain regions. In contrast, the only molecular forms of BChE were G4 and G1, and both isoforms were evenly distributed between membrane bound and soluble types. The ratio of G4 to G1 isoforms of AChE varied widely between different regions, while the G4 to G1 ratio of BChE showed considerably less variation.

Radiotelemetry and Cardiac Function after Organophosphate Exposure

Radiotelemetry is considered a humane and efficient method for observing physiological parameters in conscious, unrestrained animals (Kramer et al, 2001; Kramer et al, 2003). A combination of miniature sensors and transmitters can be used to measure physiological parameters (including blood pressure, heart rate, blood flow, electrocardiogram [ECG], respiratory rate, body temperature and other biopotentials such as EEG and EMG, pH and activity indices), which are then transmitted via a signal to a nearby receiver. It has been found previously that use of non-invasive techniques to monitor ECG, such as the use of surface electrodes, required physical restraint with potential stressor influence on the test animal, and hence produced artifacts in the results obtained including increases in heart rate, body temperature and blood pressure, among others. By using radiotelemetric devices, it is possible to monitor several physiological parameters in conscious, freely moving animals, in a humane manner. Since no restraints are required, there is reduced stress to the animal. Moreover, it is possible to obtain data

almost continuously from the animal, with minimal animal handling, which was found to reduce variability between animals (Kramer et al, 2003).

Radiotelemetry has been previously used to evaluate the effects of OP insecticides on physiological parameters such as heart rate, body temperature and motor activity in the rat model. Gordon (1993) evaluated the acute and delayed effects of diisopropylfluorophosphate (DFP) on the above-mentioned parameters using radiotelemetry. In this study, these parameters were continuously monitored for 96 hour after subcutaneous treatment of Long-Evans rats with DFP (0, 0.1 or 1 mg/kg). The reduction in core body temperature in rats treated with 1 mg/kg DFP peaked by 5 hours post-treatment and recovered to control values by 17 hours after treatment. Although motor activity and heart rate were affected during the first 24 hours (motor activity decreased; heart rate initially increased, then decreased), core body temperature was significantly elevated during the 24-96 hour recovery phase. The 0.1 mg/kg DFP group displayed a hyperthermic response throughout. It has long been known that OP toxicity is associated with hypothermia in rats. This was the first report of a delayed hyperthermic response (preceded by hypothermia) following OP exposure. Rapid blockade of this hyperthermic response was achieved by administration of sodium salicylate, an antipyretic drug that acts through inhibition of cyclooxygenase activity (Gordon, 1996). This finding corroborates many observations of fever in humans acutely exposed to OP pesticides (Namba et al, 1971; Hirshberg and Lerman, 1984; Hantson et al, 1996).

Gordon et al (1997) evaluated the thermoregulatory effects of orally administered chlorpyrifos (0, 10, 50 or 80 mg/kg) in male and female Long-Evans rats using radiotelemetry. Following treatment with CPF, both male and female rats exhibited a

significant hypothermic response that lasted ~16 hours and a delayed hyperthermia which persisted during the diurnal phase for 1-2 days after CPF exposure. Female rats were significantly more sensitive to CPF, exhibiting a significant hypothermic response at doses which did not produce hypothermia in male rats. Similar to DFP, the CPF-induced hyperthermia was blocked by administration of sodium salicylate. Castrated male rats were significantly more sensitive to the hypothermic and hyperthermic effects of CPF compared to sham operated controls, whereas, ovariectomized female rats displayed similar sensitivity to CPF compared to sham operated controls. Hence, the authors concluded that testicular function plays an important role in gender-dependent differences in sensitivity to CPF. In a subsequent study, Gordon and Yang (2000a) reported that vasodilatation of the tail skin is an important mechanism by which core body temperature decreases during the acute hypothermic stage of CPF exposure, and that these hypothermic and vasodilatory responses to CPF are mediated via a cholinergic muscarinic pathway in the CNS. A radiotelemetric probe was used to non-invasively monitor the tail skin temperature of rats (Gordon et al, 2002).

Radiotelemetric techniques were also used by Gordon and Padnos (2000b) to monitor systolic, diastolic and mean blood pressure, pulse pressure (systolic-diastolic), heart rate, core body temperature and motor activity in rats treated with various doses of CPF. The highest dose of CPF led to an increase in blood pressure within 2 hours of treatment, which persisted throughout the night and into the next day, a slight decrease in heart rate, hypothermia followed by hyperthermia, elevated pulse pressure and decreased motor activity. The authors concluded that the increase in blood pressure without a corresponding increase in heart rate could be due to CPF-induced increase in total

peripheral resistance and an alteration of the baroreflex control of blood pressure. They concluded that although the initial effects of CPF on blood pressure could be explained by cholinergic stimulation of the central nervous system, persistent pressor response probably involved neurohumoral pathways.

Specific Aims of Project

In this study, we proposed to evaluate further the role of BChE in the regulation of cardiac function. The effects of tetraisopropylpyrophosphoramide (*iso*-OMPA), an OP with high selectivity towards BChE, on cardiac function were evaluated using radiotelemetry. We also proposed to compare cardiac function in adult and aged rats following exposure to the common OPs chlorpyrifos (CPF) and parathion (PS). Chlorpyrifos has relative selectivity for inhibiting BChE while parathion has relative selectivity for inhibiting AChE. Thus, if BChE plays a role in cardiac function, chlorpyrifos may alter heart function at dosages below those leading to acute neurotoxicity mediated by AChE inhibition. Our studies also evaluated *in vitro* tissue- and age-related differences in sensitivity of cholinesterases and muscarinic receptors to chlorpyrifos oxon (CPO) and paraoxon (PO) in heart and brain of adult and aged rats.

Based on previous publications and our preliminary findings, we hypothesized that: 1) selective inhibition of cardiac BChE would disrupt heart function, 2) the relative selectivity of chlorpyrifos for inhibiting BChE would make this insecticide more effective than parathion at disrupting cardiac function, and 3) the greater sensitivity of heart BChE in aged rats to inhibition by CPO would make aged rats more sensitive than

adults to cardiotoxicity of chlorpyrifos. We hypothesized that BChE plays a role in cardiac function and that selective effects of chlorpyrifos and parathion on AChE, BChE and muscarinic receptors would lead to OP- and age-related differences in toxicity. The specific aims of this project were as follows:

Specific Aim 1: To compare the *in vitro* sensitivity of AChE, BChE and muscarinic receptor agonist binding in brain and heart of adult and aged rats to CPO and PO.

Specific Aim 2: To assess the dose-related effects of a BChE-selective OP (tetraisopropylpyrophosphoramide, *iso*-OMPA) on cardiac function.

Specific Aim 3: To compare dose- and age-related effects of chlorpyrifos (CPF) on AChE, BChE, muscarinic receptor agonist binding and cardiac function in adult (3 months) and aged (18 months) rats.

Specific Aim 4: To compare dose- and age-related effects of parathion (PS) on AChE, BChE, muscarinic receptor agonist binding and cardiac function in adult (3 months) and aged (18 months) rats.

CHAPTER 2

METHODS

Chemicals

Chlorpyrifos (CPF, O,O'-diethyl-O-(3,5,6-trichloro-2-pyridinyl)

phosphorothioate, 99% purity), chlorpyrifos oxon (CPO, O,O'-diethyl-O-(3,5,6-trichloro-2-pyridinyl) phosphate, 99.1% purity), parathion (PS, O,O'-diethyl-O-(4-nitrophenyl) phosphorothioate, 99% purity) and paraoxon (PO, O,O'-diethyl-O-(4-nitrophenyl) phosphate, 99.1% purity) were obtained from Chem Service (West Chester, PA) and were maintained dessicated under nitrogen at 4 ºC. 10 mM stock solutions of all Organophosphorus toxicants were prepared in 100% dry ethanol and stored under nitrogen in dessicators at -80°C until the day of assay. Dry ethanol (100%) was prepared using sodium sulfate.

Acetylcholine iodide (acetyl-^{3}H; specific activity 76.0 mCi/mmol), oxotremorine-M acetate (methyl-^{3}H; specific activity 75.8 Ci/mmol) and quinuclidinyl benzilate (L-benzilic-4,4'-^{3}H; specific activity 52.0 mCi/mmol) were purchased from Perkin Elmer (Boston, MA).

HEPES (N-[2-hydroxyethyl]piperazine-N'-[2-ethane sulfonic acid]), Tris (Tris [hydroxymethyl] aminomethane), EDTA (ethylenediaminetetraacetic acid), PEI (polyethylenimine, 50% w/v), absolute ethyl alcohol, sodium hydroxide, hydrochloric

acid, sodium chloride, sodium sulfate, potassium phosphate (monobasic), potassium phosphate (dibasic), atropine sulfate, acetylcholine iodide, triton X-100, chloroacetic acid, BW284C51 (1,5-bis [allyldimethylammoniumphenyl] pentane-3-dibromide), *iso*-OMPA (tetraisopropylpyrophosphoramide), BSA (bovine serum albumin), Folin and Ciocalteu's Phenol reagent, sodium potassium tartarate, cupric sulfate, PPO (2,5-diphenyloxazole), POPOP (1,4-bis[5-phenyl-2-oxazolyl]benzene), Heparin, p-nitrophenyl acetate and glutaraldehyde solution (25% in water) were purchased from Sigma Chemical Company (St. Louis, MO). Isoamyl alcohol, toluene and acetone were obtained from Fisher Scientific Company (Houston, TX). Sodium carbonate was purchased from JT Baker Chemical Company (Phillipsburg, NJ). All chemicals used in experiments were reagent grade.

Haemo-Sol Non-Sudsing enzymatic detergent was purchased from Haemo-Sol Inc. (Baltimore, MD).

Acetylcholinesterase (Type V-S) purified from electric eel was obtained from Sigma Chemical Company in the form of a lyophilized powder (1070 units per mg protein) and was resuspended in 50 mM potassium phosphate buffer (pH 7.0) at 50 units per ml.

Animals

All animals used throughout the experiments were adult (3 months-old) or aged (18 months-old) male, Sprague-Dawley rats purchased from Harlan Sprague Dawley (Indianapolis, IN). Adult male rats were housed individually in plastic cages and were

allowed 7 days to acclimate prior to the start of any studies. To obtain aging rats, six month-old, male Sprague-Dawley rats were housed 2/cage for 1 year, and were used at 18 months of age. They were also housed individually for at least 7 days prior to any studies. All animals were maintained under a 12-h light/dark cycle and were provided *ad libitum* food and tap water. All procedures involving animals followed established protocols as described in the NIH/NRC "Guide for the Care and Use of Laboratory Animals" and were approved by the Institutional Laboratory Animal Care and Use Committee (IACUC) of Oklahoma State University.

In Vitro Studies

Tissue Collection and Preparation

The adult and aged animals were sacrificed by partial asphyxiation followed by decapitation, following which the cortex and heart were collected. The cerebral cortex was dissected on ice, according to the method of Glowinski and Iversen (1966), while the heart was collected as described previously (Howard and Pope, 2002). Briefly, after the heart was removed from the thoracic cavity, it was cleared of connective tissue and blood vessels. Subsequently, it was rinsed in a buffer containing 10 mM Tris HCl and 1 mM EDTA (pH 7.4) and the whole heart was minced and stored at -70 ºC, until time of assay. The tissues were prepared depending on the biochemical assay to be performed: tissue homogenates were used for the cholinesterase assays, while membrane preparations were used for receptors binding assays. On the day of the (cholinesterase) assay, the thawed

cortex was homogenized on ice (1:20 in 50 mM Potassium phosphate buffer, pH 7) for 20 seconds at 25000 rpm using a Polytron PT 3000 homogenizer (Brinkmann Instruments, Westerbury, NY). Similarly, after rinsing the thawed heart tissue in ice-cold 0.9% saline and blotting it dry, it was homogenized (1:20 in 50 mM Potassium phosphate buffer, pH 7) twice for 30 seconds, with a 30 seconds pause in between. These crude tissue homogenates were used for the cholinesterase assays. The cardiac and cortical membranes (for the M2 receptor binding assay) were prepared as described previously (Howard and Pope, 2002; Liu et al, 1999). In brief, after the cortex was homogenized (1:20 w/v in 5mM Hepes, pH 7.4) on ice as described above, the homogenate was centrifuged at 48000g for 10 minutes. The P1 pellet obtained was then re-homogenized and re-centrifuged to obtain the P2 pellet, which was then diluted in the original volume of buffer and homogenized prior to the start of the assay. The heart tissue was homogenized (1:15, w/v in 5 mM Hepes, pH 7.4) four times, for 30 seconds each, pausing for 1 minute between the homogenizations. This cardiac homogenate was then centrifuged for 10 minutes at 1000g at 4ºC, following which, the supernatant was re-centrifuged at 40,000g for 45 minutes. The pellet thus formed was resuspended in the original volume of buffer by 10 strokes of a Dounce homogenizer, just before the assay.

Cholinesterase Assays

AChE, BChE and total ChE (AChE + BChE) activity was measured in the cortical and cardiac homogenates by the radiometric method of Johnson and Russell (1975) using 1 mM final concentration of tritiated Acetylcholine iodide as the substrate.

To estimate the levels of AChE and BChE in the adult and aged cortex and heart, as well as to ascertain the specificity and selectivity of the specific inhibitors for their respective cholinesterases, cardiac and cortical tissue homogenates were incubated with increasing concentrations of either *iso*-OMPA or BW at 37°C for 15 minutes, before assessing the residual ChE activity. For total ChE (AChE + BChE) activity, the tissue homogenate was pre-incubated in potassium phosphate buffer (no inhibitor), prior to performing the assay. Tissue homogenates that had been pre-incubated with 10 µM iso-OMPA (to obtain AChE activity only) or 10 µM BW (to obtain BChE activity only) were incubated at 37°C for 30 minutes in the presence of either vehicle (0.1% ethanol), CPO (100 pM to 300 nM) or PO (300 pM to 10 µM), prior to measuring the residual ChE activity.

Preliminary assays were carried out to determine incubation times that resulted in linear rates of substrate hydrolysis. Cholinesterase assays were carried out in 7 ml scintillation vials at room temperature. The reaction mixture consisted of 60 µl of 1% Triton X-100 (in 50 mM potassium phosphate buffer, pH 7.0), 20 µl of tissue homogenate and 20 µl of radiolabeled substrate ([^{3}H]Acetylcholine iodide) in 50 mM potassium phosphate buffer, pH 7.0. In order to determine non-enzymatic hydrolysis of substrate, blanks containing buffer only (no tissue) were included. Twenty µl of electric eel (50 units/ml in 50 mM potassium phosphate buffer, pH 7.0) was added in lieu of the tissue sample to determine total hydrolysis of radioactive substrate. The radiolabeled substrate was added to the reaction vials at staggered (10 seconds) intervals to start the incubation and reactions were terminated by staggered addition of 100 µl of ChE "stop" solution. Once the reactions had been stopped, 5 ml of organic scintillation cocktail was added to each vial. The vials were capped and vortexed for 5-10 seconds and were then

counted in a Wallac Liquid Scintillation Counter (Model 1049 DSA, PerkinElmer, Inc., Boston, MA).

Preparation of [^{3}H]Acetylcholine Iodide Substrate

The radiolabeled substrate was prepared by suspending 1 mCi of acetylcholine iodide [acetyl-^{3}H] in 2 ml of 50 mM potassium phosphate buffer, pH 7.0. This stock solution was subsequently stored at -70°C. Twenty ml of 5 mM working solution of substrate was prepared by adding 150 µl of stock radioligand solution to 10 ml of 9.90132 mM unlabeled acetylcholine iodide and making up the volume to 20 ml by adding 9.85 ml of 50 mM potassium phosphate buffer, pH 7.0. Aliquots were made in 800 µl volumes and stored at -70°C until day of assay.

Preparation of Cholinesterase Stop Solution

The cholinesterase stop solution was prepared by adding 9.45 grams of chloroacetic acid, 2 grams of sodium hydroxide and 11.6 grams of sodium chloride to 100 ml of deionized water. This solution was then stored at 4 °C and aliquots of 20 ml were made for use.

Preparation of Organic Scintillation Cocktail

Organic scintillation cocktail for the cholinesterase assay consisted of 0.5% (w/v) 2,5-diphenyloxazole (PPO), 0.03% (w/v) 1,4-bis[5-phenyl-2-oxazolyl]benzene (POPOP) and 10% (v/v) isoamyl alcohol in toluene. To make four liters of cocktail, 20 grams of PPO, 1.2 grams of POPOP and 400 ml of isoamyl alcohol were added to 3600 ml of toluene. This mixture was then stirred overnight with a magnetic stirrer and stored at room temperature.

Oxotremorine-M Displacement Assays

Muscarinic receptor binding assay was carried out according to the modified version of Silveira et al (1990), as described previously (Howard and Pope, 2002). Membranes (280-310 µl/reaction) were incubated at 21ºC for 90 minutes in the presence of [^{3}H]Oxotremorine-M acetate (1 nM final concentration) and either vehicle (0.1% ethanol) or one of a range of OP (CPO or PO) concentrations (100 pM to 10µM). Atropine (10µl final concentration) was used to determine non-specific binding. [^{3}H]OXO was prepared in 5 mM Hepes, whereas the OP toxicants were prepared in 1% ethanol (0.1% ethanol final concentration). The entire reaction up until the incubation step was carried out on ice. At the end of the incubation period, the reaction was terminated by vacuum filtration over GF/B filter paper (Brandel Inc., Gaithersburg, MD) saturated with ice-cold 0.05% polyethylenimine. Subsequently, the filter disks were immersed overnight in scintillation cocktail (Fisher Scientific, Pittsburgh, PA) prior to counting. Specific binding was calculated as the difference in total and non-specific

binding, which correspond to the reactions without and with atropine, respectively. Protein content was determined according to Lowry et al., 1951.

Tissue Protein Content Estimation

The protein content of tissue homogenates and membrane preps was determined by the method of Lowry et al, 1951, by using Bovine serum albumin (BSA) as the standard. One ml aliquots of BSA (1 mg/ml in deionized water) were prepared in advance and stored at -70°C. A standard curve consisting of 0, 10, 25, 50, 75 and 100 mg BSA per reaction was performed for each assay. For the standard curve, reactions contained BSA and the same volume of 5 mM Hepes (pH 7.4) or 50 mM potassium phosphate buffer (pH 7.0) as that used in the tissue samples for the unknowns. The amount of tissue used for the assay depended on the dilution and was adjusted in such a way that the protein content would fall within the range of the standard curve. Reactions for tissue samples were run in duplicate. The volume was adjusted to 200 µl for both the standard reactions as well as the tissue samples using deionized water. Two ml of "Reagent 1" was added to each tube, vortexed and was incubated for ten minutes at room temperature. Subsequently, 200 µl of "Reaction 2" was added, vortexed and tubes were then incubated for another 30 minutes at room temperature. The absorbance was then read using a Beckman General Purpose UV-Vis Spectrophotometer (Beckman-Coulter, Fullerton, CA) at a wavelength of 720 nM. The protein content of the samples was estimated from the absorbance values of the standard curve.

Preparation of Reagents 1 and 2 for Protein Assay

Both reagents 1 and 2 were prepared just immediately before performing the assay. Reagent 1 was prepared by combining 1 part of 0.5% copper sulfate, 1 part of 1% sodium potassium tartarate and 100 parts of 2% sodium carbonate in 0.1 N sodium hydroxide. Stock solutions of sodium carbonate, copper sulfate and sodium potassium tartarate were prepared in advance in deionized water. The sodium carbonate solution was stored at room temperature, while the copper sulfate and sodium potassium tartarate solutions were stored at 4 °C. Reagent 2 was prepared by mixing equal parts of Folin and Ciocalteu's Phenol Reagent and deionized water.

In Vivo Studies

Dose-Determination Studies

The goal of the first part of the project was to arrive at appropriate dosages of *iso*-OMPA, chlorpyrifos (CPF) parathion (PS) to be used in subsequent *in vivo* studies. Since the Maximum Tolerated Dose (MTD) of CPF and PS had already been evaluated in adult and aged rats in the past, we established treatment regimens based on this prior knowledge. Adult and aged rats were treated with CPF (MTD: 280 mg/kg in both age-groups) @ 0.1xMTD (28 mg/kg), 0.5xMTD (140 mg/kg) and 1xMTD (280 mg/kg), which served as the low, medium and high dose-groups in both ages, respectively. Similarly, based on the known MTD's of PS in adult (18 mg/kg) and aged (6 mg/kg) rats, low (0.5xMTD; adult: 9 mg/kg, aged: 3 mg/kg), medium (0.75xMTD; adult: 13.5 mg/kg,

aged: 4.5 mg/kg) and high (1xMTD; adult:18 mg/kg, aged: 6 mg/kg) doses were decided upon. Chlorpyrifos and parathion were prepared in peanut oil and administered subcutaneously at 2 ml/kg body weight. In all cases, peanut oil served as the vehicle for the control groups.

Since *iso*-OMPA had never been used *in vivo* in our lab prior to this, a dose-determination study was performed to arrive at doses of *iso*-OMPA that would selectively inhibit cardiac BChE in the absence of central cholinesterase inhibition. *Iso*-OMPA was dissolved in 0.9% saline (1 ml/kg) and rats were treated with either vehicle (normal saline) or one of a range of doses of *iso*-OMPA (1.25, 2.5, 5, 15, 25, 50 and 100 mg/kg) subcutaneously. Body weight and functional signs were observed before treatment and at the end of the study (24 hours post-treatment), when rats were sacrificed.

Treatment of Animals

Rats were treated with *iso*-OMPA at 0, 1.25 or 5 mg/kg, sc (n=6-10/group) and were sacrificed 24 and 96 hours post-treatment. For the CPF and PS studies, adult (n=4/group) and aged (n=4-5/group) rats were treated at the doses metioned above and were sacrificed 96 hours later by partial asphyxiation (using CO_2) followed by decapitation. Body weight and functional signs of toxicity were monitored every 24 hours until the end of the study. In all cases, for treatment, rats were placed in a restrainer, the skin behind the site of telemetric device placement was lifted and the OP was injected subcutaneously using a 1 cc syringe attached to a 21 guage needle, taking care not to hit the telemetric implant.

Observation of Functional Signs of Cholinergic Toxicity

Twenty four, forty eight, seventy two and ninety six hours post-treatment with either CPF or PS, adult and aged rats were weighed and graded for functional signs of cholinergic toxicity as noted by salivation, lacrimation, urination and defecation (SLUD) and involuntary movements, according to a modified method of Moser et al. (1988). All scoring of functional signs was performed in "blind". Involunatry movements were scored as follows: 1: repetitive movements of mouth and jaws; 2: normal quivering of vibrissae, head and limbs, 3: mild, fine tremor that would usually be observed in the head and forelimbs; 4: severe, whole body tremors. SLUD signs were scored as follows: 1: none; 2: slight (one symptom or multiple mild symptoms); 3: moderate (multiple moderate symptoms); 4: severe (multiple severe symptoms).

Preparation of CTA-F40 Transmitters for Surgical Implantation

A CTA-F40 telemetric transmitter device was used for implantation in rats. In order to prepare the transmitter for surgical implantation, using a sharp sterile blade, about 2-2.5 cm of the silicone tubing was cut off from the tip of one biopotential lead, so as to expose the helix of stainless steel wire inside. The tubing was cut by applying light pressure and rotating the lead. The silicone tubing was then removed and cut in half. One half was then placed over the tip of the lead, leaving some part extending over the wire, and at least 1-1.5 cm of the wire being exposed. Using 4-0 non-absorbable silk suture, the tubing was held in place by tightly applying knots. The distal part of the exposed lead

was also tightly secured using 4-0 non-absorbable silk. The purpose of securing the silicone tubing over the helix of wire was to prevent the sharp end of the proximal portion of the lead from causing injury to the animals tissues, and to prevent moisture ingress via the distal part of the exposed lead. The same process was repeated for the other lead. Figure 5 represents an image of the prepared transmitter that is ready for surgical implantation in rats.

Surgical Implantation of CTA-F40 Telemetric Device

Adult and aged rats were anesthesized using a mixture of ketamine and xylazine (0.67 ml/kg body weight, i.p.) by means of a 1 ml syringe with a 26 guage needle. This ketamine/xylazine solution was prepared by adding 1 ml of a 100 mg/ml solution of xylazine to 10 ml of 100 mg/ml ketamine solution. If anethesia was not achieved within 10-15 minutes, an additional injection of 25% of the original dose was given. The depth of anesthesia was assessed by evaluating the animals reaction to tail-pinch test.

The rat was prepped for surgery by shaving the hair above the scapula, from the base of the neck to midway down the back using hair clippers. The areas of lead placement, i.e., right shoulder and left xiphoid space were also shaved. The shaved areas were made aseptic by swabbing with 70% ethanol. The rat was placed in sternal recumbancy on a sterile drape and another surgical drape was used to cover the animal, leaving a small window with which to work. An incision was made along the dorsal midline, parallel to the long axis of the body, immediately caudal to the scapula. The incision should be large enough to accommodate the implant device body. Using artery

forceps or blunt-tipped dissecting scissors, a pouch was formed by separating the skin from the underlying subcutaneous tissue. The pouch was made just slightly larger than the device body, which would allow it to lie within the pouch without producing excessive tension on the overlying skin. The skin incision was then covered with sterile gauze and the rats was turned onto its back. Subsequently, skin incisions (~ 3 cm in length) were made in the regions of the right shoulder for the negative lead, and left of the xyphoid space, caudal to the ribcage for the positive lead. Using artery forceps, the skin was separated from underlying tissue so as to provide a greater surface area for suturing. The skin incisions (for lead placement) were then covered using sterile gauze and the animal was once again placed with its dorsal side up. The implant device body was then placed in the pouch with the suture rib side up (Figure 6). Using a trocar placed inside a plastic sleeve, a subcutaneous tunnel was formed from the dorsal incision to the lead incision. Subsequently, the trocar was removed, leaving the plastic sleeve in place. The negative lead was then passed through the sleeve to the site of lead incision, after which, the sleeve was removed. This process was repeated for the positive lead as well. Figure 7 represents an image of the positive and negative leads in place. After placing the lead in its approximate position, the excess lead was coiled up and placed beneath the implant device body. The dorsal skin incision was closed using 2-0 non-absorbable silk sutures, in a simple interrupted pattern. While suturing the skin, the needle was passed through one edge of the incision, then through the suture rib of the device and finally through the other edge before tying a knot, as can be seen in Figure 8. Once the dorsal skin incision was closed, the animal was placed on its back and the forelimbs were held down (by applying a tape) so as to have clearer access to the surgical site. The muscle

51

fibers at the site of lead placement were bluntly dissected so as to provide a shallow area in which the lead was to be placed. Care was taken to ensure that the tip of the lead lay straight and flat. The exposed part of the lead or helix of wire was held in place by suturing the muscle tissue up over the lead using 3-0 non-absorbable silk suture (Figure 9). This was done to allow the muscle tissue to grow into the lead, so as to obtain a clear telemetric signal in the absence of any extraneous noise. In order to do this, the needle was passed through the muscle tissue on one side of the helix of wire, passed over the lead, and another bite was taken on the other side of the lead. The two ends of the suture were pulled together, which resulted in the helix of the lead being embedded in the muscle tissue, and a knot was tied off. This process was repeated for the other lead as well. Finally, skin incisions (for lead placement) were closed using 9 mm EZ wound clips (Braintree Scientific Inc., MA), removing as much dead space as possible (Figure 10). All skin incisions were cleaned using Betadine®, after which an antibiotic ointment was applied topically.

For recovery, the rat was placed in a warm environment, and additional warmth was provided using a light source. The animals recovery was monitored until the rat was fully awake. Childrens ibuprofen (2 ml) was added to the drinking water to alleviate pain, and rats were allowed access to this for up to upto 3 days after surgery. The rats were given 7 days to recover from the surgery before they were used in any study.

Explantation of the CTA-F40 Transmitter

Once the study was completed, rats were sacrificed by partial asphyxiation (by CO_2) followed by decapitation. Subsequently, the sites of lead implantation were opened by cutting the skin just below the wound clips. The sutures securing the muscle around the leads were removed and the muscle was dissected so as to expose and free the leads from surrounding tissue. The rat was then placed in sternal recumbancy and the sutures at the site of device body placement were carefully cut one by one, so as to separate the skin from the suture ribs of the device body. The skin incision was then opened and the device body was freed from adjacent tissue and fascia. Subsequently, the device was removed from the subcutaneous pouch and the leads were carefully pulled out of the sites of placement (via the subcutaneous tunnels) taking care not to stretch the leads.

Sterilization of the CTA-F40 Transmitter Post-Surgery

After explantation of the transmitter from the animal, care was taken to ensure that the suture ties around each biopotential lead were intact, in order to prevent moisture ingress. If not, they were tied off using 4-0 non-absorbable silk suture. Subsequently, the transmitters were rinsed under running tap water to remove as much blood and tissue as possible, taking special care to clean the suture ribs. A three-step process was adopted for sterilization of these biopotential transmitters.

1. Enzymatic detergent: Haemo-Sol N. S. (Haemo-Sol, Inc), a non-sudsing, proteolytic powdered detergent was used to remove blood and tissue debris from the implant post-explantation. 5 grams of the powder was mixed with 1 liter of

cold water. The device was soaked in this solution for a minimum of 4 hours. If blood or tissue was found to persist, additional soaking in the detergent was carried out (upto a maximum of 72 hours). Thereafter, it was cleaned by rinsing under running tap water.

2. Chemical Sterilant: Since the DSI transmitters are heat sensitive, cold sterilization was performed by using a chemical sterilant such as Glutaraldehyde. 25% Glutaraldehyde was purchased from Sigma Chemical Company and was diluted to a 2% solution using autoclaved water, by adding 80 ml of 25% Glutaraldeyhde to 920 ml sterile, autoclaved water. The transmitter was completely immersed in 2% Glutaraldehyde for upto 24 hours.

3. Sterile Saline: Sterile saline was prepared by adding 9 grams of Sodium Chloride to 1 liter of water and then autoclaving it. The chemically sterilized transmitters were immersed in sterile saline so as to remove all traces of 2% Glutaraldehyde before implantation in the animal. For temporary storage (<48 hours) of the transmitters, until surgical implantation, the transmitters were left in the sterile saline. If use was not immediate, they were allowed to air dry and were then stored in a safe, dry place.

Acquisition of Telemetric Data

For telemetric data collection, a Chronic Use TA11CTA-F40 implant, PhysioTel Receiver Model RPC-1 and DataQuest ART (Advanced Research Technology) Version 4.0 software were used (DSI, St. Paul, MN). At the beginning of each new study, a configuration was established, which included configuration settings, name and the folder in which the data would be stored. For each configuration, eight unique animal IDs were created and subsequently, each transmitter was configured to a specific receiver by entering the manufacturers specified calibrations into the configuration window. After post-surgical recovery, baseline telemetric data (heart rate, body temperature and physical activity) were collected from rats for 24 hours prior to treatment. Thereafter, telemetric data was acquired every 24 hours for upto 96 hours post-treatment. In order to collect biopotential data from the rat, the transmitter had to be switched on. In order to turn the transmitter to the "On" operational mode, an AM radio was tuned to the low AM band and held close to the rat with the implanted device. Thereafter, a strong magnet was passed over the device body by moving it within about 1 inch from the rats back. When the transmitter was turned on, an audible tone was heard on the radio. The transmitter was turned on about 15 minutes prior to data collection. The rats were then placed in their home cages, which were placed on top of the receivers and the Acquisition program (DataQuest ART 4.0) was set up to collect data by continuous sampling. At the end of the study, the transmitter was turned off in a similar manner as described above. When the transmitters were in the "off" mode, no tone could be heard from the radio.

Telemetric Data Analysis

Once the study had been completed, parametric data (heart rate, body temperature and physical activity) that had been collected and saved by the acquisition program was exported into a Microsoft Excel spreadsheet by the Analysis program of the Dataquest ART software. Since data was collected in 10 second intervals, each cell in the Excel sheet represented that parameter over 10 seconds. For heart rate and body temperature, 360 consecutive cells were averaged to obtain an hourly estimate. For physical activity, 360 cells were summed to obtain total activity in one hour. This process was carried out for the entire 120 hours (24 hours pre-treatment and 96 hours post-treatment) of the study. Subsequently, the hourly estimates for each parameter (for each animal) were combined into 8 hour diurnal (10:30 to 18:30 hours) and nocturnal (20:30 to 04:30 hours) intervals. For heart rate and body temperature, hourly data was averaged over these diurnal and nocturnal intervals, whereas physical activity was summed over these intervals. Subsequently, for each diurnal and nocturnal time point, average and standard error were determined, based on the number of animals per treatment group.
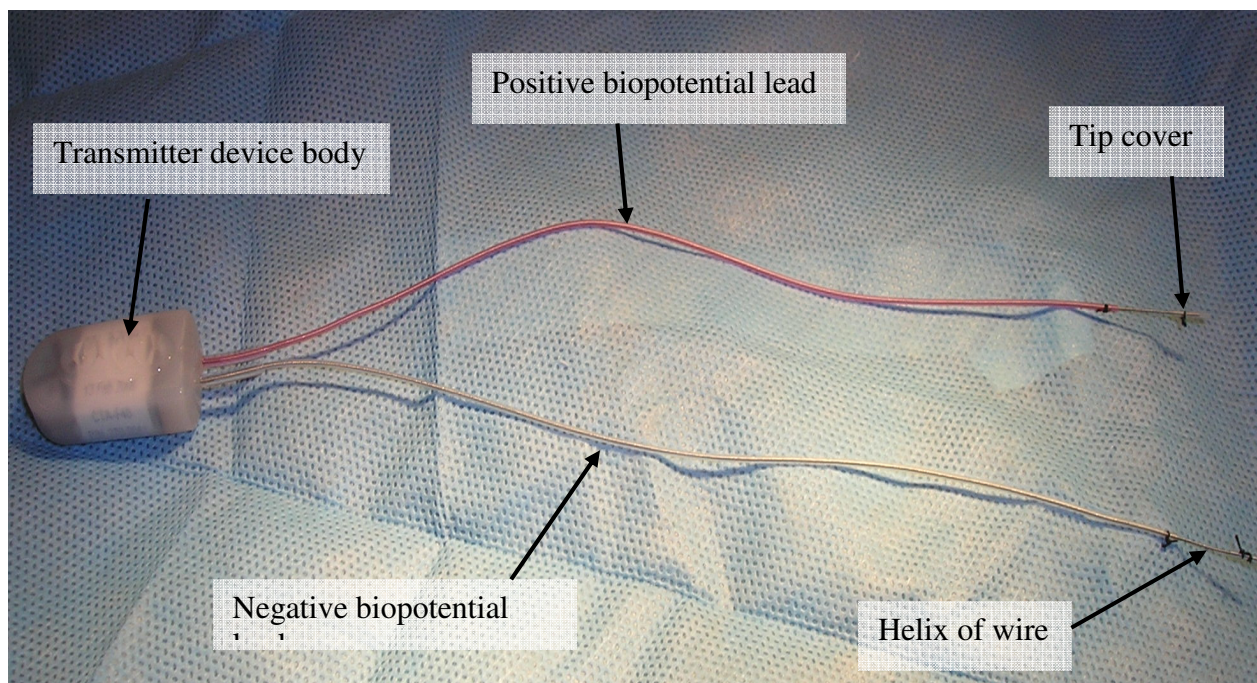
Figure 5: CTA-F40 transmitter prepared for surgical implantation in rats.
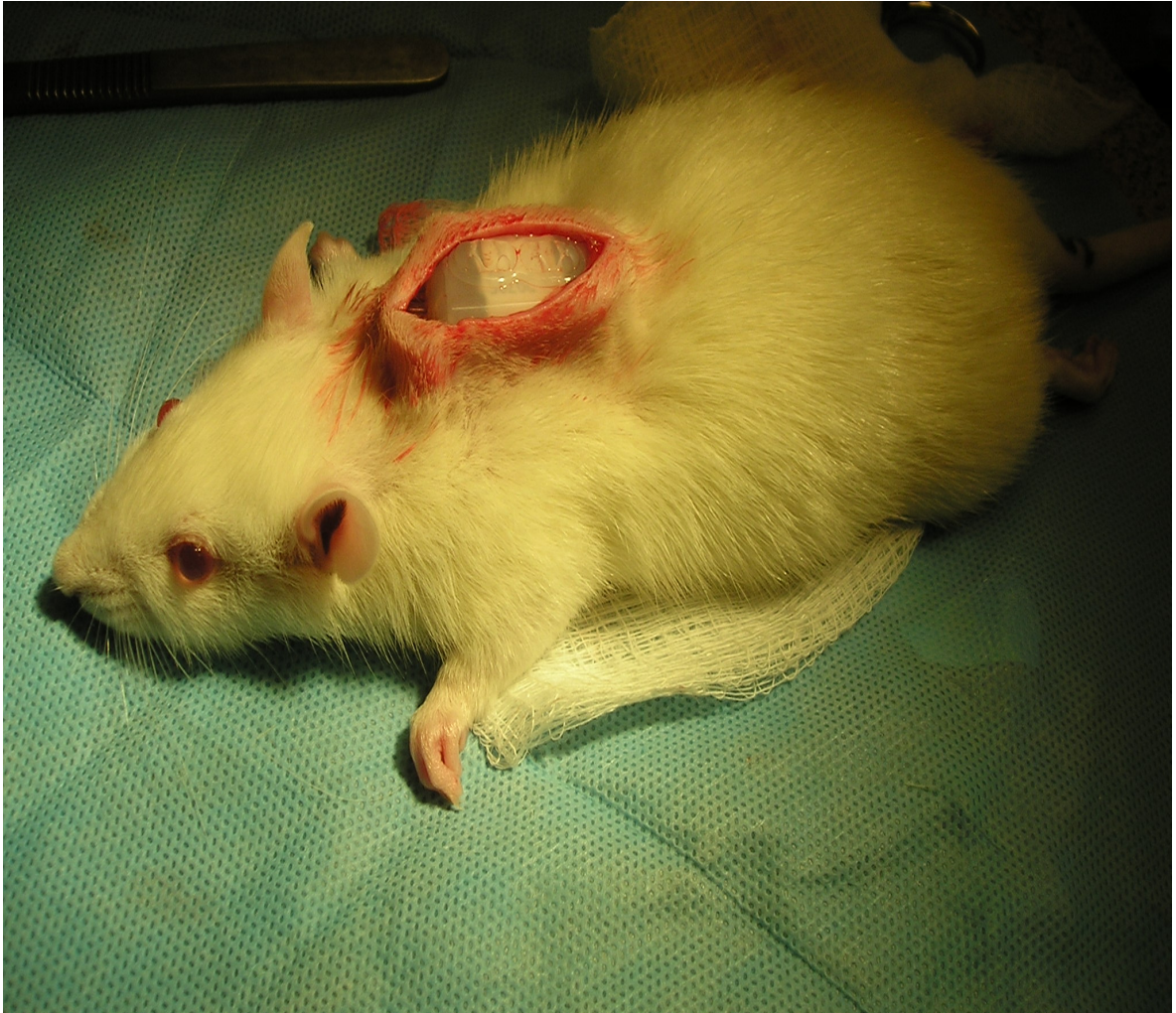
Figure 6: Placement of transmitter device body in dorsal subcutaneous pouch, suture-side up.
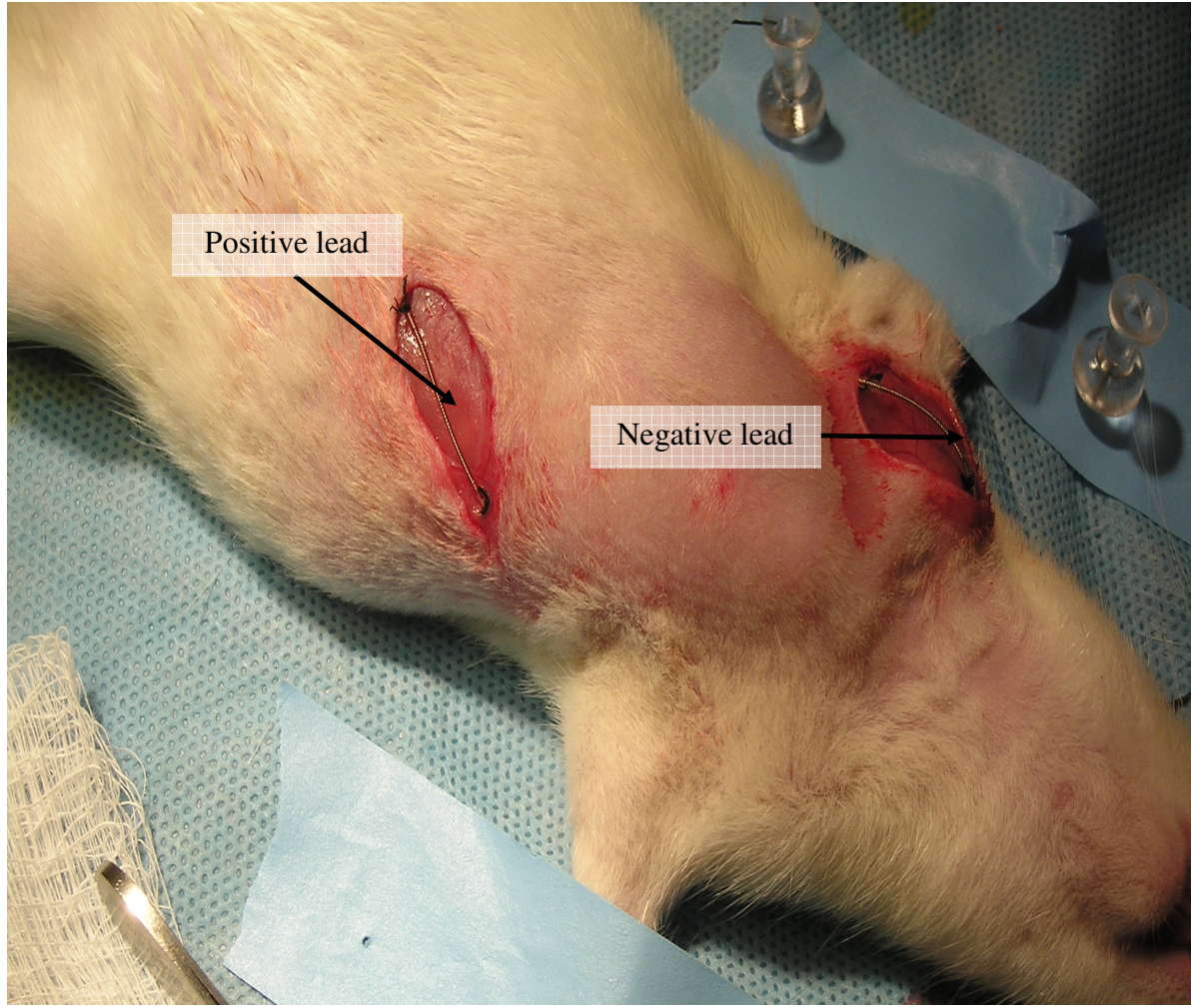
Figure 7: Placement of positive lead in the left xiphoid space, just caudal to the rib cage and negative lead in the region of the right shoulder.
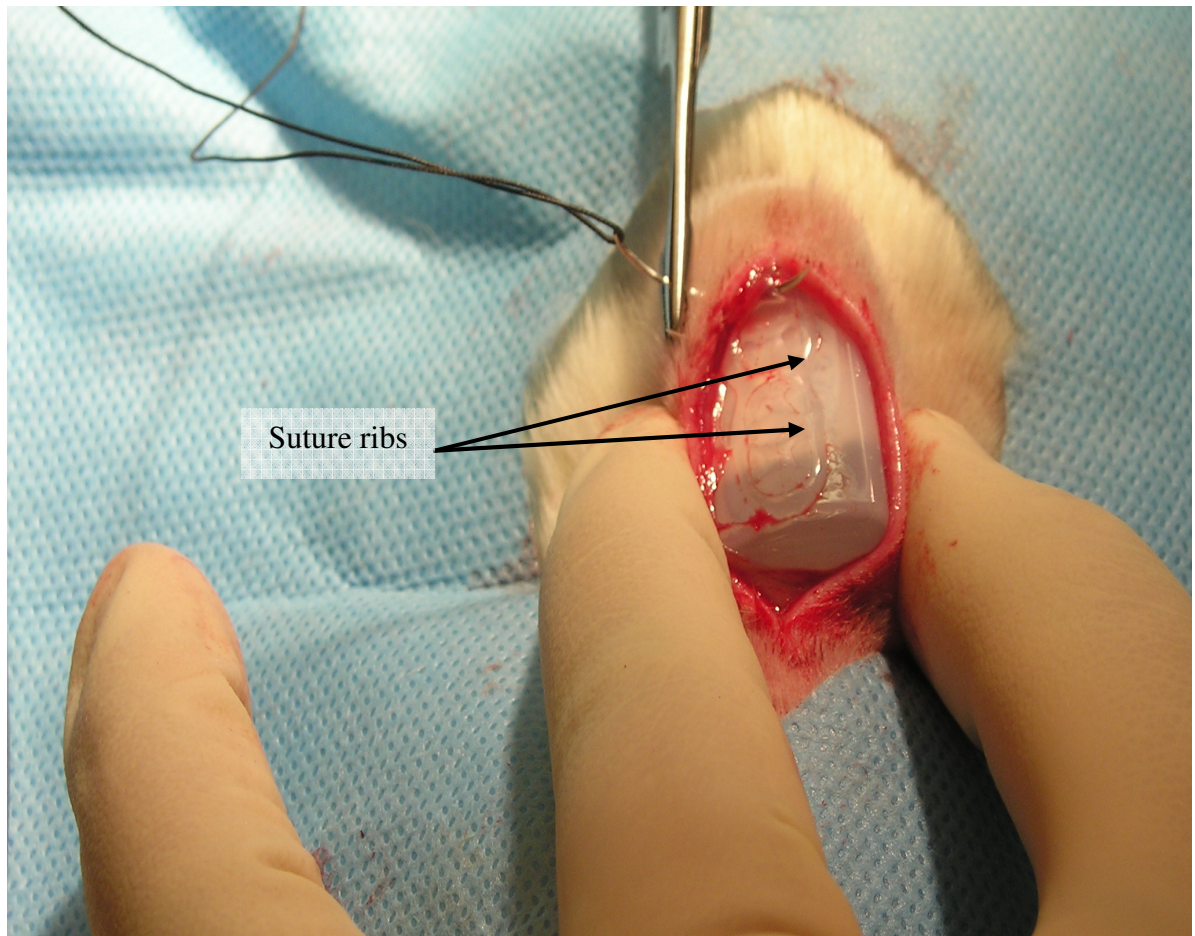
Figure 8: Suturing of dorsal skin incision through suture ribs of telemetric implant device body.

Figure 9: Suturing of the muscle up and over the exposed helix of wire of biopotential lead.
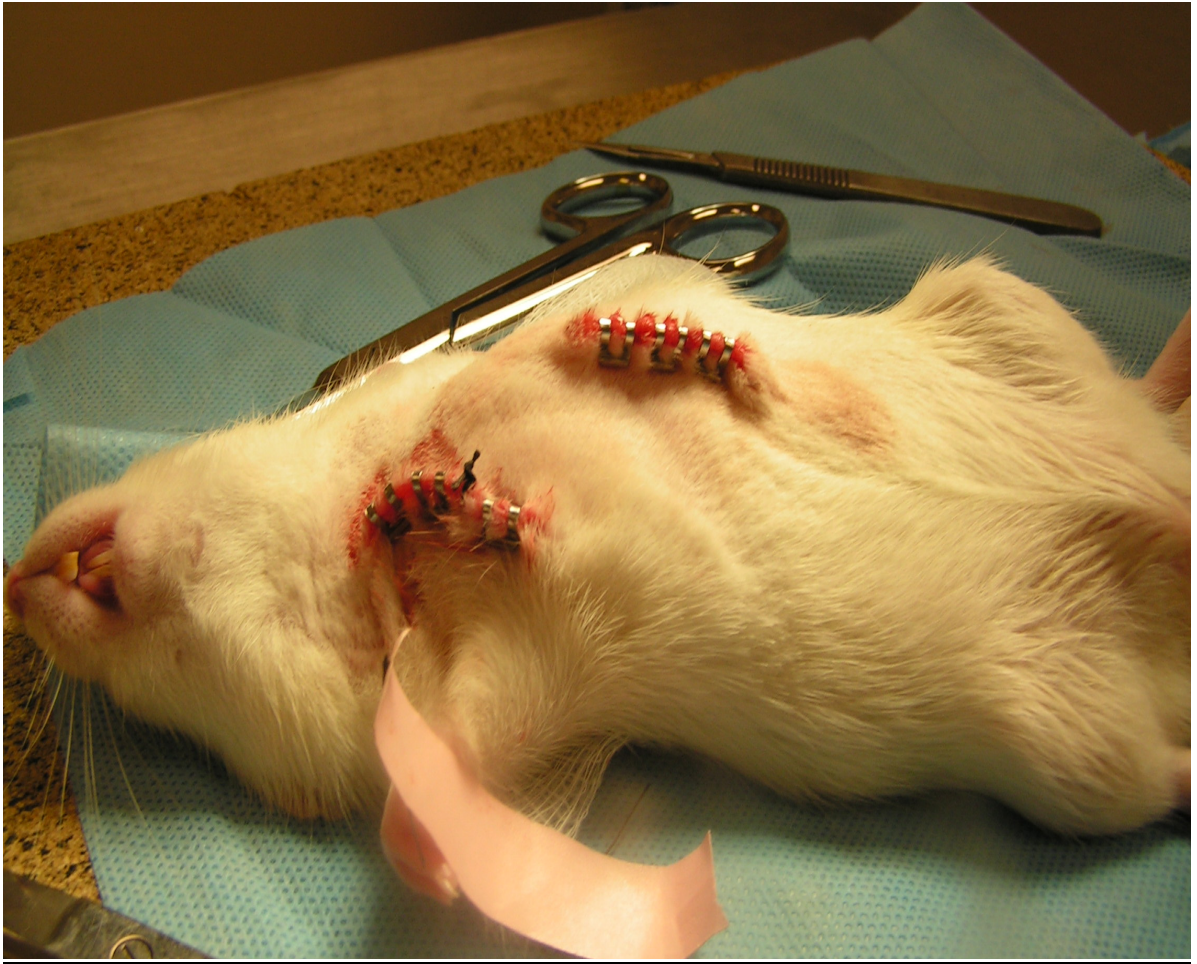
Figure 10: Closing of ventral skin incisions using skin staples.

Figure 11: Placement of rats in their home cages on top of receivers subsequent to surgery.

Biochemical Assays

Tissue Collection and Preparation

Rats were sacrificed 24 hours after treatment with iso-OMPA and 96 hours after treatment with CPF or PS by partial asphyxiation (in a CO_2 chamber) followed by decapitation. Subsequently, brain cortex, atria, ventricles and diaphragm were collected as described previously. Trunk blood was collected for plasma in heparinized vials (20 µl heparin-10,000 units/ml) and centrifuged at 12,000 rpm for 10 minutes. The supernatant plasma was then transferred to fresh eppendorf tubes and stored along with the other tissues at -70 ºC until day of assay. AChE, BChE and Lowry protein assays were performed on all tissues (except plasma); muscarinic receptor binding assays were performed on cortex, atria and ventricles; and the carboxylesterase (CarbE) assay was performed on cortex, atria, ventricles and plasma. On the day of assay, tissues were thawed, weighed and diluted (cortex 1:20; atria 1:15; ventricles 1:15; diaphragm 1:10; plasma 1:3) in 5 mM Hepes, pH 7.4 in 7 ml polycarbonate centrifuge tubes on ice. Tissues were then homogenized (cortex: 20 seconds; atria, ventricles: 30 seconds 4 times, with a 1 minute pause in between; diaphragm: 30 seconds twice with a 30 second pause in between) on ice at 28,000 rpm using a Polytron PT 3000 homogenizer (Brinkmann Instruments, Westerbury, NY). Aliquots (0.5-1 ml) of these crude tissue homogenates were separated for AChE, BChE, CarbE and protein assays, while the remaining homogenate was used to obtain membranes, as described previously.

Acetylcholinesterase and Butyrylcholinesterase Assays

AChE and BChE activities were evaluated in aliquoted tissue homogenates or diluted plasma samples as described previously in the In Vitro Studies sections. In brief, tissue homogenates were pre-incubated with either 10 µM iso-OMPA (to obtain AChE activity) or 10 µM BW (to obtain BChE activity) at 37°C for 15 minutes. Subsequently, 20 µl of tissue sample was taken in duplicate to measure the residual ChE activity. Protein content was estimated as described previously in the In Vitro Studies section.

Muscarinic Receptor Binding Assays

Cardiac (atrial and ventricular) and cortical membranes were prepared as described in the In Vitro Studies section. Muscarinic receptor binding was evaluated by following a modified version of Silveira et al (1990), as described previously (Howard and Pope, 2002). Membranes (280-310 µl/reaction) were incubated at 21°C for 90 minutes in the presence of either a non-selective muscarinic agonist, [3H]oxotremorine-M acetate (OXO, 1 nM final concentration) or a non-selective muscarinic antagonist, [3H]Quinuclidinyl benzilate (QNB, 1 nM final concentration). In both cases, atropine (10µl final concentration) was used to determine non-specific binding. Muscarinic receptor agonist and antagonist binding were evaluated as described previously in the In Vitro Studies section. Protein content was estimated as described previously in the In Vitro Studies section.

Carboxylesterase Assay

The carboxylesterase activity in tissue samples was estimated according to the method of Clement and Erhardt, 1990. 10 µl of aliquoted tissue homogenate or diluted plasma sample was added in duplicate to 980 µl of 0.1 M Tris-HCl buffer (pH 7.8) containing 2 mM EDTA and this mixture was pre-incubated at 37 °C for 5 minutes. The substrate, 50 mM p-nitrophenyl acetate (p-NPA), was freshly prepared in acetone on the day of the assay. The reaction was initiated by adding 10 µl of substrate (p-NPA, final concentration 0.5 mM) to the tubes in a staggered fashion and further incubating for a pre-determined amount of time at 37°C. Preliminary assays were carried out to determine incubation times that resulted in linear rates of substrate hydrolysis. The absorbance was then read at 405 nm in the same staggered manner against a reagent blank that contained only buffer and substrate (no tissue). A p-NPA standard curve was used to calculate the specific activity of CarbE. Protein content was estimated as described previously in the *In Vitro* Studies section.

Data Analyses

In Vitro Studies

Each assay was repeated three independent times to allow generation of mean and standard error bars for each data point. IC_{50} values were estimated by sigmoidal dose-response analysis using GraphPad Prism® 4 software (Graphpad Software, San Diego, CA, USA, www.Graphpad.com).   Assessment of the 95% confidence interval around the

IC_{50} was used to estimate significant differences in sensitivity of AChE, BChE or OXO binding to PO and CPO, as well as age-related differences in sensitivity to these OPs. GraphPad Prism $^{®}$ software was used to perform all data analyses and $p<0.05$ was considered to be statistically significant. Variability about the mean was calculated and reported as standard error (SE). The great majority of publications in toxicology-related journals present standard error and not standard deviation.

In vivo **Studies:** *iso*-**OMPA**

For the dose-determination study, enzyme assays were analyzed using one-way ANOVA, followed by Tukey's *post hoc* test. Heart rate and body temperature data were averaged over diurnal or nocturnal intervals and were expressed in terms of mean ± standard error (SE). The total physical activity over a diurnal or nocturnal interval was averaged and was expressed as mean ± SE. Data were analyzed using SAS statistical software and GraphPad Prism software. Diurnal and nocturnal data were analyzed individually using one-way repeated measures ANOVA (with time being the repeated factor), followed by multiple comparison tests with a Bonferoni adjustment factor. Heart rate, which was expressed in 4 hourly intervals (up to 48 hours post-treatment) was analyzed using one way repeated measures ANOVA, with time being the repeated factor, followed by Tukey's *post hoc* test. Biochemical assays (acetylcholinesterase, butyrylcholinesterase, carboxylesterase and muscarinic agonist binding) were analyzed using two-way ANOVA (treatment: control, low, high; time-points: 24 hours, 96 hours),

followed by a Tukey's *post hoc* test. In all cases, p<0.05 was considered to be statistically significant.

In vivo Studies: CPF and PS

Heart rate and body temperature data were averaged over diurnal or nocturnal intervals and were expressed in terms of mean ± standard error (SE). The total physical activity over a diurnal or nocturnal interval was averaged and was expressed as mean ± SE. Data were analyzed using SAS statistical software. Diurnal and nocturnal data were analyzed individually using one-way repeated measures ANOVA (with time being the repeated factor), followed by multiple comparison tests with a Bonferoni adjustment factor. In all cases, analysis was adjusted for weight as a time-dependent covariate. Body weight data, expressed in terms of percent of day 0, were represented as mean ± SE, and were analyzed using one-way repeated measures ANOVA, followed by multiple comparison tests with a Bonferoni adjustment factor. SLUD and IM data were reported as median ± interquartile range (IQR) and were analyzed using MANOVA. In all cases, p<0.05 was considered to be statistically significant. Acetylcholinesterase, butyrylcholinesterase and carboxylesterase activities were reported as mean ± SE. Muscarinic receptor agonist, [^{3}H]Oxotremorine-M and antagonist [^{3}H]Quinuclidinyl benzilate binding values were also represented as mean ± SE. For the CPF and PS adult vs aged study, these data were analyzed using two-way ANOVA (age: adult vs aged; treatment: control, low, medium, high), followed by a Tukey's *post hoc* test. GraphPad

Prism [R] software was used to perform all data analyses and $p<0.05$ was considered to be statistically significant.

CHAPTER 3

RESULTS

Distribution of Cholinesterases in Cortex & Heart of Adult and Aged rats

The distribution of AChE and BChE in the heart and brain of adult and aged rats was evaluated using the AChE-specific inhibitor BW284C51 (BW), and the BChE-specific inhibitor *iso*-OMPA. Figures 12-15 show the titration of AChE & BChE in adult heart (Figure 12), aged heart (Figure 13), adult cortex (Figure 14) and aged cortex (Figure 15), using the selective inhibitors BW & *iso*-OMPA. The IC_{50} values of BW against AChE activity in heart from adult and aged heart (0.129 µM and 2.67 µM respectively) were approximately 10 to 100-fold higher than in adult and aged cortex (30.19 nM and 48.57 nM respectively). On the other hand, the IC_{50} values for *iso*-OMPA against BChE in adult and aged heart (0.19 µM and 0.17 µM respectively) were about 10 fold lower than in adult and aged cortex (4.39 µM and 1.61 µM respectively).

Table 1 shows the AChE & BChE content in adult & aged rat heart and cortex. In the cortex, the predominant cholinesterase is AChE, with much lower levels of BChE. In the heart however, BChE was the predominant cholinesterase, with AChE being present to a much lesser extent. No age-related difference was observed in the relative composition of the two cholinesterases making up the total cholinesterase activity in either of these tissues, however.
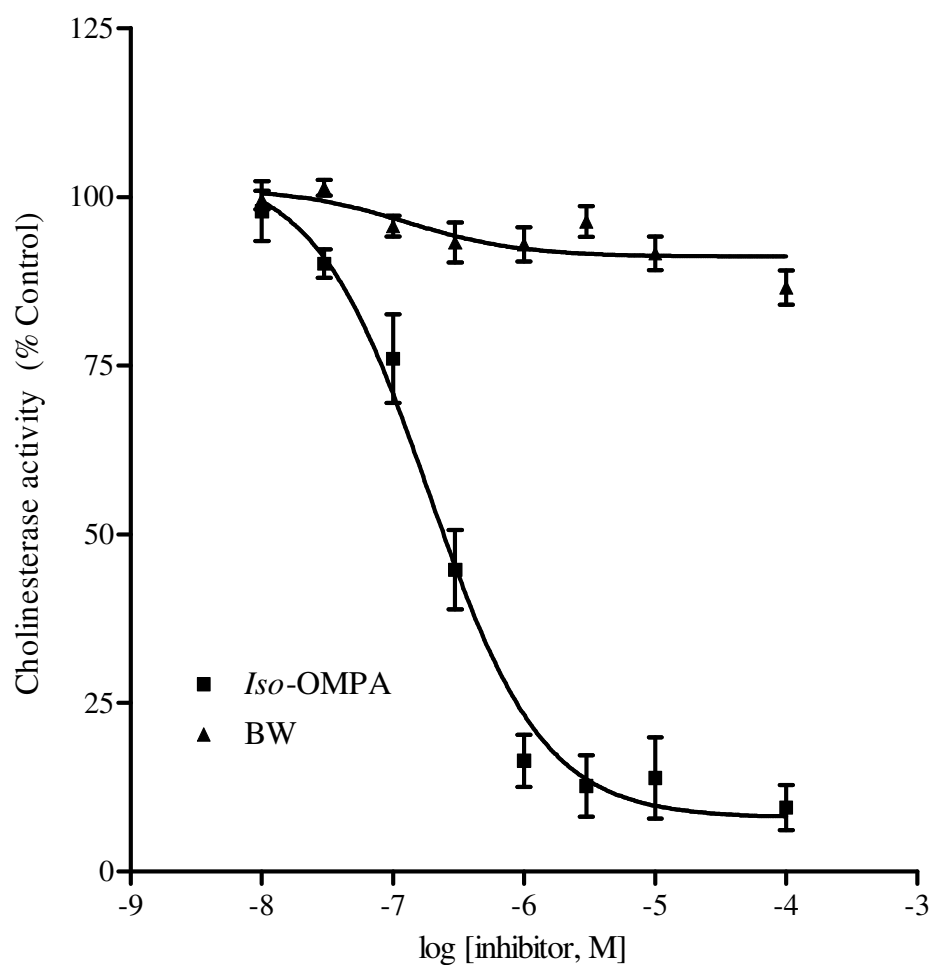
Figure 12: *In vitro* inhibition of AChE and BChE using BW284C51 and *iso*-OMPA in adult rat cardiac tissue homogenates (n=3 per group). Cardiac tissue homogenates from adult rats were incubated with *iso*-OMPA or BW (at the concentrations noted) at 37°C for 15 minutes, before assessing the residual ChE activity, as described previously. Data (mean ± standard error) represent AChE (triangle) or BChE (square) activity as percent of control (i.e., activity in the absence of either inhibitor).
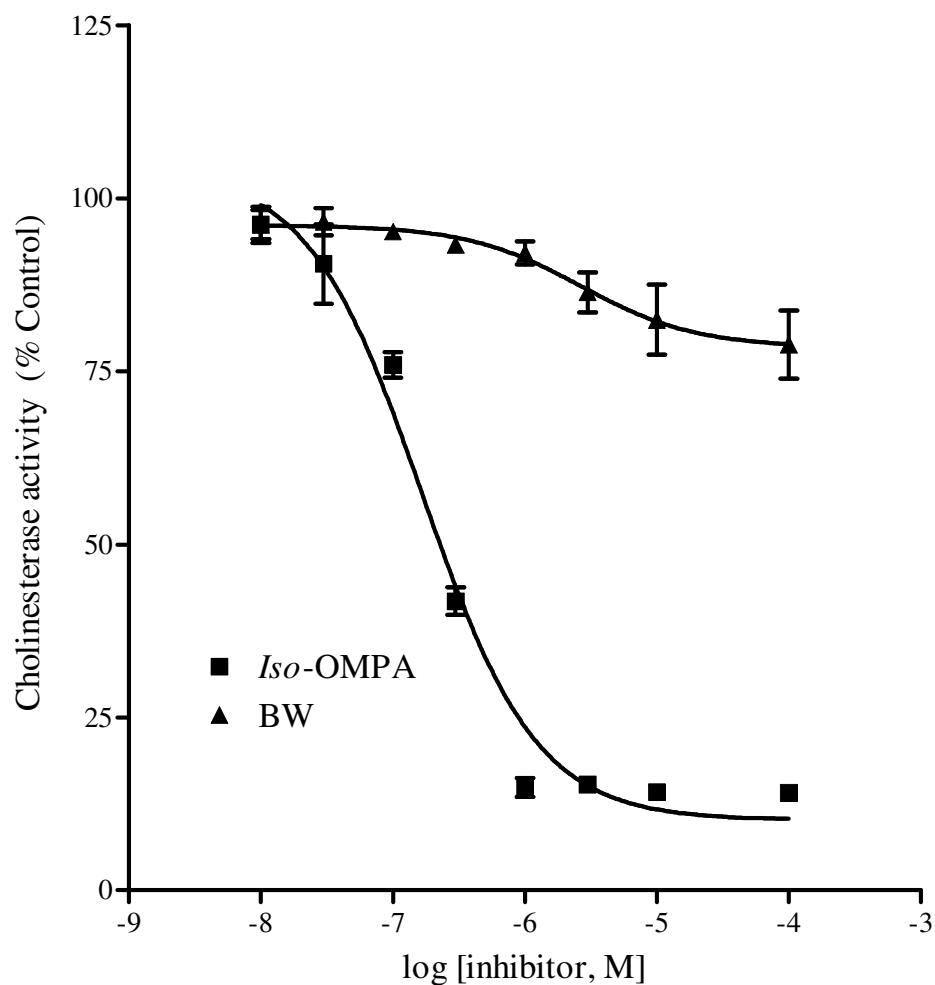
Figure 13: *In vitro* inhibition of AChE and BChE using BW284C51 and *iso*-OMPA in aged rat cardiac tissue homogenates (n=3 per group). Cardiac tissue homogenates from aged rats were incubated with *iso*-OMPA or BW (at the concentrations noted) at 37°C for 15 minutes, before assessing the residual ChE activity, as described previously. Data (mean ± standard error) represent AChE (triangle) or BChE (square) activity as percent of control (i.e., activity in the absence of either inhibitor).
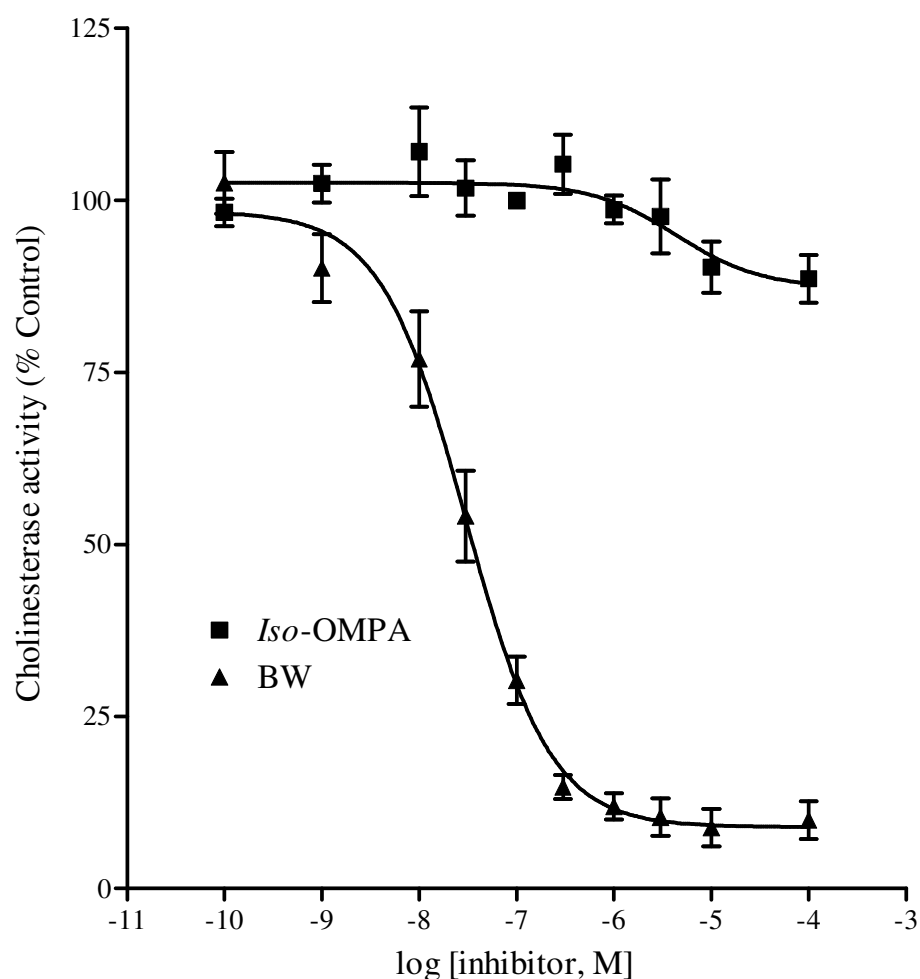
Figure 14: *In vitro* inhibition of AChE and BChE using BW284C51 and *iso*-OMPA in adult rat cortical tissue homogenates (n=3 per group). Cortical tissue homogenates from adult rats were incubated with *iso*-OMPA or BW (at the concentrations noted) at 37°C for 15 minutes, before assessing the residual ChE activity, as described previously. Data (mean ± standard error) represent AChE (triangle) or BChE (square) activity as percent of control (i.e., activity in the absence of either inhibitor).
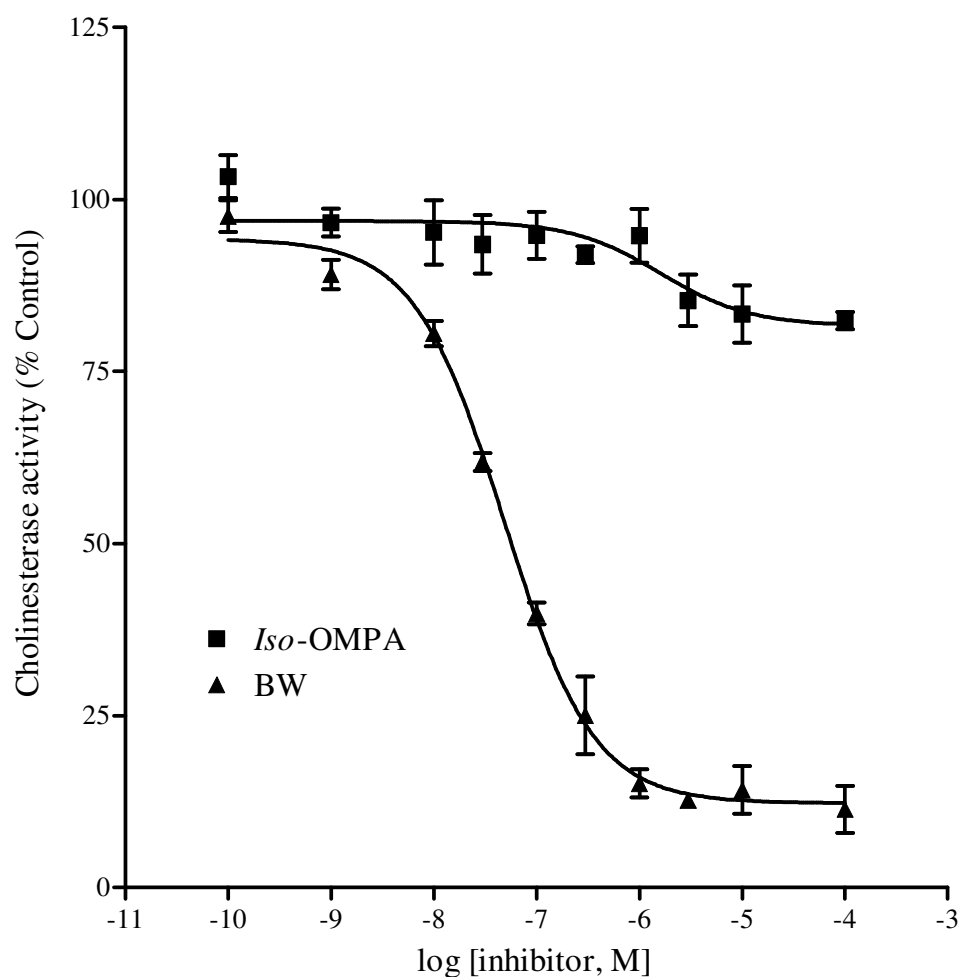
Figure 15: *In vitro* inhibition of AChE and BChE using BW284C51 and *iso*-OMPA in aged rat cortical tissue homogenates (n=3 per group). Cortical tissue homogenates from aged rats were incubated with *iso*-OMPA or BW (at the concentrations noted) at 37°C for 15 minutes, before assessing the residual ChE activity, as described previously. Data (mean ± standard error) represent AChE (triangle) or BChE (square) activity as percent of control (i.e., activity in the absence of either inhibitor).

Table 1. Distribution of AChE and BChE activity in the cortex and heart of adult and aged rats

	Cortex		Heart	
	Adult	Aged	Adult	Aged
AChE (% Total ChE)	90.27 ± 3.72	83.35 ± 4.15	13.86 ± 6.02	14.23 ± 1.18
BChE (% Total ChE)	8.85 ± 2.71	14.17 ± 3.46	91.59 ± 2.52	82.46 ± 5.07

Cardiac and cortical tissue homogenates were incubated with of *iso*-OMPA (10 µM) or BW (10 µM) at 37°C for 15 minutes, before assessing the residual ChE activity, as described in the Methods section. For total cholinesterase activity, the tissue homogenate was pre-incubated in potassium phosphate buffer only (i.e., no inhibitor), prior to performing the assay. Data (mean ± standard error) represent AChE or BChE activity as percent of total ChE activity.

In vitro inhibition of Cholinesterases (Acetylcholinesterase & Butyrylcholinesterase) in Adult and Aged Heart & Cortex by Chlorpyrifos Oxon and Paraoxon

The *in vitro* potencies of chlorpyrifos oxon (CPO) and paraoxon (PO) on cardiac and cortical acetylcholinesterase (AChE) and butyrylcholinesterase (BChE) were evaluated in crude tissue homogenates from adult and aged rats. Figures 16-23 represent the *in vitro* inhibition of AChE and BChE activity in adult and aged heart and cortex by CPO (Figures 16-19) and PO (Figures 20-23). The IC_{50} values for CPO and PO against both cholinesterase activities in the heart and cortex are shown in Tables 2 and 3, respectively. In the heart, CPO was significantly less potent against AChE (4 to 11-fold) than BChE. While there was no age-related difference in sensitivity of AChE to CPO, BChE in the heart from aged rats was significantly more sensitive to CPO than BChE in heart of adult rats (~ 2.5 fold). Similarly, CPO was significantly less potent at inhibiting cortical AChE (4 to 10-fold) than BChE in brain (cortex) of both age groups. Although BChE in the cortex of aged rats appeared about 2-fold more sensitive to the effect of CPO than BChE in the cortex of adult rats, this difference was not statistically significant.

In contrast, PO was a more potent inhibitor of heart AChE than BChE in both age groups, with relatively similar differences also being noted in the brain. Furthermore, there was no apparent age-related difference in sensitivity of AChE or BChE to PO in either tissue.
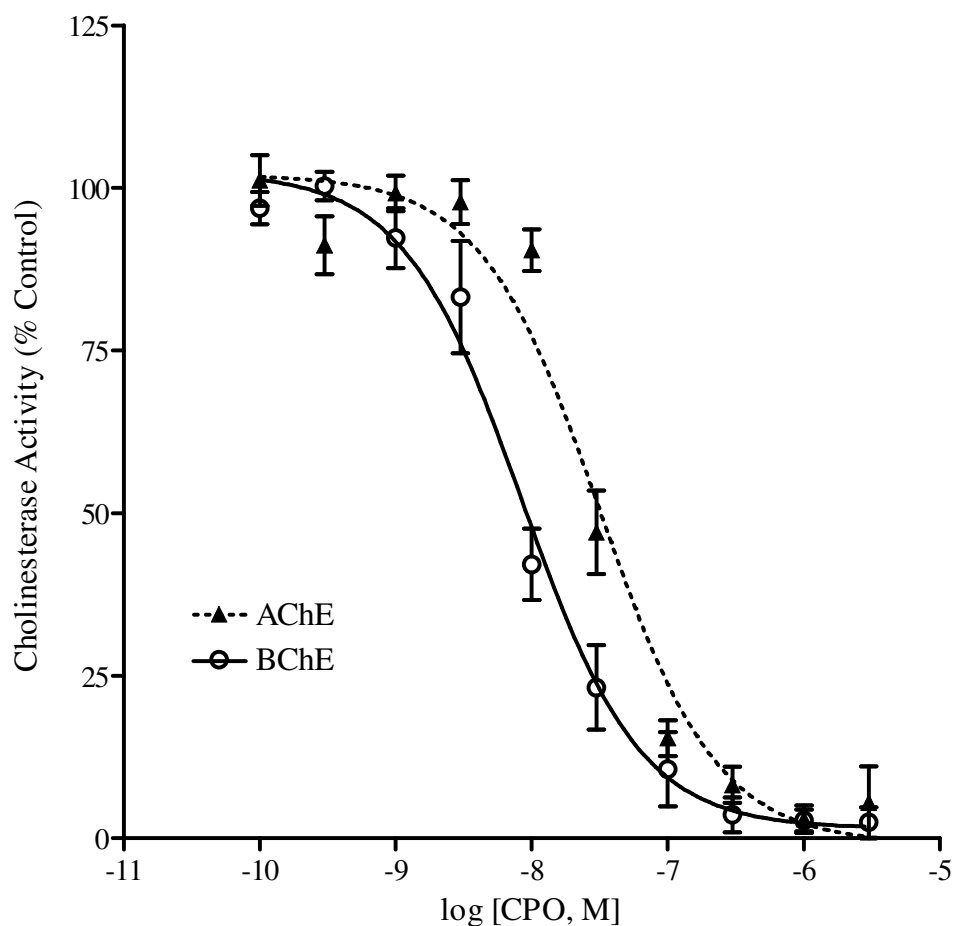
Figure 16: *In vitro* inhibition of AChE and BChE from adult heart (n=3 per group) using chlorpyrifos oxon. Cardiac tissue homogenates from adult rats were pre-incubated with either 10 µM *iso*-OMPA or 10 µM BW at 37°C for 15 minutes. Subsequently, they were incubated at 37°C for 30 minutes in the presence of CPO at the concentrations noted, prior to measuring the residual ChE activity as described previously. Data (mean ± standard error) represent AChE (triangle with dotted line) or BChE (open circle with solid line) activity in terms of percent of control.
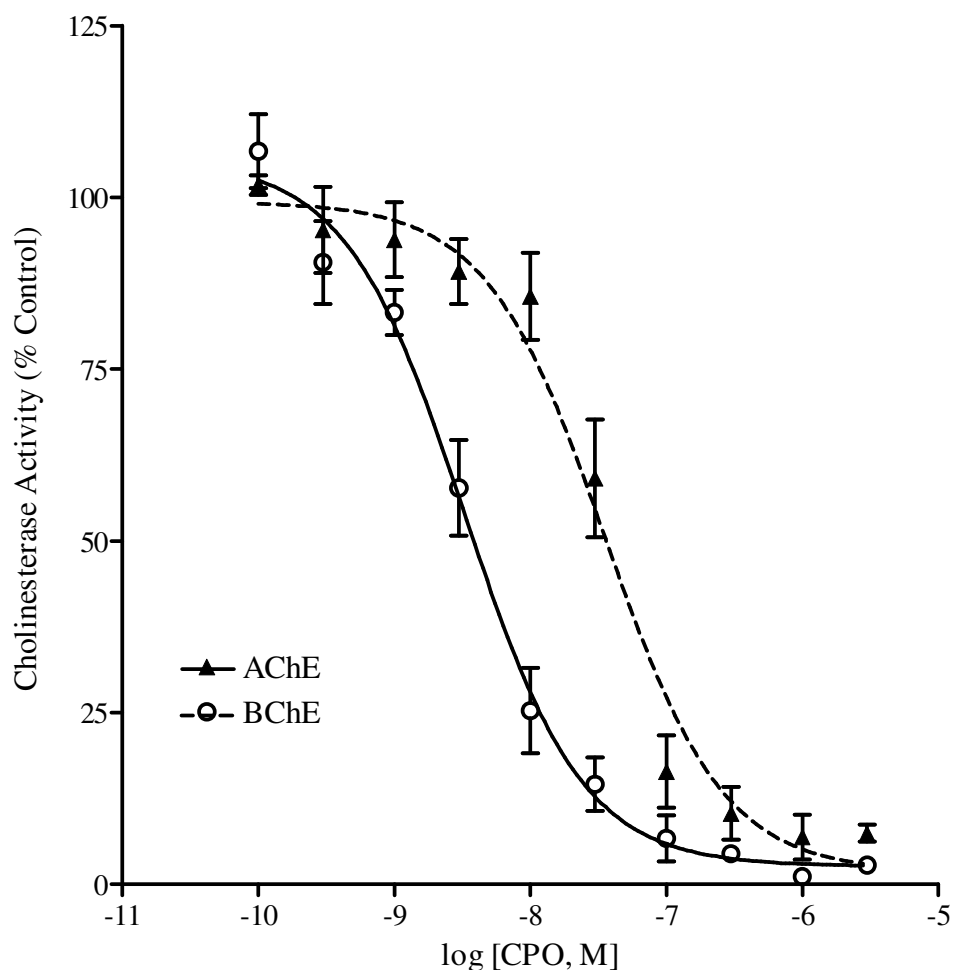
Figure 17: *In vitro* inhibition of AChE and BChE from aged heart (n=3 per group) using chlorpyrifos oxon. Cardiac tissue homogenates from aged rats were pre-incubated with either 10 μM *iso*-OMPA or 10 μM BW at 37°C for 15 minutes. Subsequently, they were incubated at 37°C for 30 minutes in the presence of CPO at the concentrations noted, prior to measuring the residual ChE activity as described previously. Data (mean ± standard error) represent AChE (triangle with dotted line) or BChE (open circle with solid line) activity in terms of percent of control.
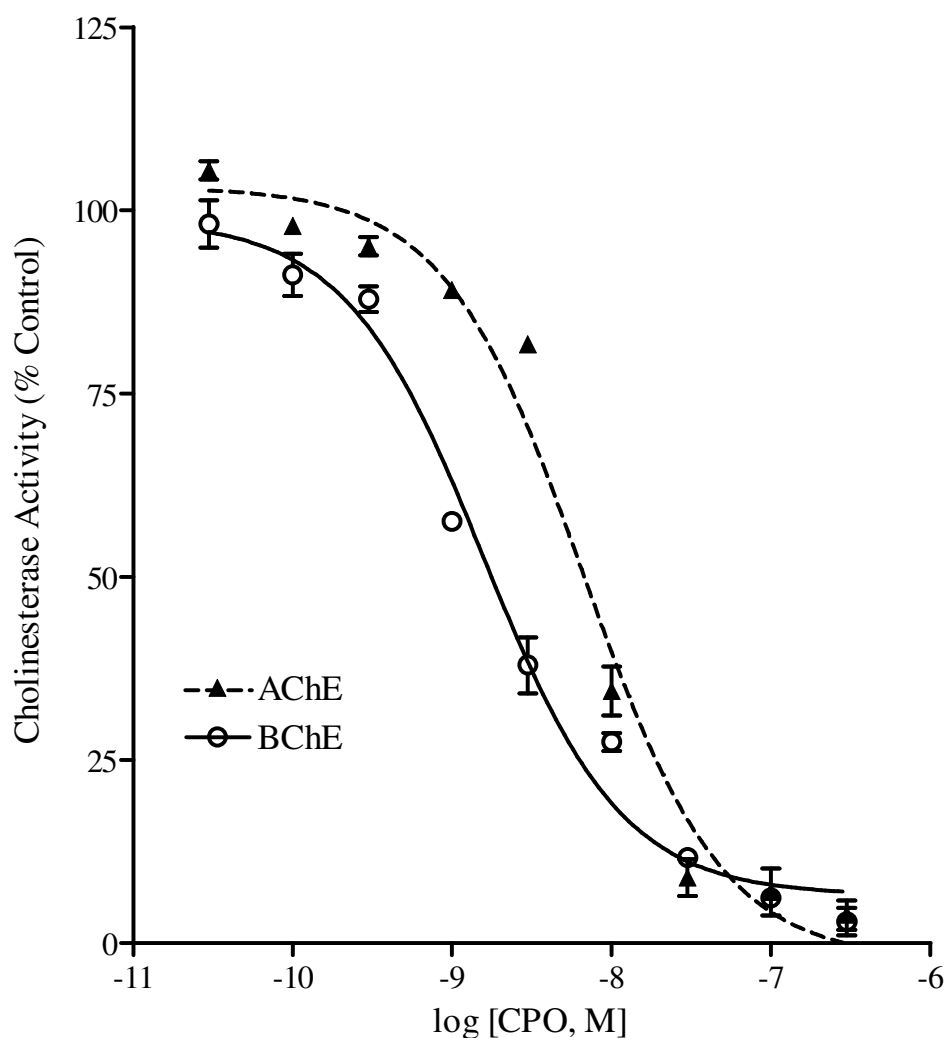
Figure 18: *In vitro* inhibition of AChE and BChE from adult cortex (n=3 per group) using chlorpyrifos oxon. Cortical tissue homogenates from adult rats were pre-incubated with either 10 μM *iso*-OMPA or 10 μM BW at 37°C for 15 minutes. Subsequently, they were incubated at 37°C for 30 minutes in the presence of CPO at the concentrations noted, prior to measuring the residual ChE activity as described previously. Data (mean ± standard error) represent AChE (triangle with dotted line) or BChE (open circle with solid line) activity in terms of percent of control.
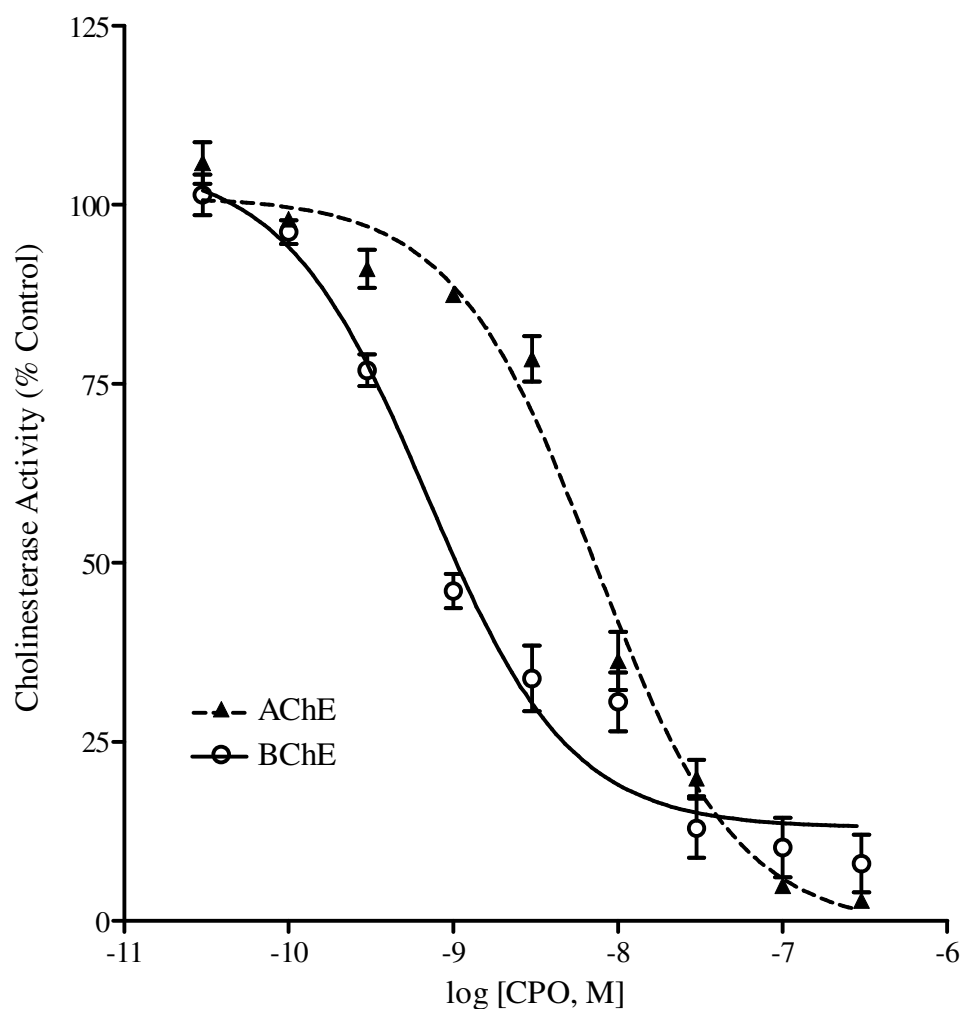
Figure 19: *In vitro* inhibition of AChE and BChE from aged cortex (n=3 per group) using chlorpyrifos oxon. Cortical tissue homogenates from aged rats were pre-incubated with either 10 µM *iso*-OMPA or 10 µM BW at 37°C for 15 minutes. Subsequently, they were incubated at 37°C for 30 minutes in the presence of CPO at the concentrations noted, prior to measuring the residual ChE activity as described previously. Data (mean ± standard error) represent AChE (triangle with dotted line) or BChE (open circle with solid line) activity in terms of percent of control.
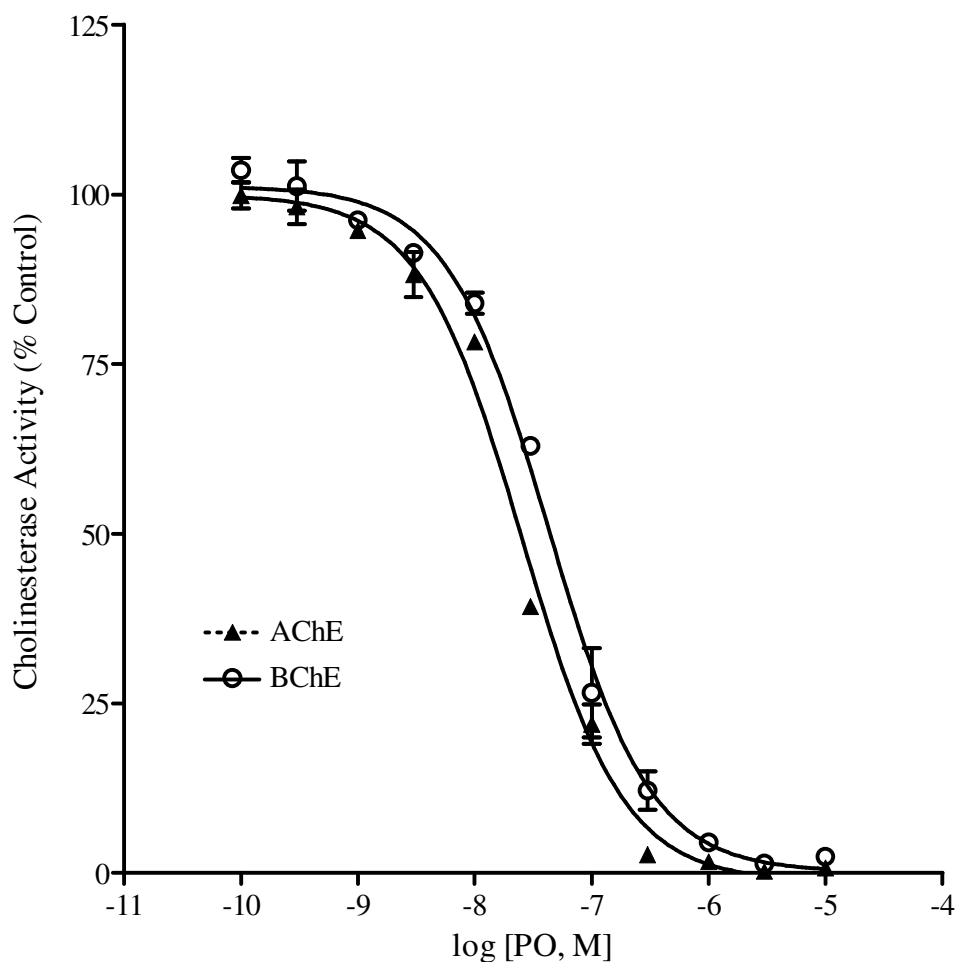
Figure 20: *In vitro* inhibition of AChE and BChE from adult heart (n=3 per group) using paraoxon. Cardiac tissue homogenates from adult rats were pre-incubated with either 10 μM *iso*-OMPA or 10 μM BW at 37°C for 15 minutes. Subsequently, they were incubated at 37°C for 30 minutes in the presence of PO at the concentrations noted, prior to measuring the residual ChE activity as described previously. Data (mean ± standard error) represent AChE (triangle with dotted line) or BChE (open circle with solid line) activity in terms of percent of control.
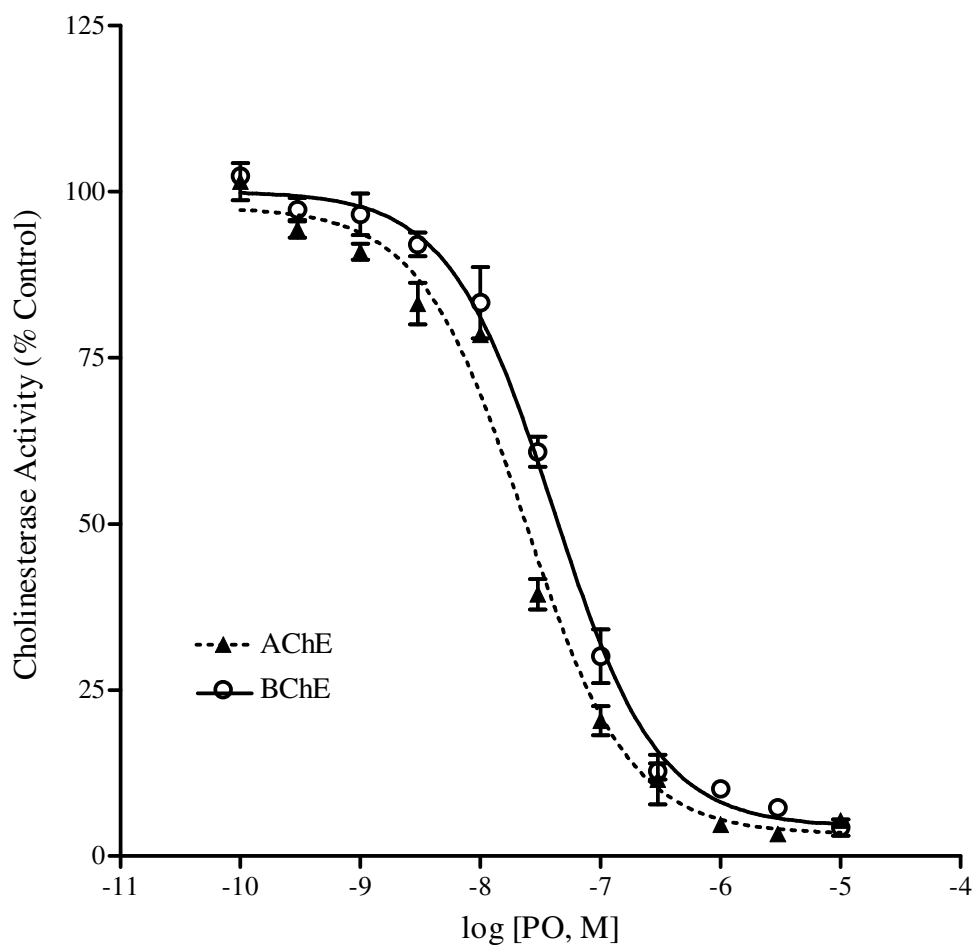
Figure 21: *In vitro* inhibition of AChE and BChE from aged heart (n=3 per group) using paraoxon. Cardiac tissue homogenates from aged rats were pre-incubated with either 10 μM *iso*-OMPA or 10 μM BW at 37°C for 15 minutes. Subsequently, they were incubated at 37°C for 30 minutes in the presence of PO at the concentrations noted, prior to measuring the residual ChE activity as described previously. Data (mean ± standard error) represent AChE (triangle with dotted line) or BChE (open circle with solid line) activity in terms of percent of control.
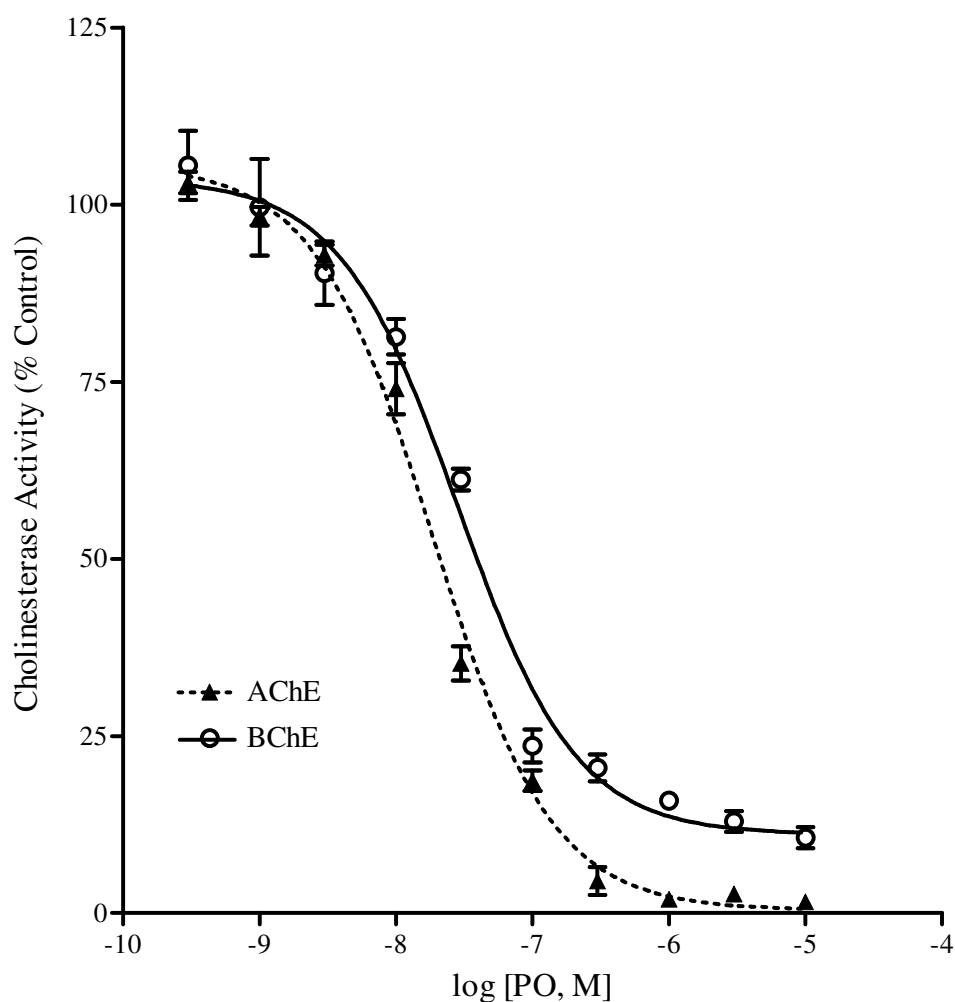
Figure 22: *In vitro* inhibition of AChE and BChE from adult cortex (n=3 per group) using paraoxon. Cortical tissue homogenates from adult rats were pre-incubated with either 10 µM *iso*-OMPA or 10 µM BW at 37°C for 15 minutes. Subsequently, they were incubated at 37°C for 30 minutes in the presence of PO at the concentrations noted, prior to measuring the residual ChE activity as described previously. Data (mean ± standard error) represent AChE (triangle with dotted line) or BChE (open circle with solid line) activity in terms of percent of control.
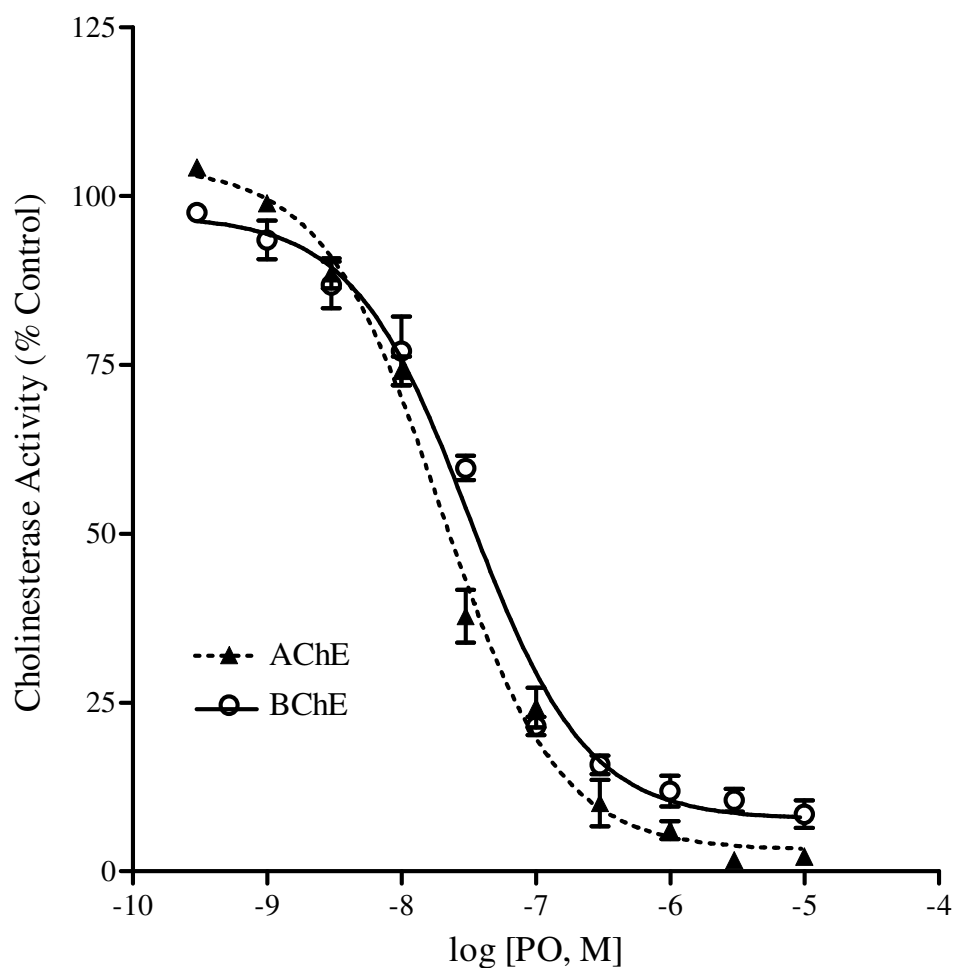
Figure 23: *In vitro* inhibition of AChE and BChE from aged cortex (n=3 per group) using paraoxon. Cortical tissue homogenates from aged rats were pre-incubated with either 10 μM *iso*-OMPA or 10 μM BW at 37°C for 15 minutes. Subsequently, they were incubated at 37°C for 30 minutes in the presence of PO at the concentrations noted, prior to measuring the residual ChE activity as described previously. Data (mean ± standard error) represent AChE (triangle with dotted line) or BChE (open circle with solid line) activity in terms of percent of control.

Table 2. IC$_{50}$ values of chlorpyrifos oxon and paraoxon against AChE and BChE activity in adult and aged rat heart

	Adult		Aged	
	AChE	BChE	AChE	BChE
CPO	31.53 nM#	8.47 nM	35.46 nM#	3.27 nM*
PO	25.3 nM	42.8 nM	23.5 nM	40.4 nM

Cardiac tissue homogenates were pre-incubated with either 10 µM *iso*-OMPA or 10 µM BW at 37°C for 15 minutes. Thereafter, they were incubated at 37°C for 30 minutes in the presence of either CPO (30 pM to 3 µM) or PO (100 pM to 10 µM), prior to measuring the residual ChE activity as described previously. Data represents the mean IC$_{50}$ for each inhibitor against each enzyme from three separate experiments. The pound signs represents values significantly different from BChE in the same age-group, while asterisks represent values significantly different from BChE in the adult (P<0.05).

Table 3. IC_{50} of chlorpyrifos oxon and paraoxon against AChE and BChE activity in adult and aged cortex

	Adult		Aged	
	AChE	BChE	AChE	BChE
CPO	6.64 nM$^{\#}$	1.58 nM	7.21 nM$^{\#}$	0.69 nM
PO	18.7 nM	28.5 nM	19.5 nM	32.1 nM

Cortical tissue homogenates were pre-incubated with either 10 µM *iso*-OMPA or 10 µM BW at 37°C for 15 minutes. Subsequently, they were incubated at 37°C for 30 minutes in the presence of either CPO (30 pM to 3 µM) or PO (100 pM to 10 µM), prior to measuring the residual ChE activity as described previously. Data represents the mean IC_{50} for each inhibitor against each enzyme from three separate experiments. Pound signs represent values significantly different from BChE in the same age-group ($P<0.05$).

In Vitro Displacement of [³H]Oxotremorine-M Binding by CPO and PO

in Adult and Aged Heart and Cortex

The abilities of chlorpyrifos oxon (CPO) and paraoxon to displace [³H]Oxotremorine-M ([³H]OXO) binding were evaluated in adult and aged cardiac and cortical membranes. Figures 24-27 show the displacement of [³H]OXO in heart and cortex from adult & aged rats by CPO (Figures 24 and 25) and PO (Figures 26 and 27). The IC_{50} and maximum percent displacement for each OP are summarized in Table 4. Both CPO and PO displaced [³H]OXO binding in heart and cortex of adult and aged rats. Of the two, CPO was the more potent displacer of [³H]OXO in the heart and cortex of both age-groups. Similarly, PO also potently displaced [³H]OXO from adult and aged cardiac and cortical membranes. Both OPs appeared to have similar efficacies in displacing [³H]OXO binding in heart and cortex of the two age-groups. No age-related difference was observed in displacement of [³H]OXO binding in either tissue.
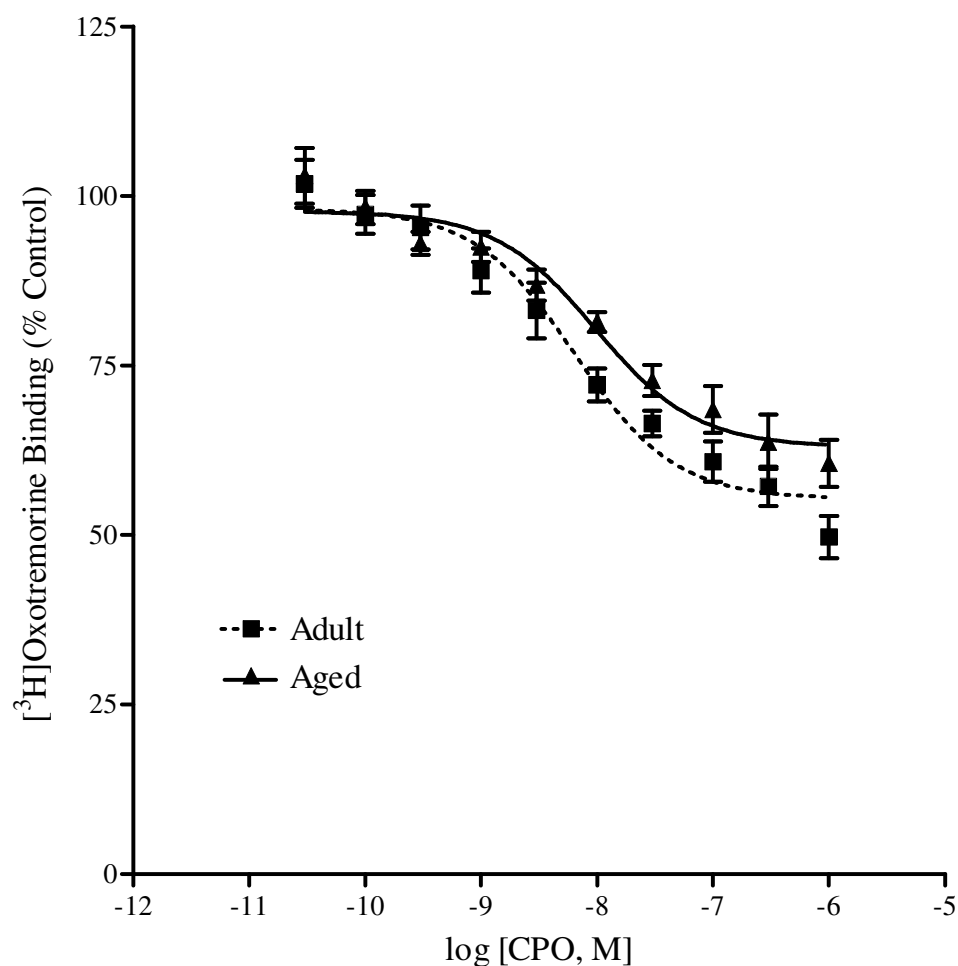
Figure 24. *In vitro* displacement of [³H]OXO by chlorpyrifos oxon in adult and aged heart (n=3 per group). Cardiac membranes from adult (square) and aged (triangle) rats were incubated at 21°C for 90 minutes in the presence of 1 nM [³H]OXO and CPO at the concentrations noted. Atropine (10 µM) was used in paired tubes to block specific binding, which was calculated as the binding between tubes incubated in the presence and absence of atropine. Data (mean ± standard error) represent specific binding in terms of percent of control.
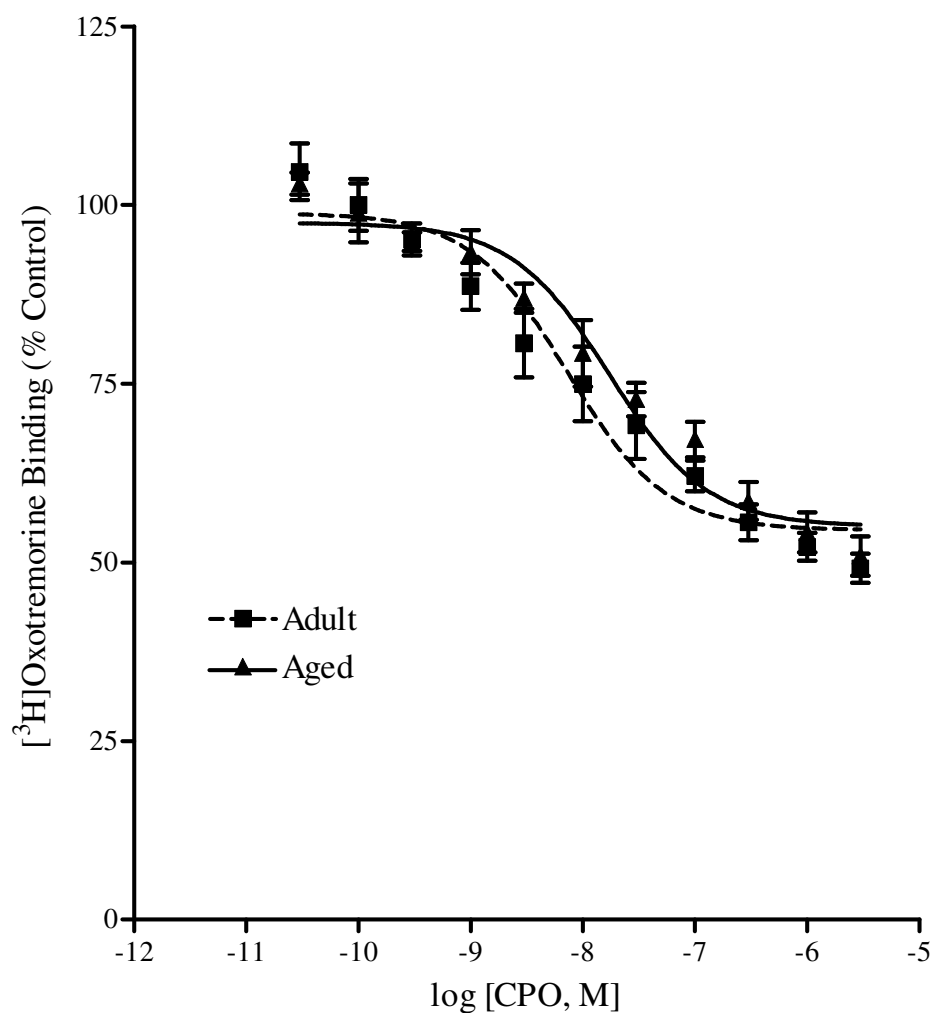
Figure 25. *In vitro* displacement of [3H]OXO by chlorpyrifos oxon in adult and aged cortex (n=3 per group). Cortical membranes from adult (square) and aged (triangle) rats were incubated at 21°C for 90 minutes in the presence of 1 nM [3H]OXO and CPO at the concentrations noted. Atropine (10 µM) was used in paired tubes to block specific binding, which was calculated as the binding between tubes incubated in the presence and absence of atropine. Data (mean ± standard error) represent specific binding in terms of percent of control.
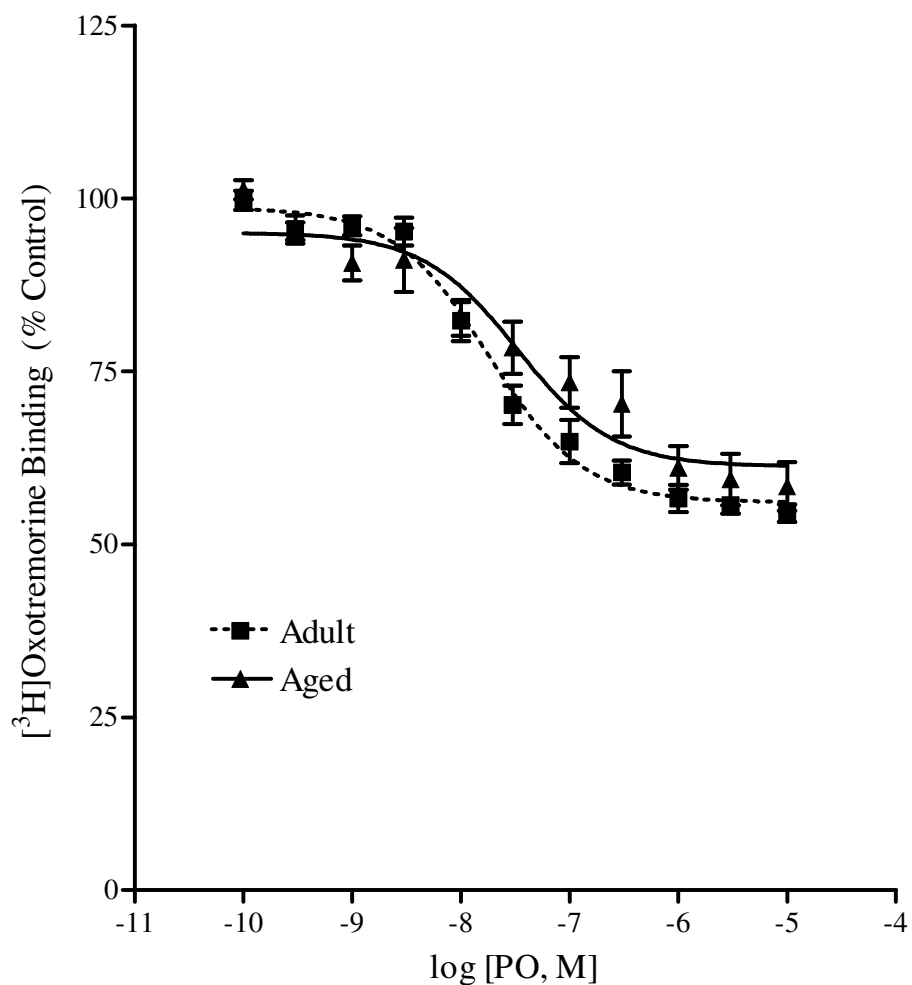
Figure 26. *In vitro* displacement of [³H]OXO by paraoxon in adult and aged heart (n=3 per group). Cardiac membranes from adult (square) and aged (triangle) rats were incubated at 21°C for 90 minutes in the presence of 1 nM [³H]OXO and PO at the concentrations noted. Atropine (10 μM) was used in paired tubes to block specific binding, which was calculated as the binding between tubes incubated in the presence and absence of atropine. Data (mean ± standard error) represent specific binding in terms of percent of control.
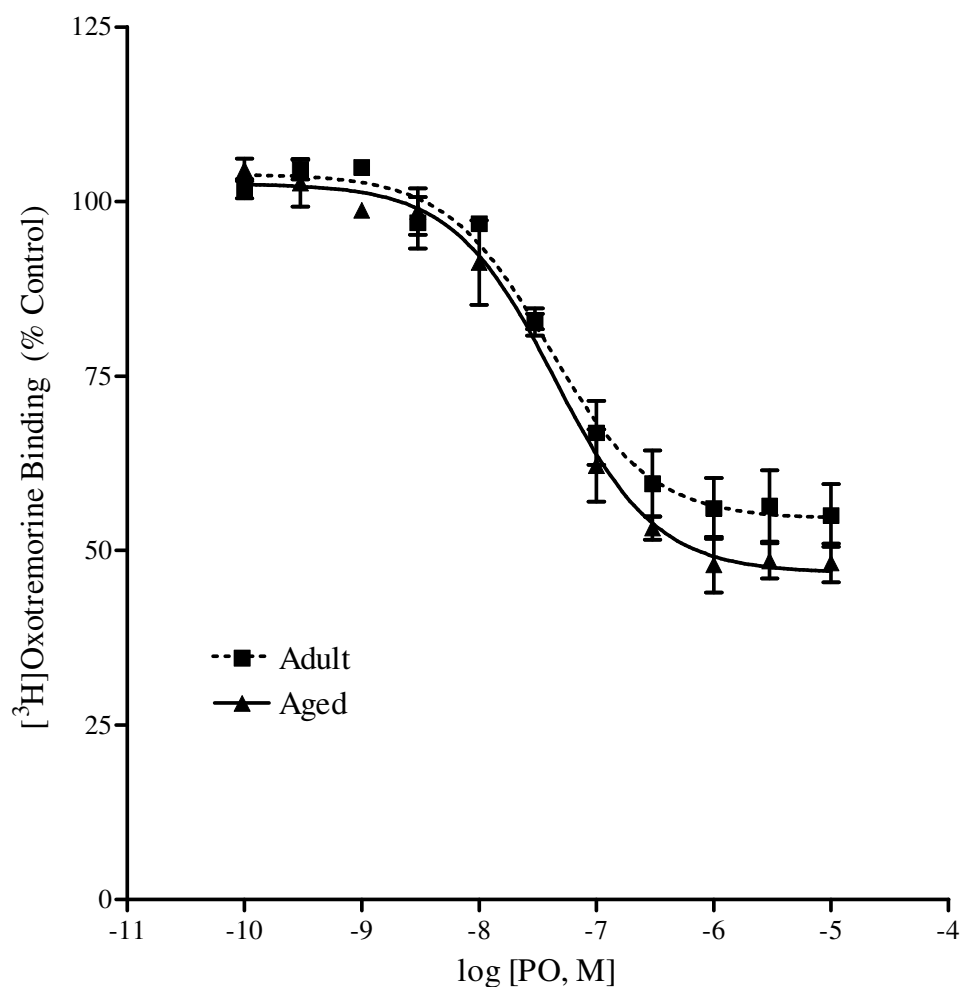
Figure 27. *In vitro* displacement of [^{3}H]OXO by paraoxon in adult and aged cortex (n=3 per group). Cortical membranes from adult (square) and aged (triangle) rats were incubated at 21ºC for 90 minutes in the presence of 1 nM [^{3}H]OXO and PO at the concentrations noted. Atropine (10 µM) was used in paired tubes to block specific binding, which was calculated as the binding between tubes incubated in the presence and absence of atropine. Data (mean ± standard error) represent specific binding in terms of percent of control.

Table 4. *In vitro* displacement of [^{3}H]Oxotremorine-M binding in adult and aged rat heart and cortex using chlorpyrifos oxon and paraoxon

	CPO		PO	
	IC_{50}	Maximum displacement	IC_{50}	Maximum displacement
Adult Heart	6.4 nM	50.27 ± 3.13%	17.9 nM	54.5 ± 1.28%
Aged Heart	9.7 nM	39.38 ± 3.47%	33.1 nM	58.39 ± 3.51%
Adult Cortex	7.3 nM	50.83 ± 2.04%	39.1 nM	55.02 ± 4.51%
Aged Cortex	17.3 nM	49.1 ± 2.75%	43.9 nM	48.22 ± 2.75%

Cardiac and cortical membranes (n=3/group) were incubated at 21ºC for 90 minutes in the presence of 1 nM [^{3}H]Oxotremorine-M acetate and one of a range of OP (CPO or PO) concentrations as described in the Methods section. Atropine (10 µM) was used in paired tubes to block specific binding, which was calculated as the binding between tubes incubated in the presence and absence of atropine. Data represent the mean IC_{50} value and percent maximum displacement (mean ± S.E.) of [^{3}H]OXO from three individual experiments.

<u>Effects of Various Doses of *iso*-OMPA on Acetylcholinesterase,</u>

<u>Butyrylcholinesterase and Carboxylesterase from Atria, Ventricles and Cortex</u>

In order to determine doses of *iso*-OMPA that would selectively inhibit only cardiac BChE in the absence of central AChE inhibition, a dose-determination study was performed *in vivo*, using various doses of *iso*-OMPA (1.25 to 100 mg/kg, sc). In addition to AChE and BChE activity, carboxylesterase (CarbE) activity was also evaluated, since *iso*-OMPA is a potent inhibitor of this enzyme. Figures 28-36 show the dose-related effects of *iso*-OMPA on AChE, BChE and CarbE in atria (Figures 28-30), ventricles (Figures 31-33) and cortex (Figures 34-36).

Iso-OMPA elicited a dose-dependent inhibition of BChE activity in the atria, ventricles and brain, with a maximal selective inhibition of ~85%. Higher doses of *iso*-OMPA led to non-specific inhibition of AChE activity. From this study, it was determined that 1.25 and 5 mg/kg of *iso*-OMPA, which selectively inhibited 60-65% and 75-80% cardiac (atrial & ventricular) BChE respectively, did not inhibit AChE activity in either any tissue. Of these two dosages, 5 mg/kg elicited significant inhibition of CarbE (10-60%) activity. We therefore selected these two dosages for subsequent studies.
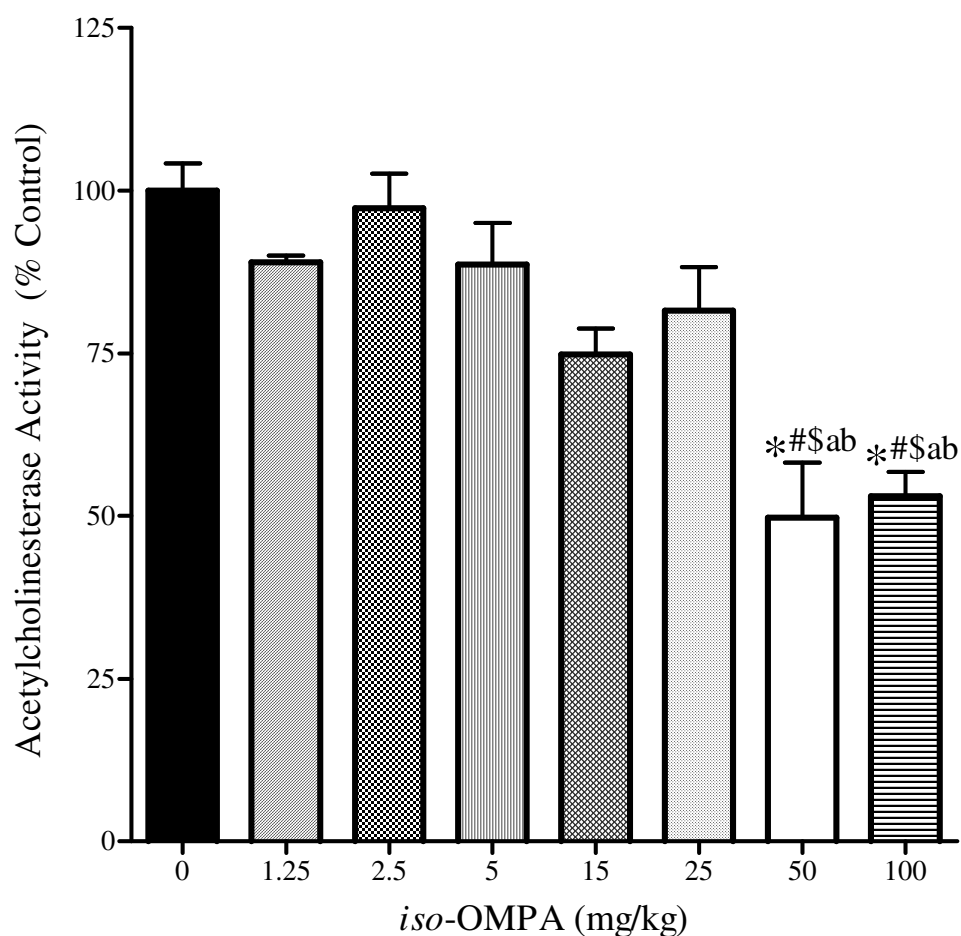
Figure 28: The effects of various doses of *iso*-OMPA on acetylcholinesterase activity in atrium. Rats (n=3-7/dose group) were treated subcutaneously with *iso*-OMPA at the doses indicated and sacrificed 24 hours later. Atrial tissue homogenates were pre-incubated with 10 µM *iso*-OMPA at 37°C for 15 minutes prior to measuring the residual ChE activity as described previously. The highest doses of *iso*-OMPA (50 and 100 mg/kg) inhibited AChE activity in the atria. Data (mean ± standard error) represent AChE activity in terms of percent of control. The asterisk, pound, dollar, a, and b signs represent values that are significantly different from control, 1.25, 2.5, 5 and 25 mg/kg dose-groups, respectively.
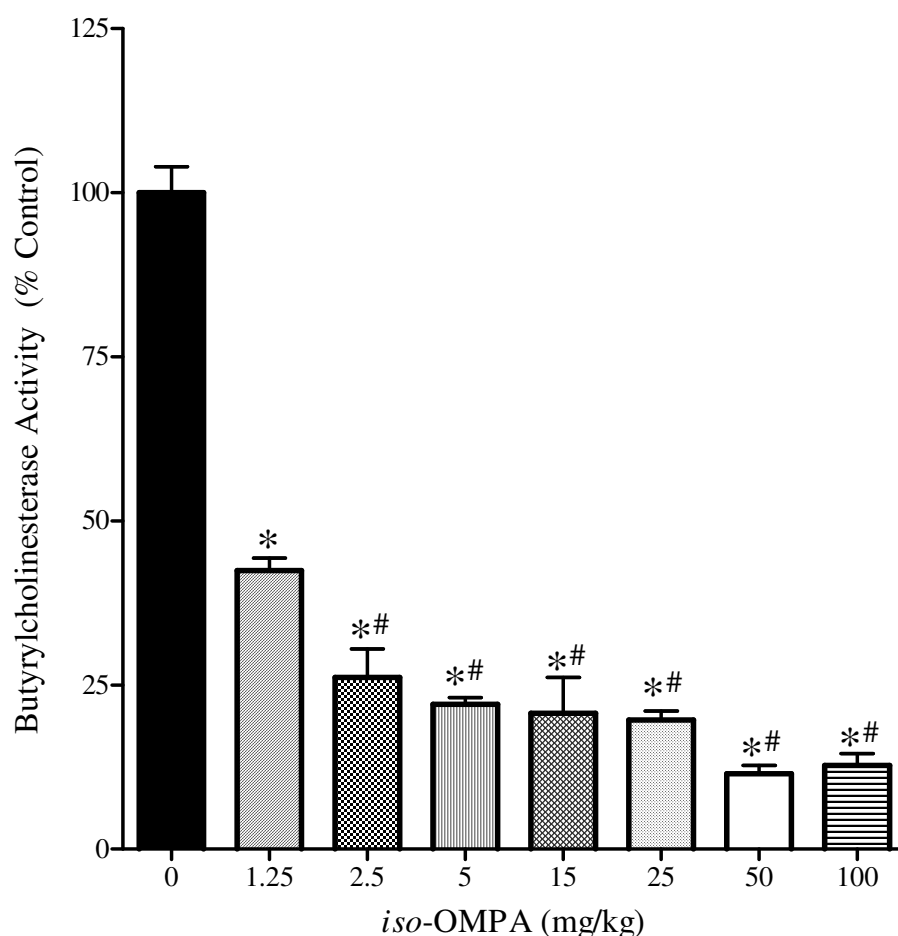
Figure 29: The effects of various doses of *iso*-OMPA on butyrylcholinesterase activity in atrium. Rats (n=3-7/dose group) were treated subcutaneously with *iso*-OMPA at the doses indicated and sacrificed 24 hours later. Atrial tissue homogenates were pre-incubated with 10 μM BW284C51 at 37°C for 15 minutes prior to measuring the residual ChE activity as described previously. A dose-dependent inhibition of BChE was observed with the lower doses, with maximal BChE inhibition plateauing at ~85% in rats treated with $\geq$ 5 mg/kg of *iso*-OMPA. Data (mean ± standard error) represent BChE activity in terms of percent of control. The asterisk and pound signs represent values that are significantly different from control and the 1.25 mg/kg dose group, respectively.
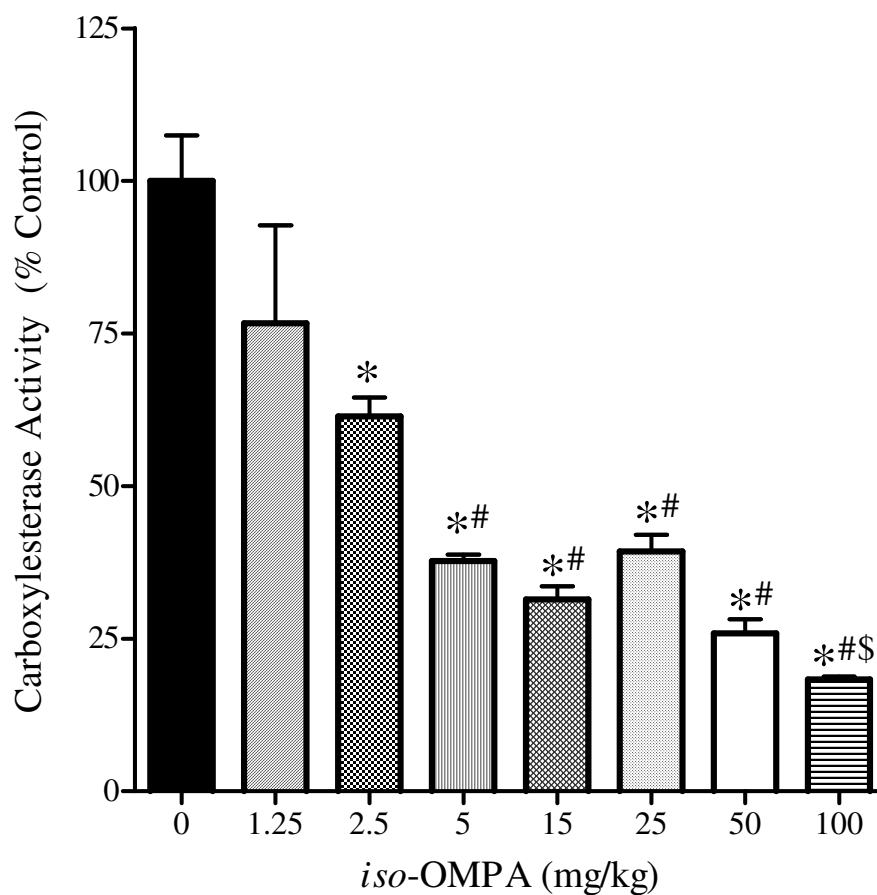
Figure 30: The effects of various doses of *iso*-OMPA on carboxylesterase activity in atrium. Rats (n=3-7/dose group) were treated subcutaneously with *iso*-OMPA at the doses indicated and sacrificed 24 hours later. Atrial tissue homogenates were incubated at 37°C in the presence of the substrate p-nitrophenyl acetate to assess CarbE activity. *Iso*-OMPA produced a dose-dependent inhibition of CarbE activity in the atria. Data (mean ± standard error) represent CarbE activity in terms of percent of control. The asterisk, pound, and dollar signs represent values that are significantly different from control, 1.25 and 2.5 mg/kg dose group, respectively.
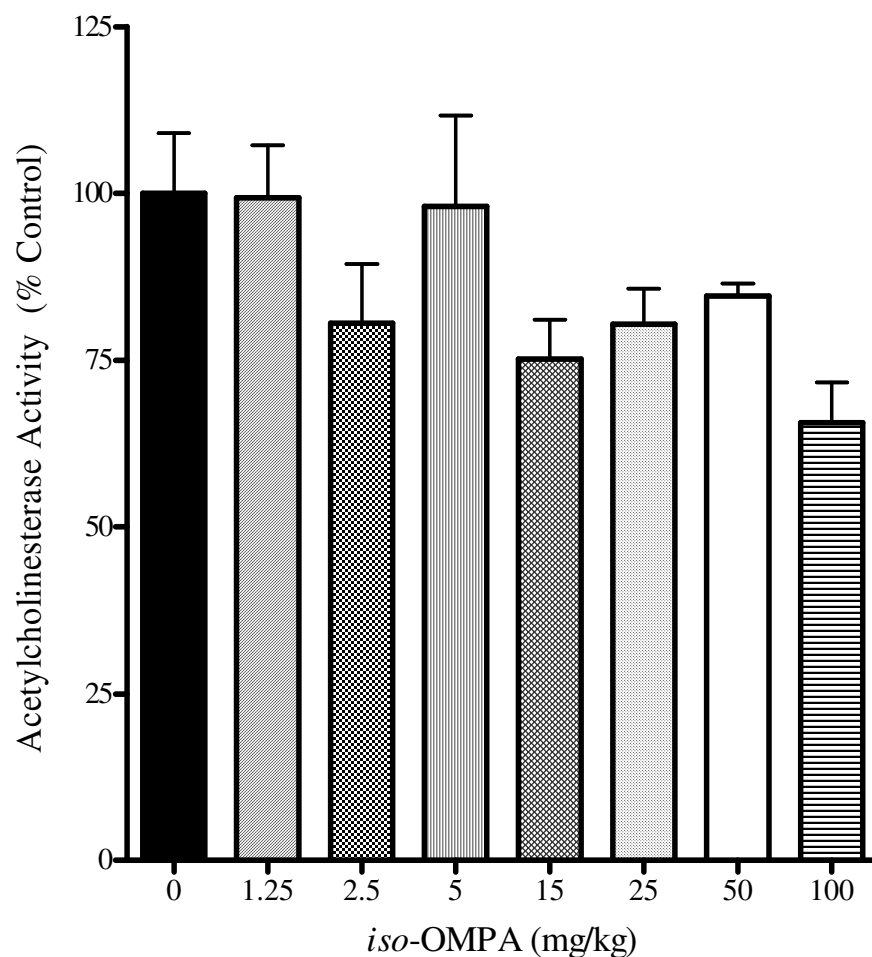
Figure 31: The effects of various doses of *iso*-OMPA on acetylcholinesterase activity in ventricular tissue homogenates. Rats (n=3-7/dose group) were treated subcutaneously with *iso*-OMPA at the doses indicated and sacrificed 24 hours later. Ventricular tissue homogenates were pre-incubated with 10 µM *iso*-OMPA at 37°C for 15 minutes prior to measuring the residual ChE activity as described previously. No significant inhibition of AChE was obtained with any of the dose groups. Data (mean ± standard error) represent AChE activity in terms of percent of control.
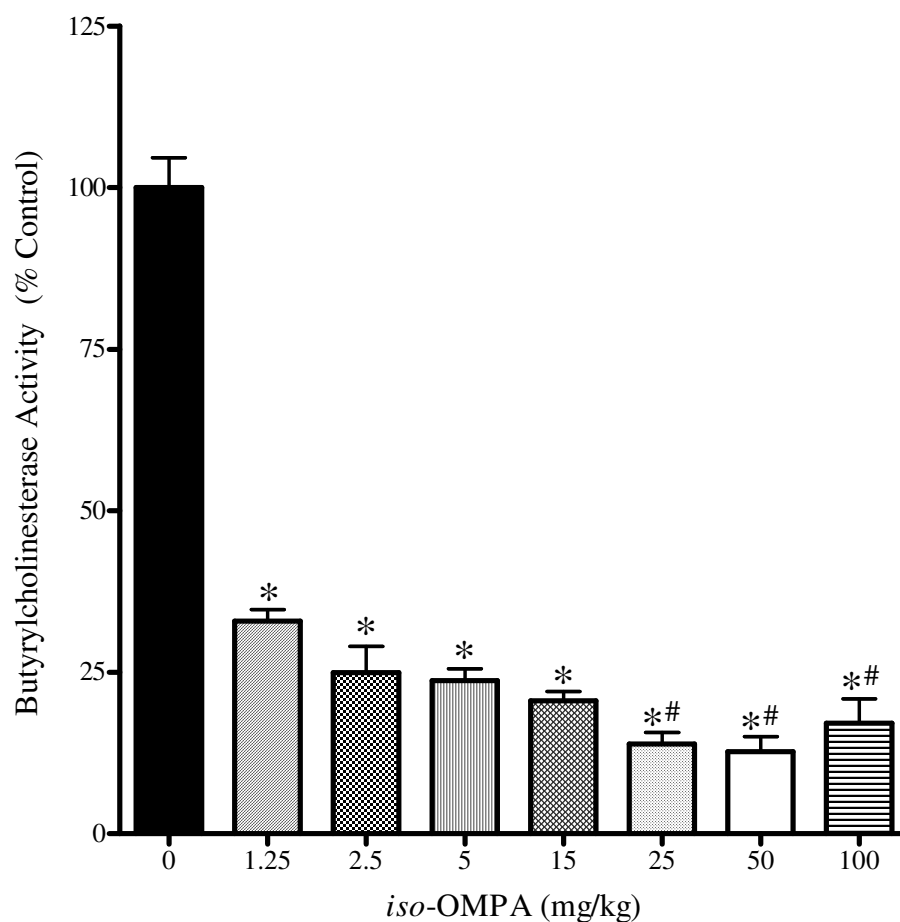
Figure 32: The effects of various doses of *iso*-OMPA on butyrylcholinesterase activity in ventricular tissue homogenates. Rats (n=3-7/dose group) were treated subcutaneously with *iso*-OMPA at the doses indicated and sacrificed 24 hours later. Ventricular tissue homogenates were pre-incubated with 10 µM BW284C51 at 37°C for 15 minutes prior to measuring the residual ChE activity as described previously. *Iso*-OMPA produced a dose-dependent inhibition of BChE activity in the ventricles. Data (mean ± standard error) represent BChE activity in terms of percent of control. The asterisk and pound signs represent values that are significantly different from control and the 1.25 mg/kg dose group, respectively.

Figure 33: The effects of various doses of *iso*-OMPA on carboxylesterase activity in ventricular tissue homogenates. Rats (n=3-7/dose group) were treated with *iso*-OMPA (sc) at the doses indicated and sacrificed 24 hours later. Ventricular tissue homogenates were incubated at 37°C in the presence of the substrate p-nitrophenyl acetate to assess CarbE activity. *Iso*-OMPA produced a dose-dependent inhibition of CarbE activity in the ventricles. Data (mean ± standard error) represent CarbE activity in terms of percent of control. The asterisk, pound, dollar, a, and b signs represent values that are significantly different from control, 1.25, 2.5, 5 and 25 mg/kg dose-groups, respectively.

Figure 34: The effects of various doses of *iso*-OMPA on acetylcholinesterase activity in cortical tissue homogenates. Rats (n=3-7/dose group) were treated subcutaneously with *iso*-OMPA at the doses indicated and sacrificed 24 hours later. Cortical tissue homogenates were pre-incubated with 10 μM iso-OMPA at 37°C for 15 minutes prior to measuring the residual ChE activity as described previously. No significant inhibition of AChE was obtained with any of the dose groups. Data (mean ± standard error) represent AChE activity in terms of percent of control.
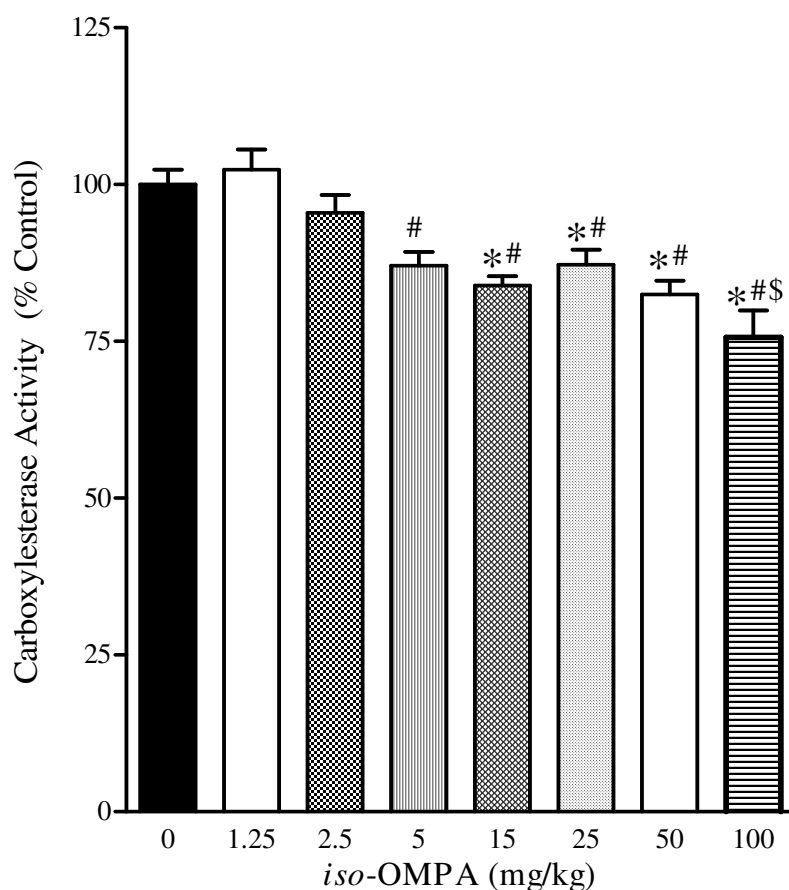
Figure 35: The effects of various doses of *iso*-OMPA on BChE activity in cortical tissue homogenates. Rats (n=3-7/dose group) were treated with *iso*-OMPA (sc) at the doses indicated and sacrificed 24 hours later. Cortical tissue homogenates were pre-incubated with 10 µM BW at 37°C for 15 minutes prior to measuring the residual ChE activity as described previously. The lower doses of *iso*-OMPA (1,25, 2.5 and 5 mg/kg) did not cause significant inhibition of cortical BChE, while the higher doses (≥15 mg/kg) produced a dose-dependent inhibition of BChE activity in the cortex. Data (mean ± standard error) represent BChE activity in terms of percent of control. The asterisk, pound, dollar, and a signs represent values that are significantly different from control, 1.25, 2.5 and 5 mg/kg dose-groups, respectively.
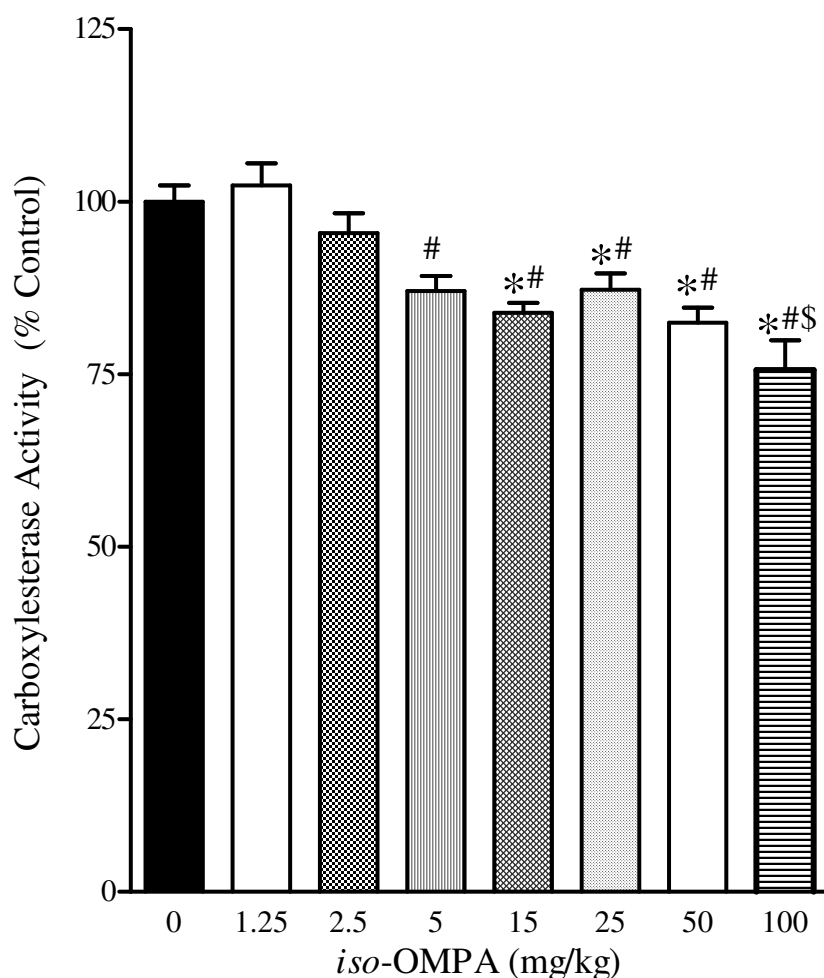
Figure 36: The effects of various doses of *iso*-OMPA on carboxylesterase activity in cortical tissue homogenates. Rats (n=3-7/dose group) were treated with *iso*-OMPA (sc) at the doses indicated and sacrificed 24 hours later. Cortical tissue homogenates were incubated at 37°C in the presence of the substrate p-nitrophenyl acetate to assess CarbE activity. *Iso*-OMPA produced a dose-dependent inhibition of CarbE activity in the cortex with doses ≥ 5 mg/kg. Data (mean ± standard error) represent CarbE activity in terms of percent of control. The asterisk, pound and dollar signs represent values that are significantly different from control, 1.25 and 2.5 mg/kg dose groups, respectively.

Effects of *iso*-OMPA on Heart Rate, Body Temperature and Physical Activity

In Adult Male Sprague-Dawley Rats

The effects of *iso*-OMPA on heart rate, body temperature and physical activity were evaluated upto 96 hours post-treatment. From the dose-determination studies, 1.25 and 5 mg/kg were selected as the low and high dose groups, respectively. Neither of the two doses of *iso*-OMPA produced any effect on body weight or functional signs of toxicity (data not shown).

The low and high doses of *iso*-OMPA produced a decrease in heart rate (Figures 37-39) at 24 hours post-treatment, with recovery occuring thereafter. The magnitude of the heart rate decrease was greater in the low dose than the high dose group. Compared to their baseline (pre-treatment) values, diurnal heart rate was significantly reduced towards the end of the study in the high dose group (84 hours post-treatment), low dose group (108 hours post-treatment), and interestingly, also in the control group. On the other hand, heart rate was significantly reduced at 24 (low and high dose groups) and 48 (low dose group) hours post-treatment, with subsequent recovery occurring thereafter. Since most of the effects of *iso*-OMPA on heart rate seemed to occur upto 48 hours post-treatment, heart rate was grouped into 4 hourly intervals and evaluated upto 48 hours post-treatment (Figure 40). The low and high doses of *iso*-OMPA produced a decrease in heart rate 16-20 hours post-treatment, with subsequent recovery occuring thereafter. Although there appeared to be a reduction of heart rate 36-40 hours post-treatment in the low and high dose-groups, it was not statistically significant.

Neither dose of *iso*-OMPA produced any effect on body temperature (Figures 41-43) at any of the time points examined. Physical activity (Figures 44-46) was only

significantly reduced in the low dose group of *iso*-OMPA at 72 hours post-treatment (in

the nocturnal phase), with subsequent recovery occurring to pre-treatment values.
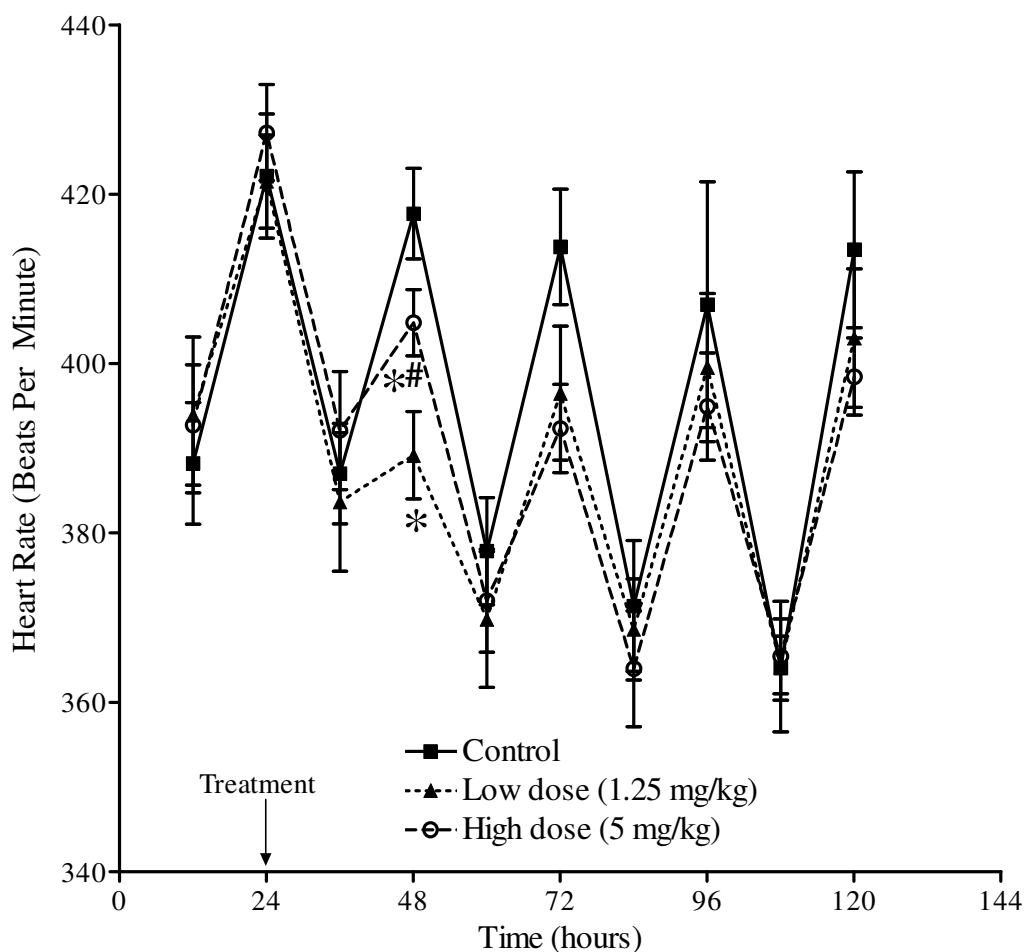
Figure 37: The effects of various doses of *iso*-OMPA on heart rate in adult rats. Rats (n=3-7/dose group) were treated with *iso*-OMPA (sc) at the doses indicated and sacrificed 24 or 96 hours later. This figure shows 24 hour baseline (pre-treatment) heart rate with the following 96 hours post-treatment data. The data (mean ± standard error) represent heart rate averaged over 8 hour diurnal and nocturnal intervals. The low and high doses of *iso*-OMPA elicited decreases in heart rate at 24 hours post-treatment, with subsequent recovery. The asterisk and pound signs represent values that are significantly different from control, and 1.25 mg/kg dose groups at the same time point, respectively.
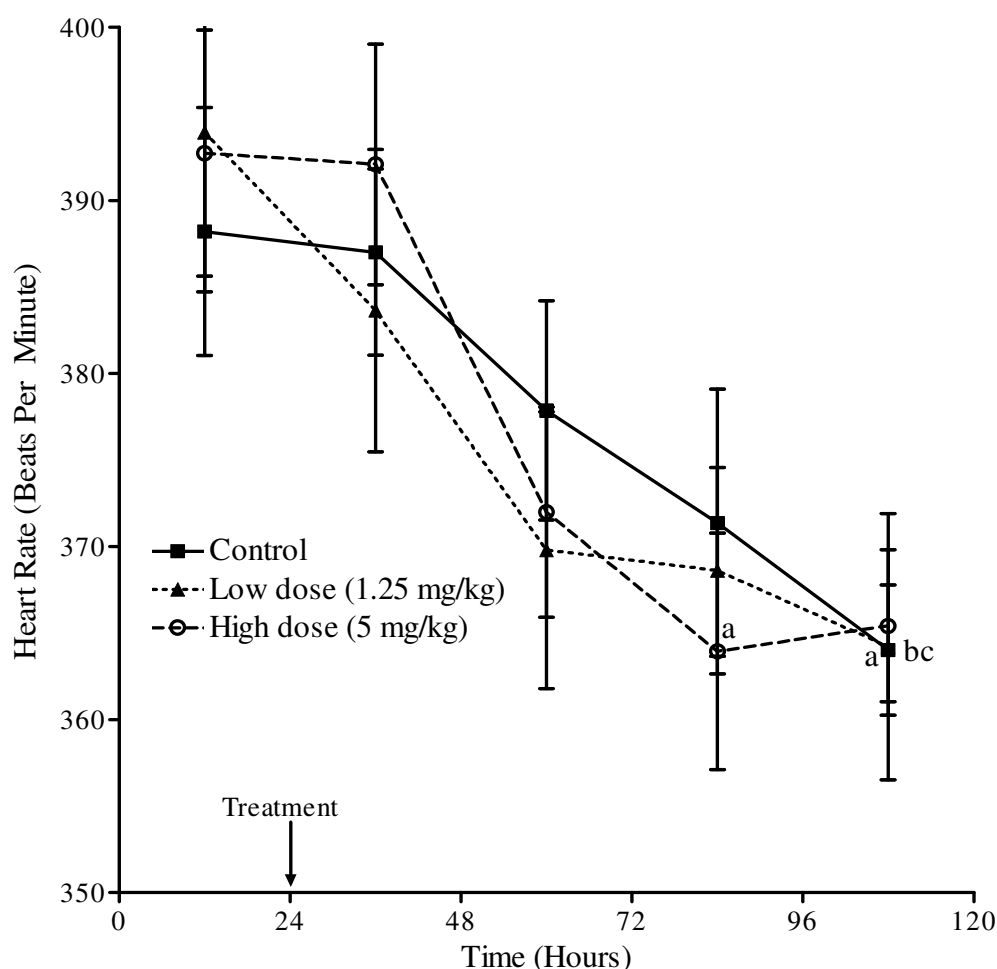
Figure 38: The effects of various doses of *iso*-OMPA on heart rate in adult rats during the diurnal (light) periods. Rats (n=3-7/dose group) were treated with *iso*-OMPA (sc) at the doses indicated and sacrificed 24 or 96 hours later. This figure shows baseline (pre-treatment) data followed by 96 hours post-treatment data. The data (mean ± standard error) represents heart rate averaged over subsequent 8-hour diurnal intervals. The low and high doses of *iso*-OMPA produced a decrease in heart rate at 108 and 84 hours post-treatment, respectively. a, b, and c represent values that are significantly different from the same dose at 12, 36 and 60 hours, respectively. Note that controls also exhibited a time-dependent reduction in diurnal heart rate.
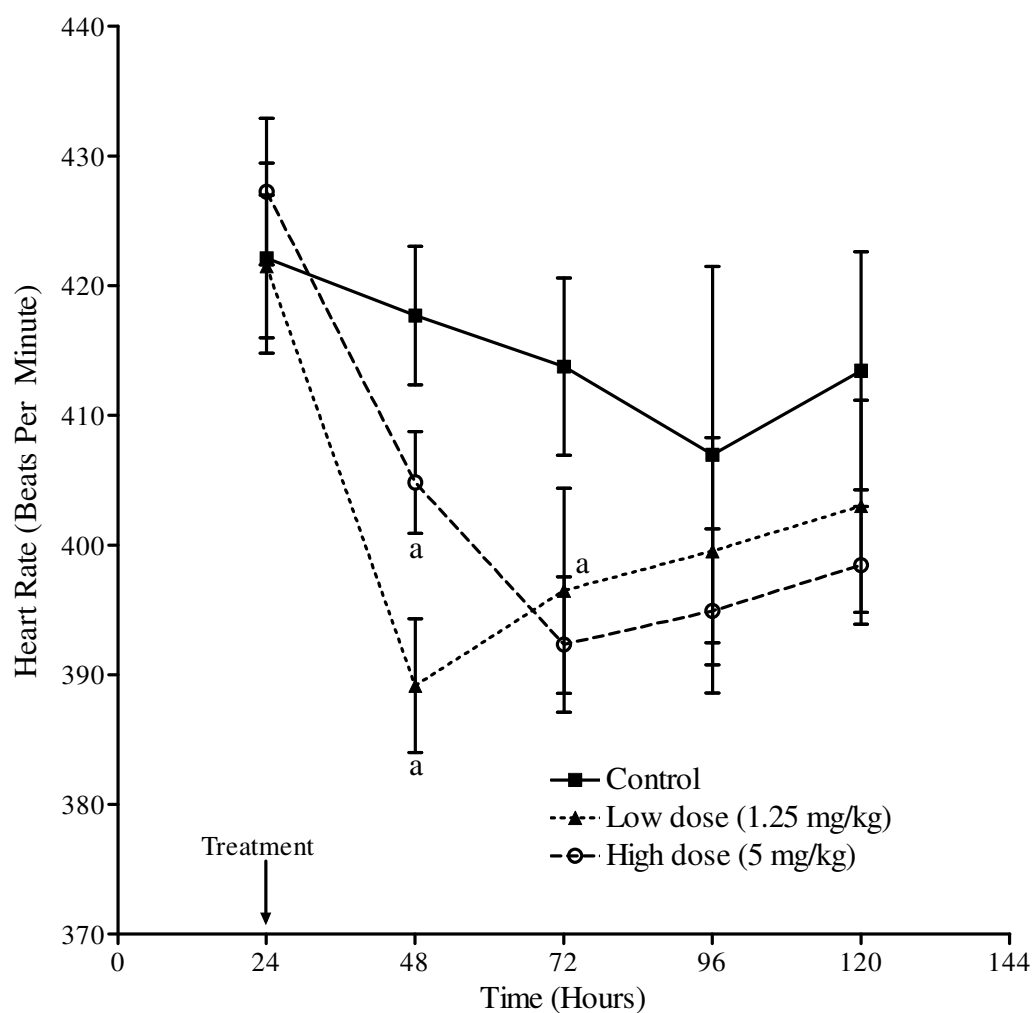
Figure 39: The effects of various doses of *iso*-OMPA on heart rate in adult rats during the nocturnal (dark) periods. Rats (n=3-7/dose group) were treated with *iso*-OMPA (sc) at the doses indicated and sacrificed 24 or 96 hours later. This figure shows 24 hour baseline (pre-treatment) data followed by 96 hours post-treatment data. The data (mean ± standard error) represents heart rate averaged over subsequent 8-hour nocturnal intervals. The low and high doses of *iso*-OMPA produced a decrease in heart rate at 24 hours post-treatment. a represents values that are significantly different from the same dose at 24 hours.
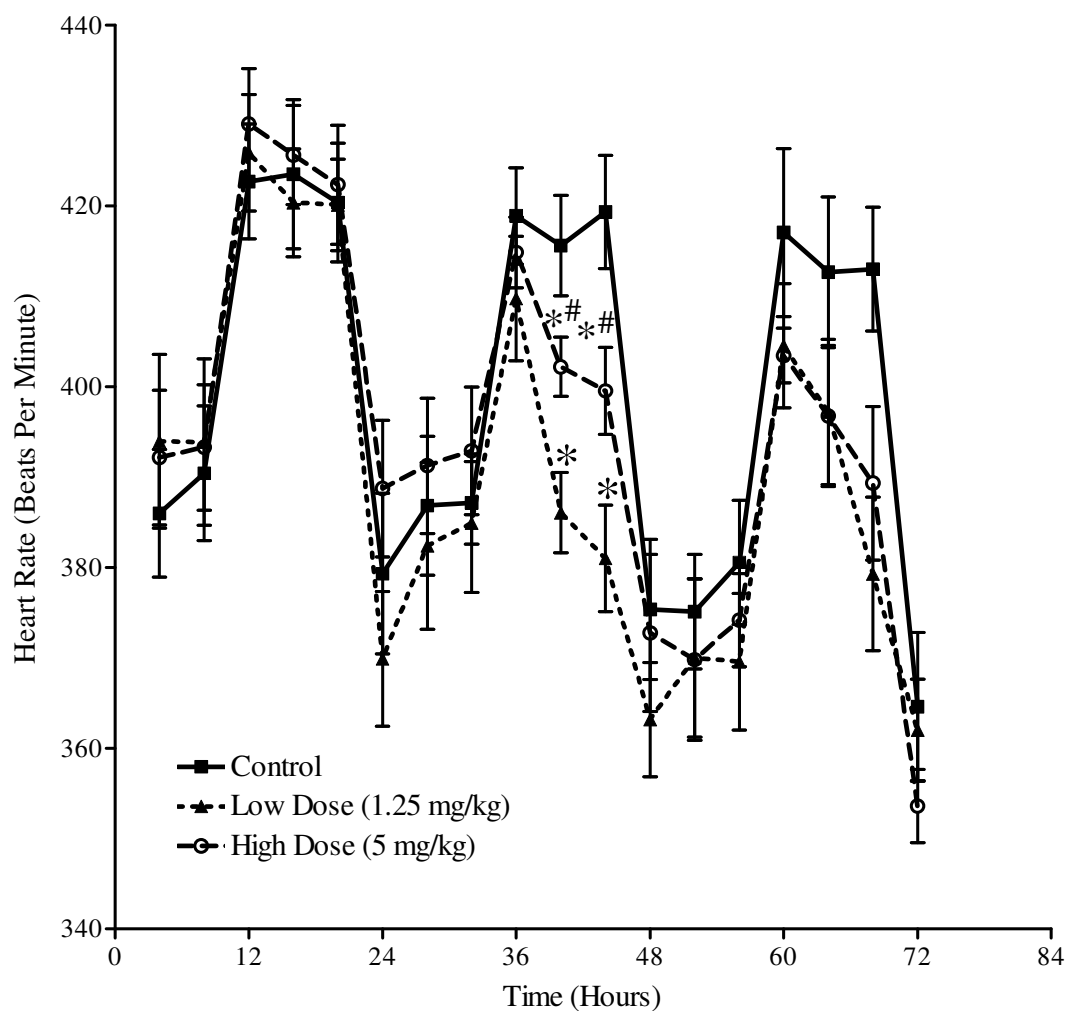
Figure 40: The effects of various doses of *iso*-OMPA on heart rate in adult rats. Rats (n=3-7/dose group) were treated with *iso*-OMPA (sc) at the doses indicated and sacrificed 24 or 96 hours later. This figure shows 24 hour baseline (pre-treatment) data followed by 48 hours post-treatment data. The data (mean ± standard error) represent heart rate averaged over 4 hourly intervals. The low and high doses of *iso*-OMPA produced a decrease in heart rate 16-20 hours post-treatment, with subsequent recovery occuring. The asterisk and pound signs represent values that are significantly different from control, and 1.25 mg/kg dose groups at the same time point, respectively.
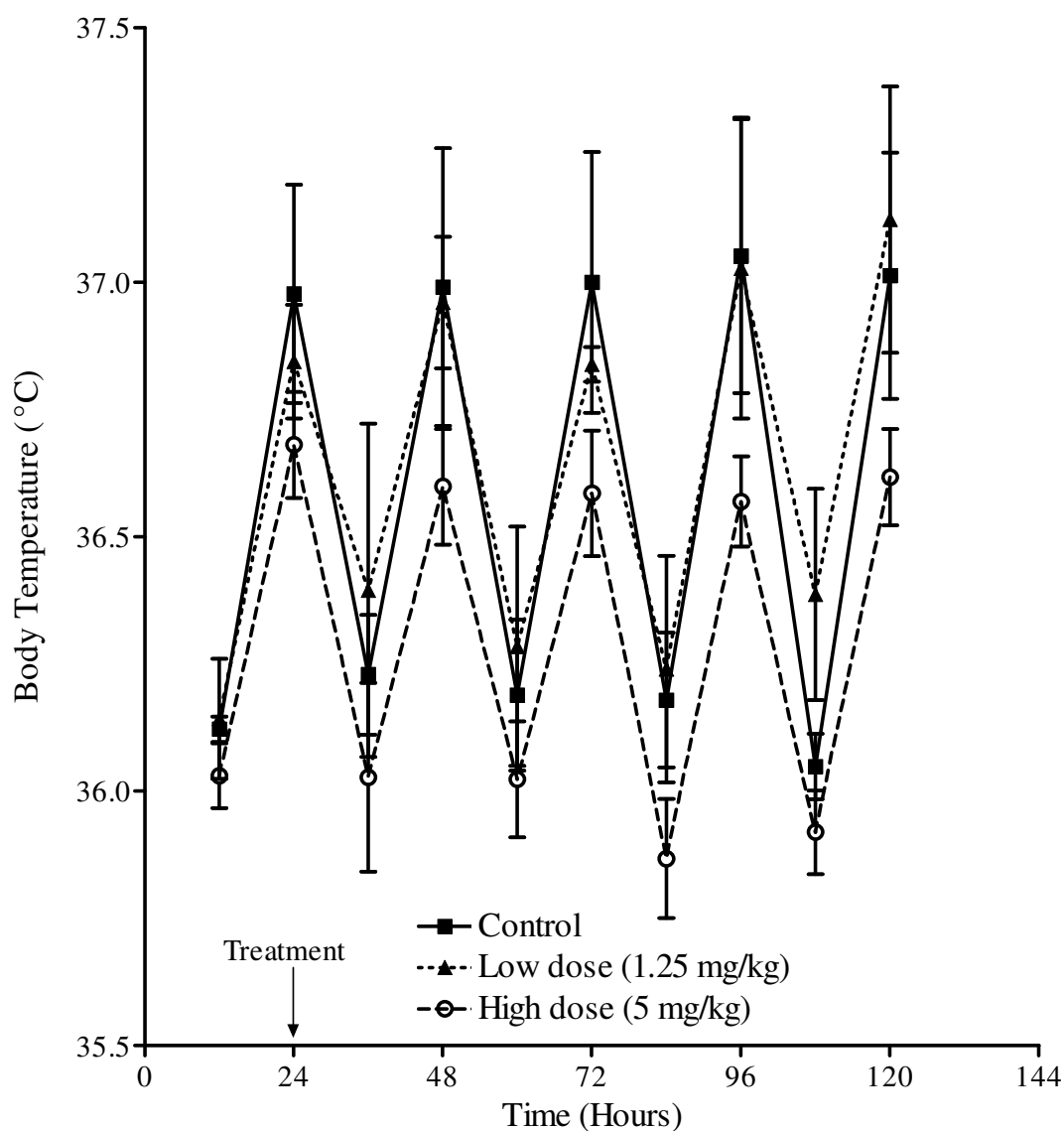
Figure 41: The effects of various doses of *iso*-OMPA on body temperature in adult rats. Rats (n=3-7/dose group) were treated with *iso*-OMPA (sc) at the doses indicated and sacrificed 24 or 96 hours later. This figure shows 24 hour baseline (pre-treatment) data followed by 96 hours post-treatment data. The data (mean ± standard error) represent body temperature averaged over diurnal and nocturnal intervals (8 hours). Body temperature was not significantly affected by *iso*-OMPA.
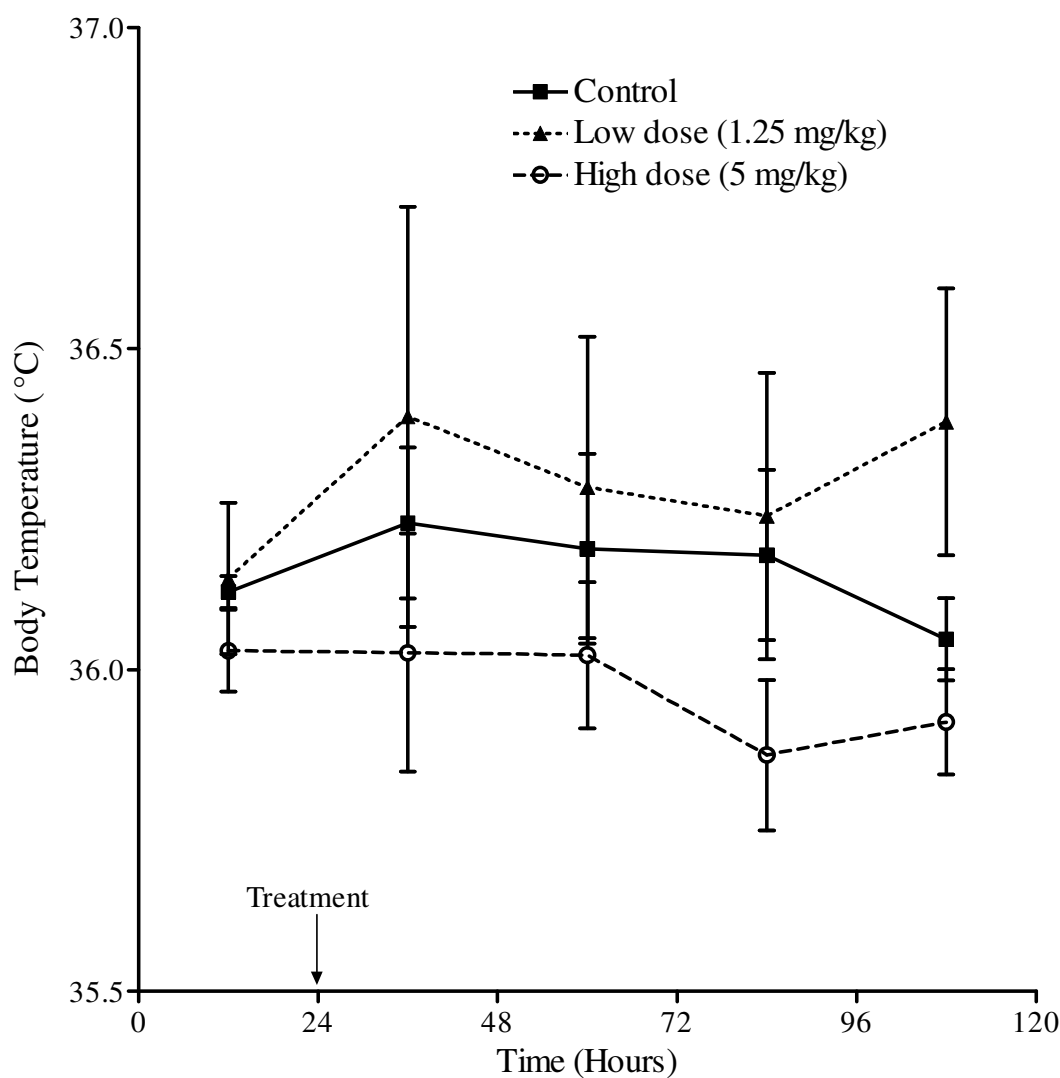
Figure 42: The effects of various doses of *iso*-OMPA on body temperature in adult rats during the diurnal (light) periods. Rats (n=3-7/dose group) were treated with *iso*-OMPA (sc) at the doses indicated and sacrificed 24 or 96 hours later. This figure shows 24 hour baseline (pre-treatment) data followed by 96 hours post-treatment data. The data (mean ± standard error) represents body temperature averaged over 8 hour diurnal intervals. Body temperature was not significantly affected by *iso*-OMPA.
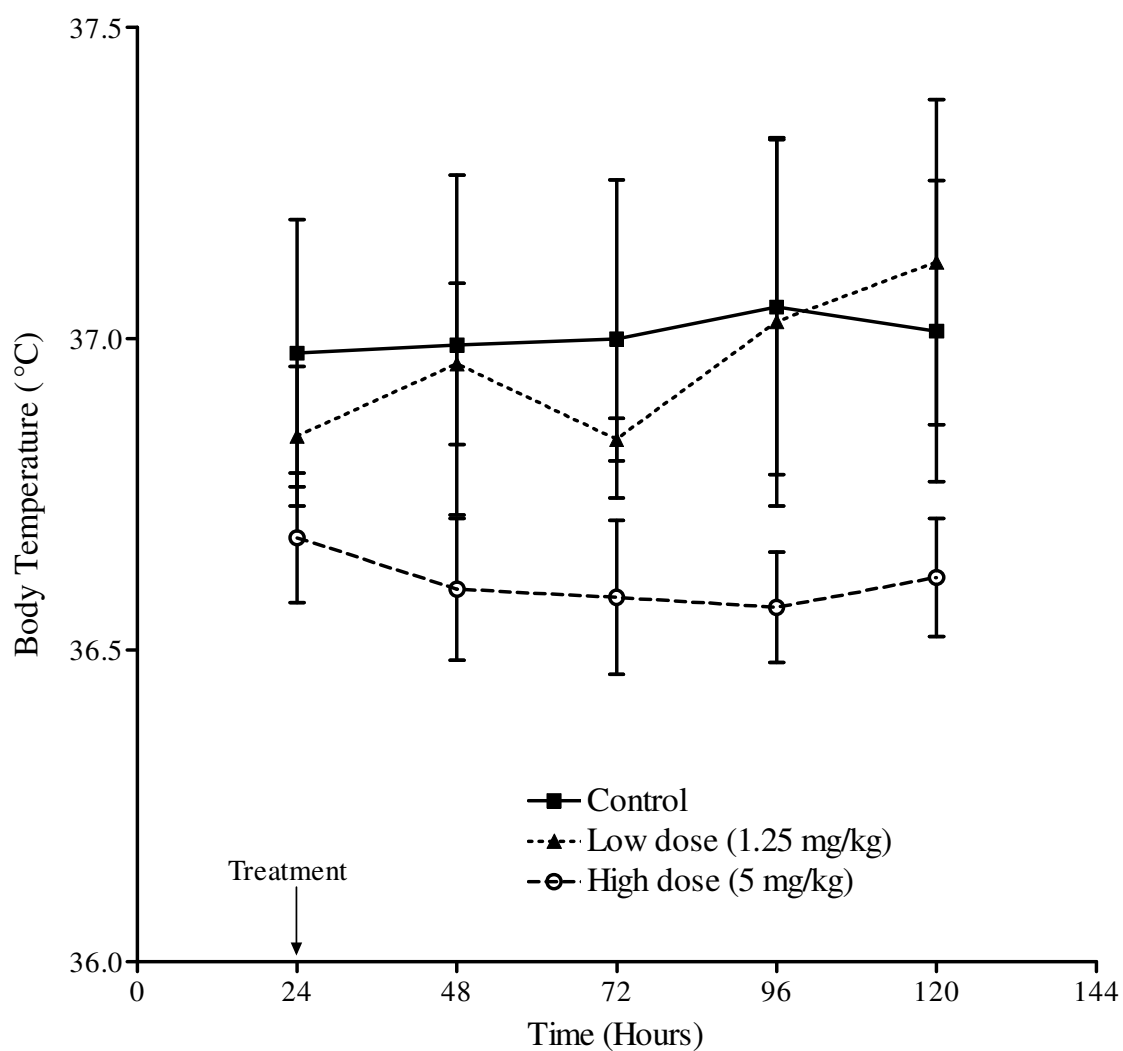
Figure 43: The effects of various doses of *iso*-OMPA on body temperature in adult rats during the nocturnal (dark) periods. Rats (n=3-7/dose group) were treated with *iso*-OMPA (sc) at the doses indicated and sacrificed 24 or 96 hours later. This figure shows 24 hour baseline (pre-treatment) data followed by 96 hours post-treatment data. The data (mean ± standard error) represents body temperature averaged over 8 hour nocturnal intervals. Body temperature was not significantly affected by *iso*-OMPA.
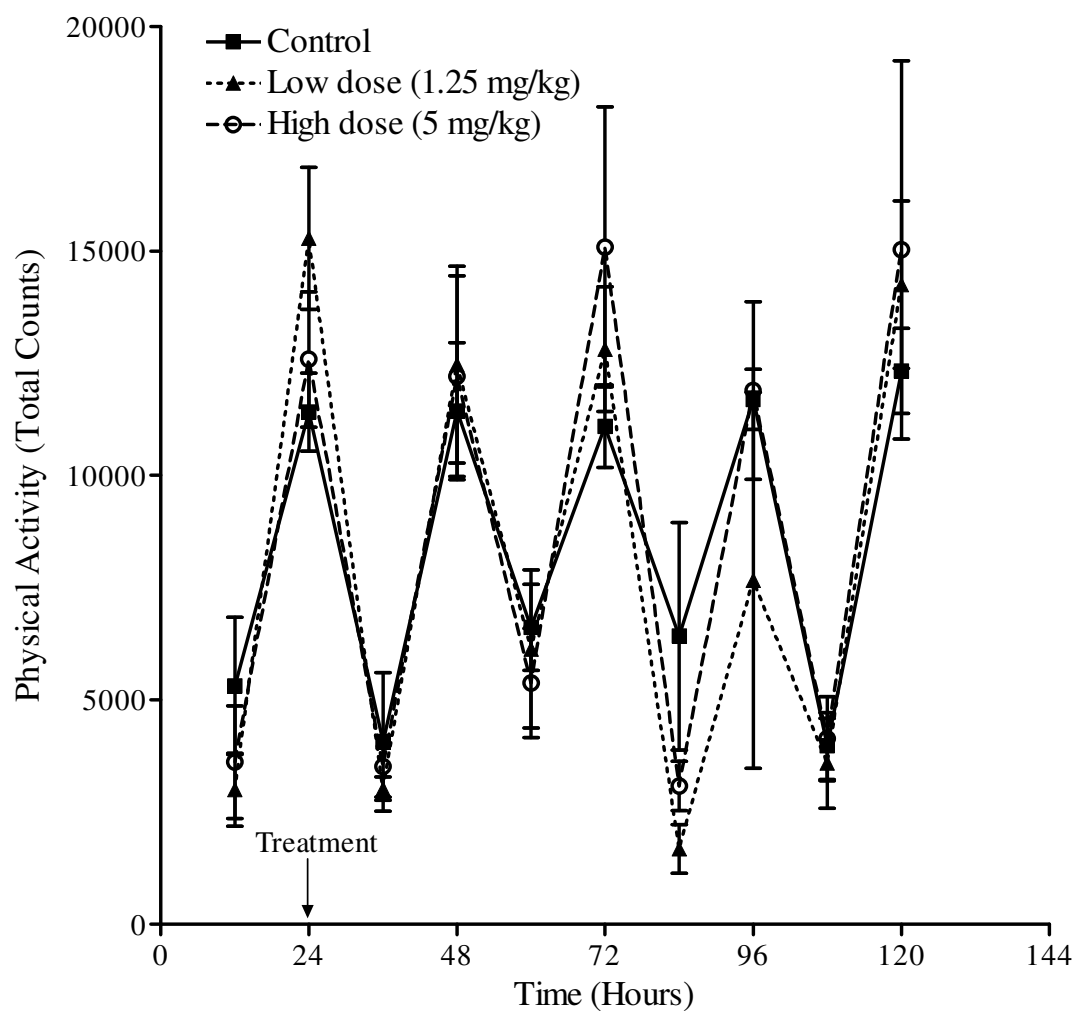
Figure 44: The effects of various doses of *iso*-OMPA on physical activity in adult rats.

Rats (n=3-7/dose group) were treated with *iso*-OMPA (sc) at the doses indicated and

sacrificed 24 or 96 hours later. This figure shows 24 hour baseline (pre-treatment) data

followed by 96 hours post-treatment data. The data (mean ± standard error) represent

physical activity averaged over 8 hour diurnal and nocturnal intervals. Physical activity

was not significantly affected by *iso*-OMPA.
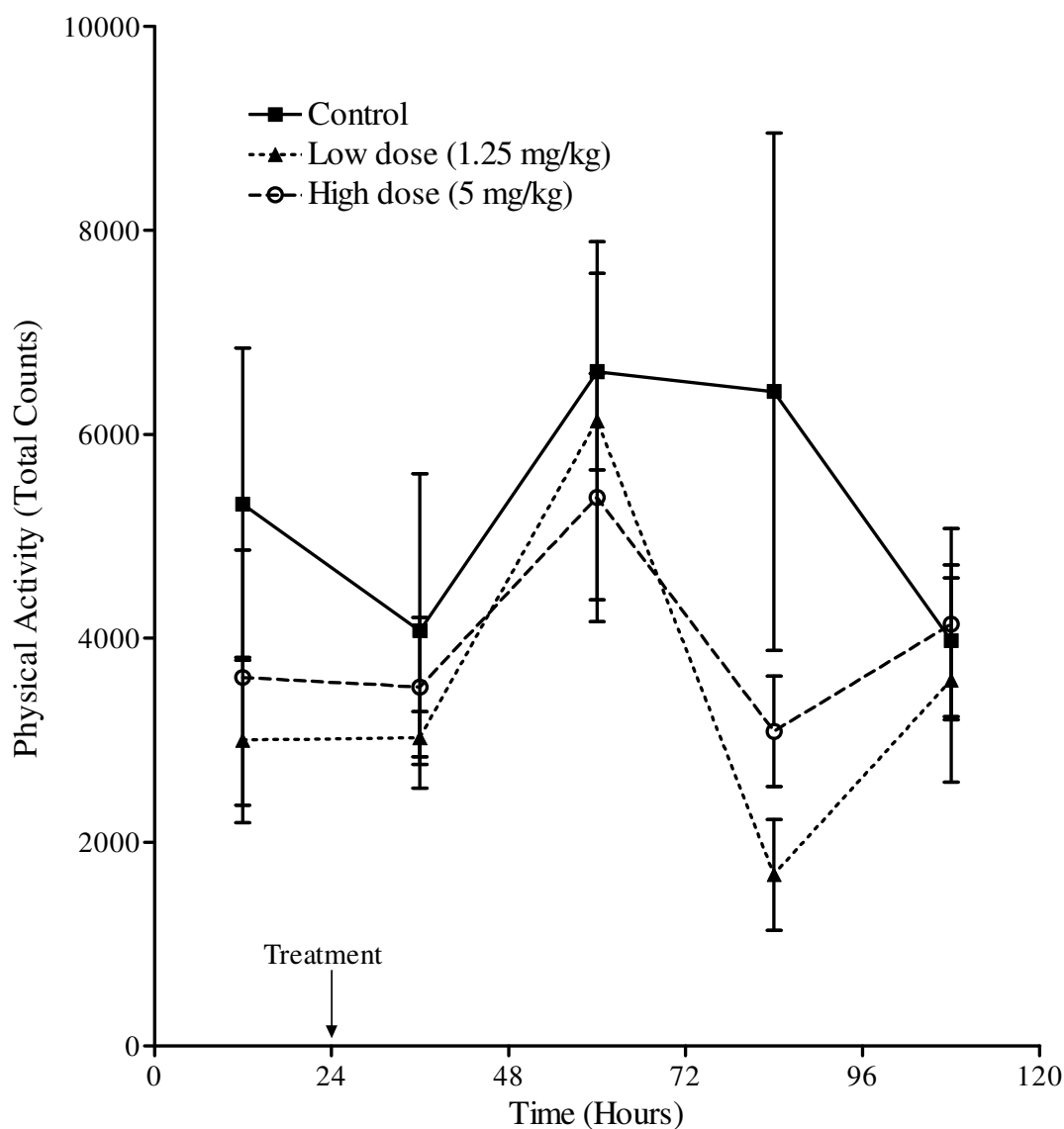
Figure 45: The effects of various doses of *iso*-OMPA on physical activity in adult rats during the diurnal (light) periods. Rats (n=3-7/dose group) were treated with *iso*-OMPA (sc) at the doses indicated and sacrificed 24 or 96 hours later. This figure shows 24 hour baseline (pre-treatment) data followed by 96 hours post-treatment data. The data (mean ± standard error) represents physical activity averaged over 8 hour diurnal intervals. Physical activity was not significantly affected by *iso*-OMPA.
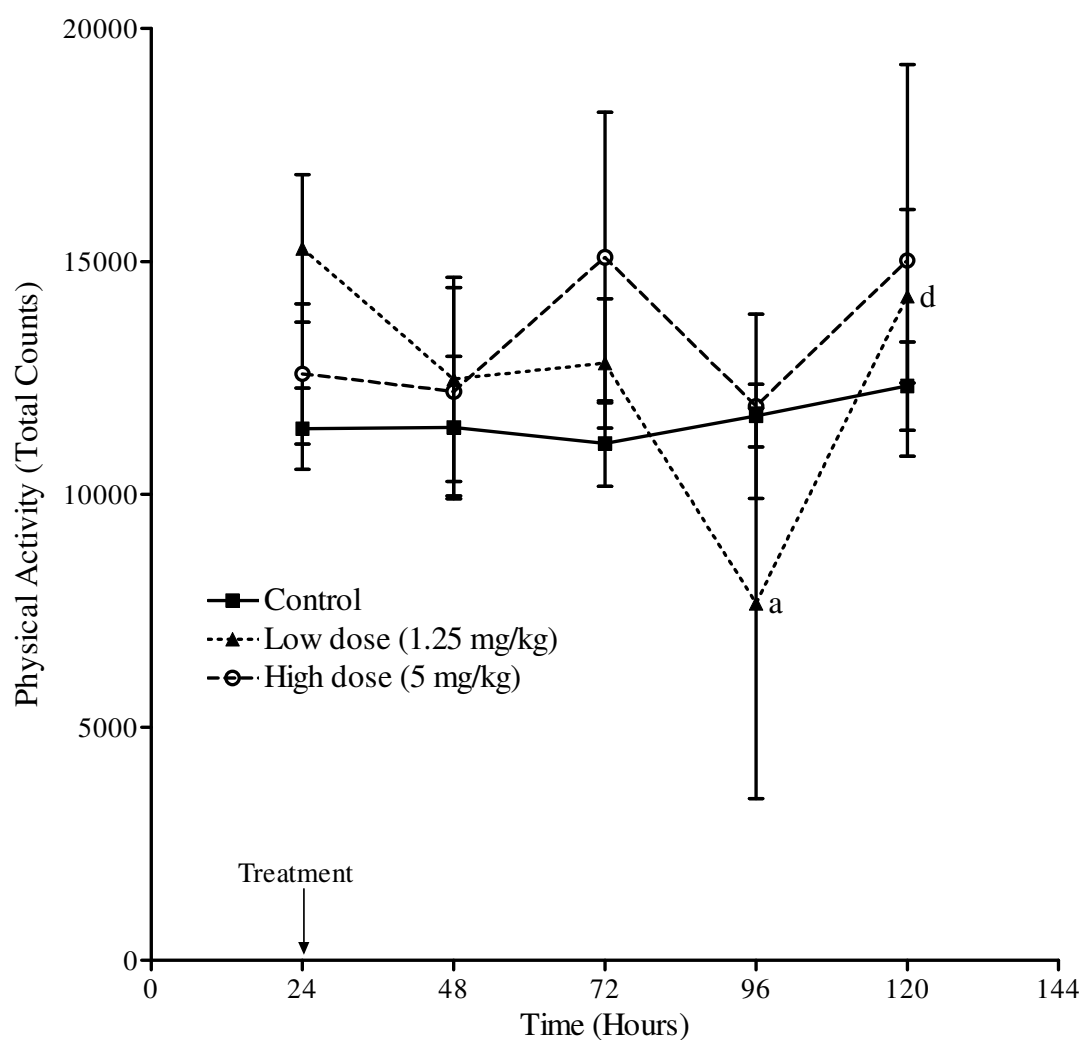
Figure 46: The effects of various doses of *iso*-OMPA on physical activity in adult rats during the nocturnal (dark) periods. Rats (n=3-7/dose group) were treated with *iso*-OMPA (sc) at the doses indicated and sacrificed 24 or 96 hours later. This figure shows 24 hour baseline (pre-treatment) data followed by 96 hours post-treatment data. The data (mean ± standard error) represents physical activity averaged over 8 hour nocturnal intervals. Physical activity was reduced by the low dose of *iso*-OMPA 72 hours post-treatment. a, and d represent values that are significantly different from the same dose at 24 and 96 hours, respectively.

In vitro Inhibition of Butyrylcholinesterase and Displacement of [^{3}H]Oxotremorine Binding by *iso*-OMPA in Adult Heart

The ability of *iso*-OMPA to inhibit BChE and displace [^{3}H]OXO binding *in vitro* was evaluated in adult rat heart. Figure 47 represents the *in vitro* inhibition of BChE and displacement of [^{3}H]OXO binding in cardiac tissue preps from adult rats. In addition to inhibiting BChE, iso-OMPA was found to be capable of displacing [^{3}H]OXO binding in the heart. *Iso*-OMPA was approximately three orders of magnitude more potent at inhibiting BChE (IC$_{50}$: 188 nM) than displacing [^{3}H]OXO binding (IC$_{50}$: 116 µM). This indicates that at low concentrations, *iso*-OMPA inhibits BChE, and as the concentration of *iso*-OMPA increases, it recruits an additional mechanism of action, via direct binding to muscarinic receptors.
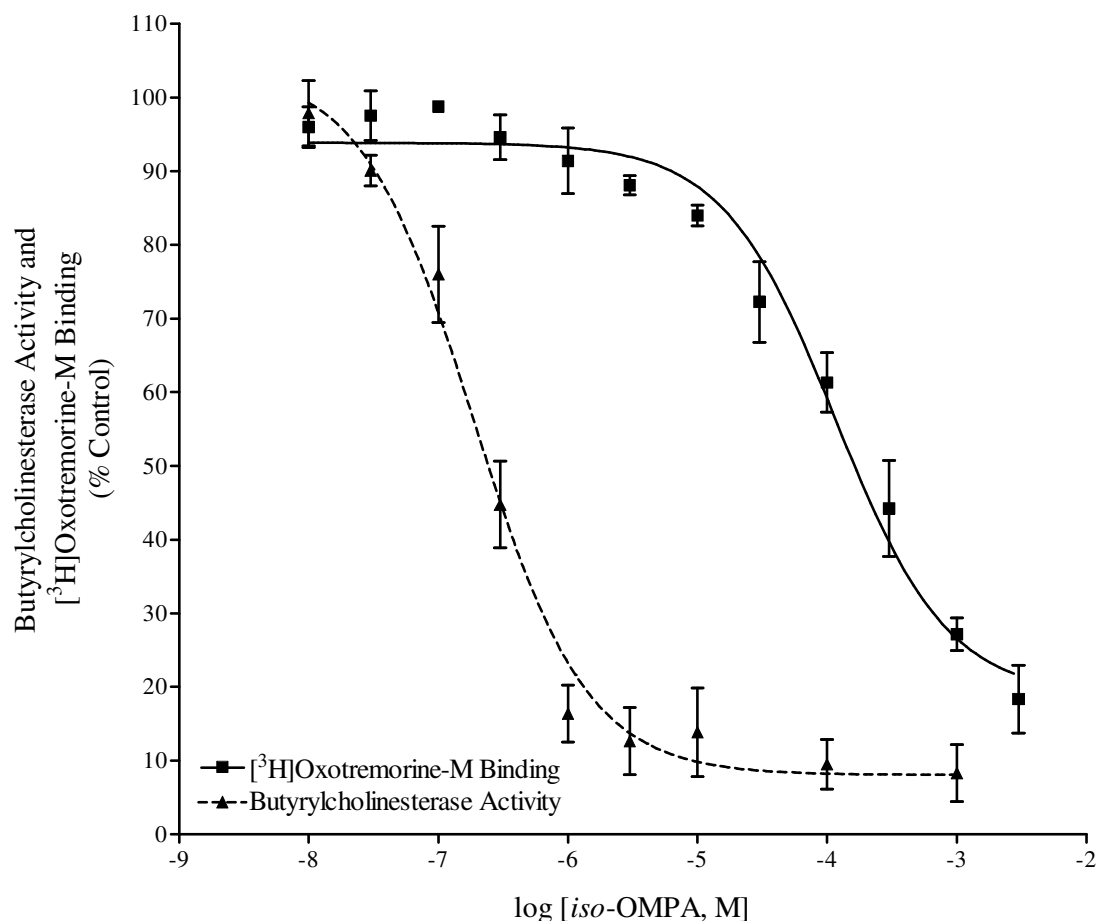
Figure 47: *In vitro* inhibition of butyrylcholinesterase and displacement of [^{3}H]Oxotremorine-M in adult rat heart. For the BChE assay, cardiac tissue homogenates were incubated with *iso*-OMPA at the concentrations noted at 37°C for 15 minutes, prior to measuring the residual ChE activity as described previously. For the [^{3}H]OXO displacement assay, cardiac membranes were incubated at 21°C for 90 minutes in the presence of 1 nM [^{3}H]Oxotremorine-M and *iso*-OMPA at the concentrations noted. Atropine (10 µM) was used in paired tubes to block specific binding, which was calculated as the binding between tubes incubated in the presence and absence of atropine. Data (mean ± standard error) represent BChE activity (triangle with dotted line) or [^{3}H]OXO (square with solid line) in terms of percent of control.

Total Cholinesterase, Acetylcholinesterase, Butyrylcholinesterase and

Carboxylesterase Activities in Atria, Ventricles, Cortex

and Plasma of Adult Rats

The levels of total ChE, AChE, BChE and CarbE in the atria, ventricles, cortex and plasma of adult rats were evaluated using the AChE-specific inhibitor BW284C51, the BChE-specific inhibitor *iso*-OMPA, and the CarbE substrate, *p*-nitrophenyl acetate. Table 5 shows the total ChE, AChE, BChE and CarbE content in the atria, ventricles, cortex and plasma of adult rats.

In agreement with our earlier observations, the total cholinesterase activity in the cortex is comprised of 90% AChE and 10% BChE. The total ChE in the ventricles is made up of ~90% BChE and 10% AChE, while in the atria, 80% BChE and 20% AChE make up the total ChE. Atria contains ~2.5-fold more cholinesterase activity (4 times more AChE activity and 2 times more BChE activity), and 1.5-fold more carboxylesterase activity than the ventricles. Plasma was found to be comprised of ~70% AChE and ~30% BChE. Plasma had the most cholinesterase and carboxylesterase activites, followed by the cortex, atria and ventricles (plasma>cortex>atria>ventricles).

Table 5. Total cholinesterase, acetylcholinesterase, butyrylcholinesterase and carboxylesterase activities in atria, ventricles, cortex and plasma of adult, male Sprague-Dawley rats.

	Total ChE	AChE	BChE	CarbE
Ventricles	8.54 ± 0.45	0.89 ± 0.09	7.83 ± 0.36	68.03 ± 3.7
Atria	19.67 ± 1.08	3.99 ± 0.39	16.92 ± 1.01	90.66 ± 4.02
Cortex	28.45 ± 2.35	26.59 ± 2.39	1.29 ± 0.13	108.36 ± 3.12
Plasma	246.04 ± 11.49	170.76 ± 10.37	79.33 ± 5.65	1806.70 ± 99.18

Atrial, ventricular and cortical tissue homogenates were incubated with 10 µM of *iso*-OMPA or BW at 37°C for 15 minutes, before assessing the residual ChE activity, to obtain AChE and BChE activities, respectively. For total ChE activity, the tissue homogenates were pre-incubated in buffer (no inhibitor), prior to performing the assay. Carboxylesterase activity was assessed following incubation of the tissue homogenates at 37°C in the presence of the substrate p-nitrophenyl acetate. Data (mean ± standard error) represent enzyme activities in terms of nmol of substrate hydrolyzed/mg protein/minute or nmol of substrate hydrolyzed/ml plasma/minute.

Effects of *iso*-OMPA on Acetylcholinesterase, Butyrylcholinesterase, Carboxylesterase and Muscarinic Receptor Binding in Ventricles, Atria, Cortex and Plasma 24 and 96 Hours Post-Treatment

The effects of *iso*-OMPA on AChE, BChE, CarbE and muscarinic receptor binding were evaluated at 24 and 96 hours post-treatment. In addition to the atria, ventricles and cortex, which were assessed during the dose-determination studies, plasma was also included in this study, since it has been found to contain significant amounts of BChE and CarbE, both of which are inhibited by *iso*-OMPA.

Iso-OMPA produced a dose-dependent inhibition of BChE (Figures 48, 52, 56 and 59) and CarbE (Figures 50, 54, 58 and 61) in all of the tissues investigated. *Iso*-OMPA inhibited ~60% (low dose) to 80% (high dose) BChE activity in the atria, ventricles and plasma at the 24 hour time point, with enzyme recovery occurring by the 96 hour time point. In the cortex, only the high dose produced a significant inhibition of BChE at the 24 hour time point, with enzyme recovery occuring by the 96 hour time point. The amount of CarbE inhibited by *iso*-OMPA at the 24 hour time point ranged from ~10% (atria and ventricles) to 30% (plasma) for the low dose, and 10% (cortex) to ~40% (atria, ventricles and plasma) for the high dose. The amount of CarbE inhibited remained approximately the same by 96 hours post-treatment for all tissues, except the ventricles, wherein the high dose of *iso*-OMPA caused further inhibition of CarbE.

Neither of the two doses of *iso*-OMPA used in the study produced any inhibition of AChE (Figures 49, 53, 57 and 60) at the 24 and 96 hour time points, thereby confirming their selectivity for BChE. However, in the atria, the high dose of iso-OMPA had significantly higher levels of AChE at the 24 hour time point. Similarly, the low dose

119

of *iso*-OMPA also had elevated levels of AChE in the cortex at the 24 and 96 hour time points.

Muscarinic receptor binding (Figures 51 and 55) was evaluated by using the agonist [^{3}H]Oxotremorine-M. Muscarinic receptors were significantly downregulated (~25%) by the high dose of *iso*-OMPA in the ventricles at 24 hours, with recovery occurring by 96 hours post-treatment. Approximately 20% downregulation of muscarinic receptors occurred in the low and high dose groups of *iso*-OMPA in the atria at 24 hours post-treatment, which persisted until 96 hours.
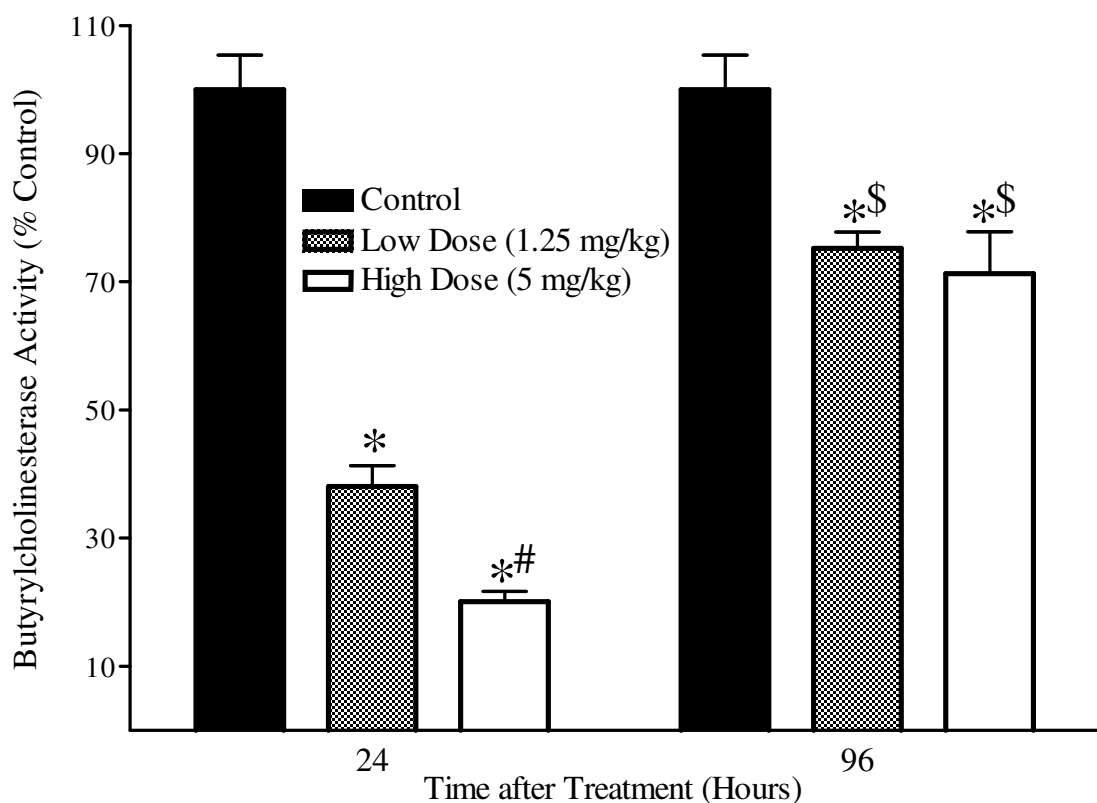
Figure 48: The effects of *iso*-OMPA on butyrylcholinesterase activity in ventricular tissue homogenates. Rats (n=3-7/dose group) were treated with *iso*-OMPA (sc) at the doses indicated and sacrificed 24 or 96 hours later. Ventricular tissue homogenates were pre-incubated with 10 µM BW284C51 at 37°C for 15 minutes prior to measuring the residual ChE activity as described previously. *Iso*-OMPA produced a dose-dependent inhibition of BChE activity in the ventricles at 24 hours with apparent enzyme recovery occurring by 96 hours post-treatment. Data (mean ± standard error) represent BChE activity in terms of percent of control. The asterisks and pound represent values that are significantly different from control and 1.25 mg/kg dose groups at the same time point, respectively, while the dollar sign represents values that are significantly different from the same dose at the 24 hour time point.
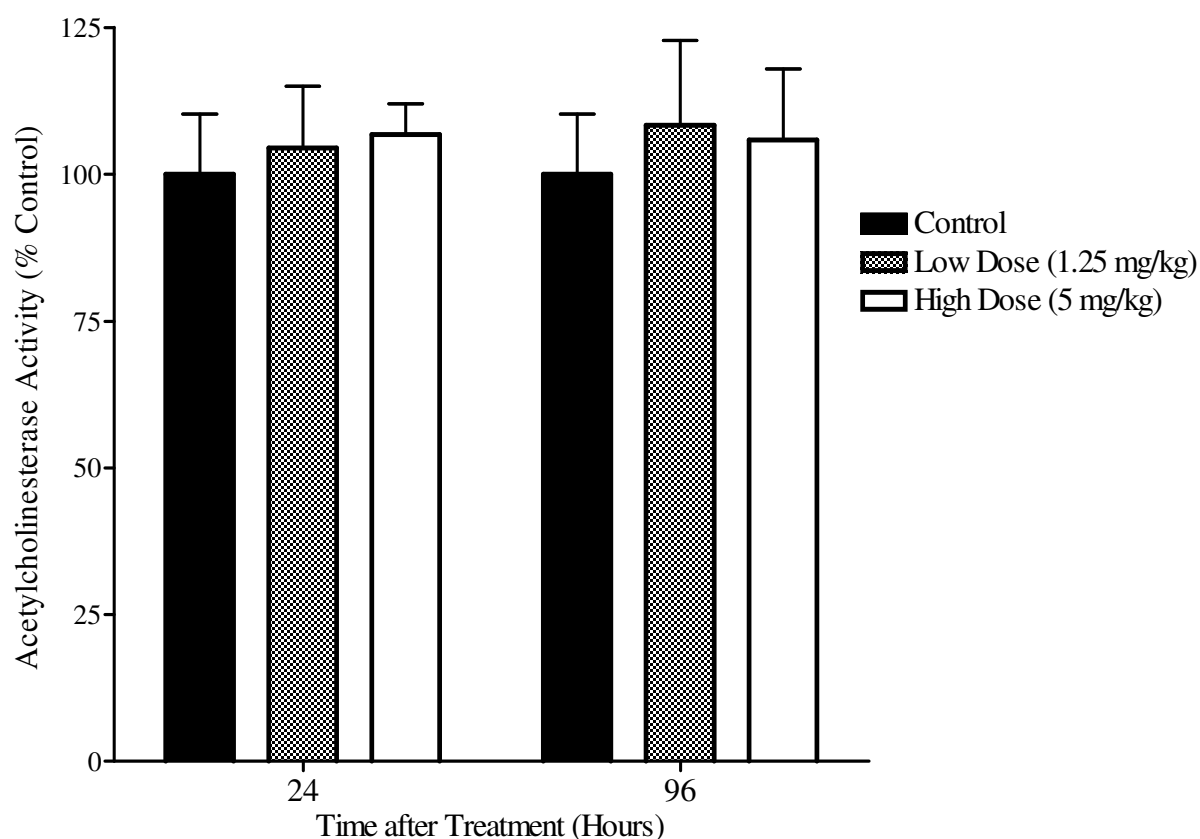
Figure 49: The effects of *iso*-OMPA on acetylcholinesterase activity in ventricular tissue homogenates. Rats (n=3-7/dose group) were treated with *iso*-OMPA (sc) at the doses indicated and sacrificed 24 or 96 hours later. Ventricular tissue homogenates were pre-incubated with 10 µM *iso*-OMPA at 37°C for 15 minutes prior to measuring the residual ChE activity as described previously. *Iso*-OMPA did not inhibit AChE at any of the doses at the 24 or 96 hour time point. Data (mean ± standard error) represent AChE activity in terms of percent of control.
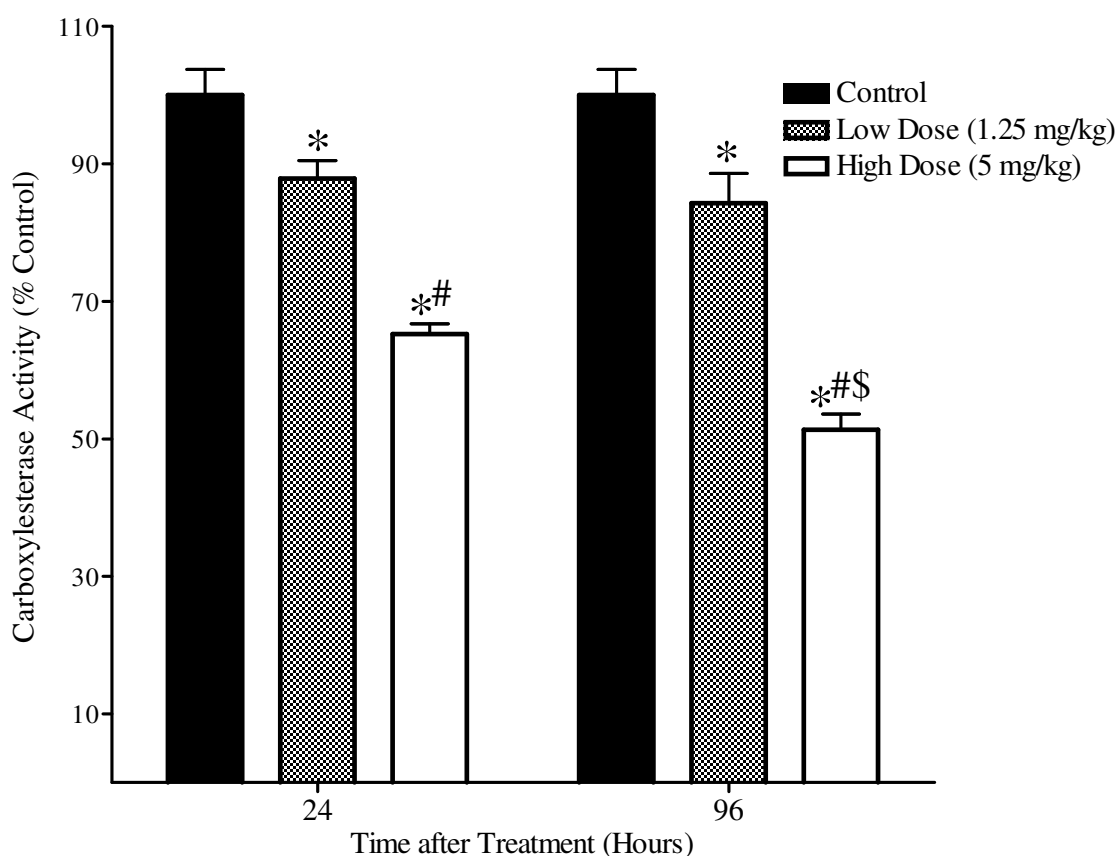
Figure 50: The effects of *iso*-OMPA on carboxylesterase activity in ventricular tissue homogenates. Rats (n=3-7/dose group) were treated with *iso*-OMPA (sc) at the doses indicated and sacrificed 24 or 96 hours later. Ventricular tissue homogenates were incubated at 37°C in the presence of the substrate p-nitrophenyl acetate to assess CarbE activity. *Iso*-OMPA produced a dose-related inhibition of CarbE activity in the ventricles at the 24 and 96 hour time points, with further enzyme inhibition occurring in the high dose group at the 96 hour time point. Data (mean ± standard error) represent CarbE activity in terms of percent of control. The asterisk and pound signs represent values that are significantly different from control and 1.25 mg/kg dose groups at the same time point, respectively, while the dollar sign represents values that are significantly different from the same dose at the 24 hour time point.
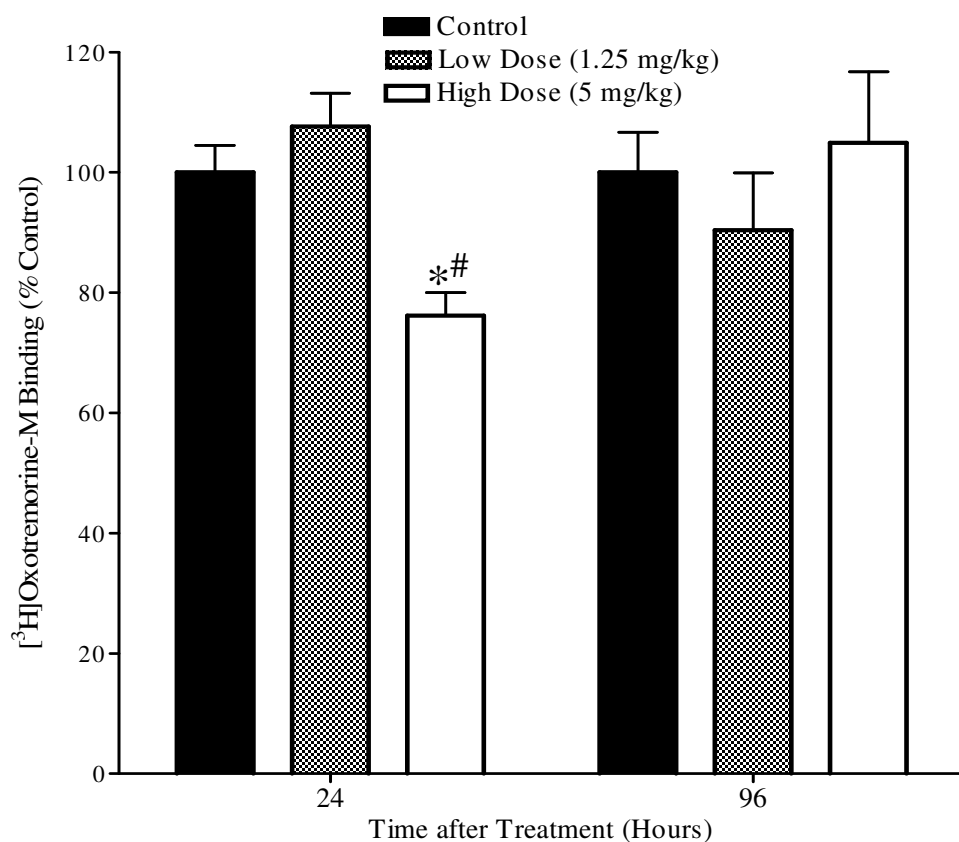
Figure 51: The effects of *iso*-OMPA on muscarinic receptor binding in ventricular membranes. Rats (n=3-7/dose group) were treated with *iso*-OMPA (sc) at the doses indicated and sacrificed 24 or 96 hours later. Membranes were incubated at 21°C for 90 minutes in the presence of 1 nM [³H]Oxotremorine-M, with or without 10 μM atropine (to determine specific binding). Data (mean ± standard error) represent specific binding in terms of percent of control. *Iso*-OMPA produced a downregulation of muscarinic receptors in the high dose-group at 24 hours post-treatment, with apparent recovery to control values by 96 hours. Data (mean ± standard error) represent [³H]OXO binding in terms of percent of control. The asterisk and pound signs represent values that are significantly different from control and 1.25 mg/kg dose groups at the same time point, respectively.
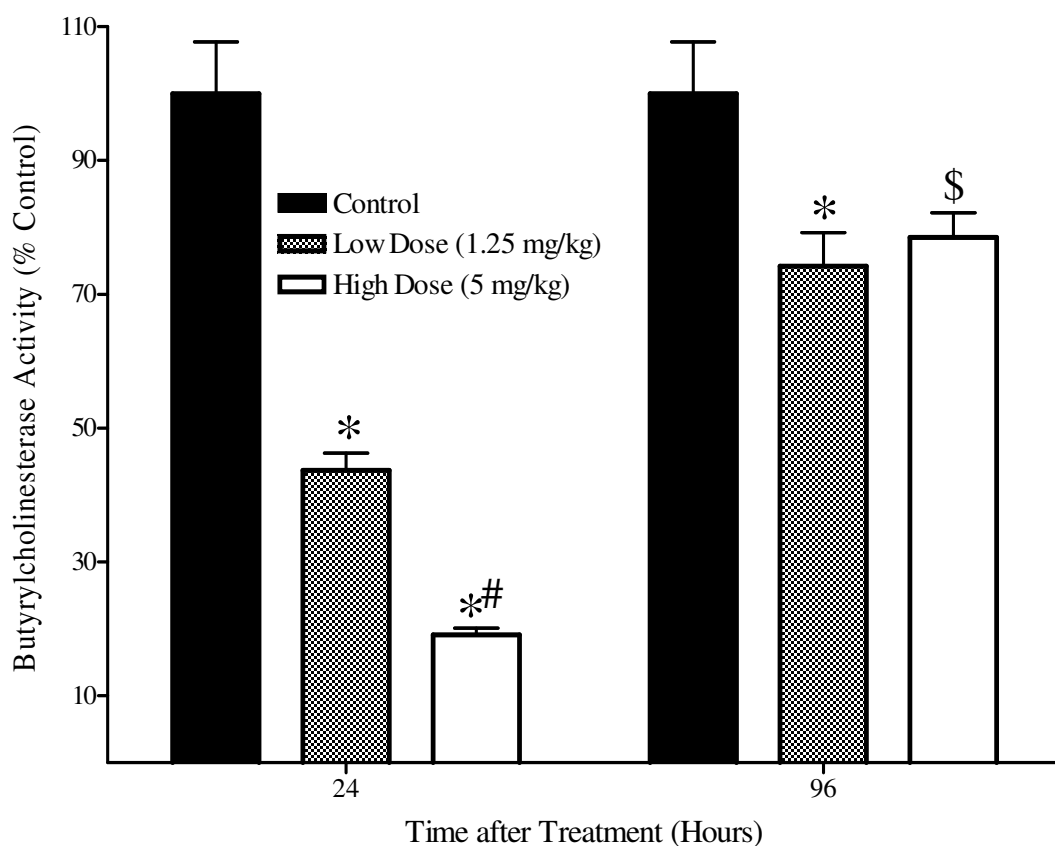
Figure 52: The effects of *iso*-OMPA on butyrylcholinesterase activity in atrial tissue homogenates. Rats (n=3-7/dose group) were treated with *iso*-OMPA (sc) at the doses indicated and sacrificed 24 or 96 hours later. Atrial tissue homogenates were pre-incubated with 10 μM BW284C51 at 37°C for 15 minutes prior to measuring the residual ChE activity as described previously. *Iso*-OMPA produced a dose-dependent inhibition of BChE activity in the atria at 24 hours with apparent enzyme recovery occurring by 96 hours post-treatment. Data (mean ± standard error) represent BChE activity in terms of percent of control. The asterisk and pound signs represent values that are significantly different from control and 1.25 mg/kg dose groups at the same time point, respectively, while the dollar sign represents values that are significantly different from the same dose at the 24 hour time point.
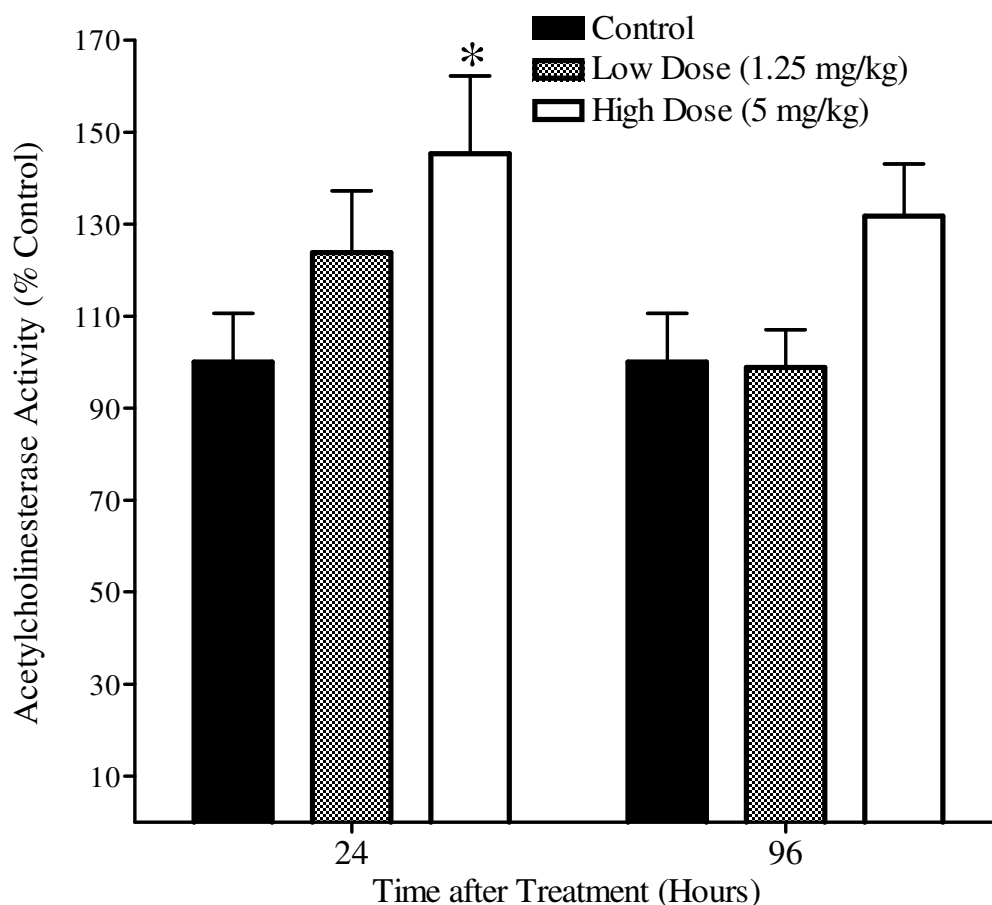
Figure 53: The effects of *iso*-OMPA on acetylcholinesterase activity in atrial tissue homogenates. Rats (n=3-7/dose group) were treated with *iso*-OMPA (sc) at the doses indicated and sacrificed 24 or 96 hours later. Atrial tissue homogenates were pre-incubated with 10 µM *iso*-OMPA at 37°C for 15 minutes prior to measuring the residual ChE activity as described previously. *Iso*-OMPA did not inhibit AChE at any of the doses at the 24 or 96 hour time point. In fact, the AChE activity in the high dose group was found to be significantly higher than the control at the 24 hour time point. Data (mean ± standard error) represent AChE activity in terms of percent of control. Asterisks represent values that are significantly different from control at the same time point.
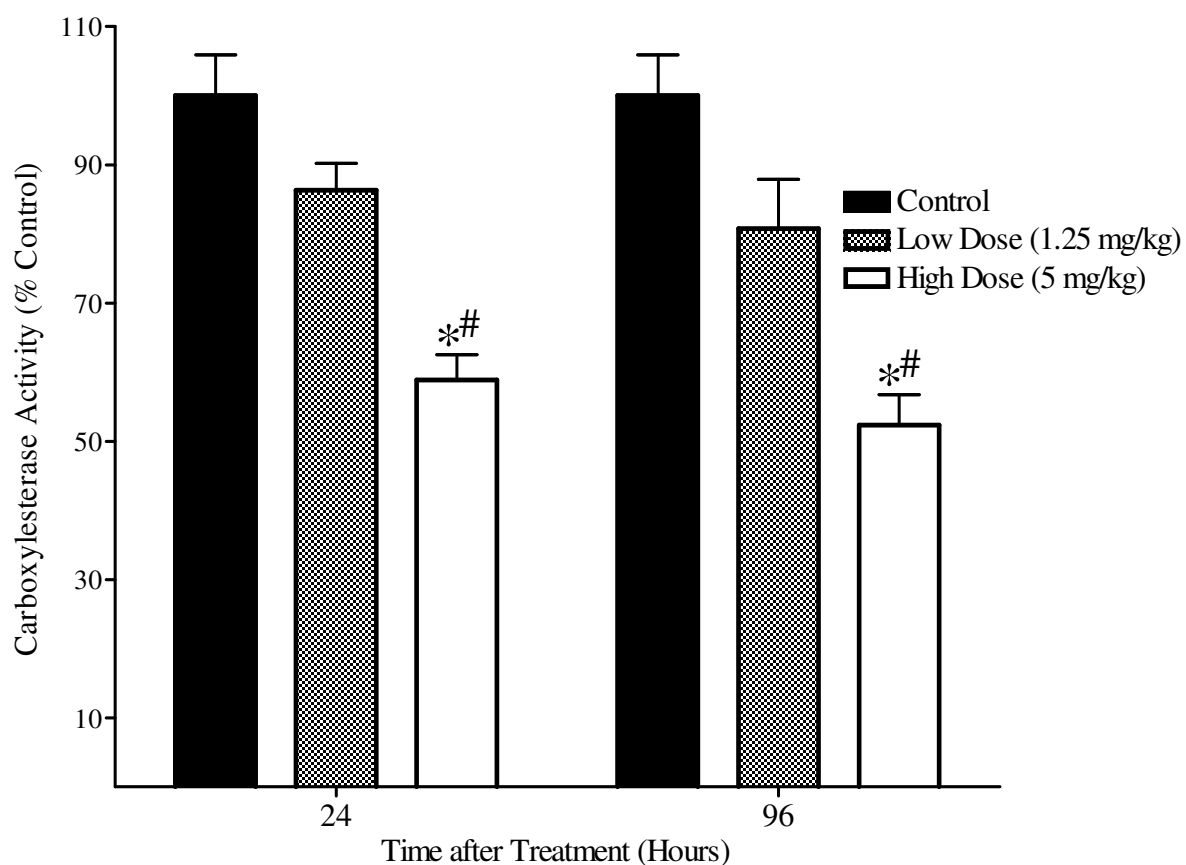
Figure 54: The effects of *iso*-OMPA on carboxylesterase activity in atrial tissue homogenates. Rats (n=3-7/dose group) were treated with *iso*-OMPA (sc) at the doses indicated and sacrificed 24 or 96 hours later. Atrial tissue homogenates were incubated at 37°C in the presence of the substrate p-nitrophenyl acetate to assess CarbE activity. *Iso*-OMPA produced a dose-dependent inhibition of CarbE activity in the ventricles at the 24 and 96 hour time points, with relatively similar amounts of enzyme being inhibited at the 2 time points. Data (mean ± standard error) represent CarbE activity in terms of percent of control. The asterisk and pound signs represent values that are significantly different from control and 1.25 mg/kg dose groups at the same time point.

Figure 55: The effects of *iso*-OMPA on muscarinic receptor binding in atrial membranes. Rats (n=3-7/dose group) were treated with *iso*-OMPA (sc) at the doses indicated and sacrificed 24 or 96 hours later. Membranes were incubated at 21°C for 90 minutes in the presence of 1 nM [³H]Oxotremorine-M, with or without 10 µM atropine (to determine specific binding). Data (mean ± standard error) represent specific binding in terms of percent of control. *Iso*-OMPA produced a downregulation of muscarinic receptors in the low and high dose-group at both, the 24 and 96 hour time points. Data (mean ± standard error) represent [³H]OXO binding in terms of percent of control. Asterisks represent values that are significantly different from control at the same time point.
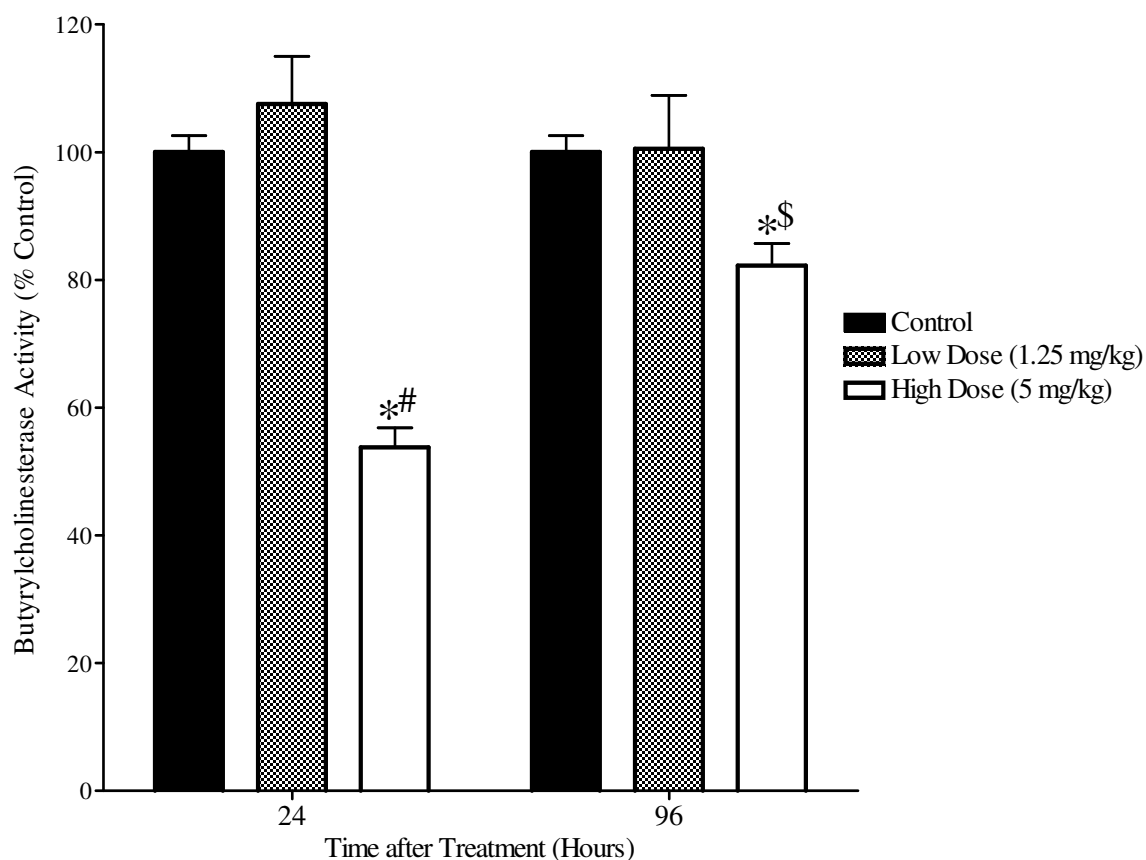
Figure 56: The effects of *iso*-OMPA on butyrylcholinesterase activity in cortical tissue homogenates. Rats (n=3-7/dose group) were treated with *iso*-OMPA (sc) at the doses indicated and sacrificed 24 or 96 hours later. Cortical tissue homogenates were pre-incubated with 10 μM BW284C51 at 37°C for 15 minutes prior to measuring the residual ChE activity as described previously. *Iso*-OMPA produced a significant inhibition of BChE activity in the cortex at 24 and 96 hours, with apparent enzyme recovery occurring by 96 hours post-treatment. Data (mean ± standard error) represent BChE activity in terms of percent of control. The asterisk and pound signs represent values that are significantly different from control and 1.25 mg/kg dose groups at the same time point, respectively, while the dollar sign represents values that are significantly different from the same dose at the 24 hour time point.
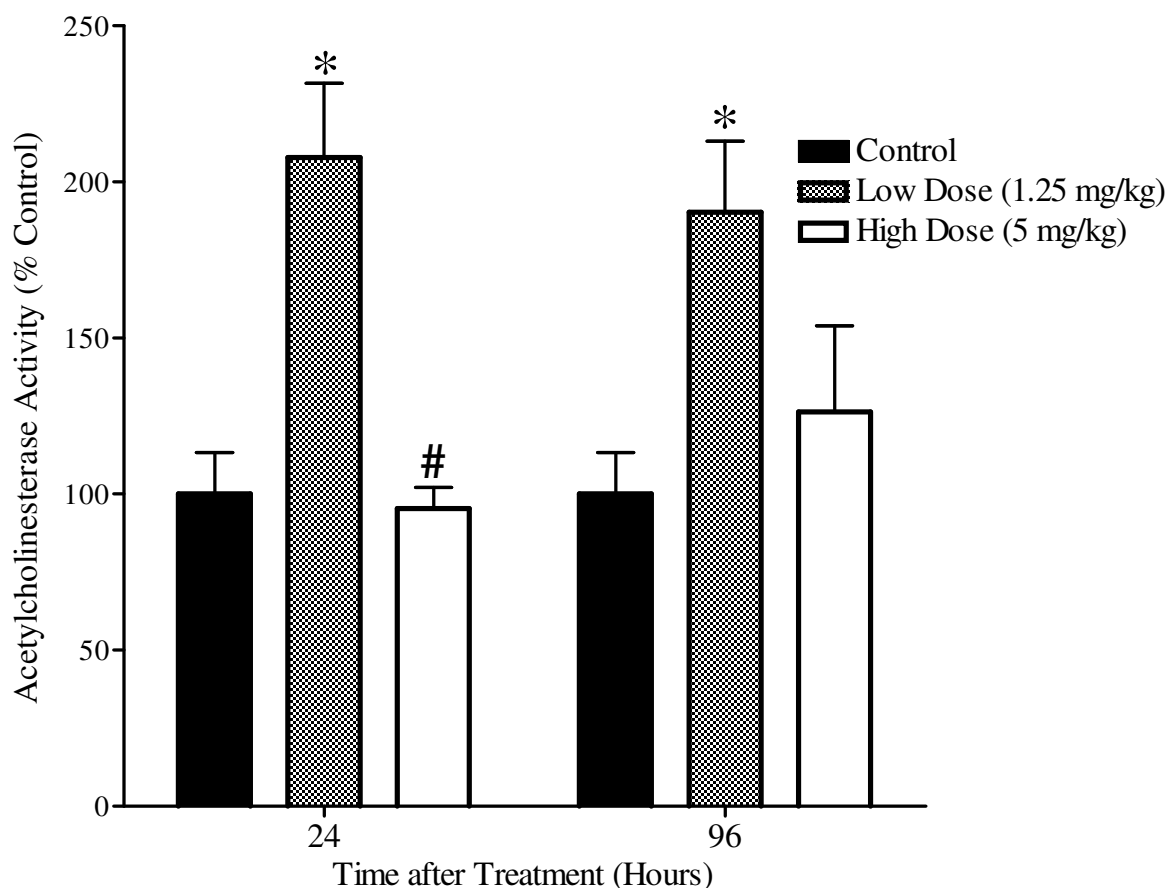
Figure 57: The effects of *iso*-OMPA on acetylcholinesterase activity in cortical tissue homogenates. Rats (n=3-7/dose group) were treated with *iso*-OMPA (sc) at the doses indicated and sacrificed 24 or 96 hours later. Cortical tissue homogenates were pre-incubated with 10 µM *iso*-OMPA at 37°C for 15 minutes prior to measuring the residual ChE activity as described previously. *Iso*-OMPA did not inhibit AChE at any of the doses at the 24 or 96 hour time point. However, the AChE activity in the low dose group was found to be significantly higher than the control at the 24 and 96 hour time points. Data (mean ± standard error) represent AChE activity in terms of percent of control. The asterisk and pound signs represent values that are significantly different from control and 1.25 mg/kg dose groups at the same time point.
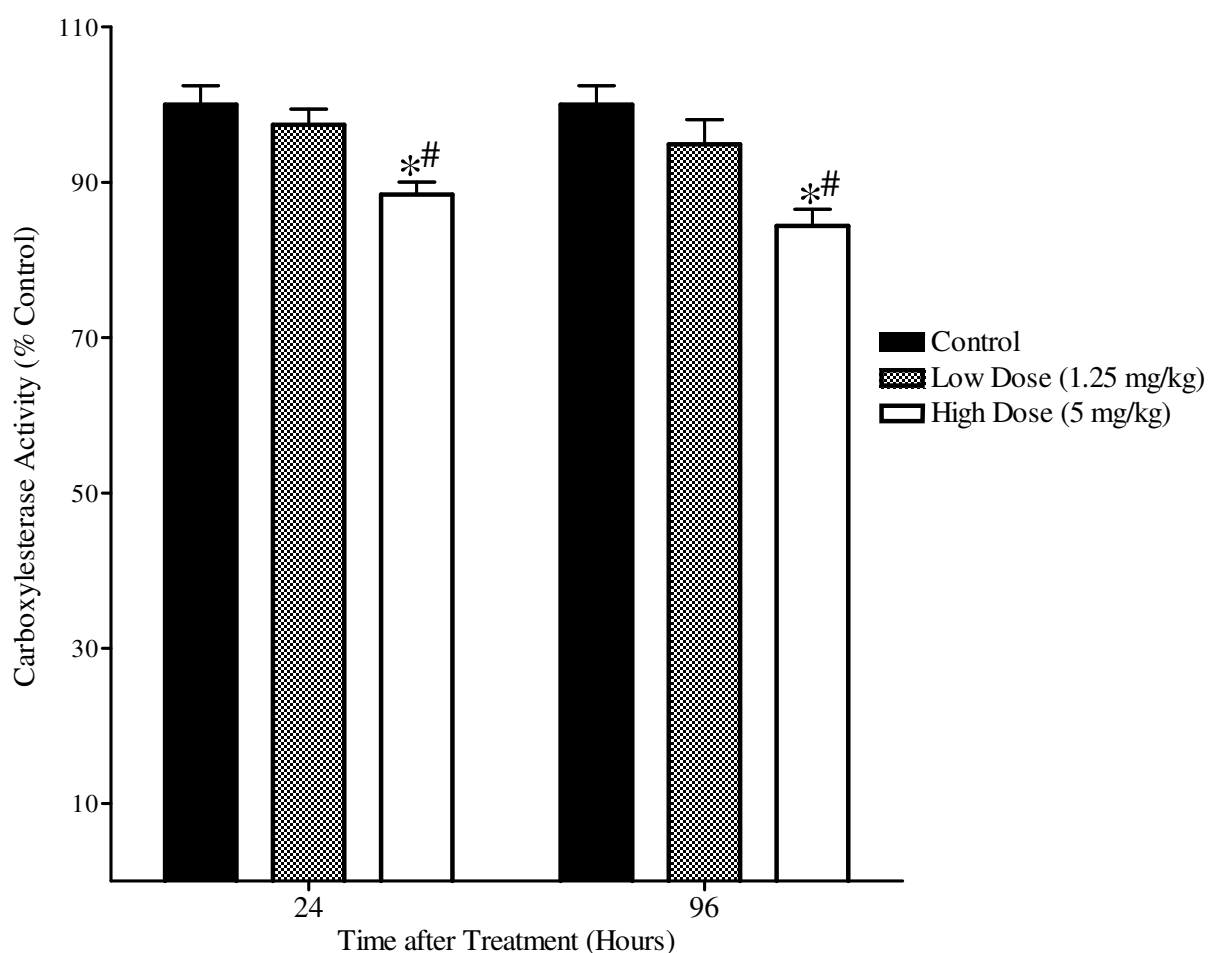
Figure 58: The effects of *iso*-OMPA on carboxylesterase activity in cortical tissue homogenates. Rats (n=3-7/dose group) were treated with *iso*-OMPA (sc) at the doses indicated and sacrificed 24 or 96 hours later. Cortical tissue homogenates were incubated at 37°C in the presence of the substrate p-nitrophenyl acetate to assess CarbE activity. *Iso*-OMPA significantly inhibited CarbE activity in the high dose group at the 24 and 96 hour time points, with relatively similar amounts of enzyme being inhibited at the 2 time points. Data (mean ± standard error) represent CarbE activity in terms of percent of control. The asterisk and pound signs represent values that are significantly different from control and 1.25 mg/kg dose groups at the same time point.
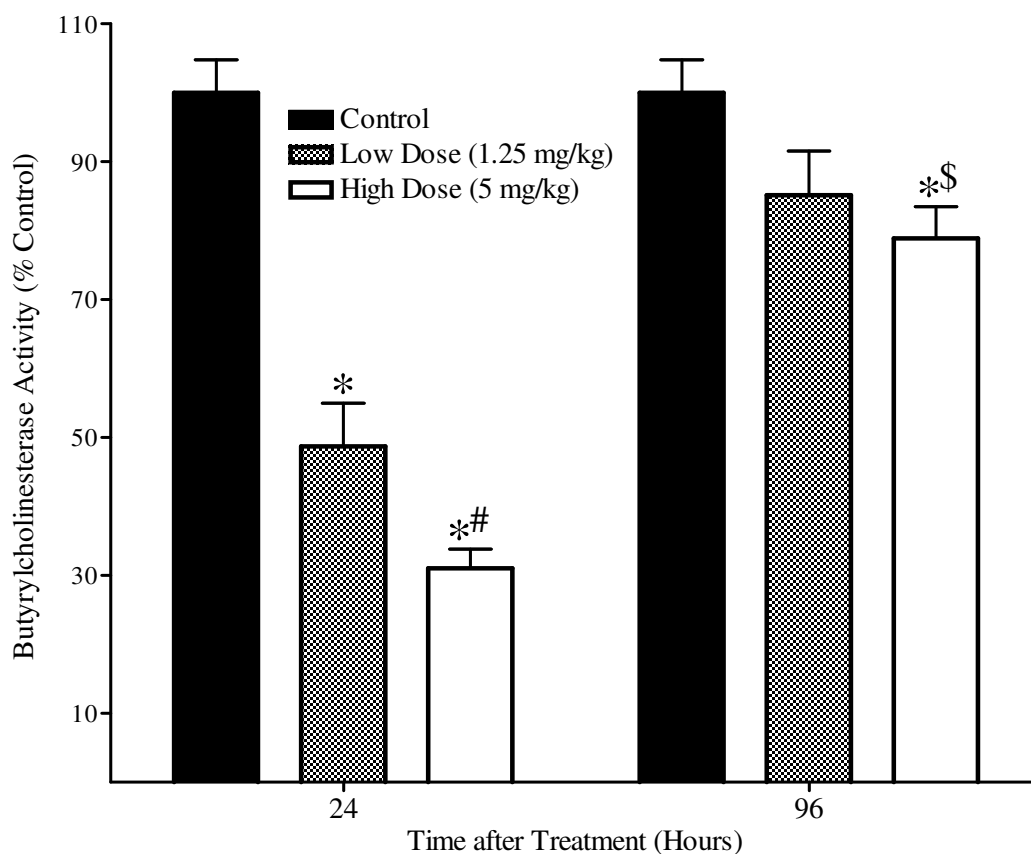
Figure 59: The effects of *iso*-OMPA on butyrylcholinesterase activity in plasma. Rats (n=3-7/dose group) were treated with *iso*-OMPA (sc) at the doses indicated and sacrificed 24 or 96 hours later. Diluted plasma samples were pre-incubated with 10 μM BW284C51 at 37°C for 15 minutes prior to measuring the residual ChE activity as described previously. *Iso*-OMPA produced a significant inhibition of BChE activity in the plasma at 24 hours, with apparent enzyme recovery occurring by 96 hours post-treatment. Data (mean ± standard error) represent BChE activity in terms of percent of control. The asterisk and pound signs represent values that are significantly different from control and 1.25 mg/kg dose groups at the same time point, respectively, while the dollar sign represents values that are significantly different from the same dose at the 24 hour time point.
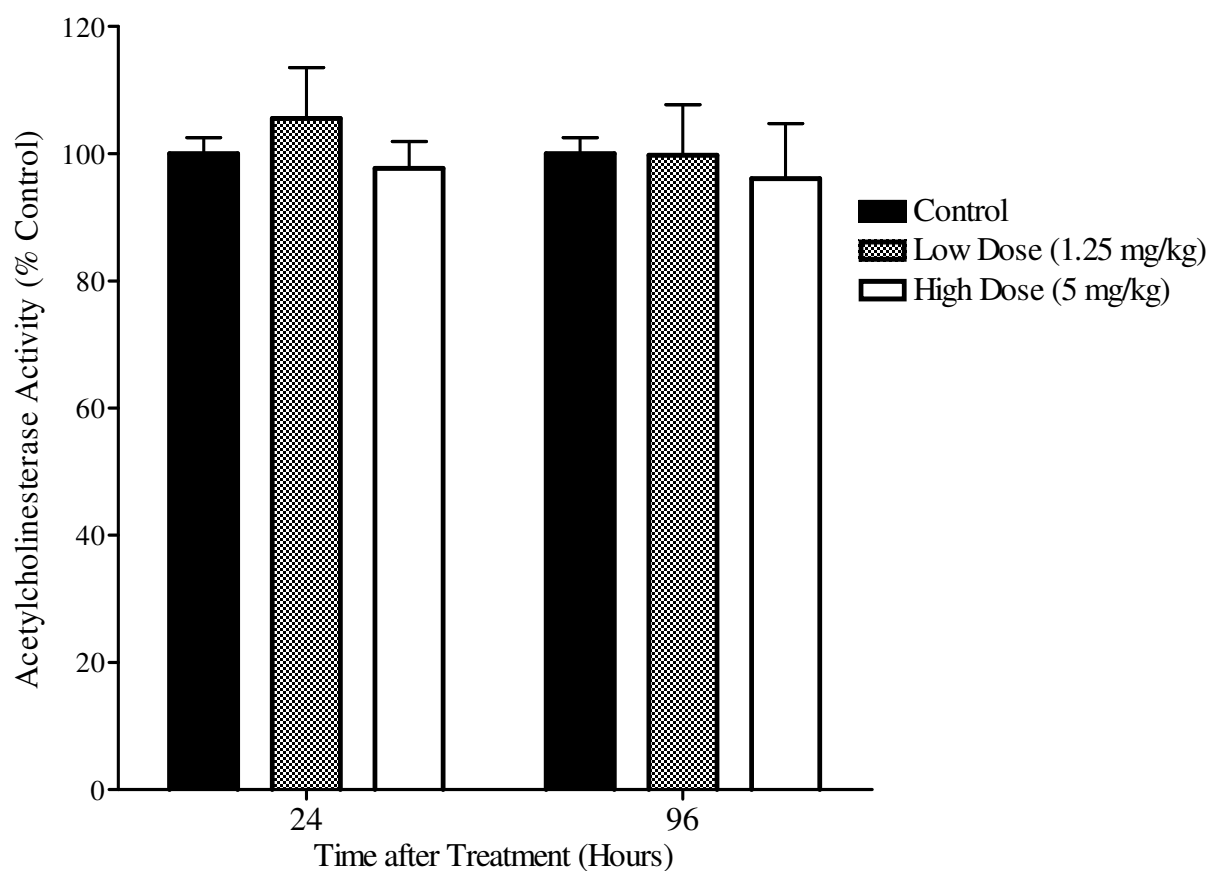
Figure 60: The effects of *iso*-OMPA on acetylcholinesterase activity in plasma. Rats (n=3-7/dose group) were treated with *iso*-OMPA (sc) at the doses indicated and sacrificed 24 or 96 hours later. Diluted plasma samples were pre-incubated with 10 μM *iso*-OMPA at 37°C for 15 minutes prior to measuring the residual ChE activity as described previously. *Iso*-OMPA did not inhibit AChE at either dose or at either the 24 or 96 hour time point. Data (mean ± standard error) represent AChE activity in terms of percent of control.
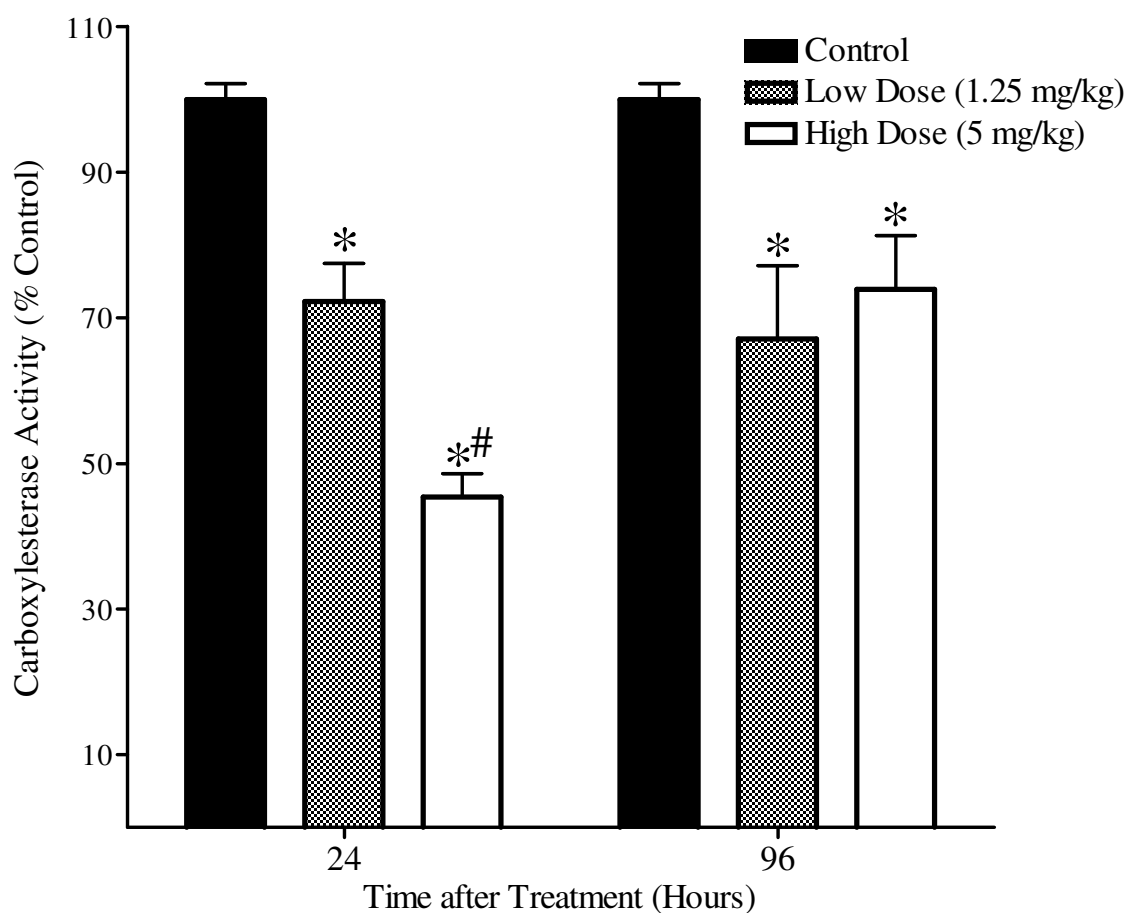
Figure 61: The effects of *iso*-OMPA on carboxylesterase activity in plasma. Rats (n=3-7/dose group) were treated with *iso*-OMPA (sc) at the doses indicated and sacrificed 24 or 96 hours later. Diluted plasma samples were incubated at 37°C in the presence of the substrate p-nitrophenyl acetate to assess CarbE activity. *Iso*-OMPA produced a dose-dependent inhibition of CarbE activity in the plasma at the 24 and 96 hour time points. Data (mean ± standard error) represent CarbE activity in terms of percent of control. The asterisk and pound signs represent values that are significantly different from control and 1.25 mg/kg dose groups at the same time point, respectively.

Effects of Acute Chlorpyrifos or Parathion Exposure on Body Weight, Involuntary Movements and SLUD Signs in Adult and Aged Rats

The effects of acute CPF and PS exposure on body weight, involuntary movements and SLUD (i.e., salivation, lacrimation, urination and defecation) were evaluated in adult and aged rats. For the CPF study, adult and aged rats were treated with vehicle (peanut oil), 0.1 x MTD (low dose), 0.5 x MTD (medium dose) and 1 x MTD (high dose), while for the PS study, rats of the two age-groups were treated with vehicle (peanut oil), 0.5 x MTD (low dose), 0.75 x MTD (medium dose) and 1 x MTD (high dose). Functional signs of toxicity (IM and SLUD) and body weight were monitored every 24 hours following CPF or PS exposure.

Figures 62 and 63 show changes in body weight following CPF exposure in adult and aged rats, respectively. CPF produced a dose-dependent decrease in body weight, which persisted until the end of the study in the medium and high dose groups of adult and aged rats. In adult rats, the decrease in body weight (15% reduction compared to day 0) peaked 48 hours after treatment in the medium and high dose-groups, after which it stayed at that level in the high dose, and showed a trend towards recovery in the medium dose, until the end of the study. In aged rats, body weight reduction peaked at 24 hours (5% reduction compared to day 0) in the medium dose group, after which it showed a trend towards recovery. In the high dose group, body weight decrease reached a maximum (10% reduction compared to day 0) by 72 hours post-treatment, and this persisted until the end of the study.

Figures 64 and 65 represent changes in body weight following PS exposure in adult and aged rats, respectively. PS produced a dose-dependent decrease in body weight,

which persisted until the end of the study in the medium and high dose groups of adult and aged rats. In adult rats, the decrease in body weight peaked 48 hours after treatment in the medium dose-group and 72 hours after treatment in the high dose-group, and this persisted until the end of the study. In aged rats, body weight decrease peaked at 48 hours in the medium dose group and at 72 hours in the medium dose group, and body weight stayed at these levels until the end of the study in both dose groups.

Tables 6-9 show the functional signs of toxicity [involuntary movements (IM) and SLUD signs (i.e., salivation, lacrimation, urination and defecation)] after acute exposure to CPF in adult and aged rats. Although CPF produced some signs of toxicity (mainly IM) in the high dose group of adult and aged rats, there was no significant difference.

Figures 66, 67, 68 and 69 show the functional signs of toxicity (IM and SLUD) in adult and aged rats after acute exposure to PS. In adult rats, the high dose of PS produced IM and SLUD signs 24 hours after treatment, which peaked by 72 hours, and these effects persisted until the end of the study. Involuntary movements had a slightly delayed onset (48 hours post-treatment) in the high dose group of aged rats, after which it peaked by 72 hours. SLUD signs were observed in the high dose group of adult rats 24 hours after treatment, and these effects start to diminish by 72 hours post-treatment.

Figure 62: The effects of various doses of CPF on body weight in adult rats. Rats (n=4/dose group) were treated subcutaneously with CPF at the doses indicated and sacrificed 96 hours later. Rats were weighed before treatment and every 24 hours after treatment. CPF produced a dose-dependent decrease in body weight, which remained lower than control values by the end of the study in the medium and high dose groups. Data (mean ± standard error) represent body weight in terms of percent of Day 0. The asterisk, pound and dollar signs represent values that are significantly different from control, 28 mg/kg and 140 mg/kg dose groups at the same time point, respectively.

Figure 63: The effects of various doses of CPF on body weight in aged rats. Rats (n=4-5/dose group) were treated subcutaneously with CPF at the doses indicated and sacrificed 96 hours later. Rats were weighed before treatment and every 24 hours after treatment. CPF produced a dose-dependent decrease in body weight, which remained lower than control values by the end of the study in the medium and high dose groups. Data (mean ± standard error) represent body weight in terms of percent of Day 0. The asterisk, pound and dollar signs represent values that are significantly different from control, 28 mg/kg and 140 mg/kg dose groups at the same time point, respectively.

Figure 64: The effects of various doses of PS on body weight in adult rats. Rats (n=4/dose group) were treated subcutaneously with PS at the doses indicated and sacrificed 96 hours later. Rats were weighed before treatment and every 24 hours after treatment. PS produced a dose-dependent decrease in body weight, which remained lower than control values by the end of the study in the medium and high dose groups. Data (mean ± standard error) represent body weight in terms of percent of Day 0. The asterisk, pound and dollar signs represent values that are significantly different from control, 9 mg/kg and 13.5 mg/kg dose groups at the same time point, respectively.

Figure 65: The effects of various doses of PS on body weight in aged rats. Rats (n=5/dose group) were treated subcutaneously with PS at the doses indicated and sacrificed 96 hours later. Rats were weighed before treatment and every 24 hours after treatment. PS produced a dose-dependent decrease in body weight, which remained lower than control values by the end of the study in the medium and high dose groups. Data (mean ± standard error) represent body weight in terms of percent of Day 0. The asterisk, pound and dollar signs represent values that are significantly different from control, 3 mg/kg and 4.5 mg/kg dose groups at the same time point, respectively.

Table 6. Involuntary movement scores for adult rats following acute exposure to chlorpyrifos.

		Time After Treatment			
		24 hours	48 hours	72 hours	96 hours
C P F D O S E S	Control	2 ± 0	2 ± 0	2 ± 0	2 ± 0
	Low Dose (28 mg/kg)	2 ± 0	2 ± 0	2 ± 0	2 ± 0
	Medium Dose (140 mg/kg)	2 ± 0	2 ± 0	2 ± 0	2 ± 0
	High Dose (280 mg/kg)	2 ± 0	2 ± 0.25	2 ± 0.25	2 ± 0.25

Rats (n=4/dose group) were treated subcutaneously with CPF at the doses indicated and sacrificed 96 hours later. Involuntary movements were evaluated every 24 hours after treatment. Data (median ± interquartile range) represent IM scores.

Table 7. SLUD scores (i.e., salivation, lacrimation, urination and defecation) in adult rats following acute exposure to chlorpyrifos.

		Time After Treatment			
		24 hours	48 hours	72 hours	96 hours
C P F D O S E S	Control	1 ± 0	1 ± 0	1 ± 0	1 ± 0
	Low Dose (28 mg/kg)	1 ± 0	1 ± 0	1 ± 0	1 ± 0
	Medium Dose (140 mg/kg)	1 ± 0	1 ± 0	1 ± 0	1 ± 0
	High Dose (280 mg/kg)	1 ± 0	1 ± 0	1 ± 0	1 ± 0

Rats (n=4/dose group) were treated subcutaneously with CPF at the doses indicated and sacrificed 96 hours later. SLUD signs were evaluated every 24 hours after treatment. Data (median ± interquartile range) represent SLUD scores.

Table 8: Involuntary movement scores for aged rats following acute exposure to chlorpyrifos.

		Time After Treatment			
		24 hours	48 hours	72 hours	96 hours
C P F D O S E S	Control	2 ± 0	2 ± 0	2 ± 0	2 ± 0
	Low Dose (28 mg/kg)	2 ± 0	2 ± 0	2 ± 0	2 ± 0
	Medium Dose (140 mg/kg)	2 ± 0	2 ± 0	2 ± 0	2 ± 0
	High Dose (280 mg/kg)	2 ± 0.25	2 ± 0.125	2 ± 0	2 ± 0

Rats (n=4/dose group) were treated subcutaneously with CPF at the doses indicated and sacrificed 96 hours later. Involuntary movements were evaluated every 24 hours after treatment. Data (median ± interquartile range) represent IM scores.

Table 9: SLUD scores (i.e., salivation, lacrimation, urination and defecation) in aged rats following acute exposure to chlorpyrifos.

		Time After Treatment			
		24 hours	48 hours	72 hours	96 hours
C P F D O S E S	Control	1 ± 0	1 ± 0	1 ± 0	1 ± 0
	Low Dose (28 mg/kg)	1 ± 0	1 ± 0	1 ± 0	1 ± 0
	Medium Dose (140 mg/kg)	1 ± 0	1 ± 0	1 ± 0	1 ± 0
	High Dose (280 mg/kg)	1 ± 0.5	1 ± 0	1 ± 0	1 ± 0

Rats (n=4/dose group) were treated subcutaneously with CPF at the doses indicated and sacrificed 96 hours later. SLUD signs were evaluated every 24 hours after treatment. Data (median ± interquartile range) represent SLUD scores.
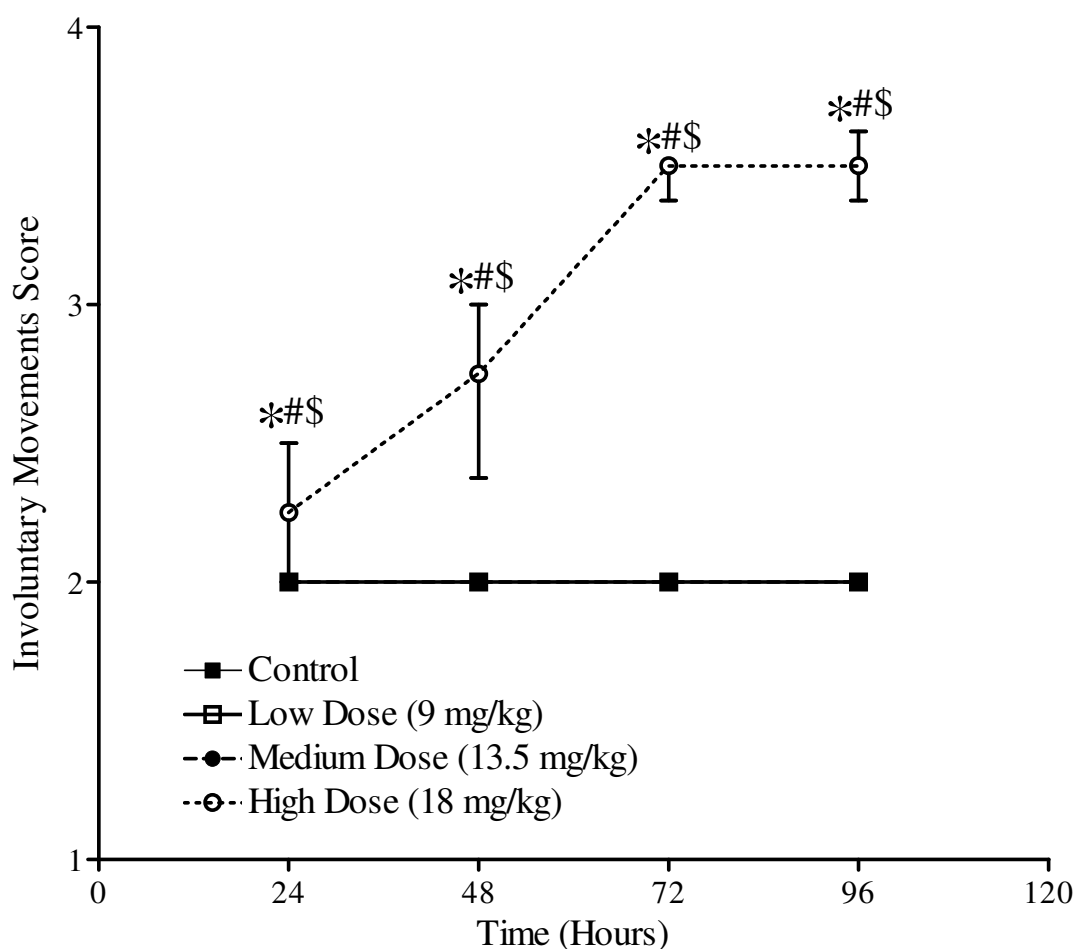
Figure 66: Involuntary movement scores for adult rats following acute exposure to parathion. Rats (n=4/dose group) were treated subcutaneously with PS at the doses indicated and sacrificed 96 hours later. Involuntary movements were evaluated every 24 hours after treatment. The high dose of PS showed an increase in IM which persisted until the end of the study. Data (median ± interquartile range) represent IM scores. The asterisk, pound and dollar signs represent values that are significantly different from control, 9 mg/kg and 13.5 mg/kg dose groups at the same time point, respectively.
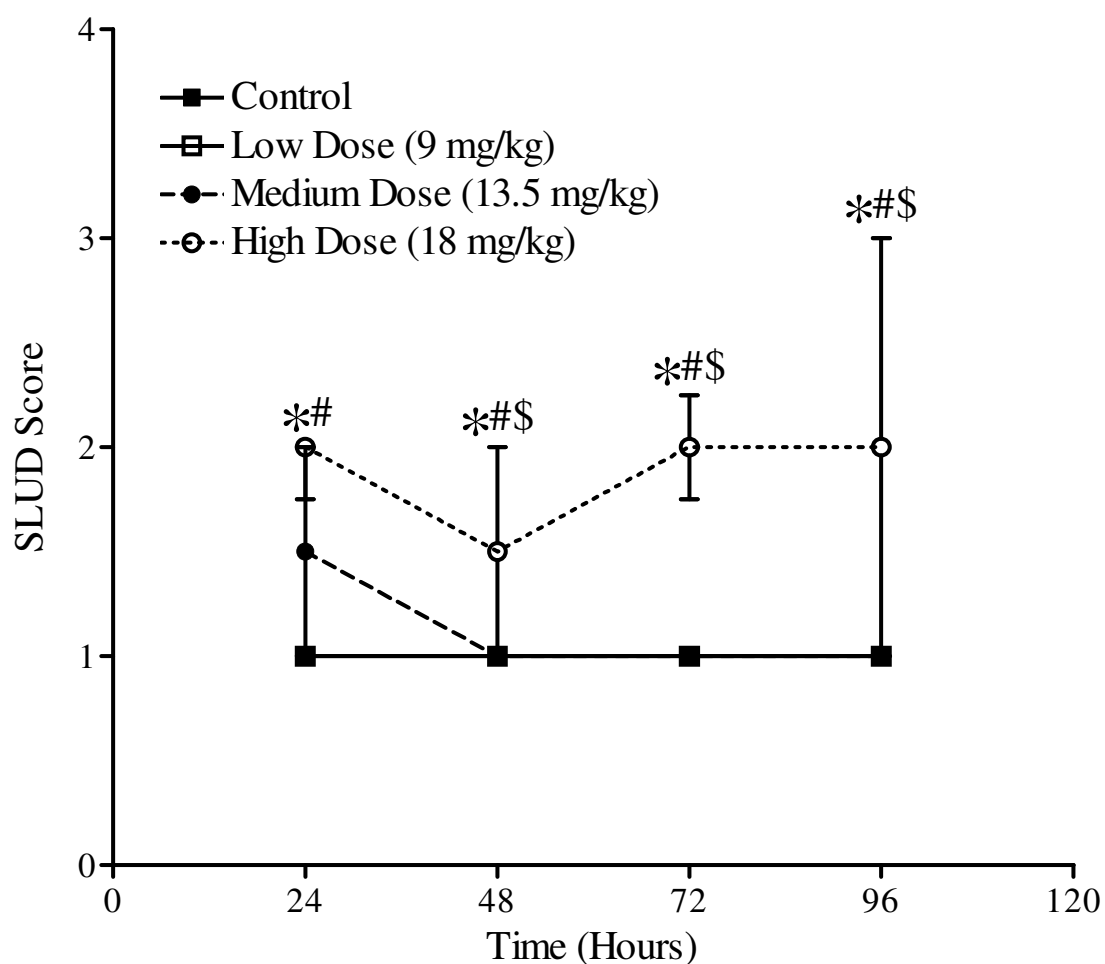
Figure 67: SLUD scores (i.e., salivation, lacrimation, urination and defecation) in adult rats following acute exposure to parathion. Rats (n=4/dose group) were treated subcutaneously with PS at the doses indicated and sacrificed 96 hours later. SLUD signs were evaluated every 24 hours after treatment. The high dose of PS showed an increase in SLUD signs which persisted until the end of the study. Data (median ± interquartile range) represent SLUD scores. The asterisk, pound and dollar signs represent values that are significantly different from control, 9 mg/kg and 13.5 mg/kg dose groups at the same time point, respectively.
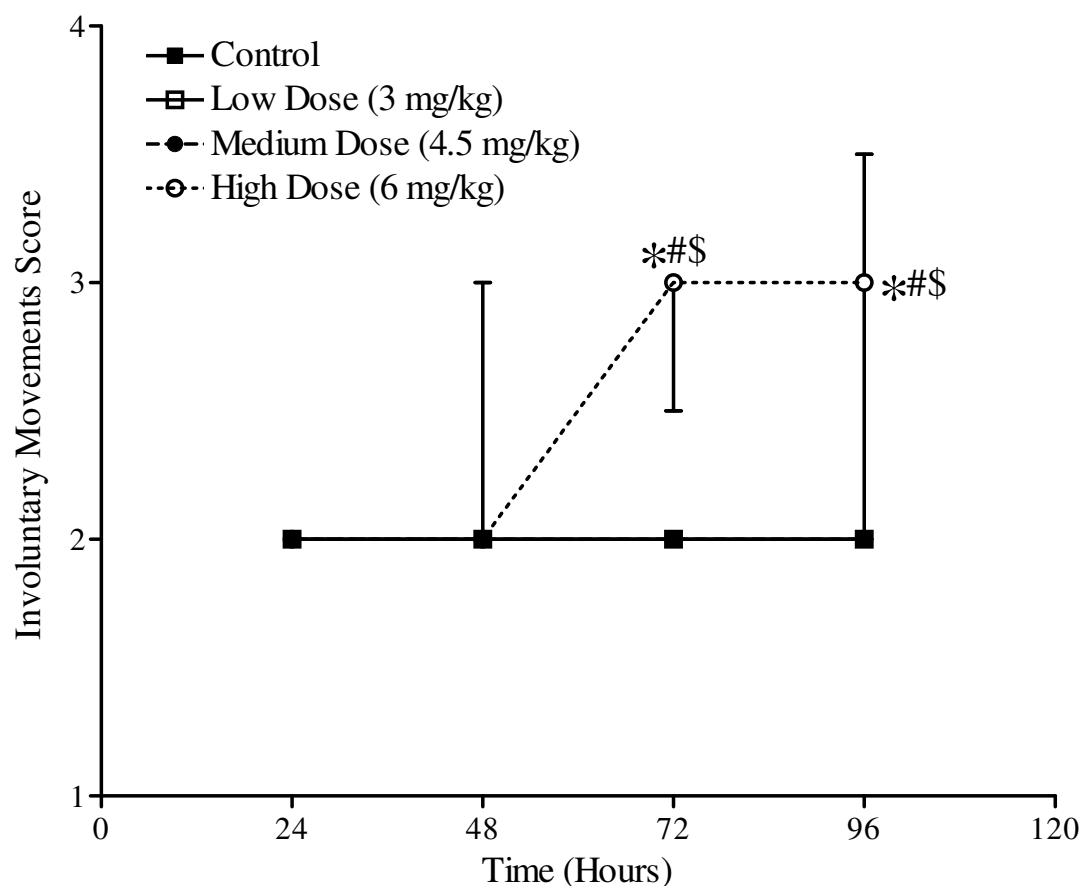
Figure 68: Involuntary movement scores for aged rats following acute exposure to parathion. Rats (n=4/dose group) were treated subcutaneously with PS at the doses indicated and sacrificed 96 hours later. Involuntary movements were evaluated every 24 hours after treatment. The high dose of PS showed an increase in IM which persisted until the end of the study. Data (median ± interquartile range) represent IM scores. The asterisk, pound and dollar signs represent values that are significantly different from control, 3 mg/kg and 4.5 mg/kg dose groups at the same time point, respectively.
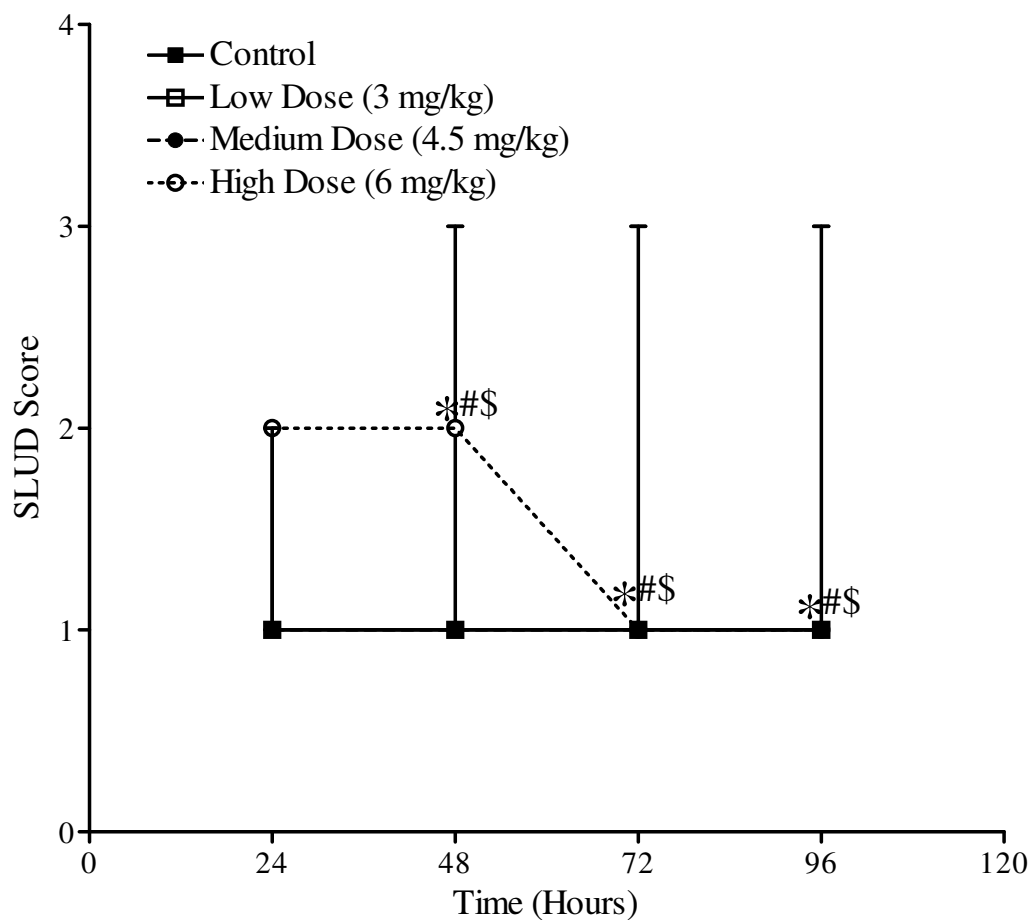
Figure 69: SLUD scores (i.e., salivation, lacrimation, urination and defecation) in aged rats following acute exposure to parathion. Rats (n=4/dose group) were treated subcutaneously with PS at the doses indicated and sacrificed 96 hours later. SLUD signs were evaluated every 24 hours after treatment. The high dose of PS showed an increase in SLUD signs which started subsiding 72 hours after treatment. Data (median ± interquartile range) represent SLUD scores. The asterisk, pound and dollar signs represent values that are significantly different from control, 3 mg/kg and 4.5 mg/kg dose groups at the same time point, respectively.

Effects of Chlorpyrifos on Heart Rate, Body Temperature and Physical Activity in Adult and Aged Rats

Basal heart rate in aged rats was considerably (~50 beats per minute) lower than that of adult rats. CPF produced a dose-dependent decrease in heart rate in the medium and high dose-groups of adult and aged rats. Figures 70-72 show the effects of the various doses of CPF on heart rate in adult rats. CPF caused a slight but significant decrease in heart rate in the medium dose group, which persisted until the end of the study. In the high dose group, the heart rate was briefly elevated, after which it was substantially decreased, and remained depressed until the end of the observation period. Figures 73-75 show the effects of the various doses of CPF on heart rate in aged rats. CPF produced a diurnal increase in heart rate in all treatment groups in the first 12 hours post-treatment, following which the heart rate showed a persistent decrease until the end of the study in the medium and high dose-groups.

CPF produced a dose-dependent decrease in body temperature in the medium and high dose-groups of adult and aged rats. Figures 76-78 show the effects of the various doses of CPF on body temperature in adult rats. The decrease in body temperature in the medium and high dose-groups predominantly occurred during the nocturnal phase and peaked 24 (medium dose group) to 48 (high dose group) hours post-treatment. This parameter recovered to baseline (pre-treatment) values by the end of the study in both dose groups. Figures 79-81 show the effects of the various doses of CPF on body temperature in aged rats. CPF produced a dose-dependent decrease in body temperature (which was evident in the diurnal and nocturnal phase) in the medium and high dose-

groups, which peaked 24 hours post-treatment. Although body temperature showed a trend towards recovery in both dose groups, it was still lower than the baseline values.

CPF elicited a dose-related effect on physical activity in the medium and high dose-groups of adult and aged rats. Figures 82-84 illustrate the effects of the various doses of CPF on physical activity in adult rats. CPF produced a dose-related decrease in physical activity which peaked 24 hours after treatment in the low, medium and high dose-groups. By 60 hours post-treatment, CPF treatment was associated with a diurnal increase in physical activity in the medium and high dose groups, which recovered to baseline values by the end of the study. Figures 85-87 show the effects of the various doses of CPF on physical activity in aged rats. During the diurnal phase, CPF produced a decrease in physical activity in the low dose-group 36 hours after treatment, and an increase in the high dose-group 60 and 84 hours post-treatment. Although the high dose of CPF did not produce any decrease in physical activity in the diurnal phase, during the nocturnal phase, physical activity was initially depressed (peaking by 24 hours after treatment) and then elevated above pre-treatment values by the end of the study.
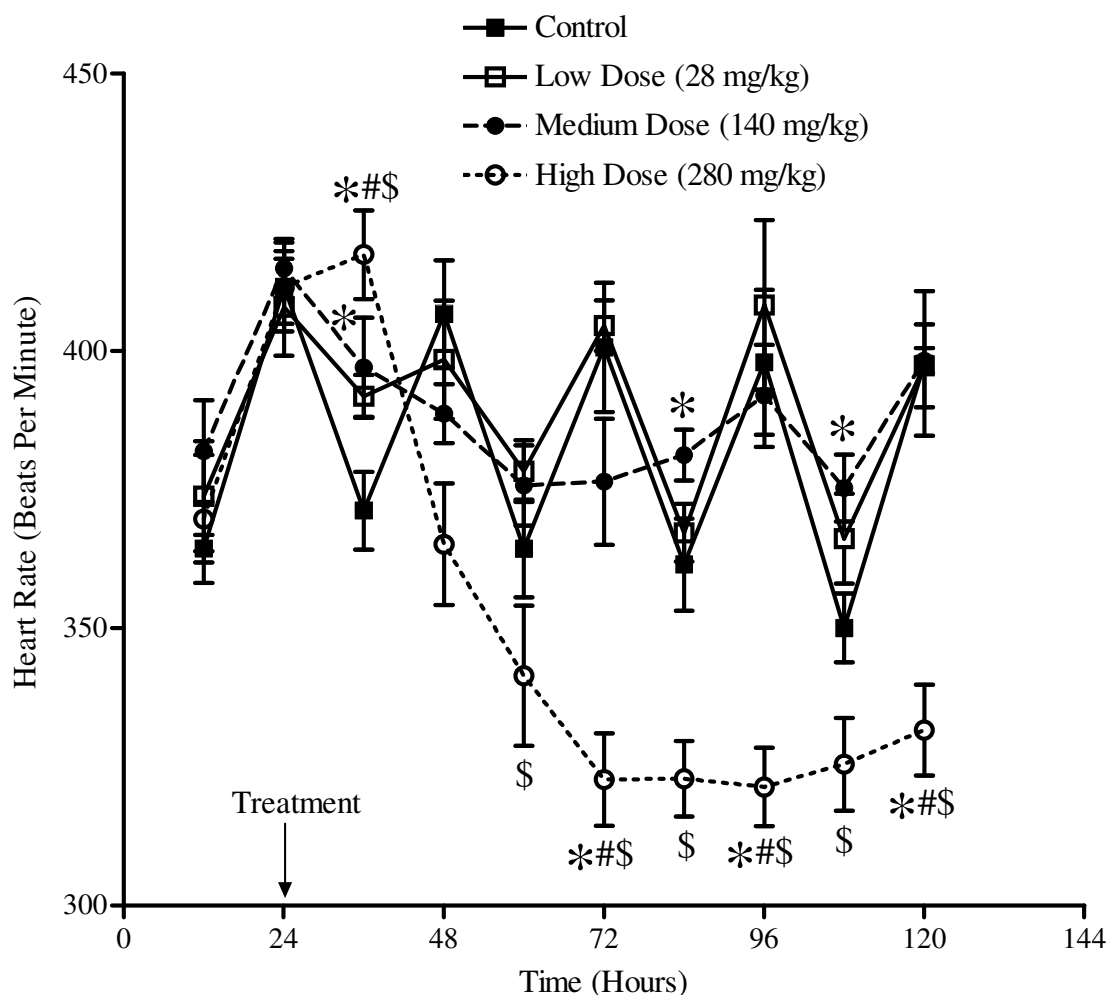
Figure 70: The effects of various doses of CPF on heart rate in adult rats. Rats (n=4/dose group) were treated subcutaneously with CPF at the doses indicated and sacrificed 96 hours later. The graph represents 24 hour baseline (pre-treatment) data followed by 96 hours post-treatment data. The data (mean ± standard error) represent heart rate averaged over 8 hour diurnal and nocturnal intervals. The medium dose of CPF caused a slight but sustained decrease in heart rate, while the high dose produced an initial increase followed by a persistent decrease in heart rate. The asterisk, pound and dollar signs represent values that are significantly different from control, 28 and 140 mg/kg dose groups at the same time point, respectively.

151
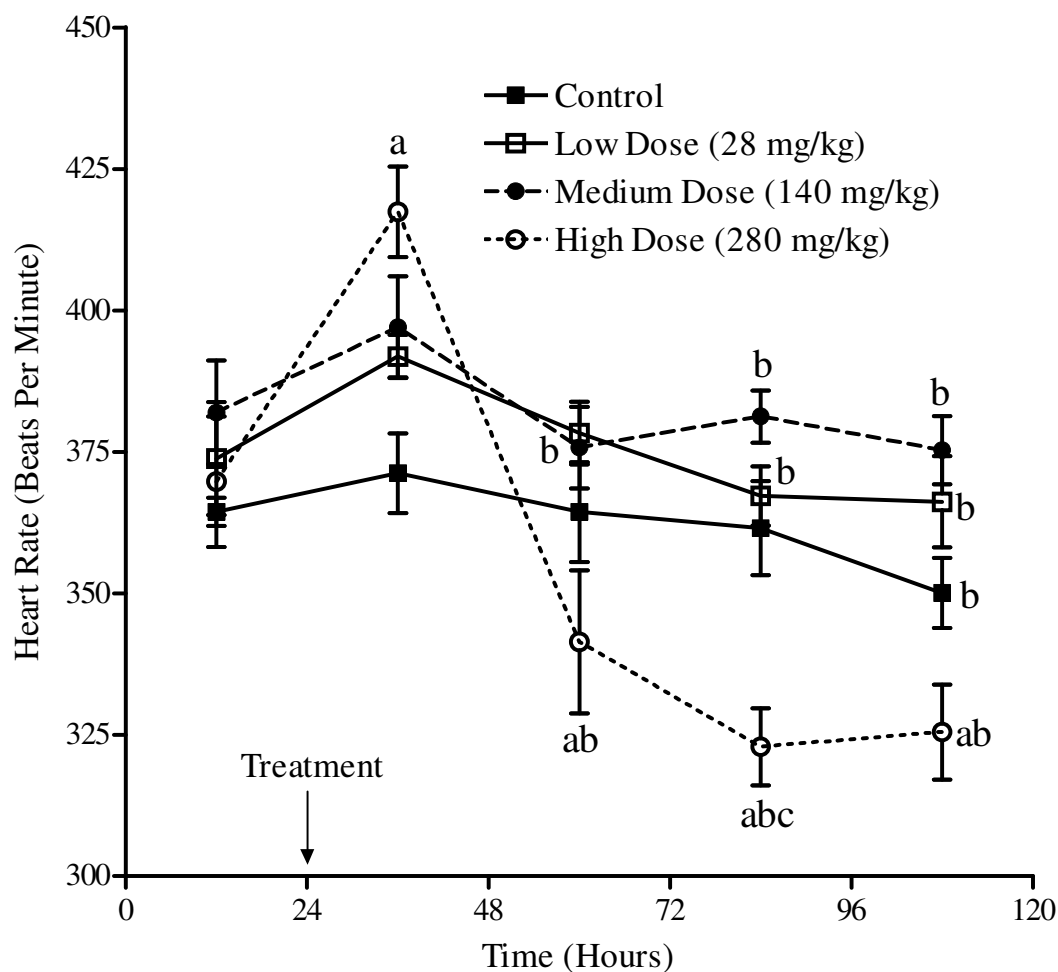
Figure 71: The effects of various doses of CPF on heart rate in adult rats during the diurnal (light) periods. Rats (n=4/dose group) were treated subcutaneously with CPF at the doses indicated and sacrificed 96 hours later. The graph represents 24 hour baseline (pre-treatment) data followed by 96 hours post-treatment data. The data (mean ± standard error) represent heart rate averaged over 8 hour diurnal intervals. CPF produced a dose-dependent decrease in heart rate. The high dose of CPF produced an initial increase followed by a persistent decrease in heart rate. a, b, and c represent values that are significantly different from the same dose at 12, 36 and 60 hours, respectively.
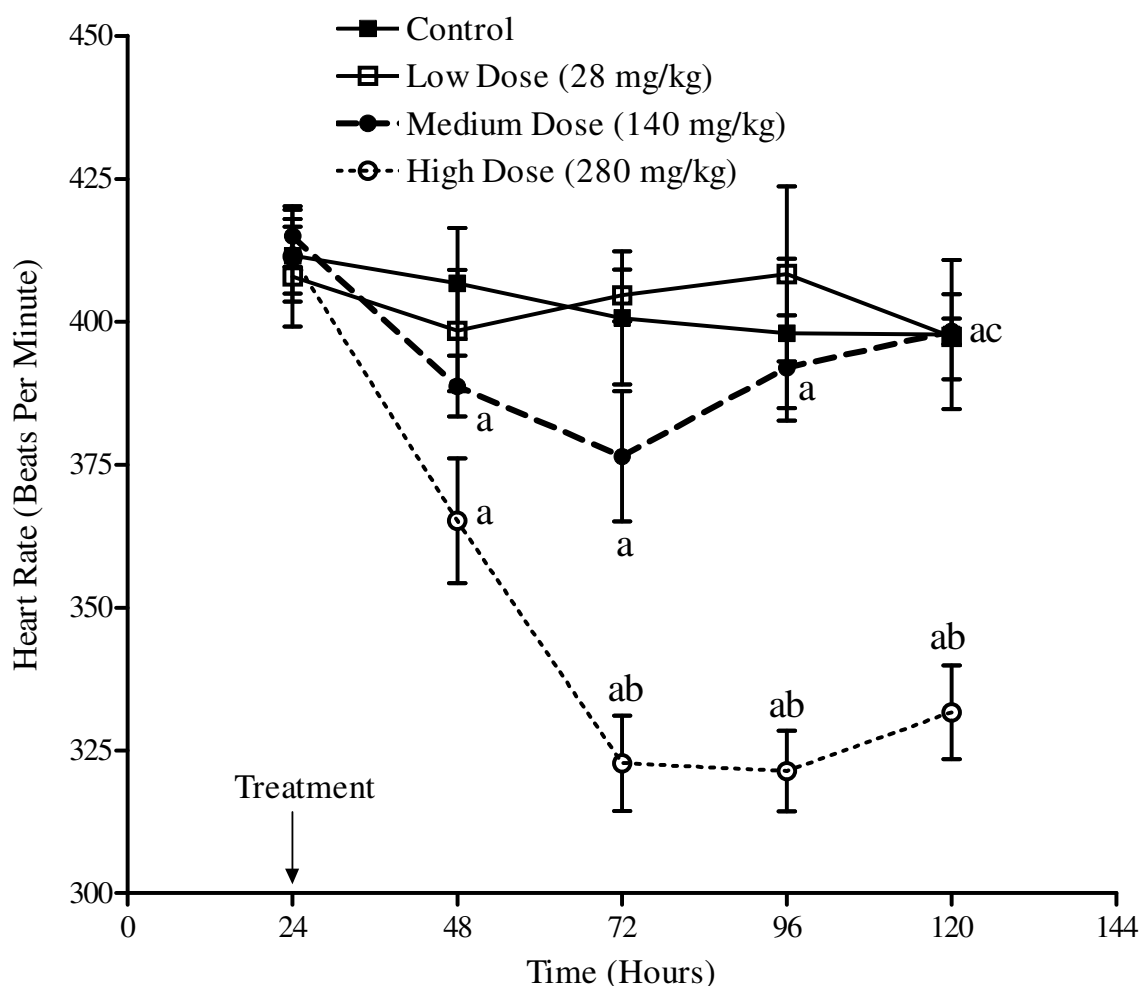
Figure 72: The effects of various doses of CPF on heart rate in adult rats during the nocturnal (dark) periods. Rats (n=4/dose group) were treated subcutaneously with CPF at the doses indicated and sacrificed 96 hours later. The graph represents 24 hour baseline (pre-treatment) data followed by 96 hours post-treatment data. The data (mean ± standard error) represent heart rate averaged over 8 hour nocturnal intervals. CPF produced a dose-dependent decrease in heart rate. Both the medium and high dose of CPF produced a decrease in heart rate, which persisted until the end of the study. a, b, and c represent values that are significantly different from the same dose at 24, 48 and 72 hours, respectively.
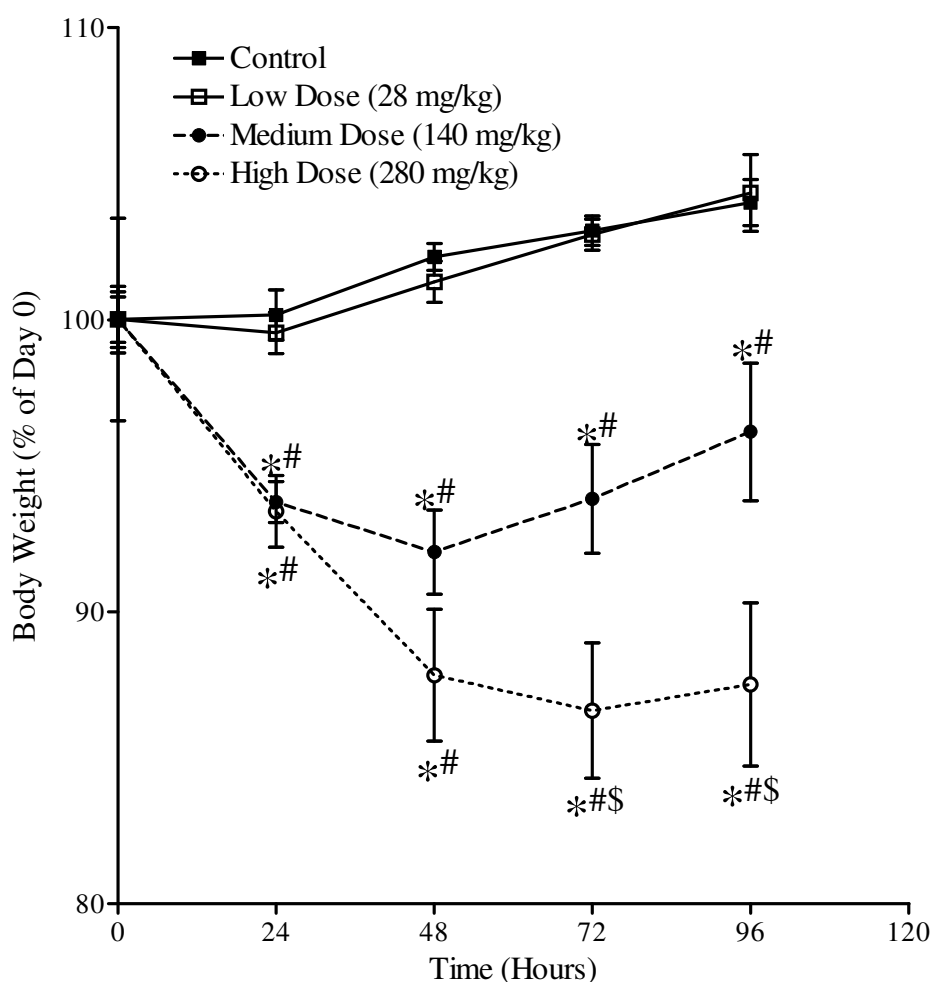
153

Figure 73: The effects of various doses of CPF on heart rate in aged rats. Rats (n=4-5/treatment group) were treated subcutaneously with CPF at the doses indicated and sacrificed 96 hours later. The graph represents 24 hour baseline (pre-treatment) data followed by 96 hours post-treatment data. The data (mean ± standard error) represent heart rate averaged over 8 hour diurnal and nocturnal intervals. CPF produced a dose-dependent decrease in heart rate, which persisted until the end of the study in the medium and high dose-groups. The asterisk, pound and dollar signs represent values that are significantly different from control, 28 and 140 mg/kg dose groups at the same time point, respectively.
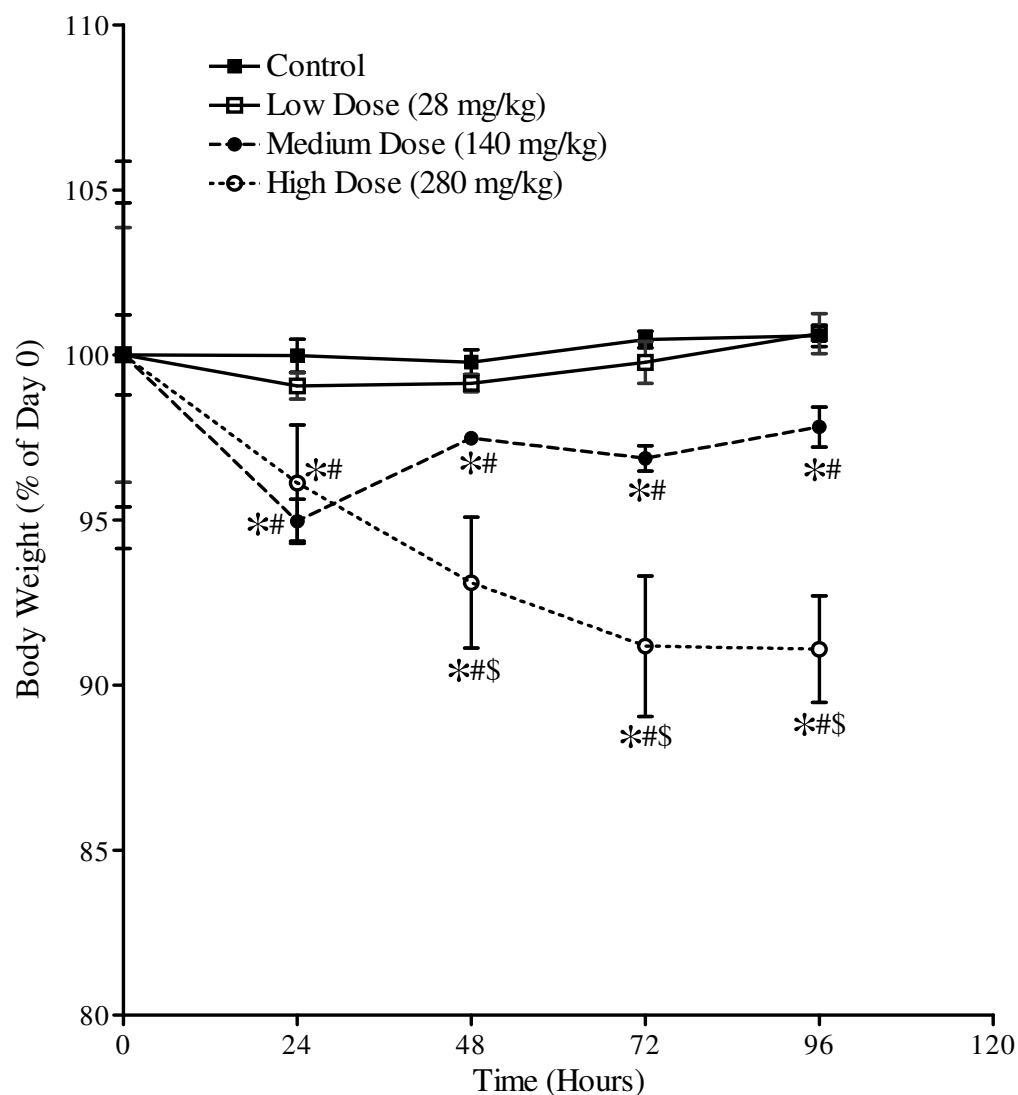
154

Figure 74: The effects of various doses of CPF on heart rate in aged rats during the diurnal (light) periods. Rats (n=4-5/dose group) were treated subcutaneously with CPF at the doses indicated and sacrificed 96 hours later. The graph represents 24 hour baseline (pre-treatment) data followed by 96 hours post-treatment data. The data (mean ± standard error) represent heart rate averaged over 8 hour diurnal intervals. CPF produced a diurnal increase in heart rate in all the dose-groups 12 hours after treatment, with apparent recovery to pre-treatment levels by the end of the study. a, b, and c represent values that are significantly different from the same dose at 12, 36 and 60 hours, respectively.

Figure 75: The effects of various doses of CPF on heart rate in aged rats during the nocturnal (dark) periods. Rats (n=4-5/dose group) were treated subcutaneously with CPF at the doses indicated and sacrificed 96 hours later. The graph represents 24 hour baseline (pre-treatment) data followed by 96 hours post-treatment data. The data (mean ± standard error) represent heart rate averaged over 8 hour nocturnal intervals. CPF produced a dose-dependent decrease in heart rate in the medium and high dose-groups, which persisted until the end of the study. a, b, and c represent values that are significantly different from the same dose at 24, 48 and 72 hours, respectively.

Figure 76: The effects of various doses of CPF on body temperature in adult rats. Rats (n=4/dose group) were treated subcutaneously with CPF at the doses indicated and sacrificed 96 hours later. The graph represents 24 hour baseline (pre-treatment) data followed by 96 hours post-treatment data. The data (mean ± standard error) represent body temperature averaged over 8 hour diurnal and nocturnal intervals. CPF produced a dose-dependent decrease in body temperature. The body temperature recovered to control values by the end of the study in all three dose-groups. The asterisk, pound and dollar signs represent values that are significantly different from control, 28 and 140 mg/kg dose groups at the same time point, respectively.
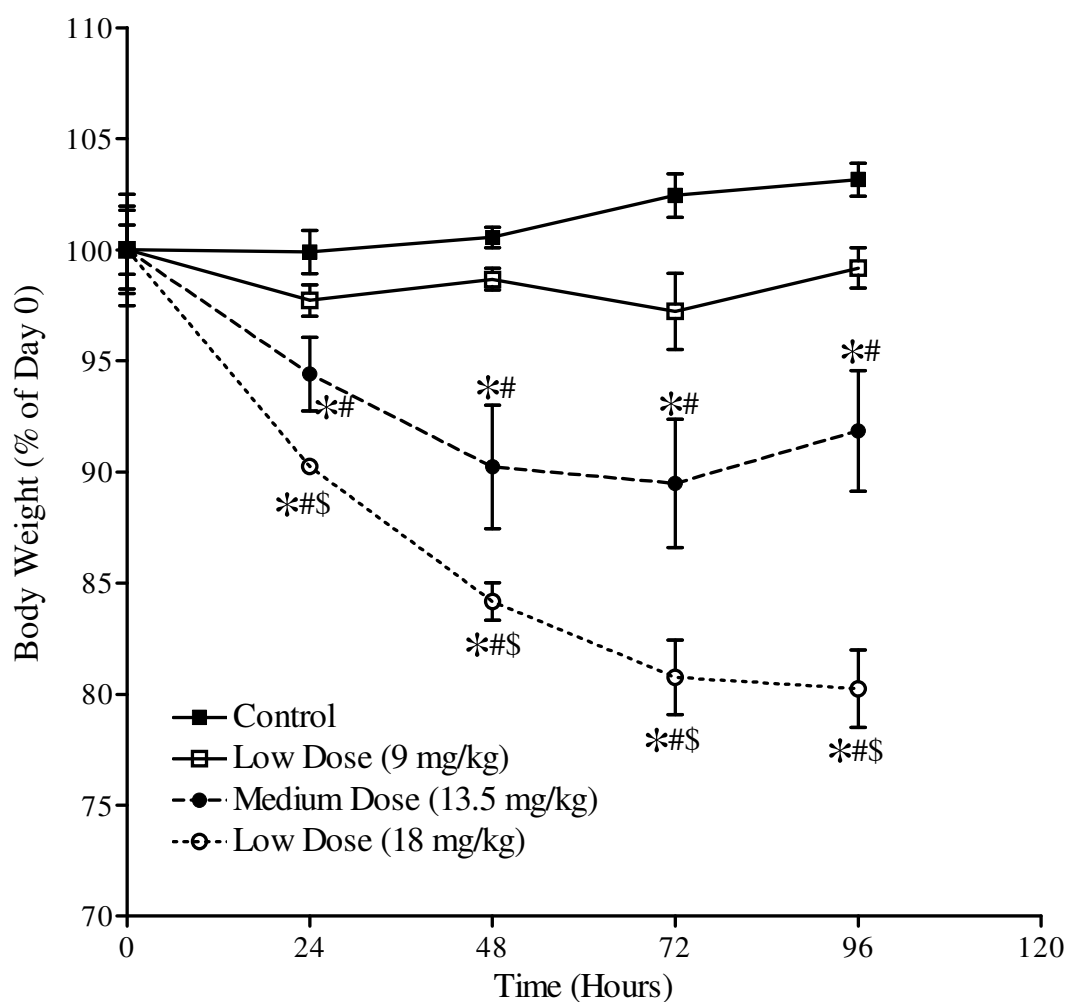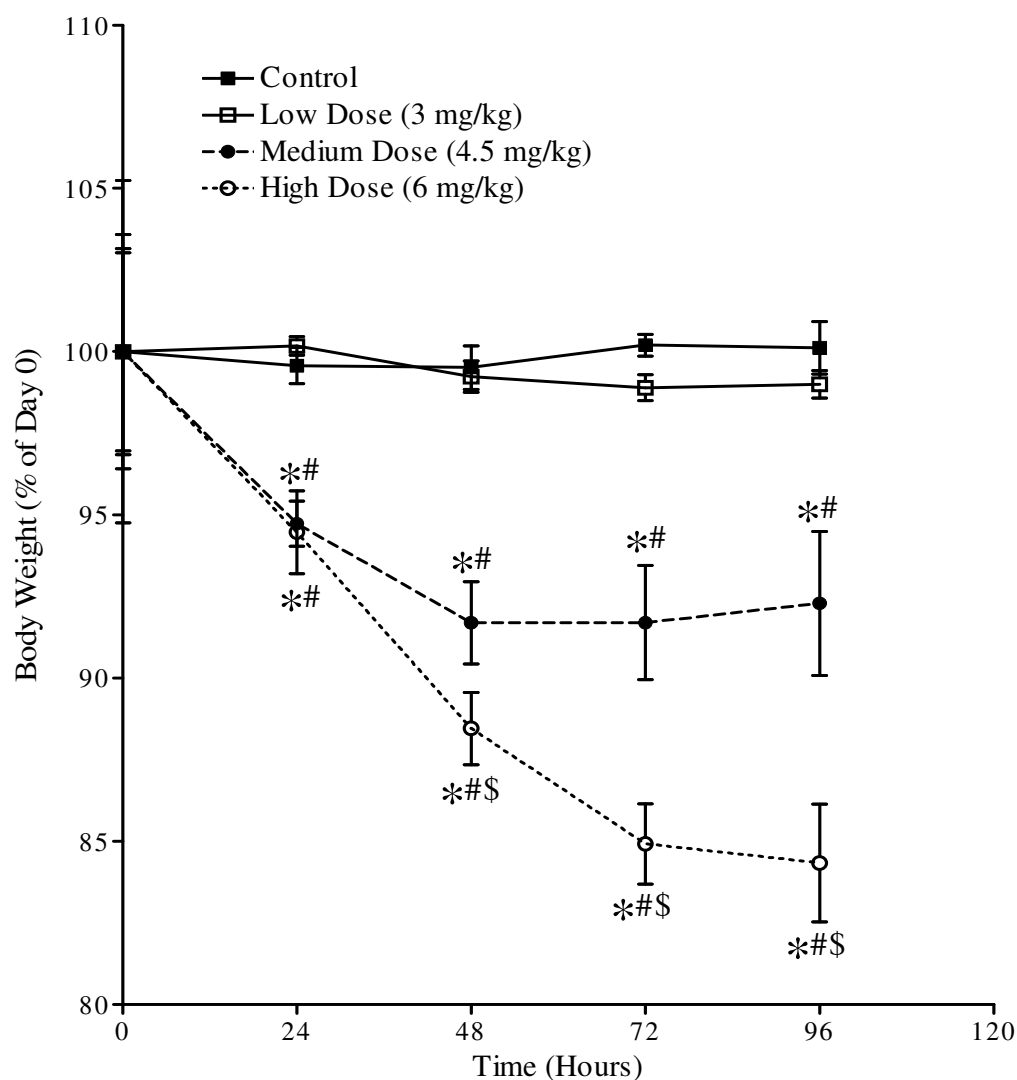
Figure 77: The effects of various doses of CPF on body temperature in adult rats during the diurnal (light) periods. Rats (n=4/dose group) were treated subcutaneously with CPF at the doses indicated and sacrificed 96 hours later. The graph represents 24 hour baseline (pre-treatment) data followed by 96 hours post-treatment data. The data (mean ± standard error) represent body temperature averaged over 8 hour diurnal intervals. CPF produced a significant decrease in body temperature during the diurnal phase, that peaked by 12 hours (low dose group) and 36 hours (high dose group) post-treatment. a, and b represent values that are significantly different from the same dose at 12 and 36 hours, respectively.

Figure 78: The effects of various doses of CPF on body temperature in adult rats during the nocturnal (dark) periods. Rats (n=4/dose group) were treated subcutaneously with CPF at the doses indicated and sacrificed 96 hours later. The graph represents 24 hour baseline (pre-treatment) data followed by 96 hours post-treatment data. The data (mean ± standard error) represent body temperature averaged over 8 hour nocturnal intervals. CPF produced a dose-dependent decrease in body temperature which peaked at 48 hours post-treatment and recovered to baseline values by the end of the study. a, b, and c represent values that are significantly different from the same dose at 24, 48 and 72 hours, respectively.

Figure 79: The effects of various doses of CPF on body temperature in aged rats. Rats (n=4-5/dose group) were treated subcutaneously with CPF at the doses indicated and sacrificed 96 hours later. The graph represents 24 hour baseline (pre-treatment) data followed by 96 hours post-treatment data. The data (mean ± standard error) represents body temperature averaged over 8 hour diurnal and nocturnal intervals. CPF produced a significant decrease in body temperature, which peaked 24 hours post-treatment and started recovering to control values thereafter. The asterisk, pound and dollar signs represent values that are significantly different from control, 28 and 140 mg/kg dose groups at the same time point, respectively.

Figure 80: The effects of various doses of CPF on body temperature in aged rats during the diurnal (light) periods. Rats (n=4-5/dose group) were treated subcutaneously with CPF at the doses indicated and sacrificed 96 hours later. The graph represents 24 hour baseline (pre-treatment) data followed by 96 hours post-treatment data. The data (mean ± standard error) represents body temperature averaged over 8 hour diurnal intervals. CPF produced a decrease in body temperature in the high dose-group 36 hours after treatment, with apparent recovery to pre-treatment levels by the end of the study. a, b, c, and d represent values that are significantly different from the same dose at 12, 36, 60 and 84 hours, respectively.

161

Figure 81: The effects of various doses of CPF on body temperature in aged rats during the nocturnal (dark) periods. Rats (n=4-5/dose group) were treated subcutaneously with CPF at the doses indicated and sacrificed 96 hours later. The graph represents 24 hour baseline (pre-treatment) data followed by 96 hours post-treatment data. The data (mean ± standard error) represents body temperature averaged over 8 hour nocturnal intervals. CPF produced a dose-dependent decrease in body temperature in the medium and high dose-groups, which persisted until the end of the study. a, b, c, and d represent values that are significantly different from the same dose at 24, 48, 72 and 96 hours, respectively.

Figure 82: The effects of various doses of CPF on physical activity in adult rats. Rats (n=4/dose group) were treated subcutaneously with CPF at the doses indicated and sacrificed 96 hours later. The graph represents 24 hour baseline (pre-treatment) data followed by 96 hours post-treatment data. The data (mean ± standard error) represents physical activity averaged over 8 hour diurnal and nocturnal intervals. CPF produced a dose-dependent decrease in physical activity, which recovered to control values by the end of the study in all dose-groups. Asterisks represent values that are significantly different from the control group at the same time point.

Figure 83: The effects of various doses of CPF on physical activity in adult rats during the diurnal (light) periods. Rats (n=4/dose group) were treated subcutaneously with CPF at the doses indicated and sacrificed 96 hours later. The graph represents 24 hour baseline (pre-treatment) data followed by 96 hours post-treatment data. The data (mean ± standard error) represents physical activity averaged over 8 hour diurnal intervals. CPF produced a diurnal increase in physical activity in the medium and high dose groups 60 hours post-treatment, which recovered to pre-treatment levels by the end of the study. a, b, and c represent values that are significantly different from the same dose at 12, 36 and 60 hours, respectively.

Figure 84: The effects of various doses of CPF on physical activity in adult rats during the nocturnal (dark) periods. Rats (n=4/dose group) were treated subcutaneously with CPF at the doses indicated and sacrificed 96 hours later. The graph represents 24 hour baseline (pre-treatment) data followed by 96 hours post-treatment data. The data (mean ± standard error) represents physical activity averaged over 8 hour nocturnal intervals. CPF produced a dose-dependent decrease in physical activity which peaked 24 hours post-treatment in all 3 dose groups and recovered to baseline values by the end of the study. a, b, c, and d represent values that are significantly different from the same dose at 24, 48, 72 and 96 hours, respectively.

Figure 85: The effects of various doses of CPF on physical activity in aged rats. Rats (n=4-5/dose group) were treated subcutaneously with CPF at the doses indicated and sacrificed 96 hours later. The graph represents 24 hour baseline (pre-treatment) data followed by 96 hours post-treatment data. The data (mean ± standard error) represents physical activity averaged over 8 hour diurnal and nocturnal intervals. CPF produced a significant decrease in physical activity in the high dose-group, which peaked 24 hours post-treatment and started increasing above control values by 60 hours post-treatment. The asterisk, pound and dollar signs represent values that are significantly different from control, 28 and 140 mg/kg dose groups at the same time point, respectively.

Figure 86: The effects of various doses of CPF on physical activity in aged rats during the diurnal (light) periods. Rats (n=4-5/dose group) were treated subcutaneously with CPF at the doses indicated and sacrificed 96 hours later. The graph represents 24 hour baseline (pre-treatment) data followed by 96 hours post-treatment data. The data (mean ± standard error) represents physical activity averaged over 8 hour diurnal intervals. CPF produced a decrease in physical activity in the low dose-group 36 hours after treatment, and a diurnal increase in physical activity in the high dose-group 60 and 84 hours post-treatment. a, b, c, and d represent values that are significantly different from the same dose at 12, 36, 60 and 84 hours, respectively.

167

Figure 87: The effects of various doses of CPF on physical activity in aged rats during the nocturnal (dark) periods. Rats (n=4-5/dose group) were treated subcutaneously with CPF at the doses indicated and sacrificed 96 hours later. The graph represents 24 hour baseline (pre-treatment) data followed by 96 hours post-treatment data. The data (mean ± standard error) represents physical activity averaged over 8 hour nocturnal intervals. The physical activity in the high dose-group was initially depressed and then elevated above pre-treatment (baseline) values by the end of the study. a, b, c, and d represent values that are significantly different from the same dose at 24, 48, 72 and 96 hours, respectively.

Effects of Parathion on Heart Rate, Body Temperature and Physical Activity in

Adult and Aged Rats

PS produced a dose-dependent decrease in heart rate in the medium and high dose-groups of adult and aged rats. Figures 88-90 represent the effects of the various doses of PS on heart rate in adult rats. PS produced a brief diurnal (12 hours post-treatment) increase in heart rate in the medium dose group, followed by a prolonged decrease, with a trend towards recovery by the end of the study. Relative to the control group, the high dose of PS caused an increase in heart rate 12 hours post-treatment, followed by a significant and prolonged decrease in heart rate, which persisted until the end of the study. Figures 91-93 represent the effects of the various doses of PS on heart rate in aged rats. In the medium dose group of aged rats, PS produced an initial diurnal increase (12 hours post-treatment) in heart rate, followed by a decrease and a subsequent trend towards recovery (by the end of the study). In the high dose group, an initial decrease in heart rate (24 hours post-treatment) was followed by a brief period of increase (48 hours after treatment), after which the heart rate continued to decrease significantly until the end of the study (72 hours post-treatment onwards). This transient increase in heart rate response was absent in adult rats and in other treatment groups of aged rats.

PS produced a dose-dependent decrease in body temperature in the medium and high dose-groups of adult and aged rats. Figures 94-96 represent the effects of the various doses of PS on body temperature in adult rats. PS produced a dose-dependent decrease in body temperature in the medium and high dose-groups, which peaked 24 hours after treatment. By the end of the study, body temperature recovered to pre-treatment values in the medium dose-group and remained depressed in the high dose-group. Figures 97-99

169

represent the effects of the various doses of PS on body temperature in aged rats. Similar to the observation in adult rats, PS produced a dose-dependent decrease in body temperature (which peaked at 24 hours post-treatment in the high dose group and at 36 hours post-treatment in the medium dose-group). By the end of the study, the body temperature in the medium dose group had recovered to baseline values, while it remained depressed in the high dose group.

PS produced a dose-dependent effect on physical activity in adult and aged rats. Figures 100-102 represent the effects of the various doses of PS on physical activity in adult rats. PS produced a dose-dependent decrease in physical activity, which peaked 24 hours post-treatment in the low, medium and high dose groups. By the end of the study, physical activity in the low dose group recovered to baseline values, while in the medium and high dose-groups, it remained depressed. Figures 103-105 represent the effects of the various doses of PS on physical activity in aged rats. PS produced a dose-dependent decrease in physical activity in the low, medium and high dose-groups, which peaked at 24 hours post-treatment. In the nocturnal phase, physical activity recovered to baseline values in all 3 treatment groups by the end of the study. Interestingly, in the diurnal phase, PS produced an increase in physical activity around 60 hours post-treatment in the medium and high dose-groups, which persisted until the end of the study.
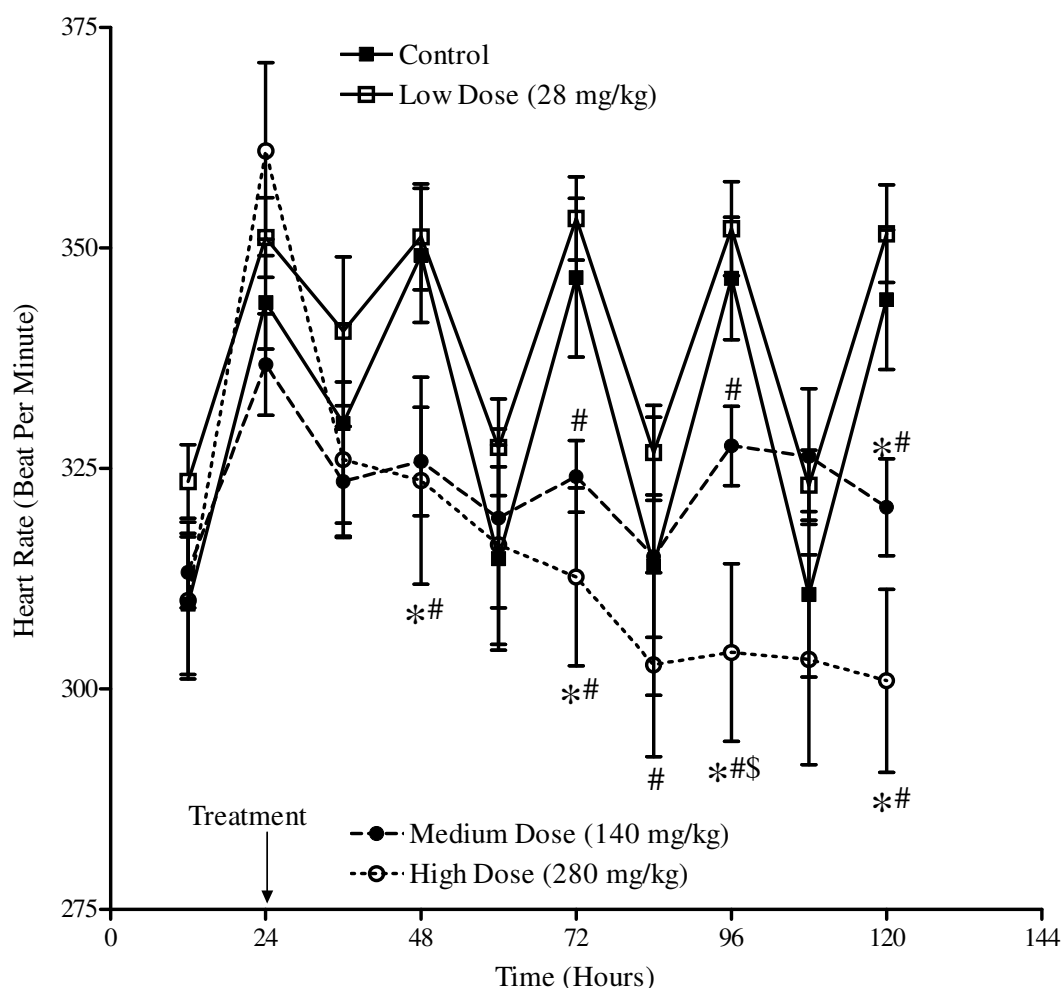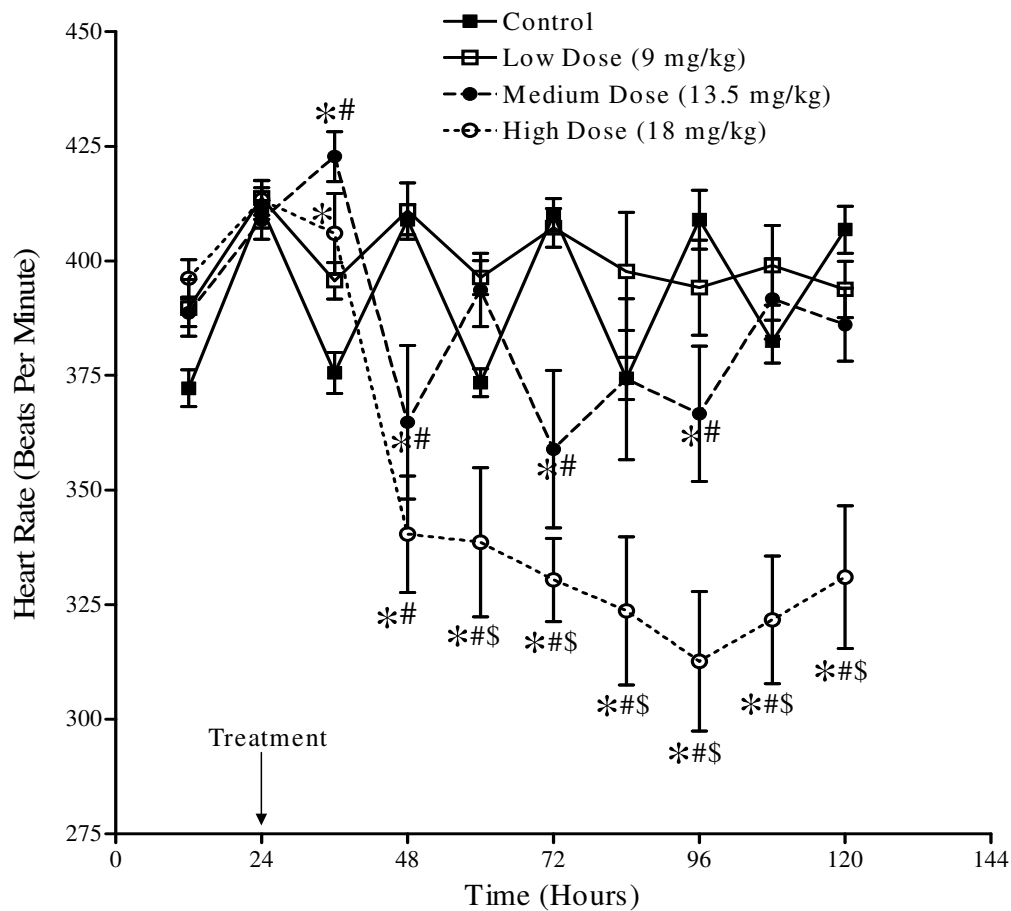
Figure 88: The effects of various doses of PS on heart rate in adult rats. Rats (n=4/dose group) were treated subcutaneously with PS at the doses indicated and sacrificed 96 hours later. The graph represents 24 hour baseline (pre-treatment) data followed by 96 hours post-treatment data. The data (mean ± standard error) represent heart rate averaged over 8 hour diurnal and nocturnal intervals. The medium and high dose-groups of PS caused an initial increase followed by a prolonged decrease in heart rate, which remained depressed in the high dose-group and recovered to control values in the medium dose-group by the end of the study. The asterisk, pound and dollar signs represent values that are significantly different from control, 9 and 13.5 mg/kg dose groups at the same time point, respectively.
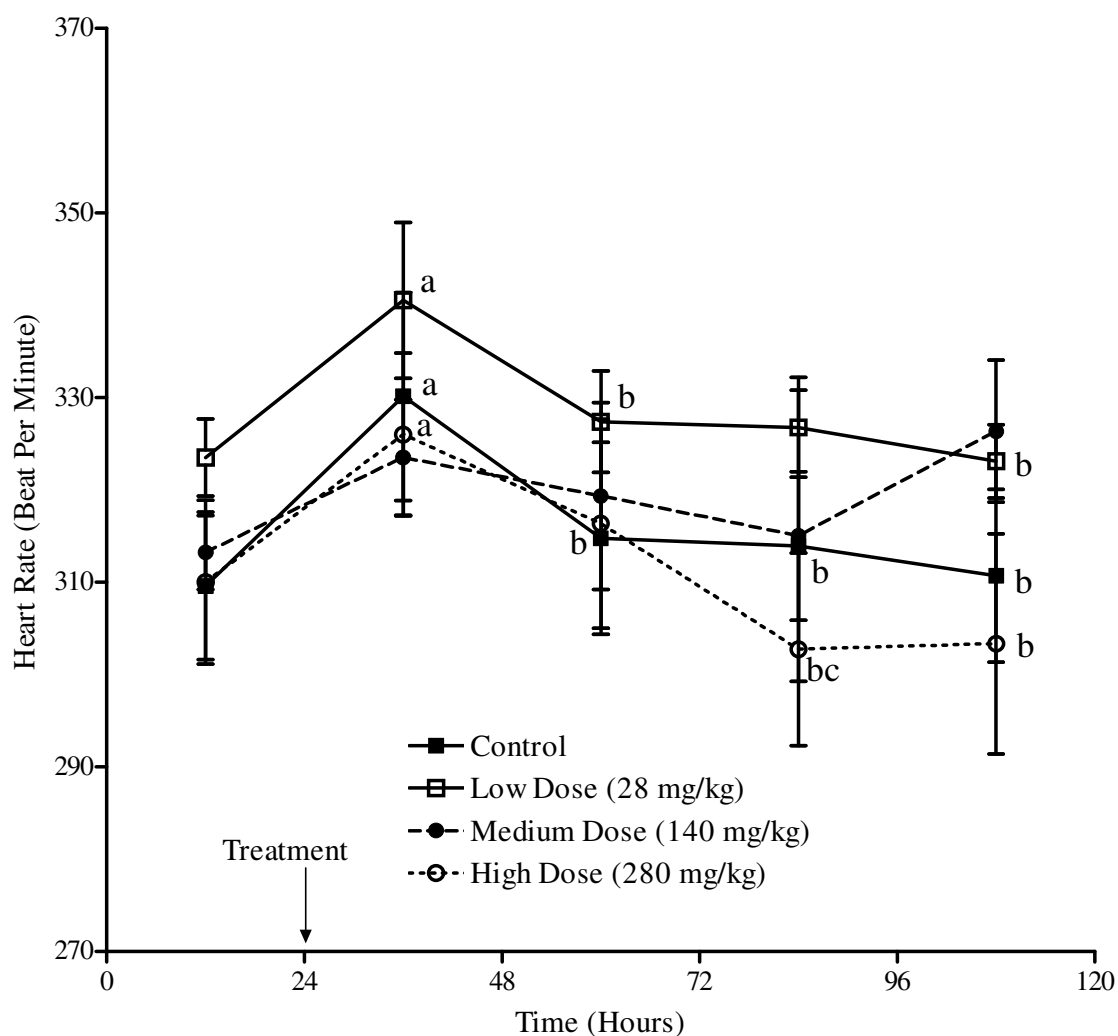
171
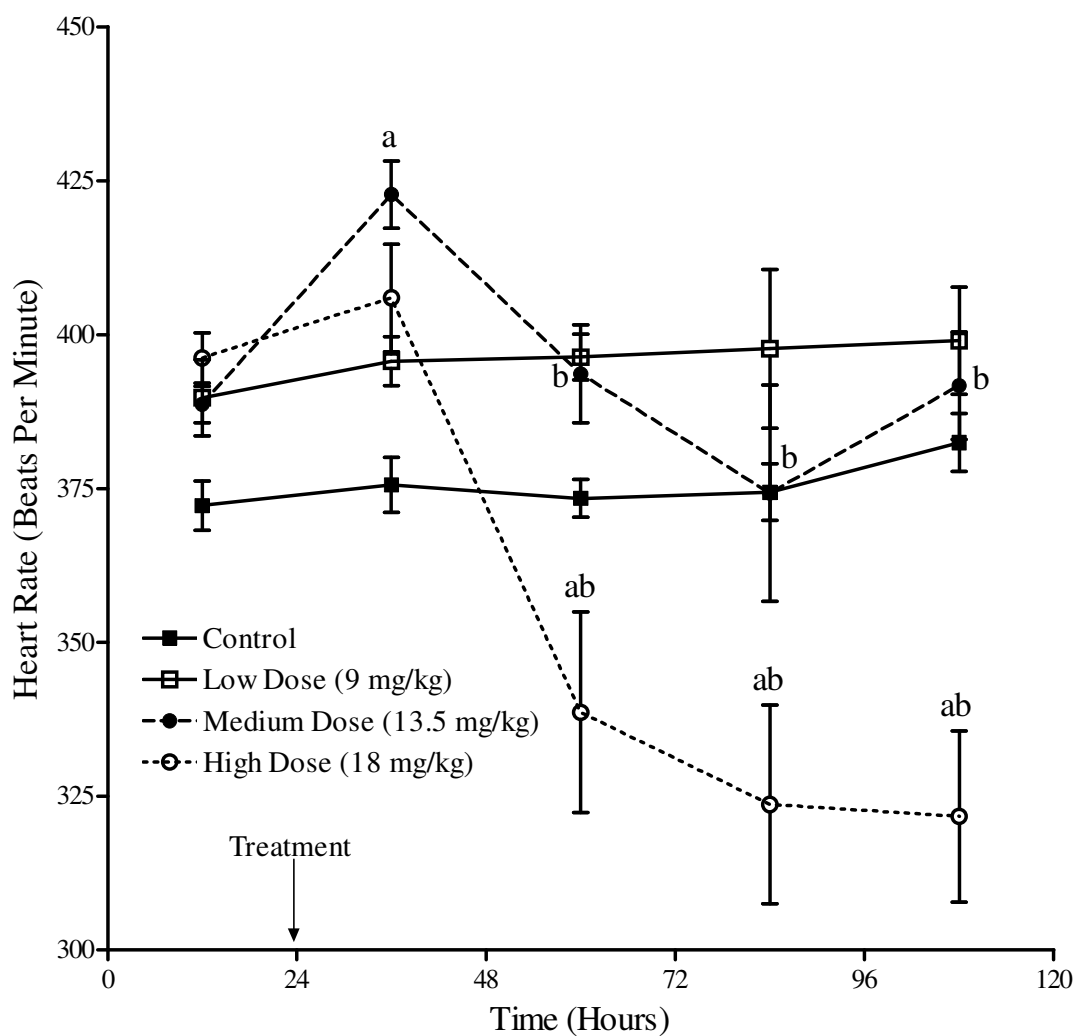
Figure 89: The effects of various doses of PS on heart rate in adult rats during the diurnal (light) periods. Rats (n=4/dose group) were treated subcutaneously with PS at the doses indicated and sacrificed 96 hours later. The graph represents 24 hour baseline (pre-treatment) data followed by 96 hours post-treatment data. The data (mean ± standard error) represents heart rate averaged over 8 hour diurnal intervals. PS produced an initial increase followed by a decrease in heart rate in the medium dose-group and a persistent decrease in the high dose-group. a, and b represent values that are significantly different from the same dose at 12 and 36 hours, respectively.
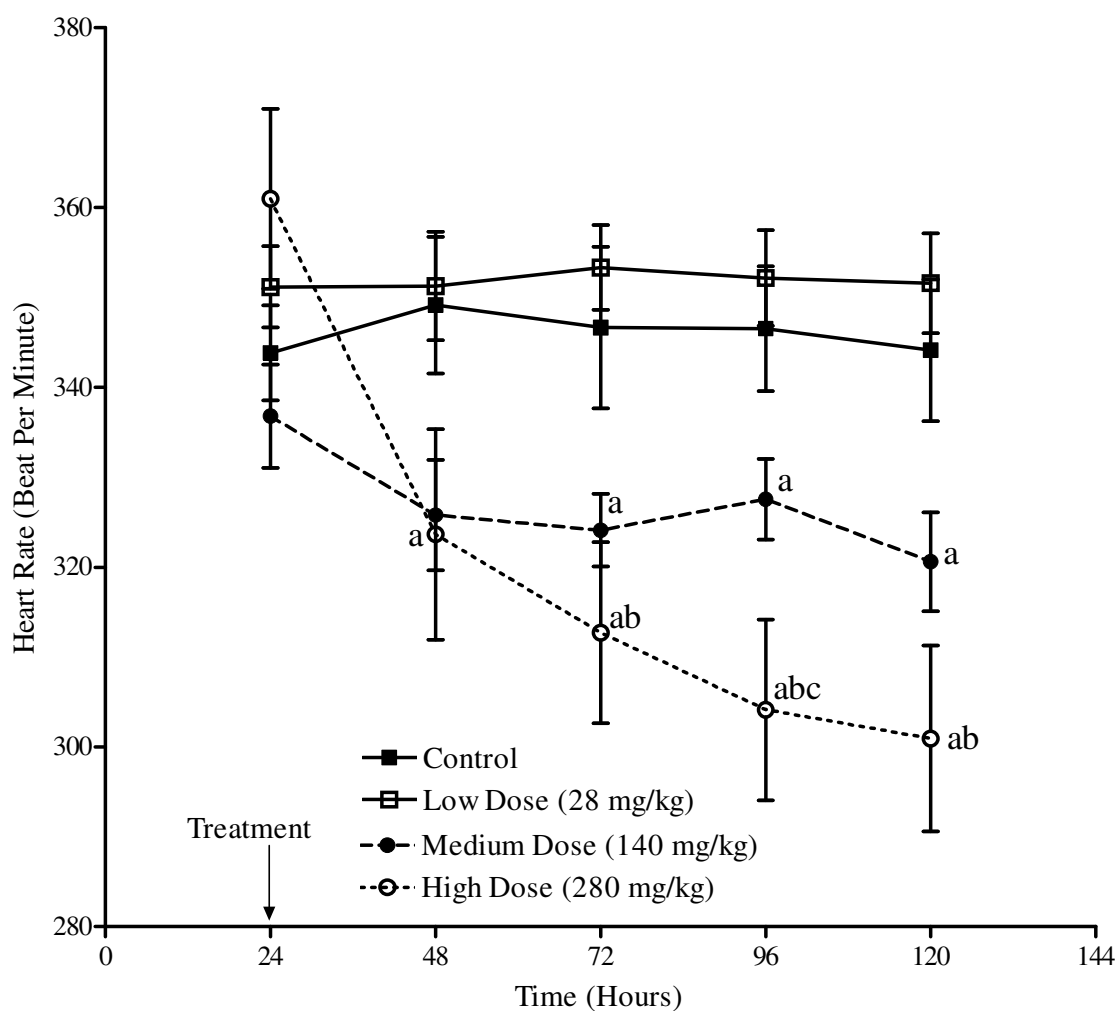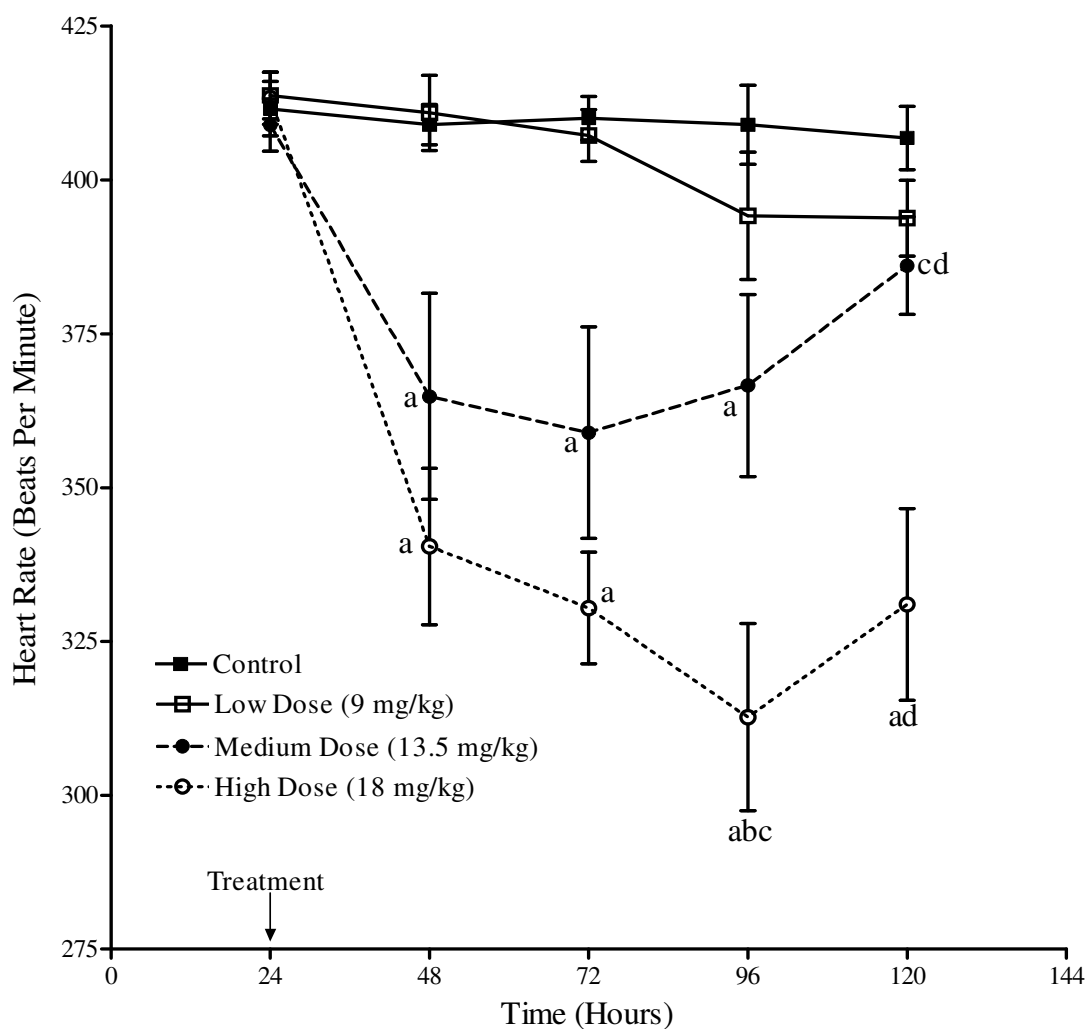
Figure 90: The effects of various doses of PS on heart rate in adult rats during the nocturnal (dark) periods. Rats (n=4/dose group) were treated subcutaneously with PS at the doses indicated and sacrificed 96 hours later. The graph represents 24 hour baseline (pre-treatment) data followed by 96 hours post-treatment data. The data (mean ± standard error) represents heart rate averaged over 8 hour nocturnal intervals. PS produced a dose-dependent decrease in heart rate in the medium and high dose-groups, which persisted until the end of the study. a, b, c, and d represent values that are significantly different from the same dose at 24, 48, 72 and 96 hours, respectively.
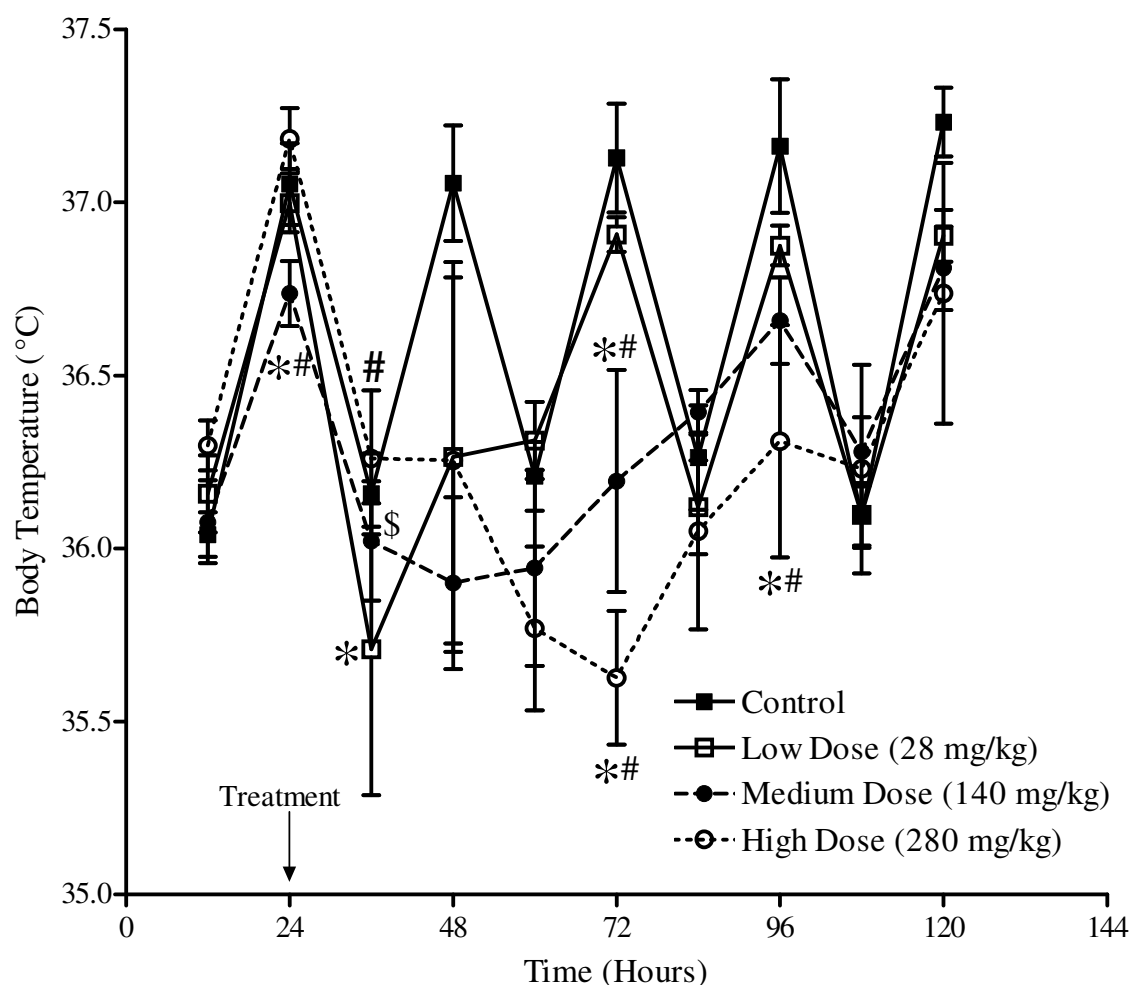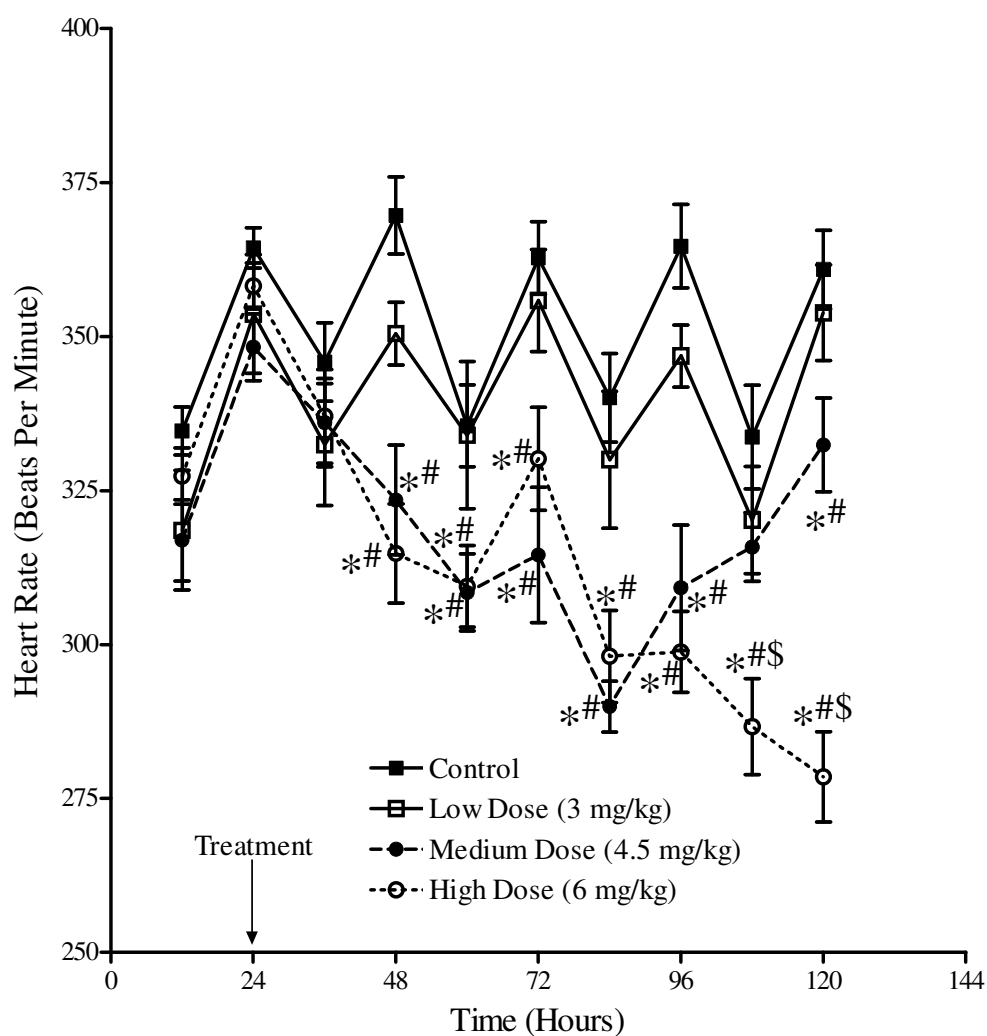
Figure 91: The effects of various doses of PS on heart rate in aged rats. Rats (n=5/dose group) were treated subcutaneously with PS at the doses indicated and sacrificed 96 hours later. The graph represents 24 hour baseline (pre-treatment) data followed by 96 hours post-treatment data. The data (mean ± standard error) represent heart rate averaged over 8 hour diurnal and nocturnal intervals. PS produced a significant and persistent decrease in heart rate in the medium and high dose-groups. The asterisk, pound and dollar signs represent values that are significantly different from control, 3 and 4.5 mg/kg dose groups at the same time point, respectively.
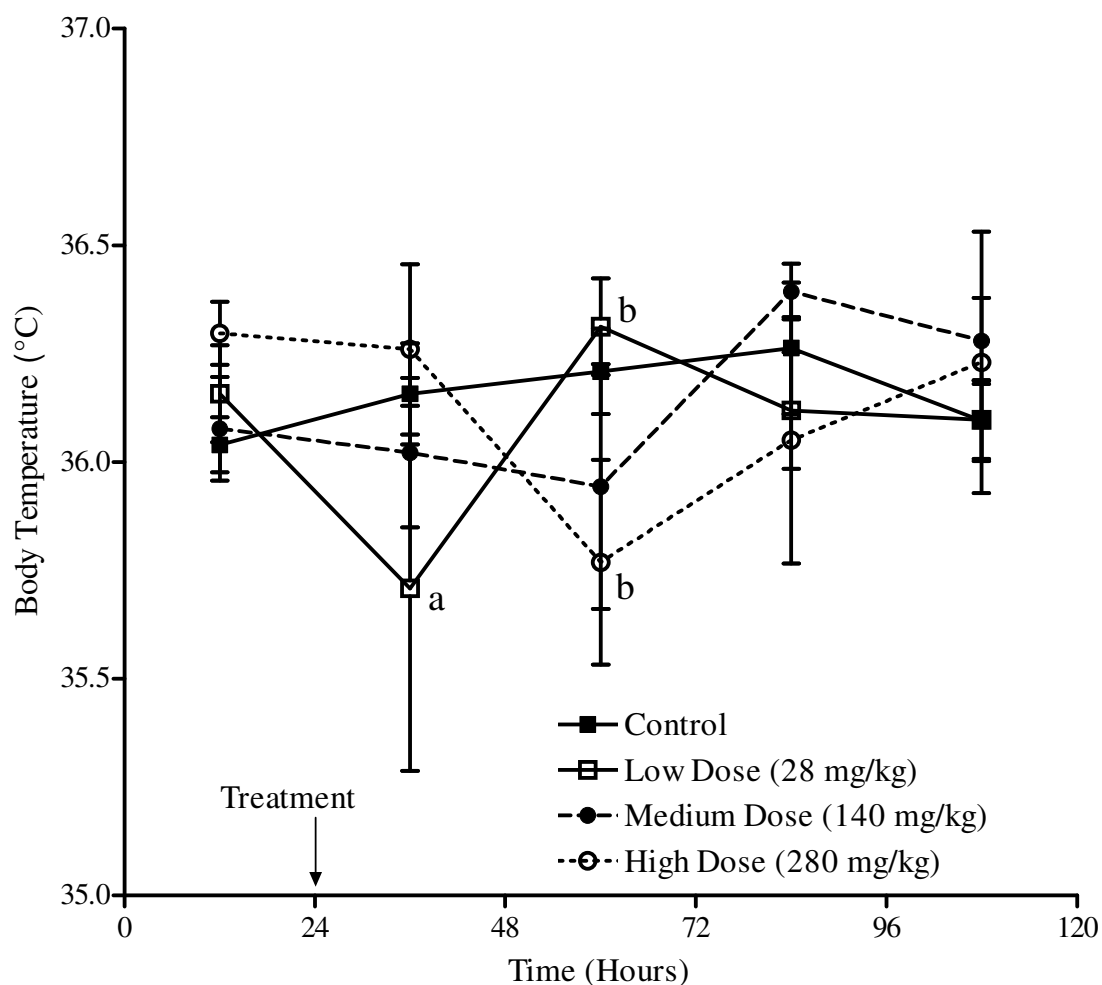
174
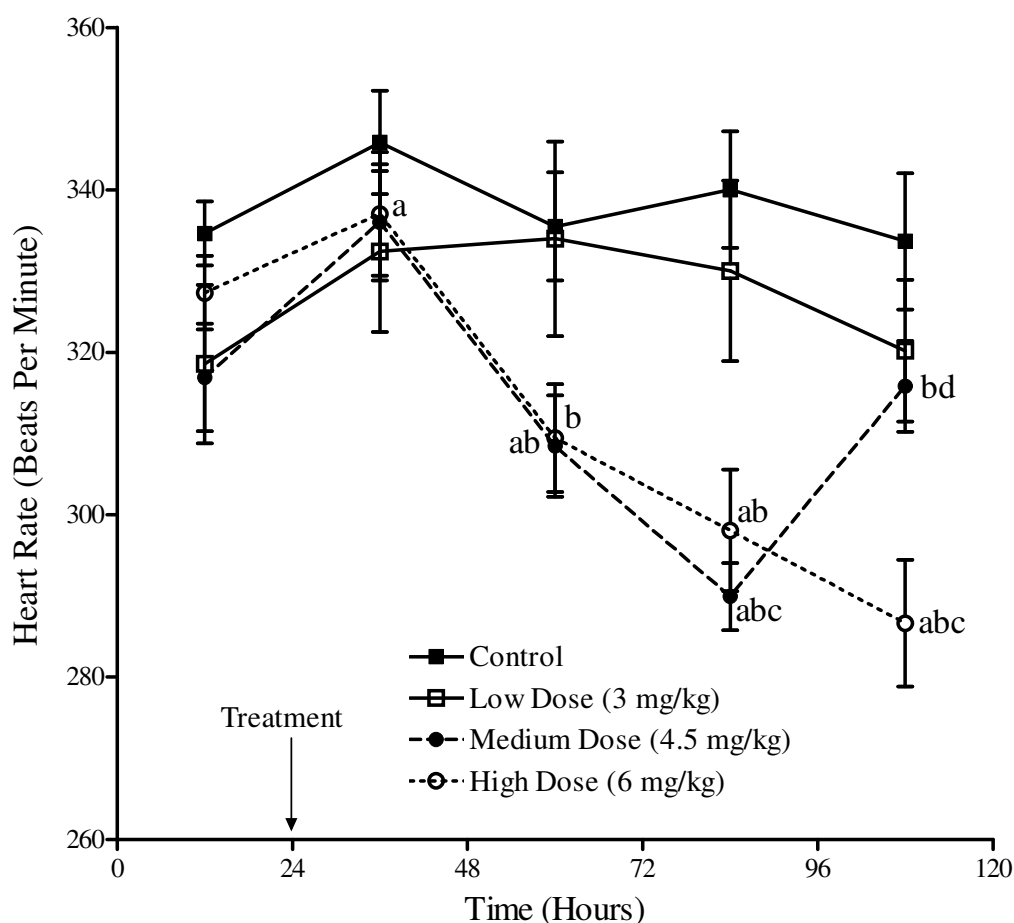
Figure 92: The effects of various doses of PS on heart rate in aged rats during the diurnal (light) periods. Rats (n=5/dose group) were treated subcutaneously with PS at the doses indicated and sacrificed 96 hours later. The graph represents 24 hour baseline (pre-treatment) data followed by 96 hours post-treatment data. The data (mean ± standard error) represents heart rate averaged over 8 hour diurnal intervals. PS produced an initial increase followed by a decrease and a trend towards recovery in heart rate in the medium dose-group, and a persistent decrease in the high dose-group. a, b, c, and d represent values that are significantly different from the same dose at 12, 36, 60 and 84 hours, respectively.
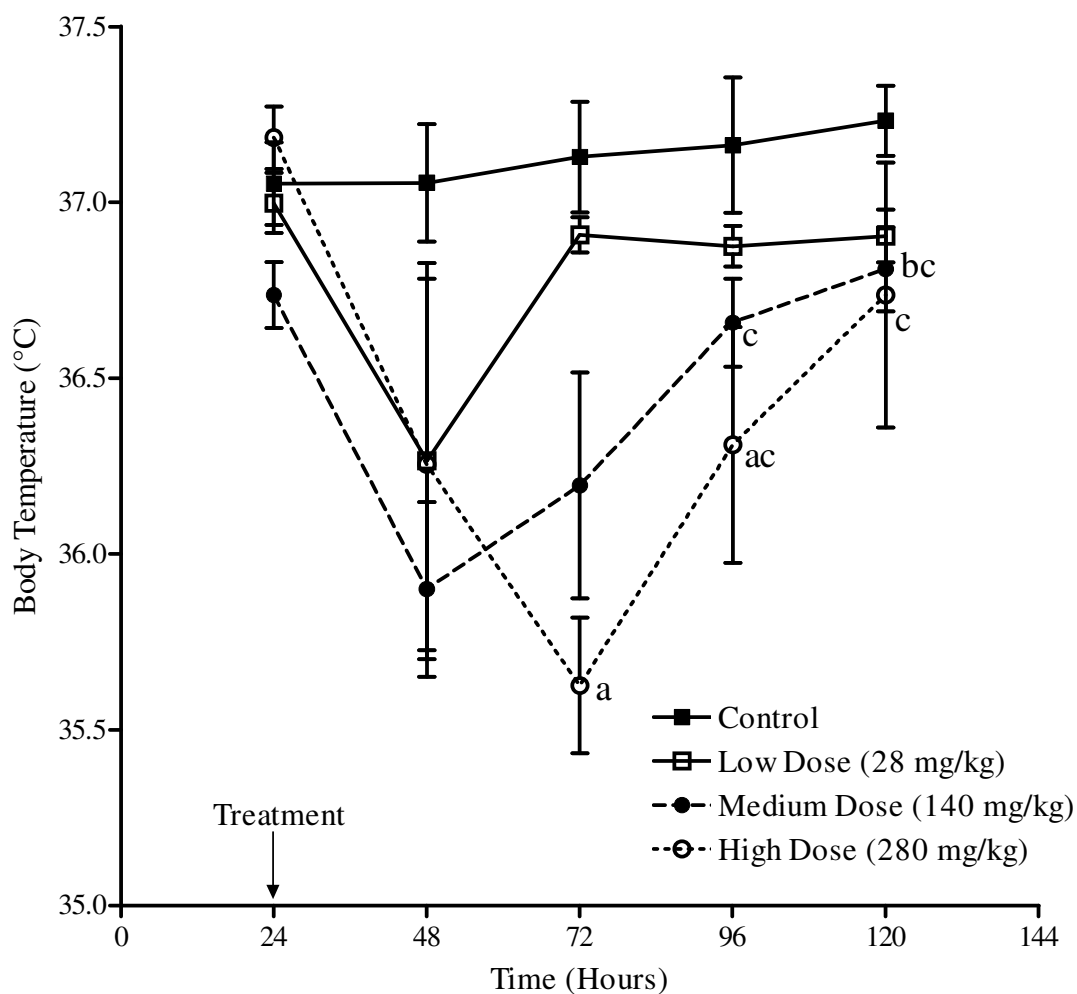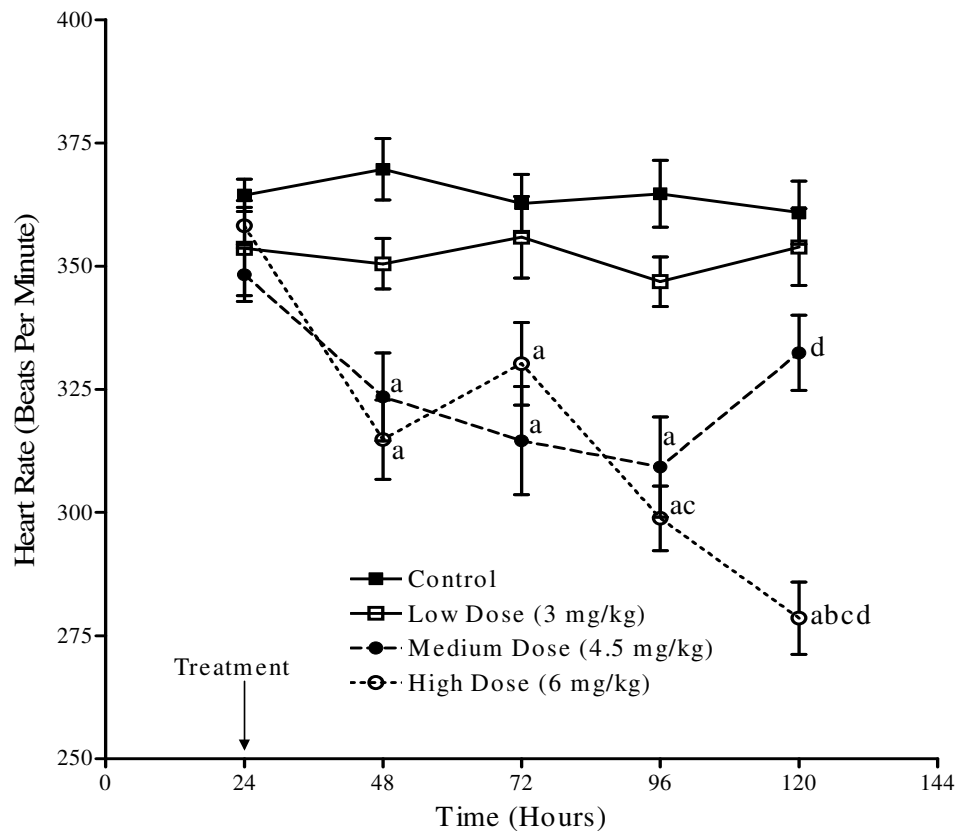
Figure 93: The effects of various doses of PS on heart rate in aged rats during the nocturnal (dark) periods. Rats (n=4/dose group) were treated subcutaneously with PS at the doses indicated and sacrificed 96 hours later. The graph represents 24 hour baseline (pre-treatment) data followed by 96 hours post-treatment data. The data (mean ± standard error) represents heart rate averaged over 8 hour nocturnal intervals. PS produced a dose-dependent decrease in heart rate. The medium dose group showed a trend towards recovery 96 hours post-treatment, while in the high dose group, an initial decrease was followed by a brief period of increase (48 hours after treatment), after which the heart rate continued to decrease significantly until the end of the study. a, b, c, and d represent values that are significantly different from the same dose at 24, 48, 72 and 96 hours, respectively.
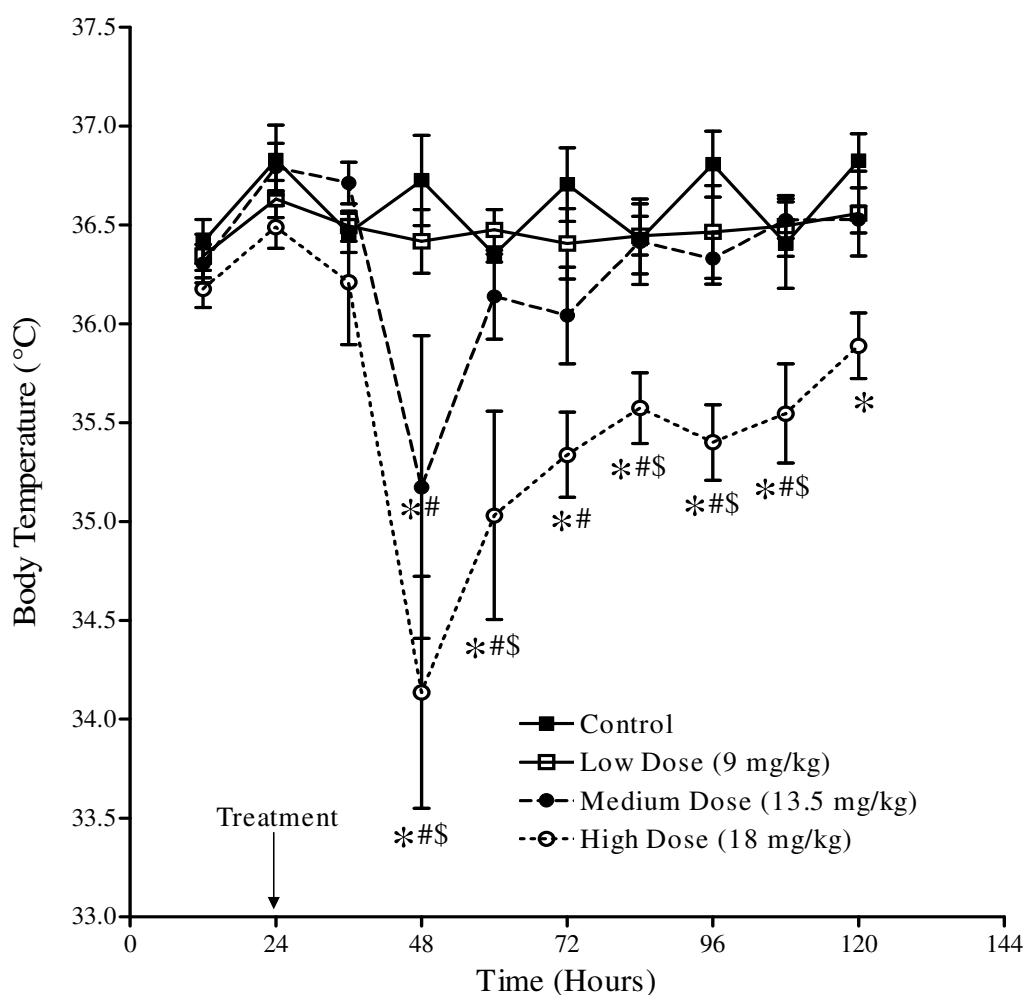
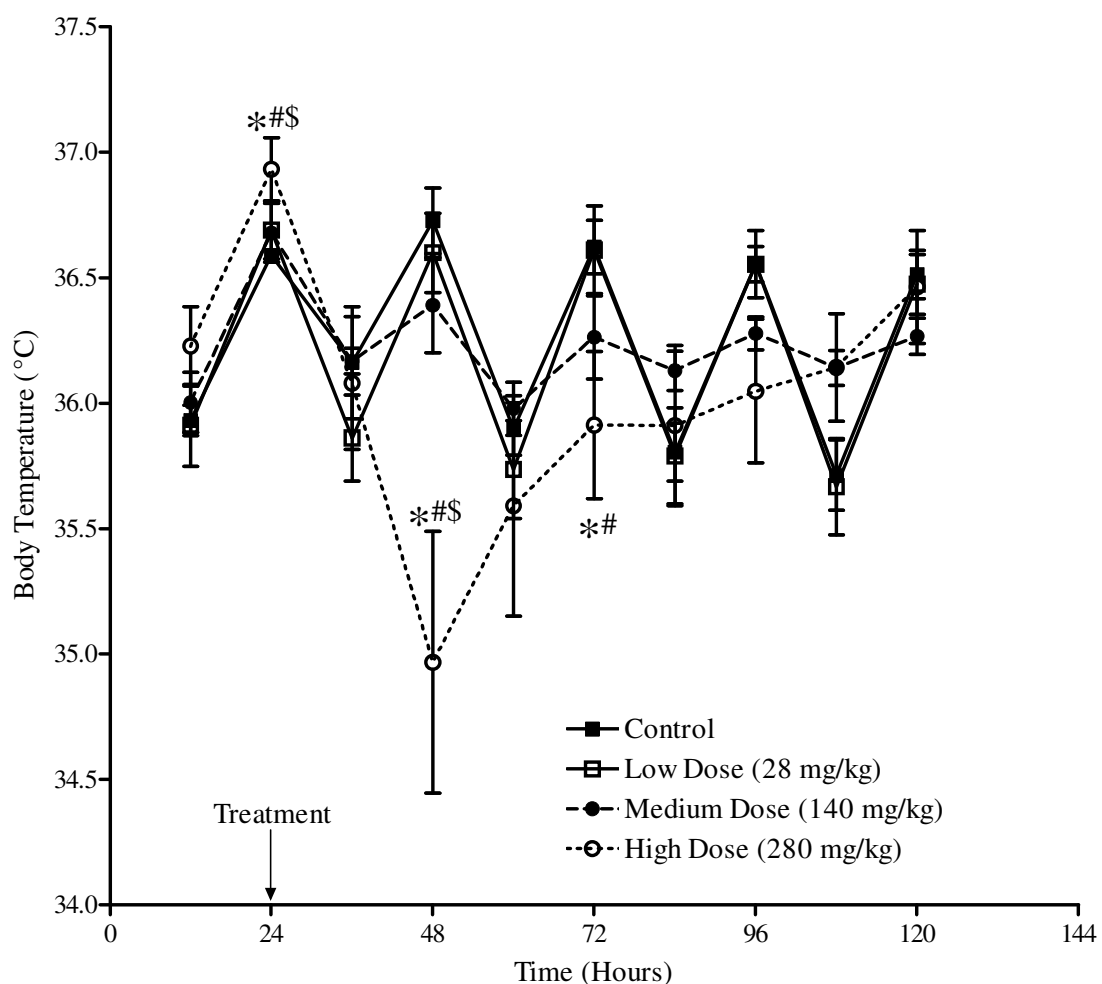Figure 94: The effects of various doses of PS on body temperature in adult rats. Rats (n=4/dose group) were treated subcutaneously with PS at the doses indicated and sacrificed 96 hours later. The graph represents 24 hour baseline (pre-treatment) data followed by 96 hours post-treatment data. The data (mean ± standard error) represents body temperature averaged over 8 hour diurnal and nocturnal intervals. PS produced a dose-dependent decrease in body temperature, which recovered to control values in the medium dose-group, and remained depressed in the high dose-group by the end of the study. The asterisk, pound and dollar signs represent values that are significantly different from control, 9 and 13.5 mg/kg dose groups at the same time point, respectively.
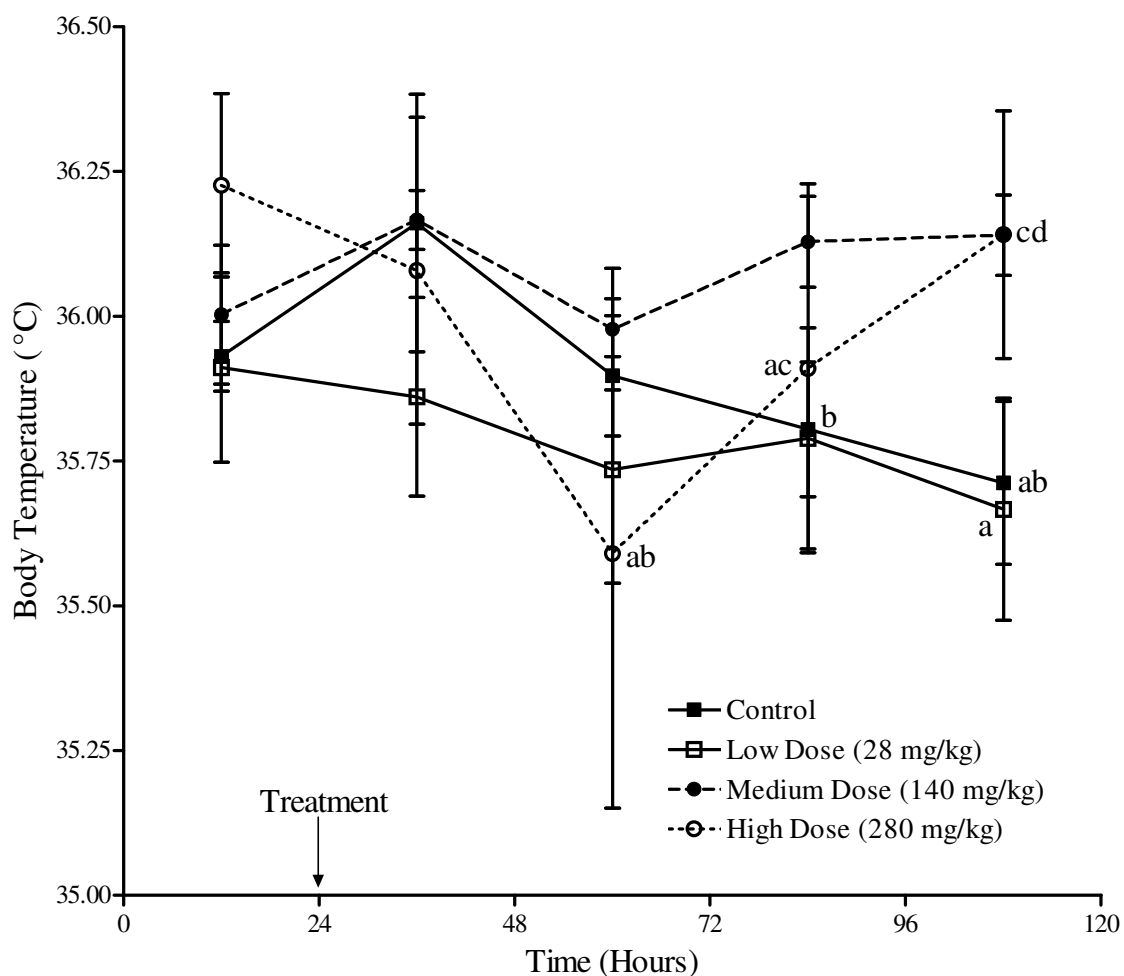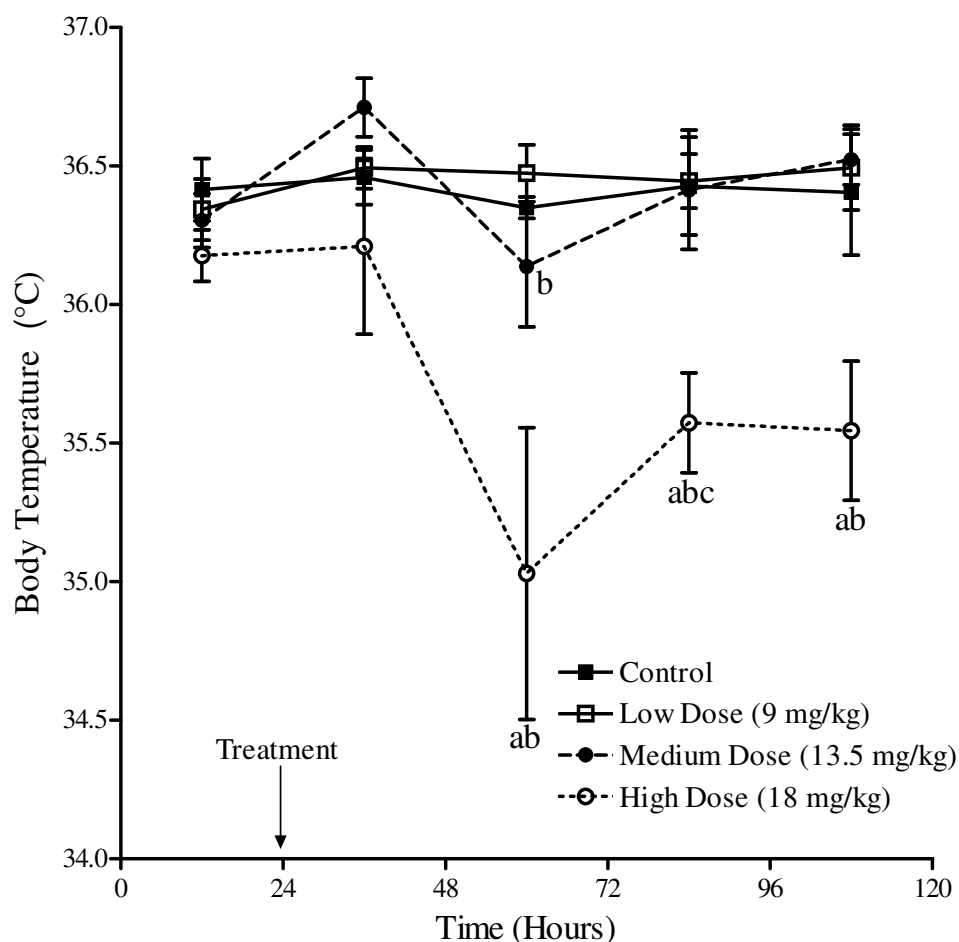
Figure 95: The effects of various doses of PS on body temperature in adult rats during the diurnal (light) periods. Rats (n=4/dose group) were treated subcutaneously with PS at the doses indicated and sacrificed 96 hours later. The graph represents 24 hour baseline (pre-treatment) data followed by 96 hours post-treatment data. The data (mean ± standard error) represents body temperature averaged over 8 hour diurnal intervals. PS produced a diurnal decrease in body temperature in the high dose-group which peaked 36 hours post-treatment and remained depressed until the end of the study. a, b, and c represent values that are significantly different from the same dose at 12, 36 and 60 hours respectively.
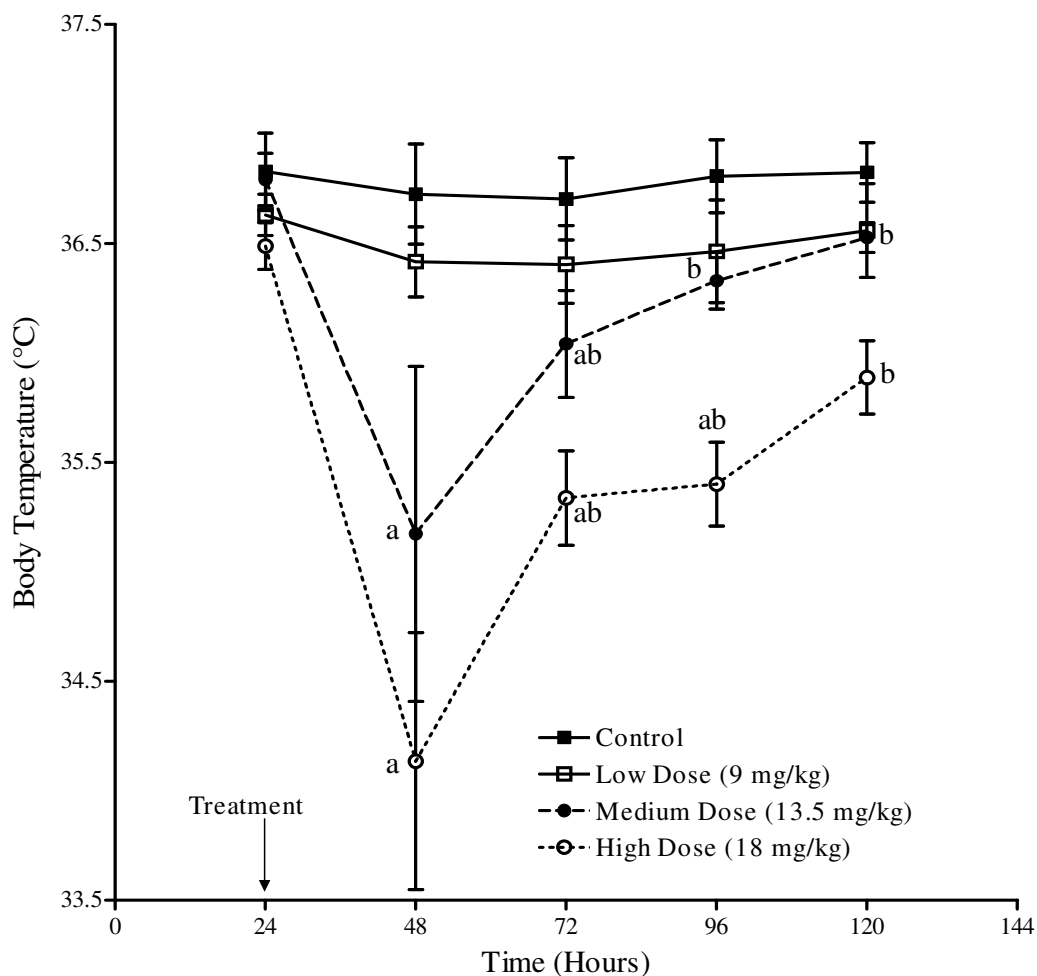
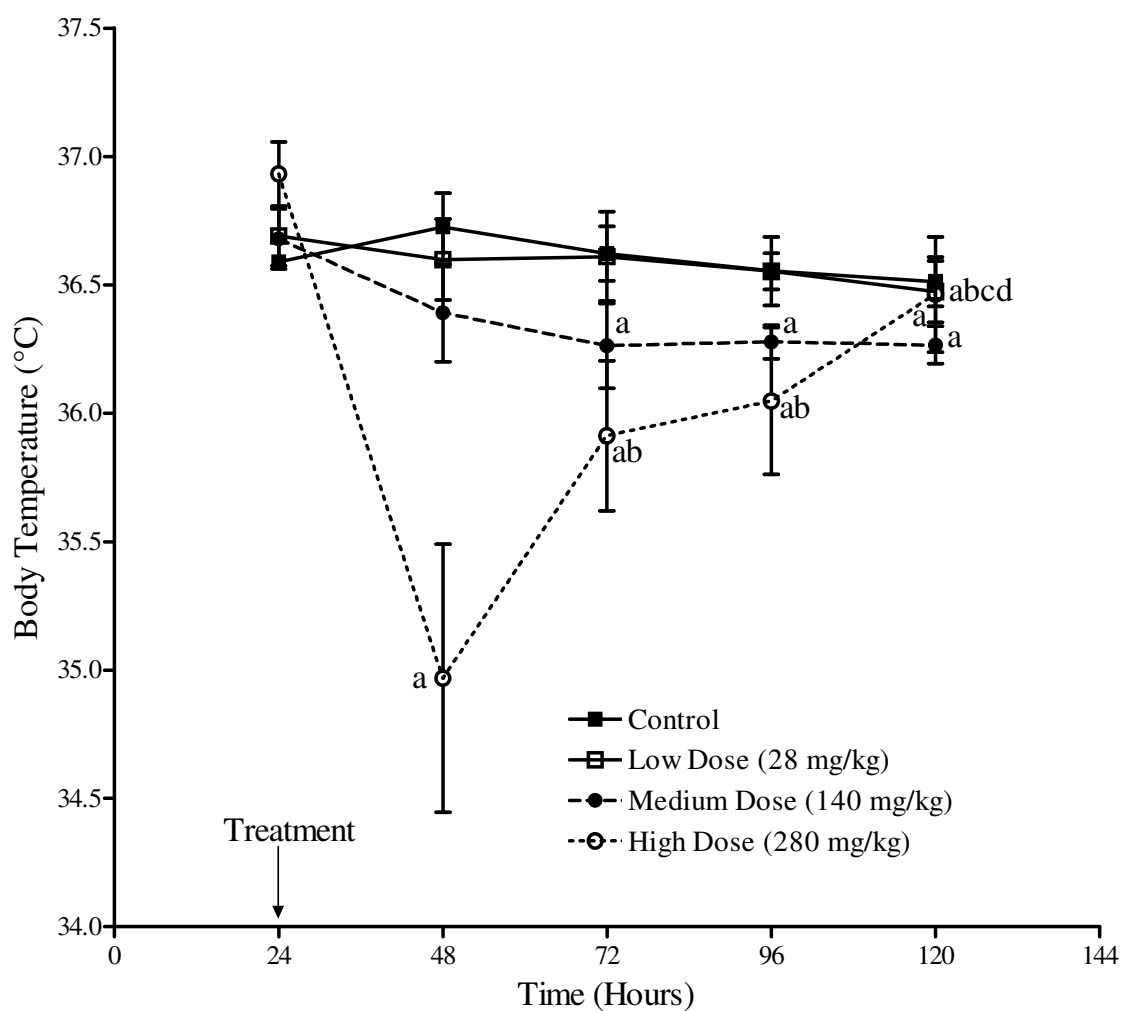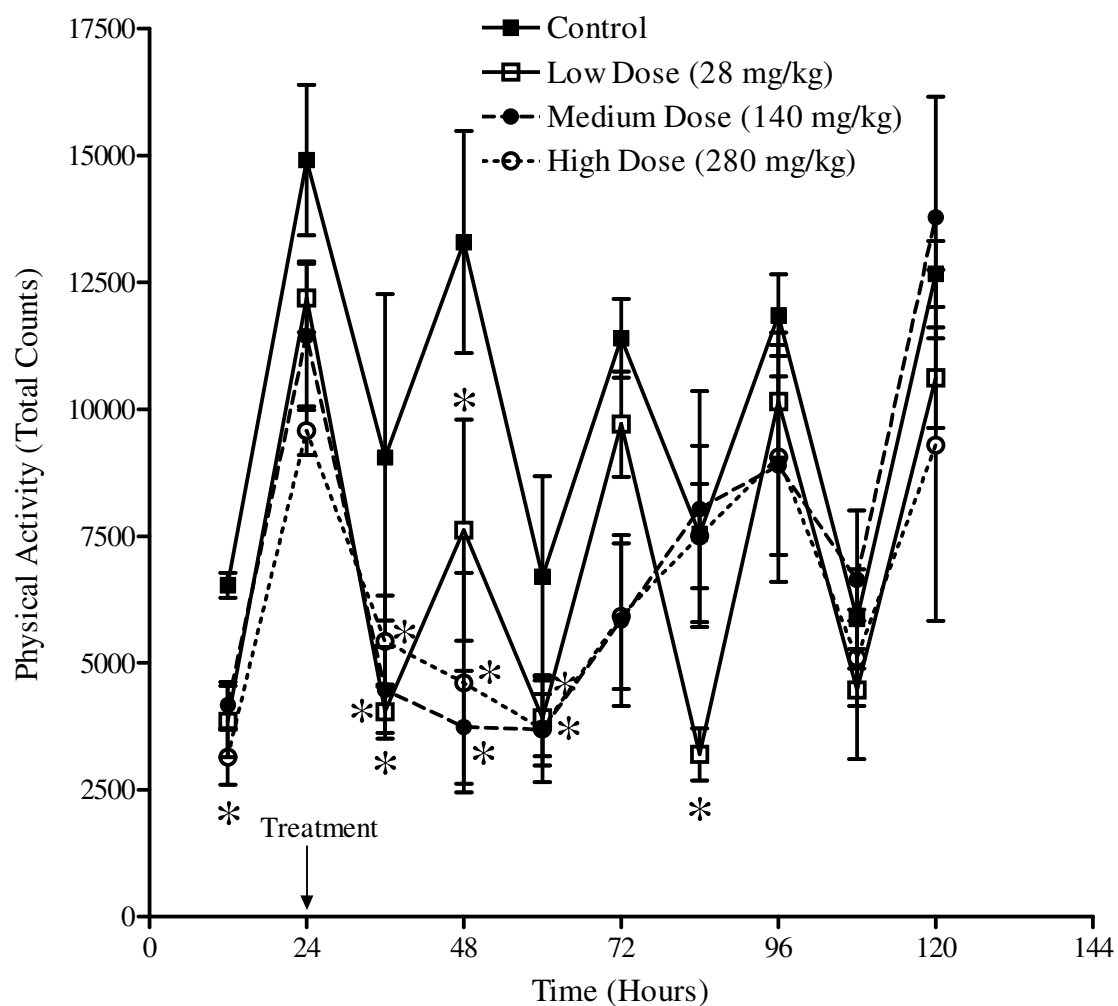Figure 96: The effects of various doses of PS on body temperature in adult rats during the nocturnal (dark) periods. Rats (n=4/dose group) were treated subcutaneously with PS at the doses indicated and sacrificed 96 hours later. The graph represents 24 hour baseline (pre-treatment) data followed by 96 hours post-treatment data. The data (mean ± standard error) represents body temperature averaged over 8 hour nocturnal intervals. PS produced a dose-dependent decrease in body temperature in the medium and high dose-groups, which recovered to pre-treatment values in the medium dose-group and persisted until the end of the study in the high dose-group. a, and b represent values that are significantly different from the same dose at 24 and 48 hours, respectively.
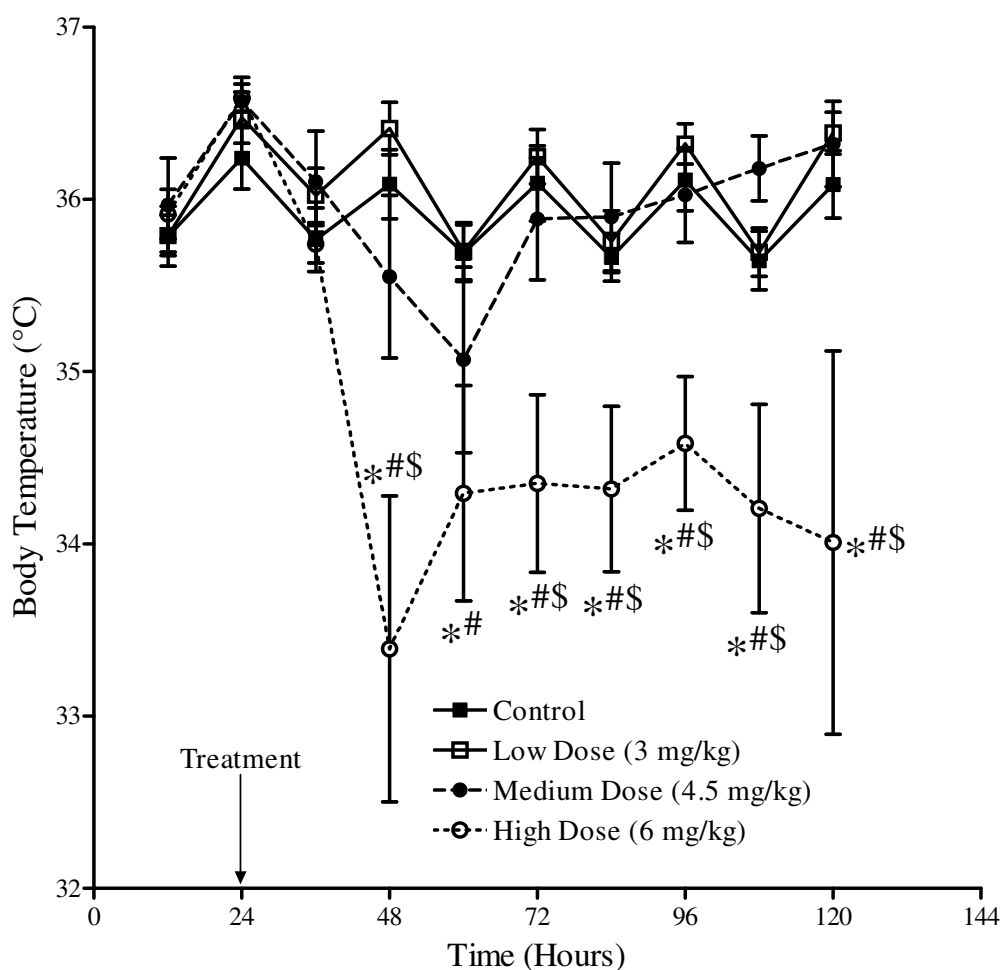
Figure 97: The effects of various doses of PS on body temperature in aged rats. Rats (n=5/dose group) were treated subcutaneously with PS at the doses indicated and sacrificed 96 hours later. The graph represents 24 hour baseline (pre-treatment) data followed by 96 hours post-treatment data. The data (mean ± standard error) represent body temperature averaged over 8 hour diurnal and nocturnal intervals. PS produced a significant and persistent decrease in body temperature in the high dose-group. The asterisk, pound and dollar signs represent values that are significantly different from control, 3 and 4.5 mg/kg dose groups at the same time point, respectively.
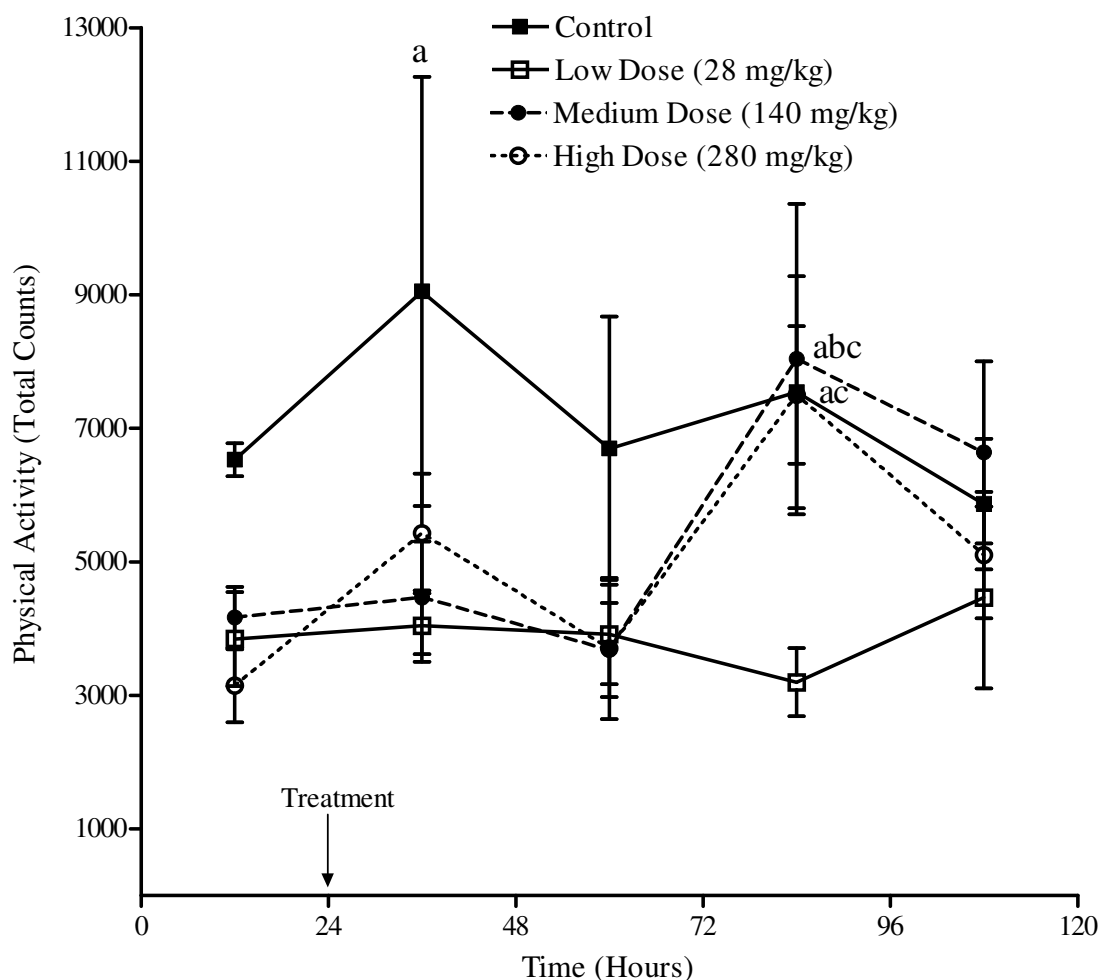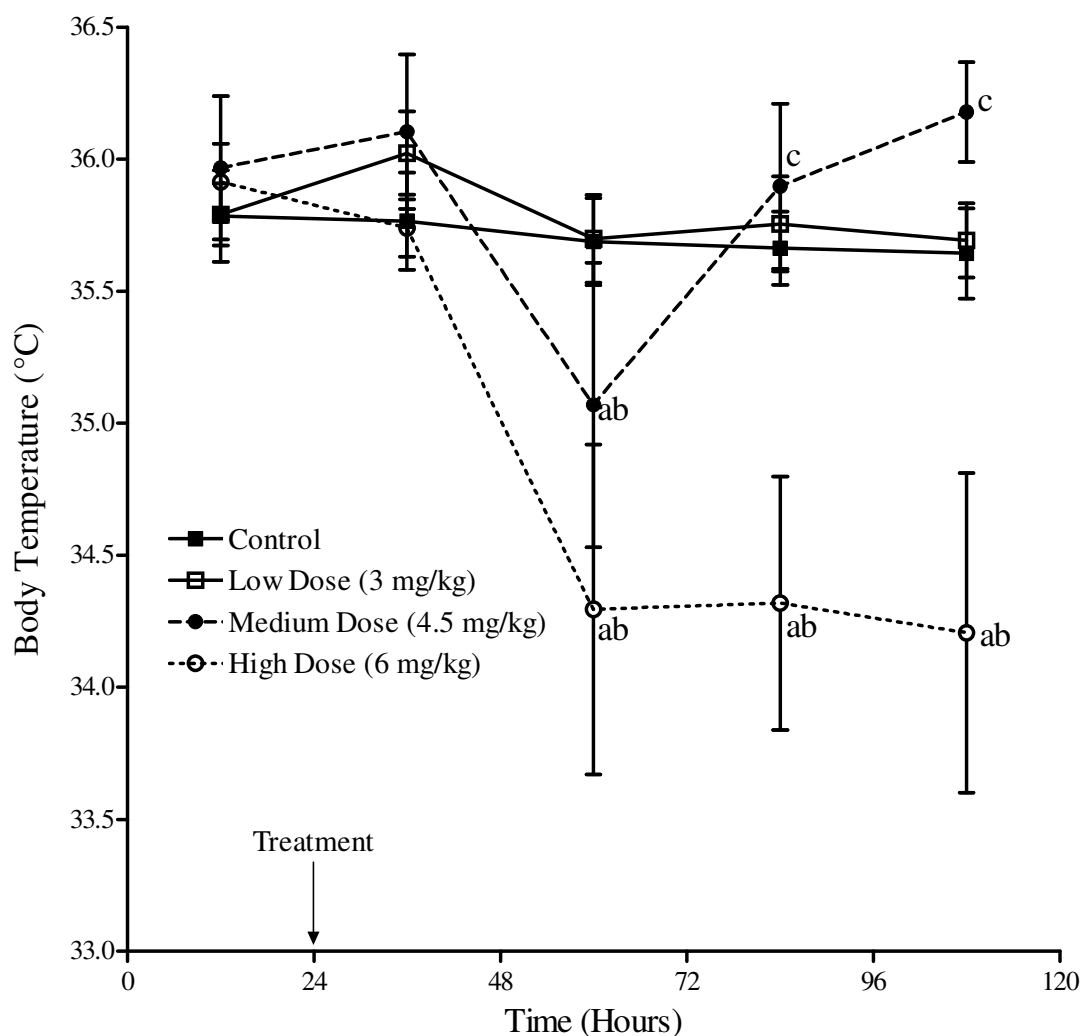
Figure 98: The effects of various doses of PS on body temperature in aged rats during the diurnal (light) periods. Rats (n=5/dose group) were treated subcutaneously with PS at the doses indicated and sacrificed 96 hours later. The graph represents 24 hour baseline (pre-treatment) data followed by 96 hours post-treatment data. The data (mean ± standard error) represents body temperature averaged over 8 hour diurnal intervals. PS produced a decrease in body temperature followed by a trend towards recovery in the medium dose-group, and a persistent decrease in the high dose-group. a, b, and c represent values that are significantly different from the same dose at 12, 36 and 60 hours, respectively.
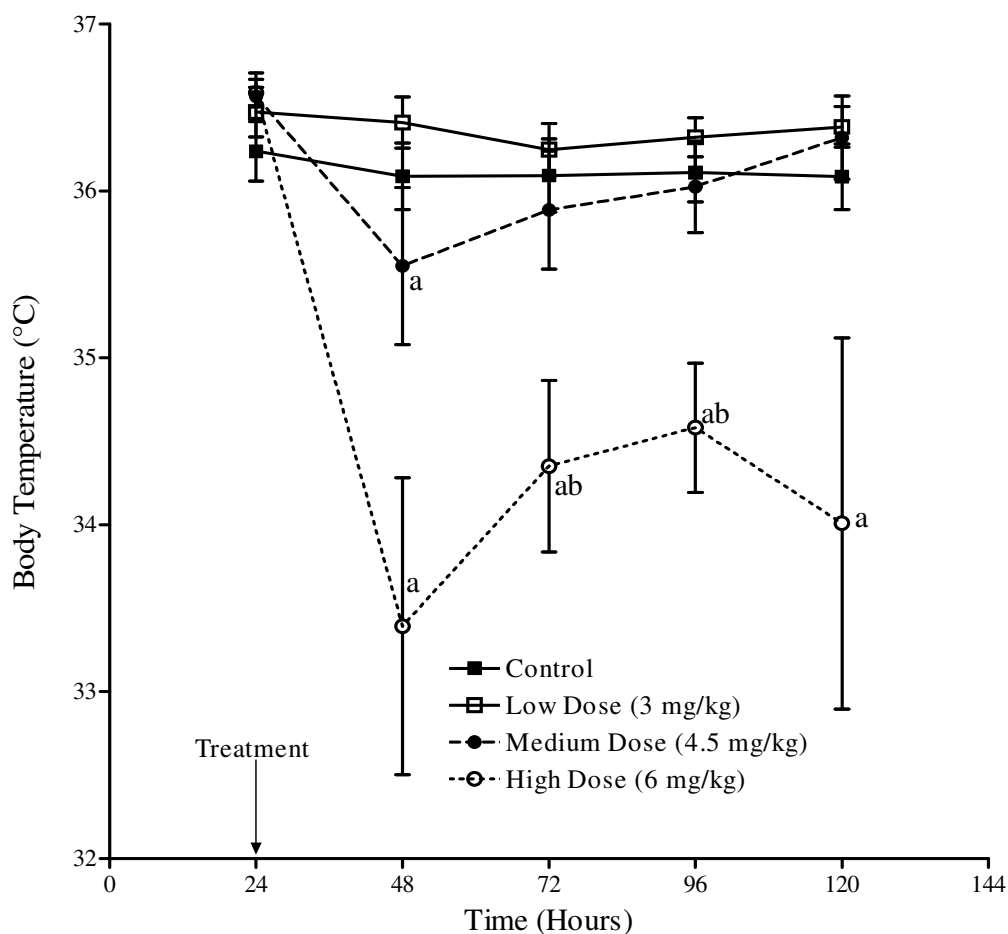
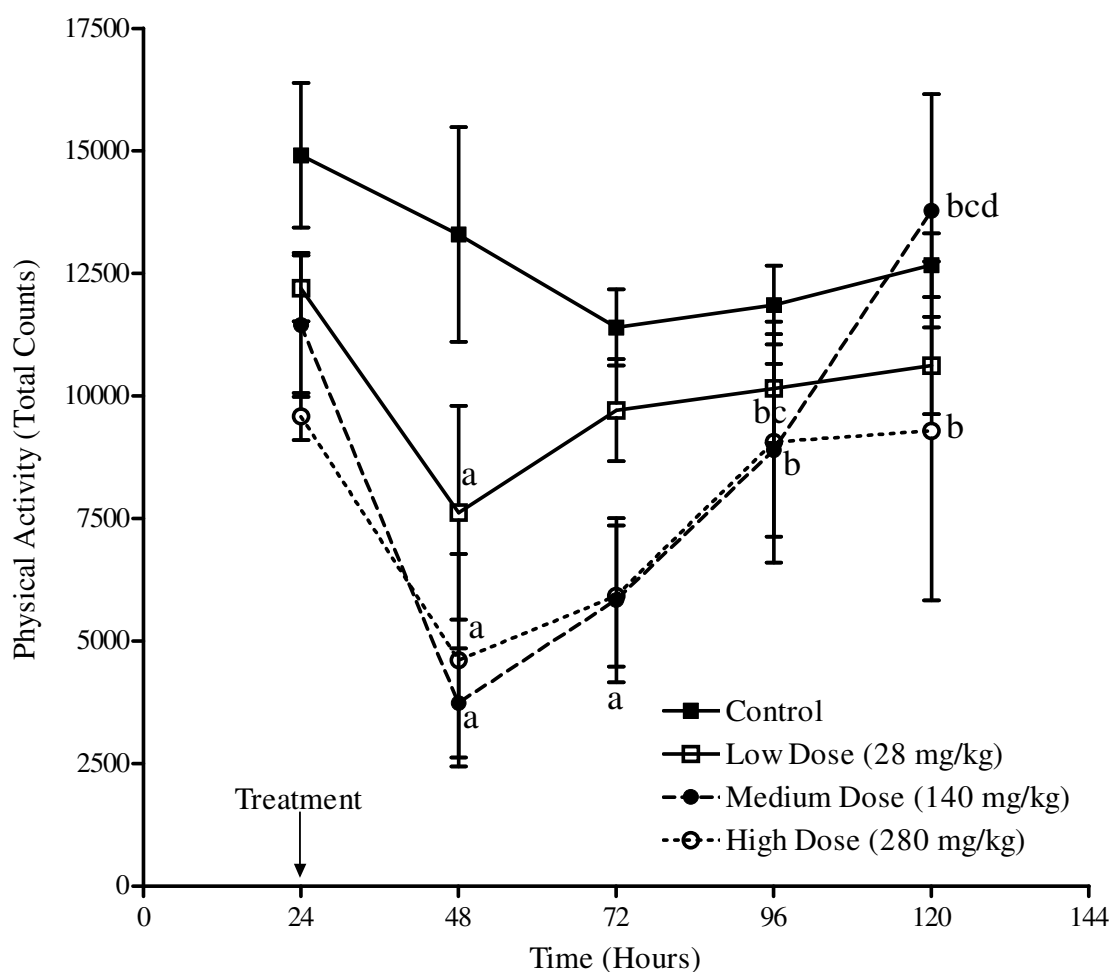Figure 99: The effects of various doses of PS on body temperature in aged rats during the nocturnal (dark) periods. Rats (n=4/dose group) were treated subcutaneously with PS at the doses indicated and sacrificed 96 hours later. The graph represents 24 hour baseline (pre-treatment) data followed by 96 hours post-treatment data. The data (mean ± standard error) represents body temperature averaged over 8 hour nocturnal intervals. PS produced a dose-dependent decrease in body temperature. By the end of the study, the body temperature in the medium dose group had recovered to baseline values, while it remained depressed in the high dose group. a, and b represent values that are significantly different from the same dose at 24 and 48 hours, respectively.
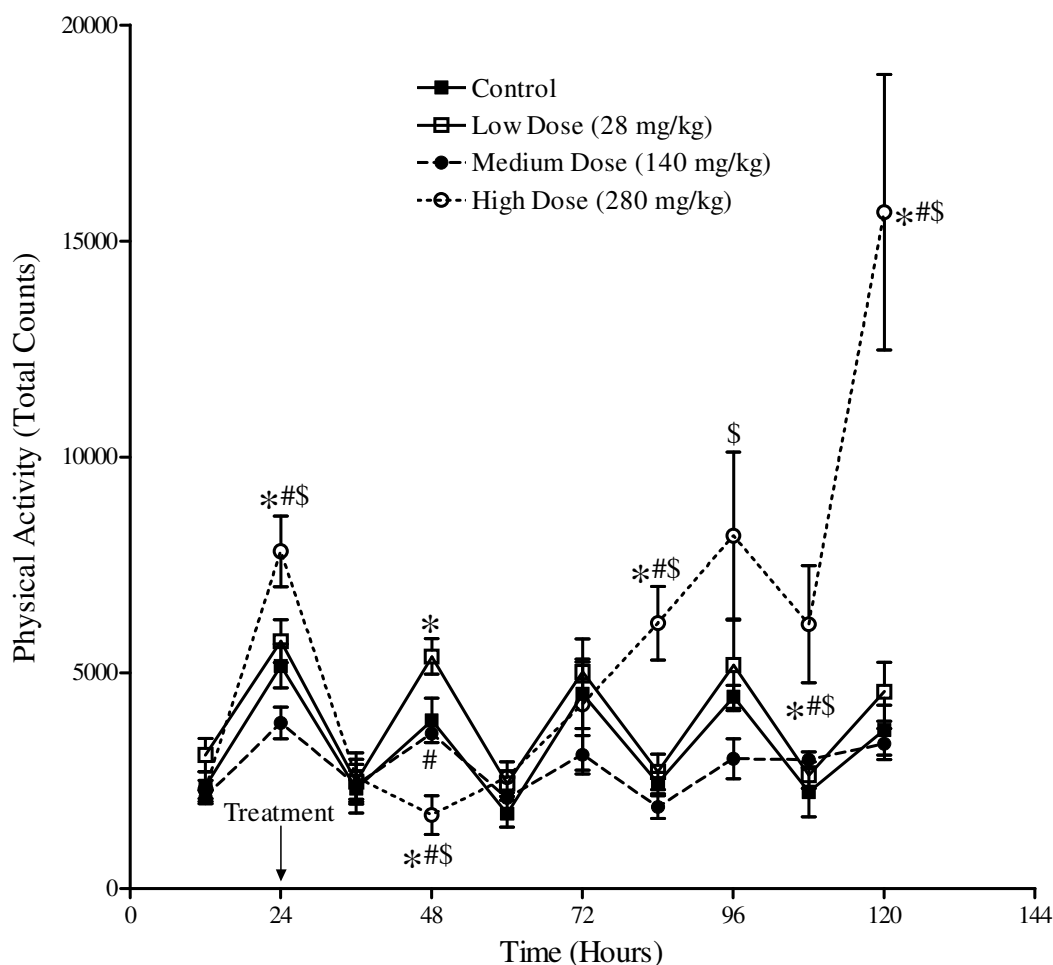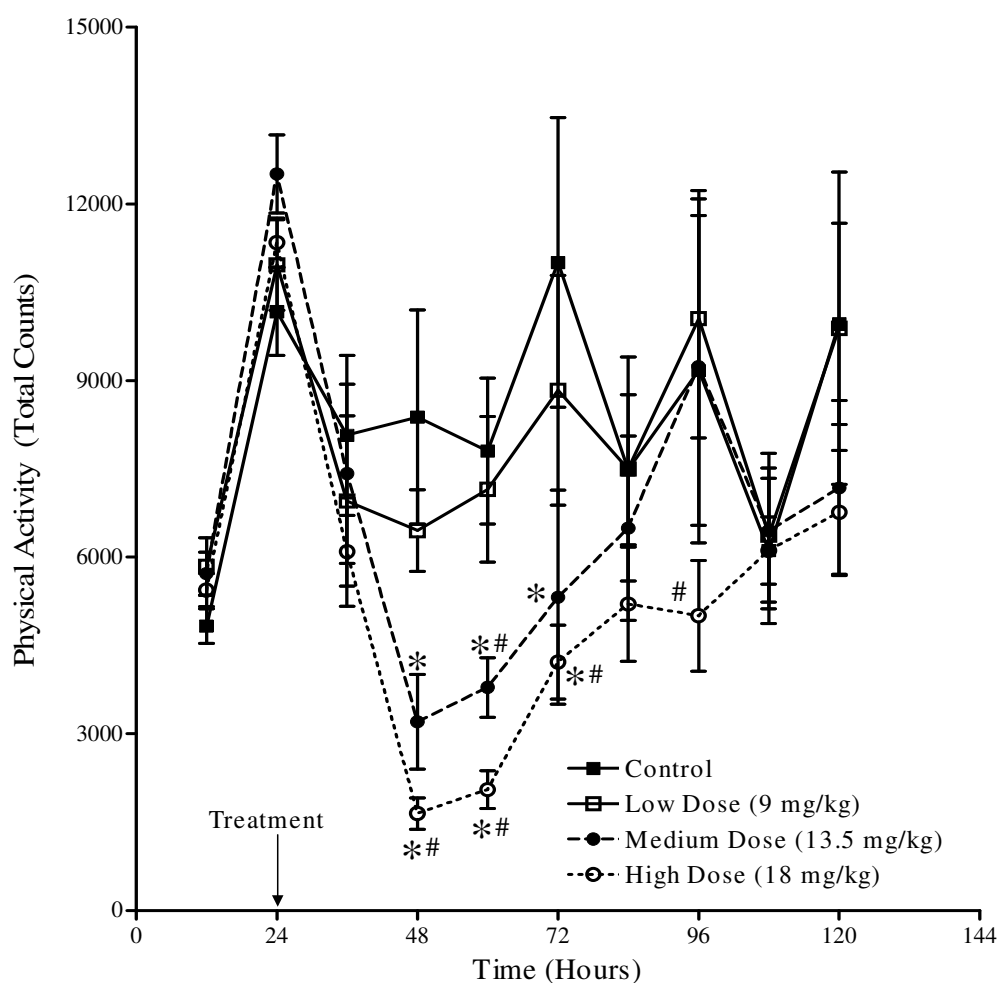
Figure 100: The effects of various doses of PS on physical activity in adult rats. Rats (n=4/dose group) were treated subcutaneously with PS at the doses indicated and sacrificed 96 hours later. The graph represents 24 hour baseline (pre-treatment) data followed by 96 hours post-treatment data. The data (mean ± standard error) represents physical activity averaged over 8 hour diurnal and nocturnal intervals. PS produced a dose-dependent decrease in physical activity in the medium and high dose-groups, which peaked at 24 hours post-treatment, and started recovering thereafter. The asterisk and pound signs represent values that are significantly different from control and 9 mg/kg dose groups at the same time point, respectively.
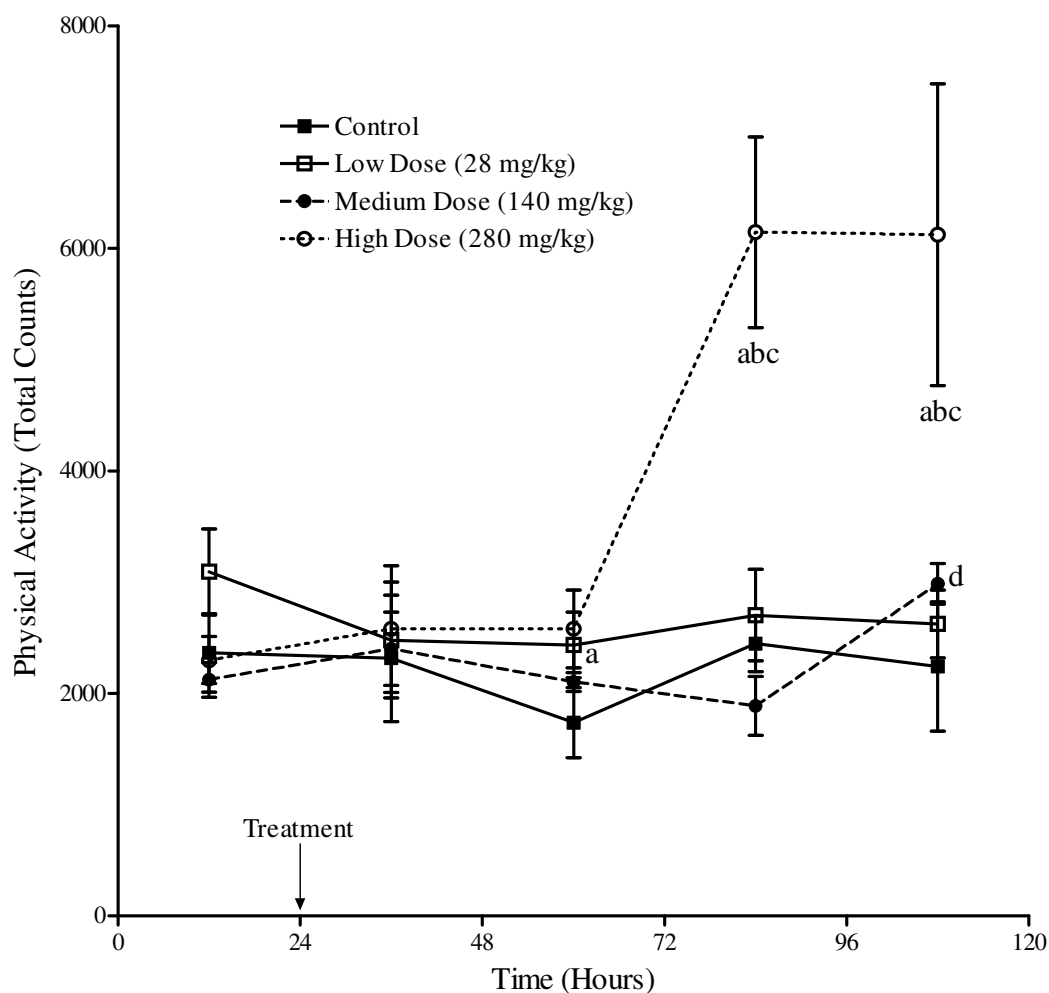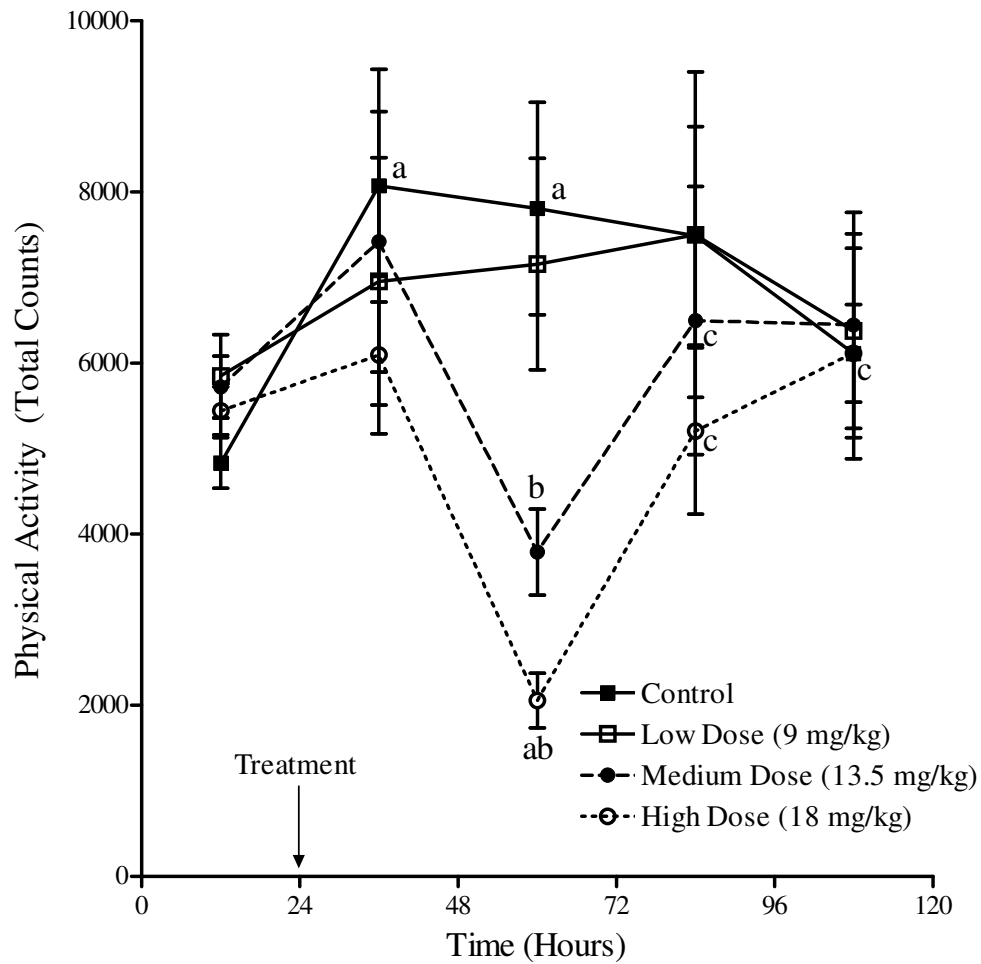
Figure 101: The effects of various doses of PS on physical activity in adult rats during the diurnal (light) periods. Rats (n=4/dose group) were treated subcutaneously with PS at the doses indicated and sacrificed 96 hours later. The graph represents 24 hour baseline (pre-treatment) data followed by 96 hours post-treatment data. The data (mean ± standard error) represents physical activity averaged over 8 hour diurnal intervals. PS produced a diurnal decrease in physical activity in the medium and high dose-group, which peaked 36 hours post-treatment and recovered to baseline values thereafter. a, b, and c represent values that are significantly different from the same dose at 12, 36 and 60 hours, respectively.
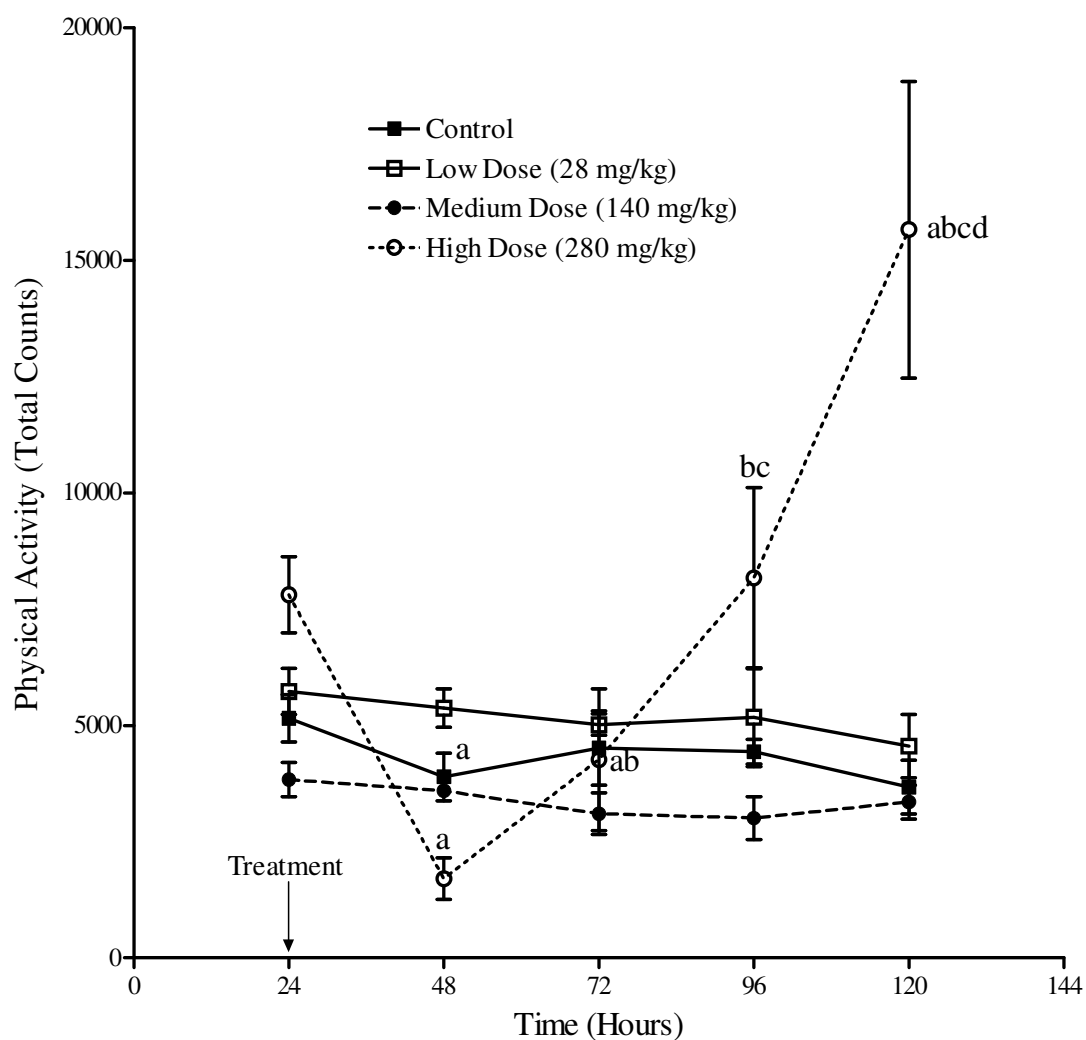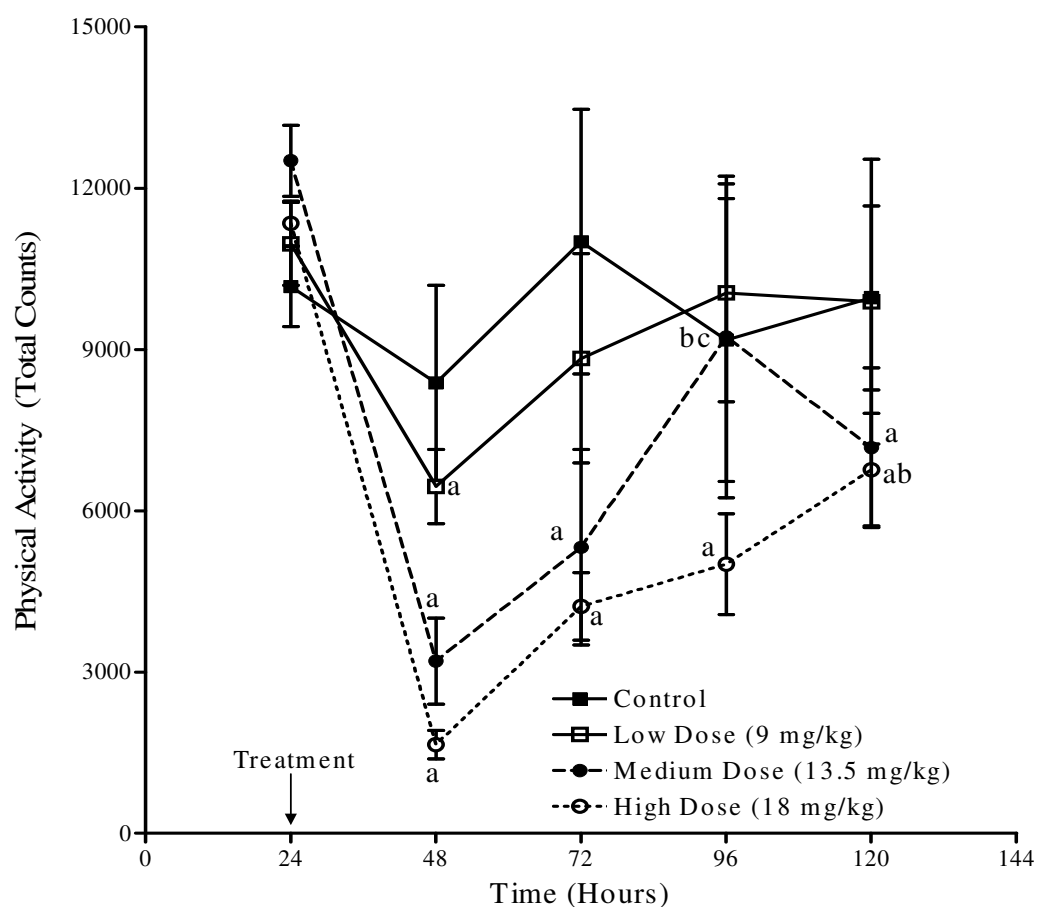
Figure 102: The effects of various doses of PS on physical activity in adult rats during the nocturnal (dark) periods. Rats (n=4/dose group) were treated subcutaneously with PS at the doses indicated and sacrificed 96 hours later. The graph represents 24 hour baseline (pre-treatment) data followed by 96 hours post-treatment data. The data (mean ± standard error) represents physical activity averaged over 8 hour nocturnal intervals. PS produced a dose-dependent decrease in nocturnal physical activity, which peaked 24 hours after treatment. The physical activity in the low dose-group recovered to baseline values, while in the medium and high dose-groups, it remained depressed until the end of the study. a, b, and c represent values that are significantly different from the same dose at 24, 48 and 72 hours, respectively.
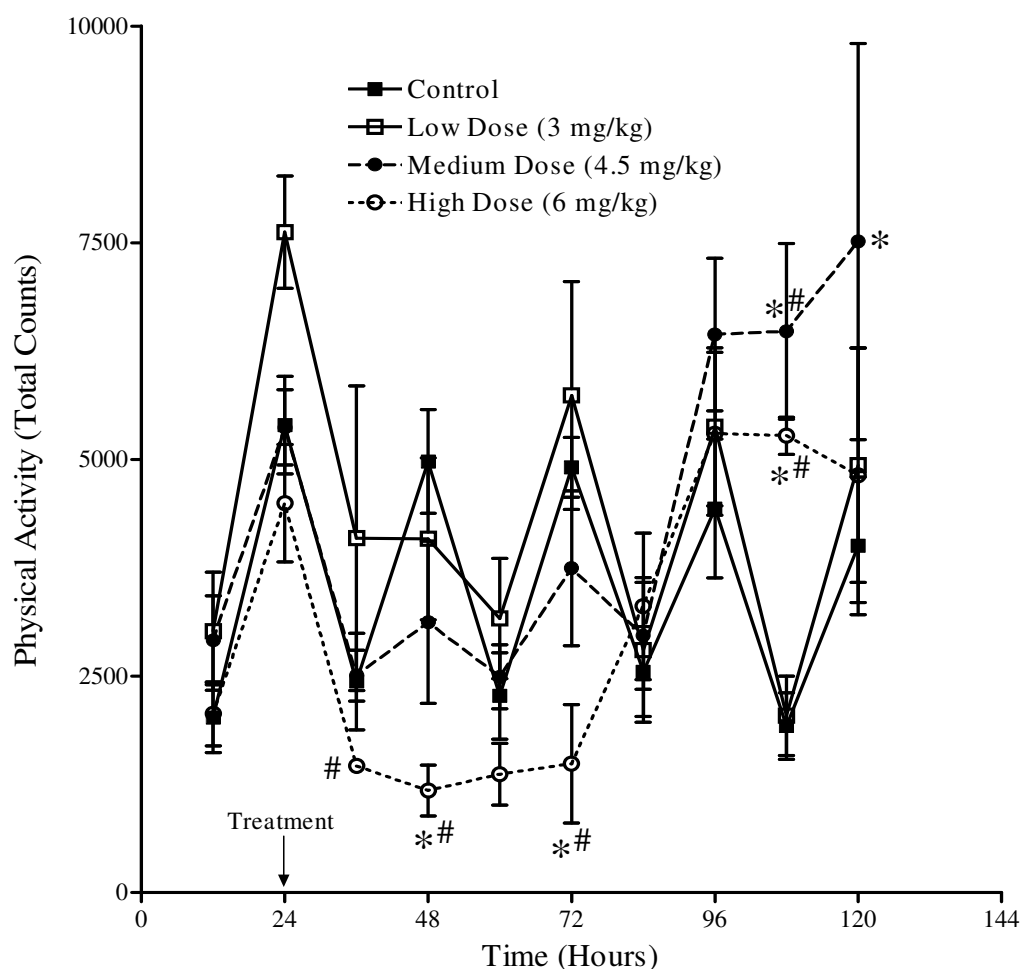
Figure 103: The effects of various doses of PS on physical activity in aged rats. Rats (n=5/dose group) were treated subcutaneously with PS at the doses indicated and sacrificed 96 hours later. The graph represents 24 hour baseline (pre-treatment) data followed by 96 hours post-treatment data. The data (mean ± standard error) represent physical activity averaged over 8 hour diurnal and nocturnal intervals. PS produced a decrease in physical activity in the high dose-group, followed by an increase 96 hours post-treatment in the medium and high dose-groups. The asterisk and pound signs represent values that are significantly different from control and 3 mg/kg dose groups at the same time point, respectively.
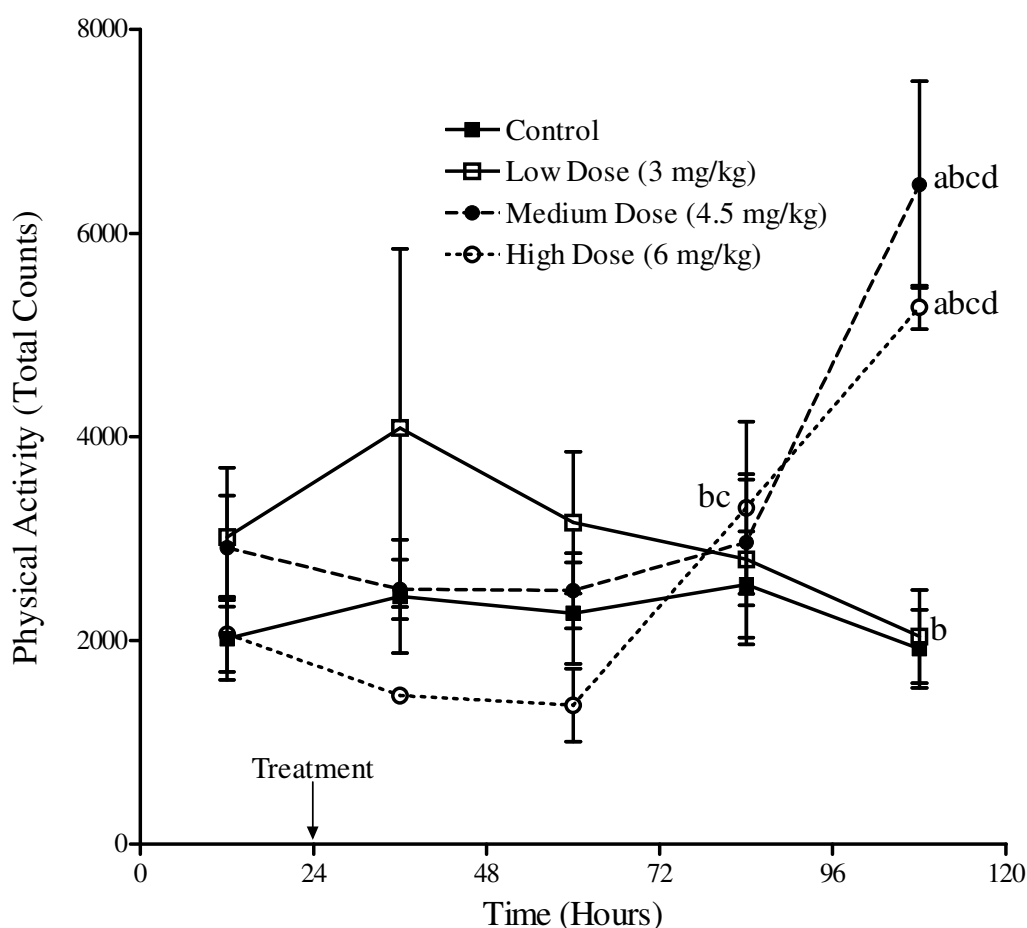
Figure 104: The effects of various doses of PS on physical activity in aged rats during the diurnal (light) periods. Rats (n=5/dose group) were treated subcutaneously with PS at the doses indicated and sacrificed 96 hours later. The graph represents 24 hour baseline (pre-treatment) data followed by 96 hours post-treatment data. The data (mean ± standard error) represents physical activity averaged over 8 hour diurnal intervals. PS produced a diurnal increase in physical activity around 60 hours post-treatment in the medium and high dose-groups, which persisted until the end of the study. a, b, c, and d represent values that are significantly different from the same dose at 12, 36, 60 and 84 hours, respectively.

Figure 105: The effects of various doses of PS on physical activity in aged rats during the nocturnal (dark) periods. Rats (n=4/dose group) were treated subcutaneously with PS at the doses indicated and sacrificed 96 hours later. The graph represents 24 hour baseline (pre-treatment) data followed by 96 hours post-treatment data. The data (mean ± standard error) represents body physical activity averaged over 8 hour nocturnal intervals. PS produced a dose-dependent decrease in physical activity in all 3 dose-groups, which peaked at 24 hours post-treatment, with a subsequent trend towards recovery until the end of the study. a, b, and c represent values that are significantly different from the same dose at 24, 48 and 72 hours, respectively.

<u>Total Cholinesterase, Acetylcholinesterase, Butyrylcholinesterase and</u>

<u>Carboxylesterase Activities in Atria, Ventricles, Cortex, Plasma</u>

<u>and Diaphragm of Adult and Aged Rats</u>

The levels of total ChE, AChE, BChE and CarbE in the atria, ventricles, cortex, plasma and diaphragm of adult (3 months) and aged (18 moths) rats were evaluated using the AChE-specific inhibitor BW284C51, the BChE-specific inhibitor iso-OMPA, and the CarbE substrate, *p*-nitrophenyl acetate. Table 5 summarizes these values in adult atria, ventricles, cortex and plasma. Information on these values in aged rats was lacking, however. In order to assess the effects of the various doses of CPF and PS on these enzymes in adult and aged rats, it was critical to evaluate the normal levels of these enzymes in tissues from these two age-groups. Figures 106-110 show the comparative ChE, AChE, BChE and CarbE content in the ventricles, atria, cortex, plasma and diaphragm, respectively, in adult and aged rats.

The ventricles of adult and aged rats contain approximately 10% AChE and 90% BChE. In both adult and aged rats, atria are comprised of 80% BChE and ~20% AChE, while the cortex has ~90% AChE and 10% BChE. The plasma in both ages was made up of ~70% AChE and 30% BChE, while the diaphragm in adult and aged rats contains 90% AChE and 10% BChE. Although the ventricles and cortex in aged rats appear to contain less amounts total ChE, AChE, BChE and CarbE as compared to adults, this difference was not significant. The atria and diaphragm in adult and aged rats contain essentially the same amount of each enzyme. In contrast, plasma in aged rats has ~1.5-fold higher levels of total ChE, AChE and BChE, and 35% lower CarbE activity than aged rats. Since both

AChE and BChE levels in the plasma increase during aging, the ratio of AChE:BChE remains the same as in adults.
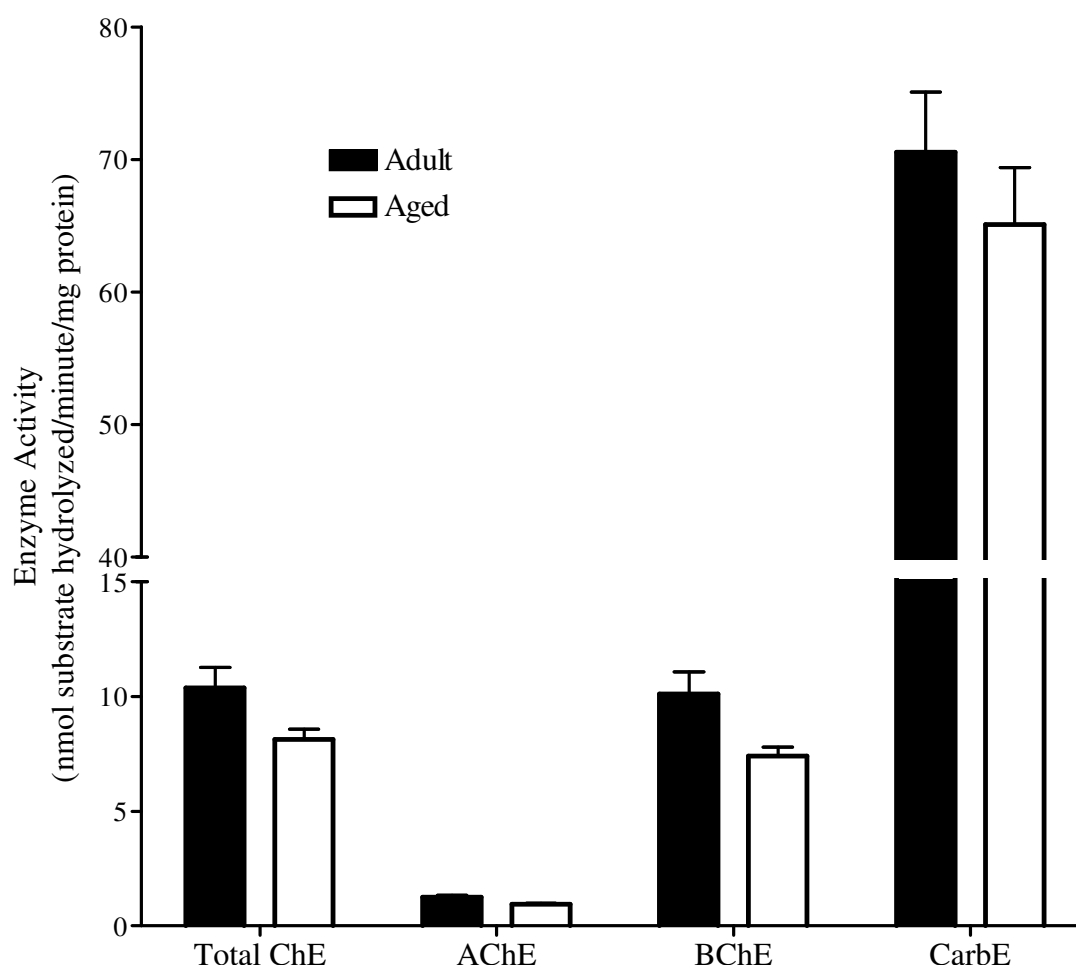
Figure 106: Total cholinesterase, acetylcholinesterase, butyrylcholinesterase and carboxylesterase activities in the ventricles of adult and aged rats. Ventricular tissue homogenates were incubated with 10 µM of *iso*-OMPA or BW at 37°C for 15 minutes, before assessing the residual ChE activity, to obtain AChE and BChE activities, respectively. For total ChE activity, the tissue homogenates were pre-incubated in buffer (no inhibitor), prior to performing the assay. Carboxylesterase activity was assessed following incubation of the tissue homogenates at 37°C in the presence of the substrate p-nitrophenyl acetate. Data (mean ± standard error) represent enzyme activities in terms of nmol of substrate hydrolyzed/mg protein/minute.

191
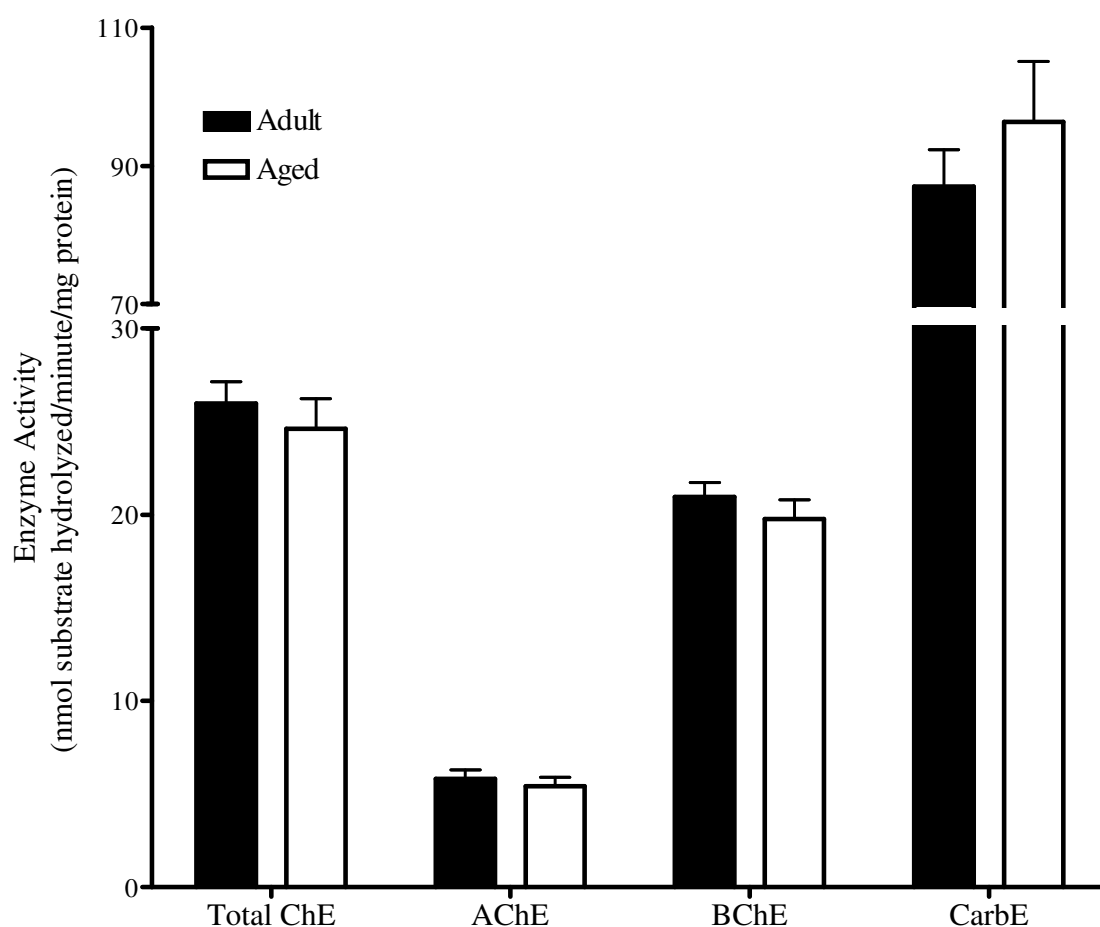
Figure 107: Total cholinesterase, acetylcholinesterase, butyrylcholinesterase and carboxylesterase activities in the atria of adult and aged rats. Atrial tissue homogenates were incubated with 10 µM of *iso*-OMPA or BW at 37°C for 15 minutes, before assessing the residual ChE activity, to obtain AChE and BChE activities, respectively. For total ChE activity, the tissue homogenates were pre-incubated in buffer (no inhibitor), prior to performing the assay. Carboxylesterase activity was assessed following incubation of the tissue homogenates at 37°C in the presence of the substrate p-nitrophenyl acetate. Data (mean ± standard error) represent enzyme activities in terms of nmol of substrate hydrolyzed/mg protein/minute.
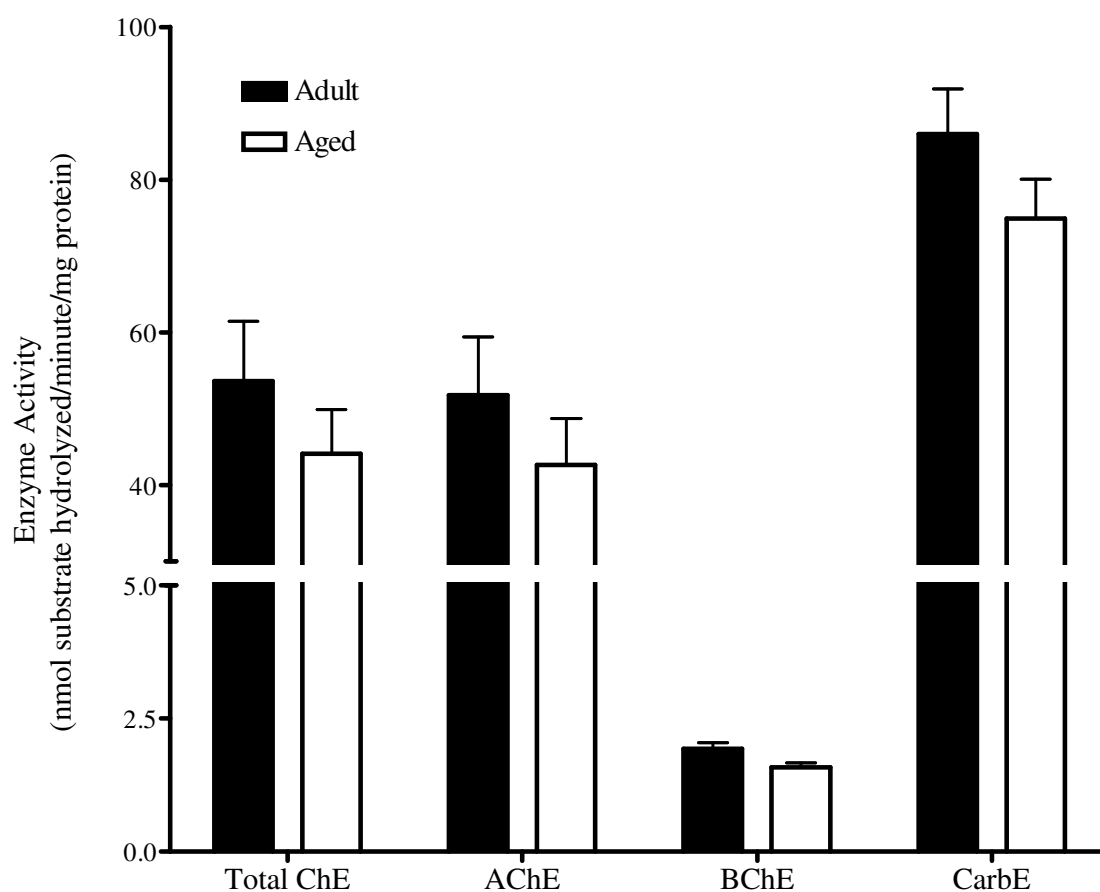
Figure 108: Total cholinesterase, acetylcholinesterase, butyrylcholinesterase and carboxylesterase activities in the cortex of adult and aged rats. Cortical tissue homogenates were incubated with 10 µM of *iso*-OMPA or BW at 37°C for 15 minutes, before assessing the residual ChE activity, to obtain AChE and BChE activities, respectively. For total ChE activity, the tissue homogenates were pre-incubated in buffer (no inhibitor), prior to performing the assay. Carboxylesterase activity was assessed following incubation of the tissue homogenates at 37°C in the presence of the substrate p-nitrophenyl acetate. Data (mean ± standard error) represent enzyme activities in terms of nmol of substrate hydrolyzed/mg protein/minute.
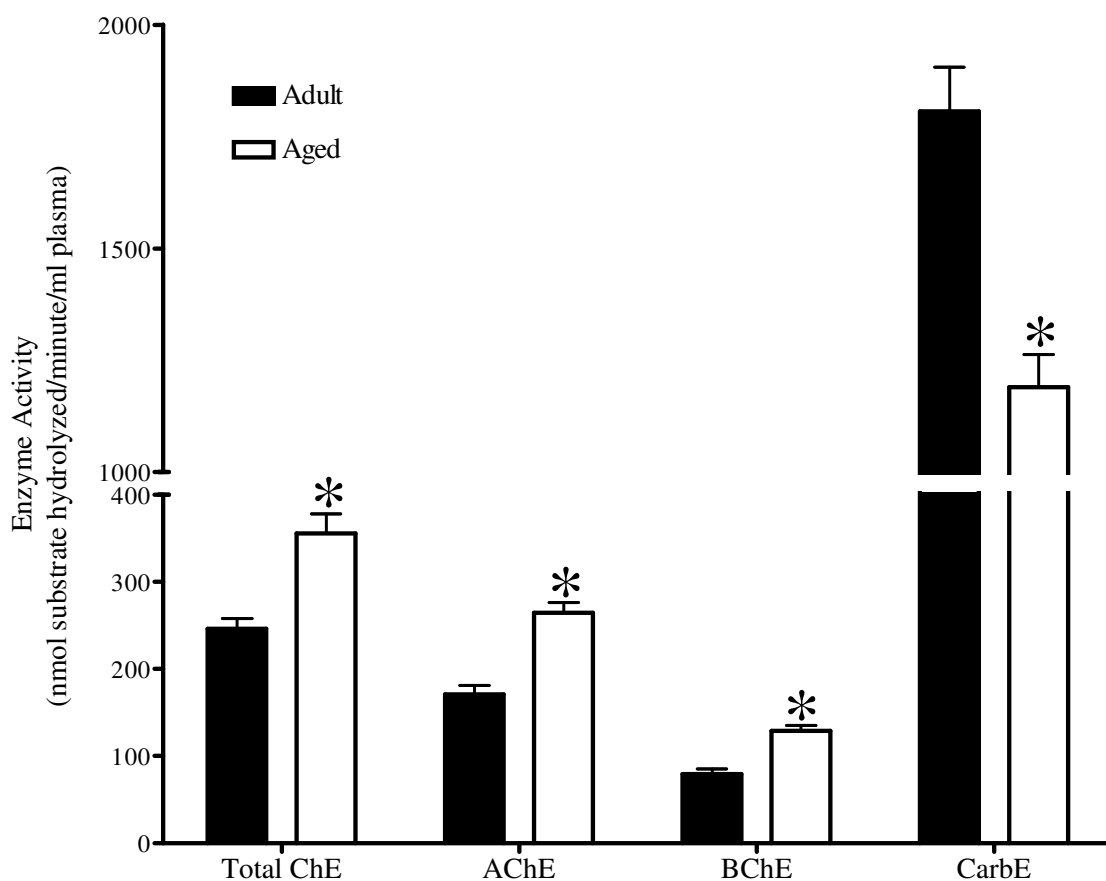
Figure 109: Total cholinesterase, acetylcholinesterase, butyrylcholinesterase and carboxylesterase activities in the plasma of adult and aged rats. Diluted plasma samples were incubated with 10 µM of *iso*-OMPA or BW at 37°C for 15 minutes, before assessing the residual ChE activity, to obtain AChE and BChE activities, respectively. For total ChE activity, the diluted plasma samples were pre-incubated in buffer (no inhibitor), prior to performing the assay. Carboxylesterase activity was assessed following incubation of the diluted plasma samples at 37°C in the presence of the substrate p-nitrophenyl acetate. Data (mean ± standard error) represent enzyme activities in terms of nmol of substrate hydrolyzed/ml plasma/minute. Asterisks represent values that are significantly different from adults.
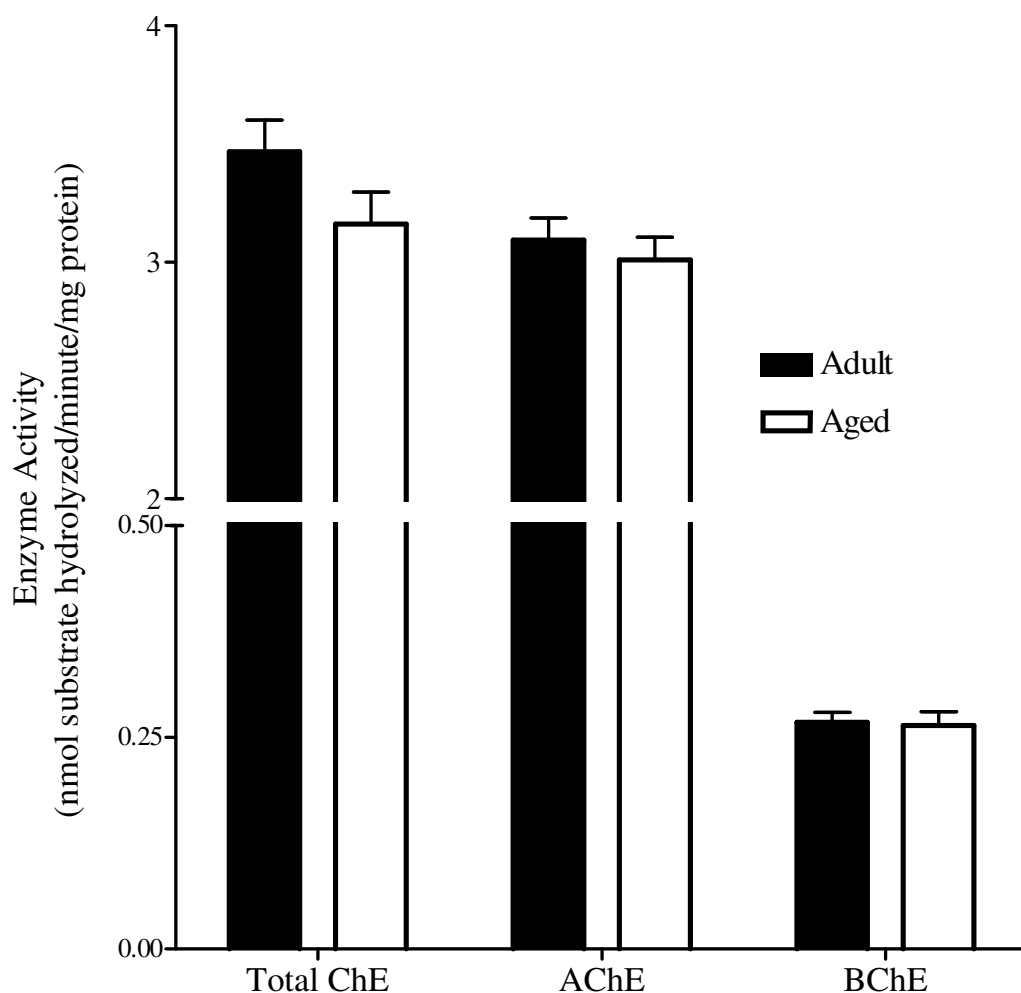
Figure 110: Total cholinesterase, acetylcholinesterase and butyrylcholinesterase activities in the diaphragm of adult and aged rats. Diaphragm tissue homogenates were incubated with 10 µM of *iso*-OMPA or BW at 37°C for 15 minutes, before assessing the residual ChE activity, to obtain AChE and BChE activities, respectively. For total ChE activity, the tissue homogenates were pre-incubated in buffer (no inhibitor), prior to performing the assay. Data (mean ± standard error) represent enzyme activities in terms of nmol of substrate hydrolyzed/mg protein/minute.

Effects of Chlorpyrifos on Acetylcholinesterase, Butyrylcholinesterase,

Carboxylesterase and Muscarinic Receptor Binding in Ventricles, Atria,

Cortex, Plasma and Diaphragm of Adult and Aged Rats

The effects of CPF on AChE, BChE, CarbE, muscarinic receptor agonist and antagonist binding were evaluated in adult and aged rats. The tissues examined were atria, ventricles, cortex, plasma and diaphragm. CPF produced a dose-dependent inhibition of AChE (Figures 111, 116, 121, 126 and 129) and BChE (Figures 112, 117, 122, 127 and 130) in all of the tissues examined in adult and aged rats. In general, the same dose of CPF inhibited BChE to a greater extent (~2 to 2.5 fold) than AChE, and this was especially obvious with the low (28 mg/kg) and medium (140 mg/kg) dose groups of CPF. AChE and BChE in the ventricles were inhibited to a greater extent than in the atria, with all doses of CPF. In the atria, both AChE and BChE were inhibited to a greater extent in aged than in adult rats by the same dose of CPF (evident with the low dose of CPF). Similarly, AChE and BChE in the plasma and diaphragm of aged rats were also inhibited to a greater extent in aged as compared to adult rats. In the ventricles and cortex, both enzymes were inhibited to a similar degree by the same dose of CPF in both age-groups. The maximum amount of enzyme inhibited by the highest dose of CPF was ~85-90% for AChE and 90-95% for BChE.

Carboxylesterase was also inhibited in a dose-dependent manner by CPF (Figures 113, 118, 123 and 128) in adult and aged rats. The amount of CarbE inhibited ranged from 35% (low dose) to 80% (high dose). Other than the ventricles, there did not appear to be any age-related difference in the amount of CarbE inhibited by a certain dose of CPF. The highest dose of CPF inhibited a maximum of ~80% of the total CarbE activity

in a tissue, with the exception of the cortex, which had ~40% residual enzyme after treatment with 280 mg/kg CPF.

Muscarinic receptor binding was also evaluated through the use of a radiolabeled agonist ($[^3H]$OXO) (Figures 114, 119 and 124) and antagonist ($[^3H]$QNB) (Figures 115, 120 and 125). Muscarinic antagonist binding was found to be reduced by ~20% in adult ventricles (Figure 115) in the group treated with the high dose of CPF. A similar reduction in $[^3H]$QNB binding was observed in the cortex (Figure 125), wherein ~20% of the receptors were downregulated in the medium and high dose groups of adults, and in the high dose group of aged rats. Muscarinic agonist binding was also reduced in the cortex (Figure 124) to a similar extent (~25%) in the high dose groups of adult and aged rats. A more robust decrease in $[^3H]$OXO binding was observed in the atria (Figure 119), wherein ~50% reduction in receptor binding was noted in the high dose group of adult and aged rats.
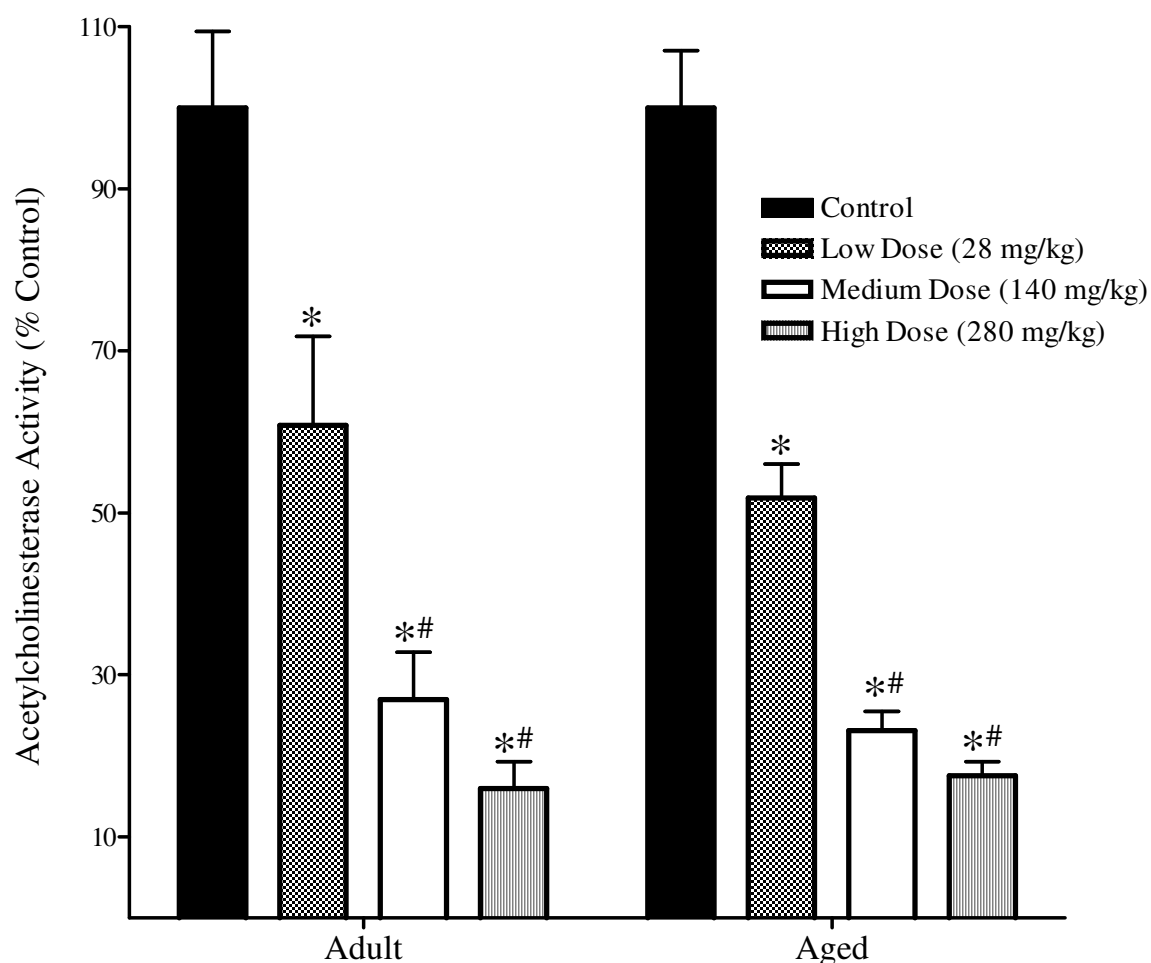
Figure 111: The effects of CPF on acetylcholinesterase activity in ventricles from adult and aged rats. Rats (n=4-5/dose group) were treated with CPF (sc) at the doses indicated and sacrificed 96 hours later. Ventricular tissue homogenates were pre-incubated with 10 μM *iso*-OMPA at 37°C for 15 minutes prior to measuring the residual ChE activity as described previously. CPF produced a dose-dependent inhibition of AChE activity in the ventricles of adult and aged rats. Data (mean ± standard error) represent AChE activity in terms of percent of control. The asterisk and pound signs represent values that are significantly different from control and 28 mg/kg dose groups, respectively.

Figure 112: The effects of CPF on butyrylcholinesterase activity in ventricles from adult and aged rats. Rats (n=4-5/dose group) were treated with CPF (sc) at the doses indicated and sacrificed 96 hours later. Ventricular tissue homogenates were pre-incubated with 10 μM BW284C51 at 37°C for 15 minutes prior to measuring the residual ChE activity as described previously. CPF produced a dose-dependent inhibition of BChE activity in the ventricles of adult and aged rats. Data (mean ± standard error) represent BChE activity in terms of percent of control. The asterisk and pound signs represent values that are significantly different from control and 28 mg/kg dose groups, respectively.

Figure 113: The effects of CPF on carboxylesterase activity in ventricles from adult and aged rats. Rats (n=4-5/dose group) were treated with CPF (sc) at the doses indicated and sacrificed 96 hours later. Ventricular tissue homogenates were incubated at 37°C in the presence of the substrate p-nitrophenyl acetate to assess CarbE activity. CPF produced a dose-dependent inhibition of CarbE activity in the ventricles of adult and aged rats, with slightly more CarbE being inhibited by the high dose of CPF in aged than adult rats. Data (mean ± standard error) represent CarbE activity in terms of percent of control. Asterisks represent values that are significantly different from control, while the plus sign represents values that are significantly different from the same dose in adult rats.
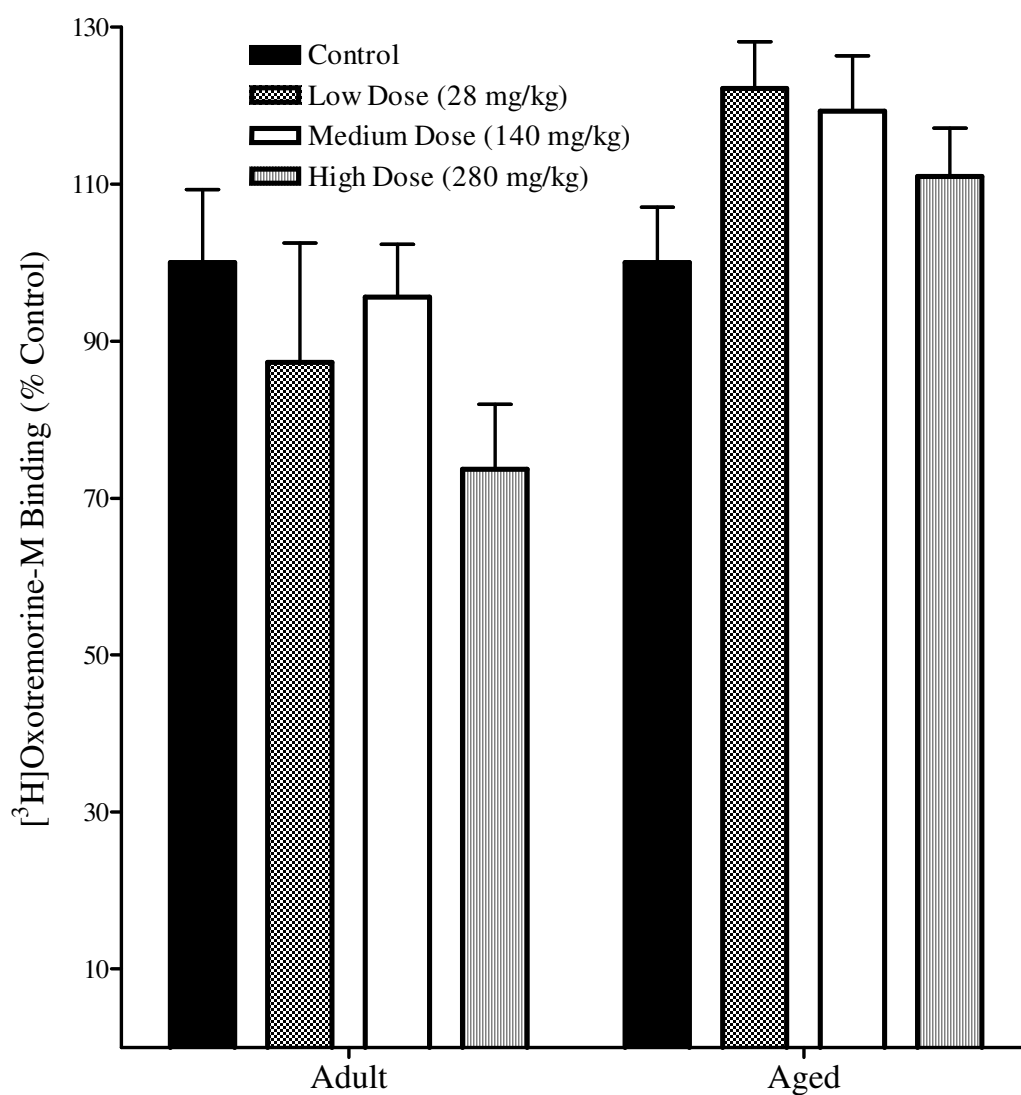
Figure 114: The effects of CPF on muscarinic agonist binding in ventricles from adult and aged rats. Rats (n=4-5/dose group) were treated with CPF (sc) at the doses indicated and sacrificed 96 hours later. Ventricular membranes were incubated at 21°C for 90 minutes in the presence of 1 nM [^{3}H]Oxotremorine-M, with or without 10 μM atropine (to determine specific binding). CPF did not affect muscarinic receptor binding in adult or aged rats at any of the doses used. Data (mean ± standard error) represent specific binding in terms of percent of control.

Figure 115: The effects of CPF on muscarinic antagonist binding in ventricles from adult and aged rats. Rats (n=4-5/dose group) were treated with CPF (sc) at the doses indicated and sacrificed 96 hours later. Ventricular membranes were incubated at 21°C for 90 minutes in the presence of 1 nM [³H]Quinuclidinyl benzilate, with or without 10 µM atropine (to determine specific binding). CPF significantly downregulated muscarinic receptors in the high dose group of adult rats. Data (mean ± standard error) represent specific binding in terms of percent of control. The asterisk, pound and dollar signs represent values that are significantly different from control, 28 mg/kg and 140 mg/kg dose groups, respectively.
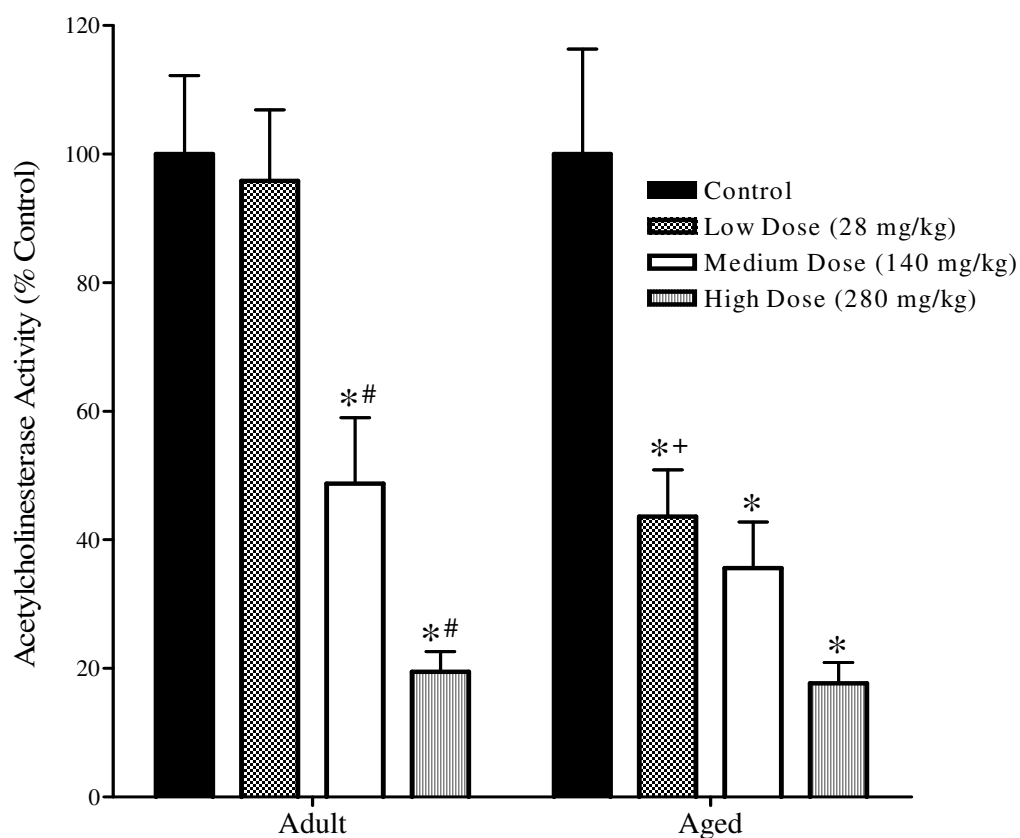
Figure 116: The effects of CPF on acetylcholinesterase activity in atria from adult and aged rats. Rats (n=4-5/dose group) were treated with CPF (sc) at the doses indicated and sacrificed 96 hours later. Atrial tissue homogenates were pre-incubated with 10 μM *iso-OMPA* at 37°C for 15 minutes prior to measuring the residual ChE activity as described previously. CPF produced a dose-dependent inhibition of AChE activity in the atria of adult and aged rats. AChE in aged rats was inhibited to a significantly greater extent by the low dose of CPF than AChE in adults. Data (mean ± standard error) represent AChE activity in terms of percent of control. The asterisk and pound signs represent values that are significantly different from control and 28 mg/kg dose groups, respectively, while the plus sign represents values that are significantly different from the same dose group in adults.

Figure 117: The effects of CPF on butyrylcholinesterase activity in atria from adult and aged rats. Rats (n=4-5/dose group) were treated with CPF (sc) at the doses indicated and sacrificed 96 hours later. Atrial tissue homogenates were pre-incubated with 10 μM BW284C51 at 37°C for 15 minutes prior to measuring the residual ChE activity as described previously. CPF produced a dose-dependent inhibition of BChE activity in the atria of adult and aged rats. BChE in aged rats was inhibited to a significantly greater extent by the low dose of CPF than BChE in adults. Data (mean ± standard error) represent BChE activity in terms of percent of control. The asterisk and pound signs represent values that are significantly different from control and 28 mg/kg dose groups, respectively, while the plus sign represents values that are significantly different from the same dose group in adults.

Figure 118: The effects of CPF on carboxylesterase activity in atria from adult and aged rats. Rats (n=4-5/dose group) were treated with CPF (sc) at the doses indicated and sacrificed 96 hours later. Atrial tissue homogenates were incubated at 37°C in the presence of the substrate p-nitrophenyl acetate to assess CarbE activity. CPF produced a dose-dependent inhibition of CarbE activity in the atria of adult and aged rats. Data (mean ± standard error) represent CarbE activity in terms of percent of control. The asterisk and pound signs represent values that are significantly different from control and 28 mg/kg dose groups, respectively.

Figure 119: The effects of CPF on muscarinic agonist binding in atria from adult and aged rats. Rats (n=4-5/dose group) were treated with CPF (sc) at the doses indicated and sacrificed 96 hours later. Atrial membranes were incubated at 21°C for 90 minutes in the presence of 1 nM [³H]Oxotremorine-M, with or without 10 µM atropine (to determine specific binding). The high dose of CPF produced a significant downregulation of muscarinic receptors in adult and aged rats. Data (mean ± standard error) represent specific binding in terms of percent of control. Asterisks represent values that are significantly different from control.

Figure 120: The effects of CPF on muscarinic antagonist binding in atria from adult and aged rats. Rats (n=4-5/dose group) were treated with CPF (sc) at the doses indicated and sacrificed 96 hours later. Atrial membranes were incubated at 21°C for 90 minutes in the presence of 1 nM [³H]Quinuclidinyl benzilate, with or without 10 μM atropine (to determine specific binding). CPF did not affect muscarinic receptor binding in adult or aged rats at any of the doses used. Data (mean ± standard error) represent specific binding in terms of percent of control.
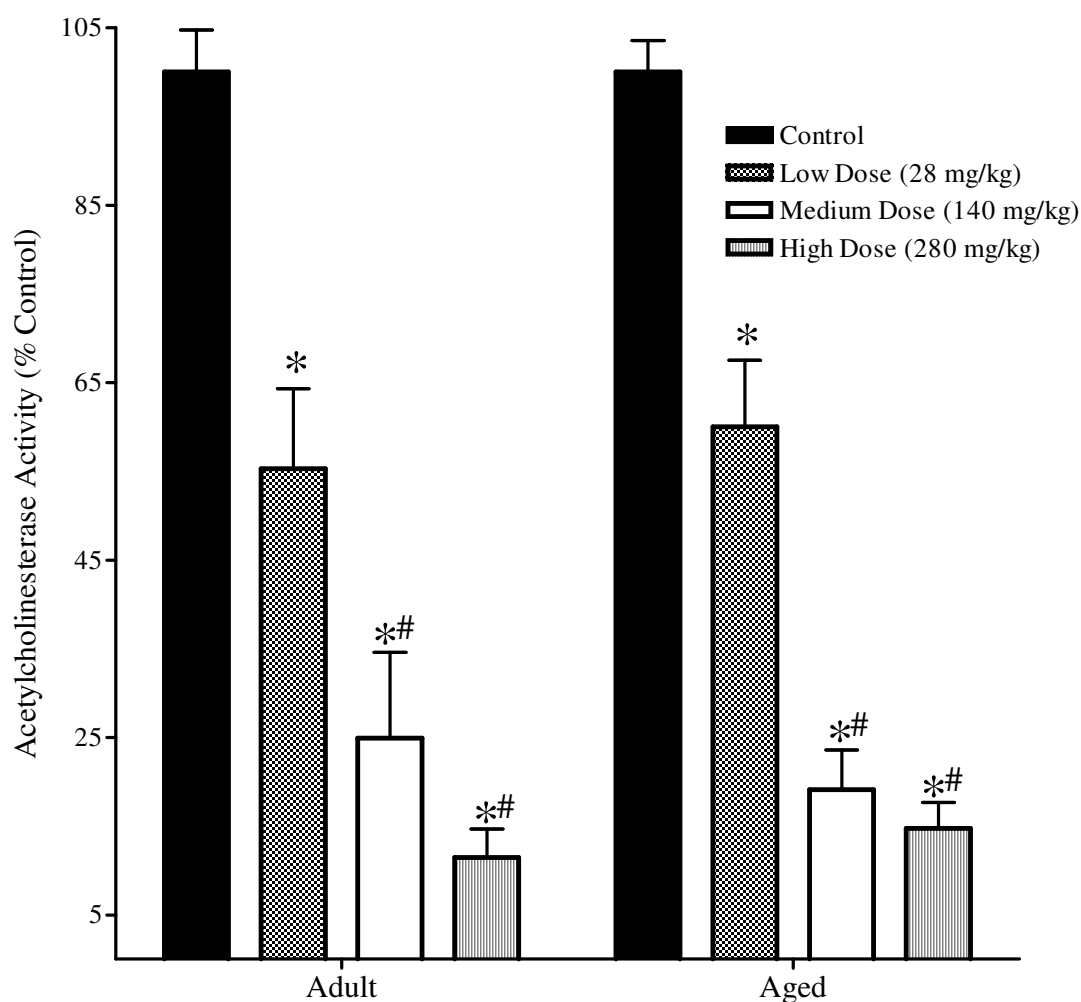
Figure 121: The effects of CPF on acetylcholinesterase activity in cortex from adult and aged rats. Rats (n=4-5/dose group) were treated with CPF (sc) at the doses indicated and sacrificed 96 hours later. Cortical tissue homogenates were pre-incubated with 10 μM *iso*-OMPA at 37°C for 15 minutes prior to measuring the residual ChE activity as described previously. CPF produced a dose-dependent inhibition of AChE activity in the cortex of adult and aged rats. Data (mean ± standard error) represent AChE activity in terms of percent of control. The asterisk and pound signs represent values that are significantly different from control and 28 mg/kg dose groups, respectively.

Figure 122: The effects of CPF on butyrylcholinesterase activity in cortex from adult and aged rats. Rats (n=4-5/dose group) were treated with CPF (sc) at the doses indicated and sacrificed 96 hours later. Cortical tissue homogenates were pre-incubated with 10 µM BW284C51 at 37°C for 15 minutes prior to measuring the residual ChE activity as described previously. CPF produced a dose-dependent inhibition of BChE activity in the cortex of adult and aged rats. Data (mean ± standard error) represent BChE activity in terms of percent of control. The asterisk and pound signs represent values that are significantly different from control and 28 mg/kg dose groups, respectively.

Figure 123: The effects of CPF on carboxylesterase activity in cortex from adult and aged rats. Rats (n=4-5/dose group) were treated with CPF (sc) at the doses indicated and sacrificed 96 hours later. Cortical tissue homogenates were incubated at 37°C in the presence of the substrate p-nitrophenyl acetate to assess CarbE activity. CPF produced a dose-dependent inhibition of CarbE activity in the cortex of adult and aged rats. Data (mean ± standard error) represent CarbE activity in terms of percent of control. The asterisk, pound and dollar signs represent values that are significantly different from control, 28 mg/kg and 140 mg/kg dose groups, respectively.

Figure 124: The effects of CPF on muscarinic agonist binding in cortex from adult and aged rats. Rats (n=4-5/dose group) were treated with CPF (sc) at the doses indicated and sacrificed 96 hours later. Cortical membranes were incubated at 21°C for 90 minutes in the presence of 1 nM [^{3}H]Oxotremorine-M, with or without 10 μM atropine (to determine specific binding). The high dose of CPF produced a significant downregulation of muscarinic receptors in adult and aged rats. Data (mean ± standard error) represent specific binding in terms of percent of control. Asterisks represent values that are significantly different from control.

Figure 125: The effects of CPF on muscarinic antagonist binding in cortex from adult and aged rats. Rats (n=4-5/dose group) were treated with CPF (sc) at the doses indicated and sacrificed 96 hours later. Cortical membranes were incubated at 21°C for 90 minutes in the presence of 1 nM [³H]Quinuclidinyl benzilate, with or without 10 μM atropine (to determine specific binding). CPF produced a significant downregulation of muscarinic receptors in the low and high dose-groups of adult rats, and in the high dose-group of aged rats. Data (mean ± standard error) represent specific binding in terms of percent of control. The asterisk and pound signs represent values that are significantly different from control and 28 mg/kg dose group, respectively.

Figure 126: The effects of CPF on acetylcholinesterase activity in plasma from adult and aged rats. Rats (n=4-5/dose group) were treated with CPF (sc) at the doses indicated and sacrificed 96 hours later. Diluted plasma samples were pre-incubated with 10 μM *iso*-OMPA at 37°C for 15 minutes prior to measuring the residual ChE activity as described previously. CPF produced a dose-dependent inhibition of AChE activity in the plasma of adult and aged rats. Data (mean ± standard error) represent AChE activity in terms of percent of control. The asterisk and pound signs represent values that are significantly different from control and 28 mg/kg dose groups, respectively.

Figure 127: The effects of CPF on butyrylcholinesterase activity in plasma from adult and aged rats. Rats (n=4-5/dose group) were treated with CPF (sc) at the doses indicated and sacrificed 96 hours later. Diluted plasma samples were pre-incubated with 10 µM BW284C51 at 37°C for 15 minutes prior to measuring the residual ChE activity as described previously. CPF produced a dose-dependent inhibition of BChE activity in the plasma of adult and aged rats. Data (mean ± standard error) represent BChE activity in terms of percent of control. The asterisk and pound signs represent values that are significantly different from control and 28 mg/kg dose groups, respectively.

Figure 128: The effects of CPF on carboxylesterase activity in plasma from adult and aged rats. Rats (n=4-5/dose group) were treated with CPF (sc) at the doses indicated and sacrificed 96 hours later. Diluted plasma samples were incubated at 37°C in the presence of the substrate p-nitrophenyl acetate to assess CarbE activity. CPF produced a dose-dependent inhibition of CarbE activity in the plasma of adult and aged rats. CarbE in aged rats was inhibited to a significantly greater extent by the low dose of CPF than CarbE in adults. Data (mean ± standard error) represent CarbE activity in terms of percent of control. The asterisk and pound signs represent values that are significantly different from control and 28 mg/kg dose groups, respectively, while the plus sign represents values that are significantly different from the same dose group in adults.

215

Figure 129: The effects of CPF on acetylcholinesterase activity in diaphragm from adult and aged rats. Rats (n=4-5/dose group) were treated with CPF (sc) at the doses indicated and sacrificed 96 hours later. Diaphragm tissue homogenates were pre-incubated with 10 μM *iso*-OMPA at 37°C for 15 minutes prior to measuring the residual ChE activity as described previously. CPF produced a dose-dependent inhibition of AChE activity in the diaphragm of adult and aged rats. Data (mean ± standard error) represent AChE activity in terms of percent of control. The asterisk, pound and dollar signs represent values that are significantly different from control, 28 mg/kg and 140 mg/kg dose groups, respectively.

Figure 130: The effects of CPF on butyrylcholinesterase activity in diaphragm from adult and aged rats. Rats (n=4-5/dose group) were treated with CPF (sc) at the doses indicated and sacrificed 96 hours later. Diaphragm tissue homogenates were pre-incubated with 10 µM BW284C51 at 37°C for 15 minutes prior to measuring the residual ChE activity as described previously. CPF produced a dose-dependent inhibition of BChE activity in the diaphragm of adult and aged rats. Data (mean ± standard error) represent BChE activity in terms of percent of control. The asterisk and pound signs represent values that are significantly different from control and 28 mg/kg dose groups, respectively.

Effects of Parathion on Acetylcholinesterase, Butyrylcholinesterase, Carboxylesterase and Muscarinic Receptor Binding in Ventricles, Atria, Cortex, Plasma and Diaphragm of Adult and Aged Rats

The effects of PS on AChE, BChE, CarbE, muscarinic receptor agonist and antagonist binding were evaluated in the atria, ventricles, cortex, diaphragm and plasma of adult and aged rats. PS produced a dose-dependent inhibition of AChE (Figures 131, 136, 141, 146 and 149) and BChE (Figures 132, 137, 142, 147 and 150) in all of the tissues examined in adult and aged rats. In general, the same dose of PS was found to inhibit AChE to a greater extent (~1.5 fold) than BChE, and this was especially obvious with the low (adult: 9 mg/kg; aged: 3 mg/kg) and medium (adult: 13.5 mg/kg; aged: 4.5 mg/kg) dose groups. All the doses of PS used in the study inhibited AChE and BChE to a greater extent in the ventricles as compared to the atria. In the atria, both AChE and BChE were inhibited to a greater extent in aged than in adult rats by the same dose of PS, as was seen with the low dose of PS. Although not significant, BChE in the plasma of aged rats appeared to be inhibited to a greater degree than in adult rats. No such age-related difference was observed for plasma AChE activity. The maximum amount of enzyme inhibited by the highest dose of PS was ~90-95% for AChE and 70-75% for BChE.

Carboxylesterase was also inhibited in a dose-dependent manner by PS (Figures 133, 138, 143 and 148) in adult and aged rats. There did not appear to be any age-related difference in the amount of CarbE inhibited by any dose of PS. The highest dose of PS inhibited a maximum of ~70% of the total CarbE activity in any of the tissues examined,

with the exception of the cortex, which had ~50% residual enzyme after treatment with the highest dose of PS.

Muscarinic receptor binding was also evaluated through the use of a radiolabeled agonist ([^{3}H]OXO) (Figures 134, 139 and 144) and antagonist ([^{3}H]QNB) (Figure 135, 140 and 145). Muscarinic antagonist binding in the cortex (Figure 145) was found to be reduced by ~25% in aged rats in the group treated with the high dose of PS. Conversely, an increase in [^{3}H]QNB binding was observed in the ventricles (Figure 135), wherein ~30% of the receptors were upregulated in the high dose group of aged rats. Muscarinic agonist binding in the ventricles (Figure 134) was reduced by ~25% in the medium and high dose groups of adults. A similar downregulation of receptors (20%) in the atria (Figure 139) was observed in the low dose of adult rats and high dose of aged rats, with a more robust decrease being observed in the medium and high dose groups of adult rats, wherein ~35-40% of the receptors were downregulated. Muscarinic receptors were also found to be downregulated in the cortex (Figure 144), wherein, [^{3}H]OXO binding in the cortex of aged rats was reduced by ~45% in the high dose group.
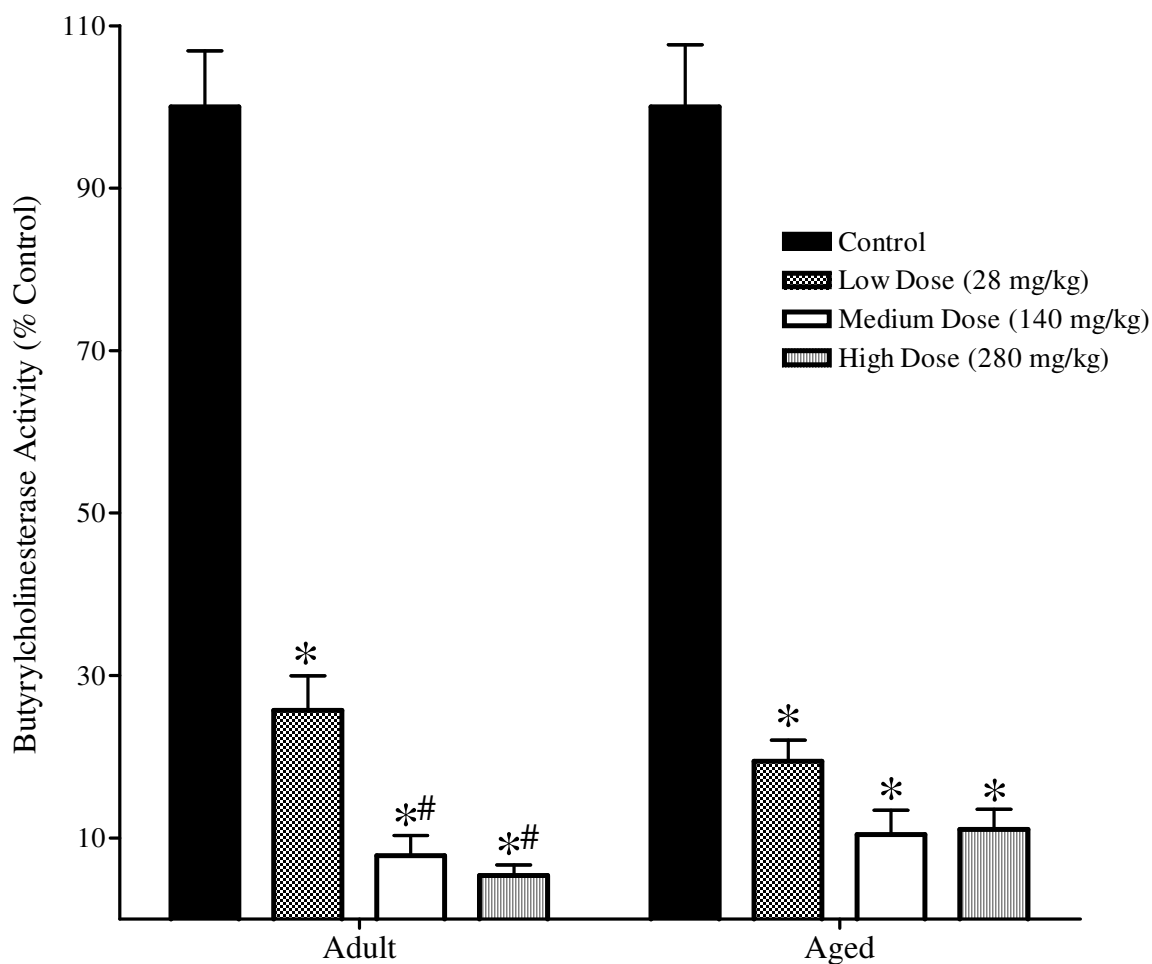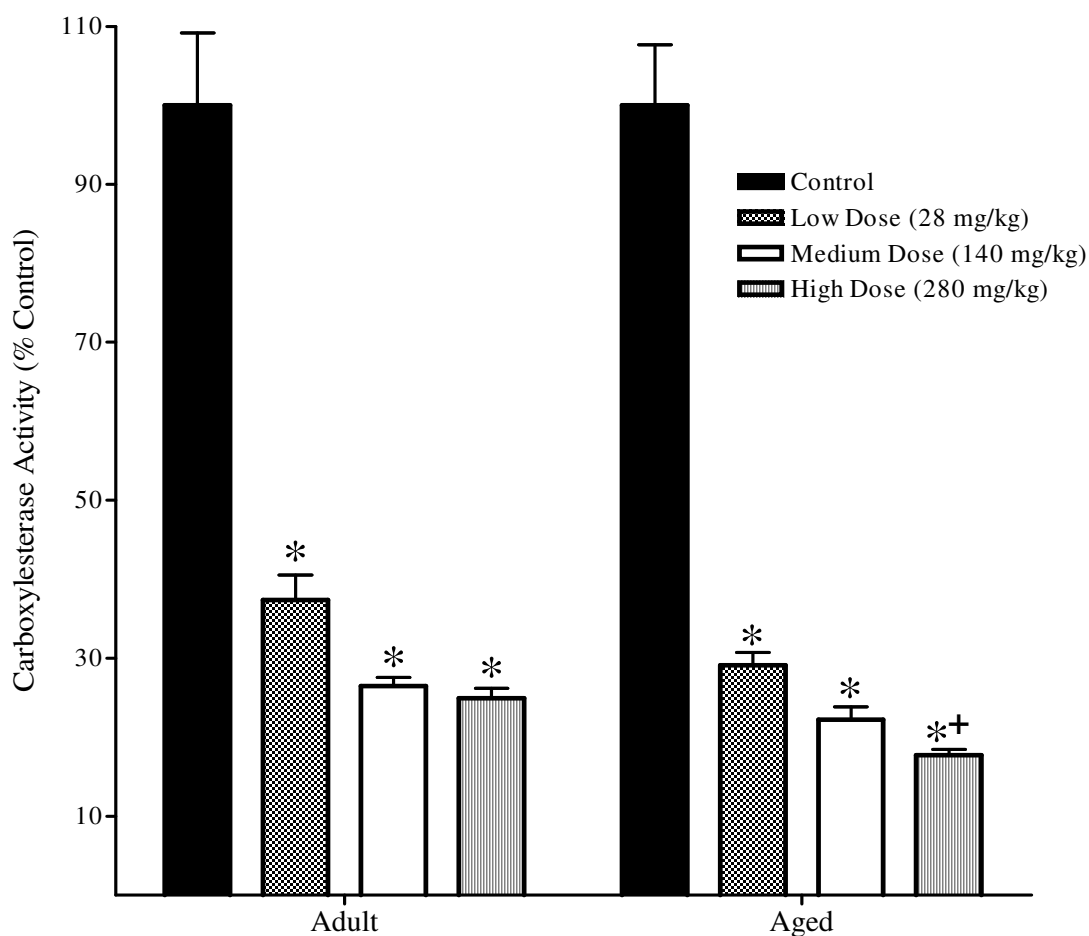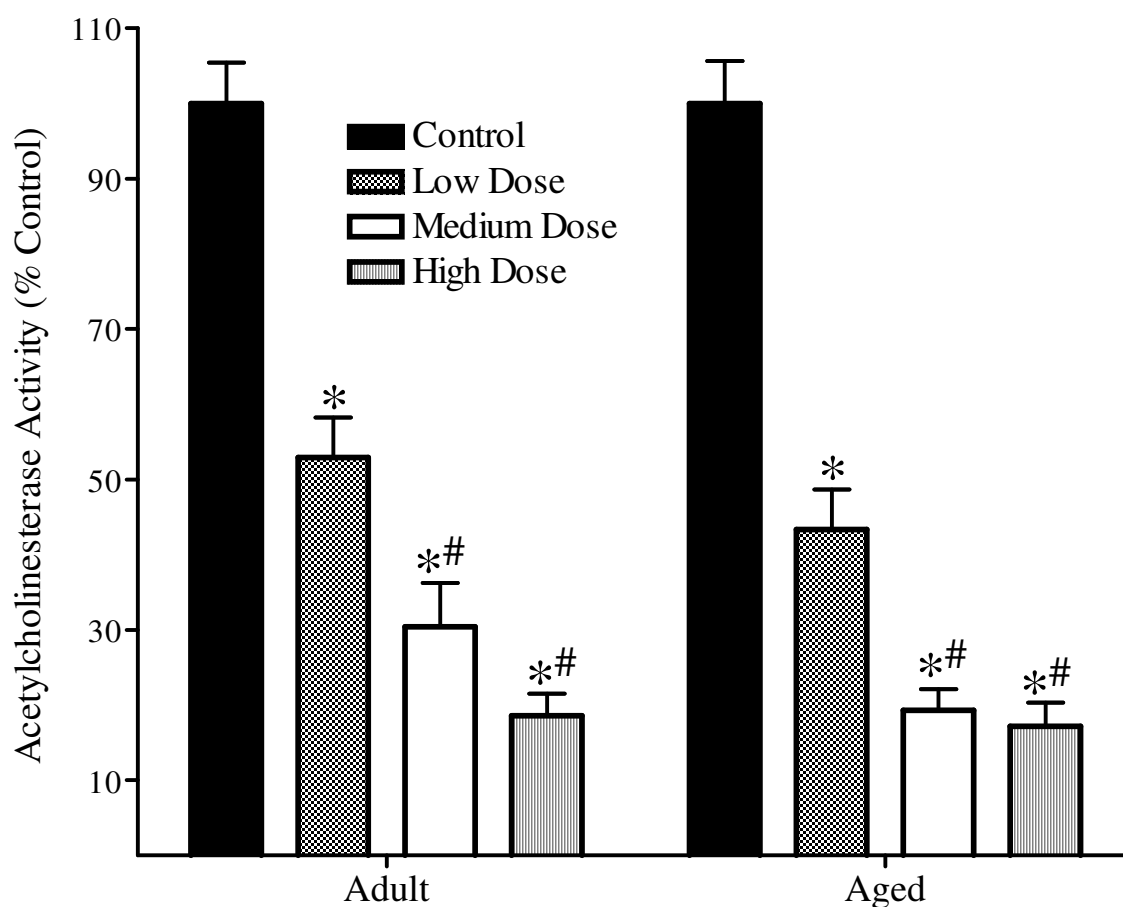
Figure 131: The effects of PS on acetylcholinesterase activity in ventricles from adult and aged rats. Rats (n=4-5/dose group) were treated with PS (sc) at the doses indicated and sacrificed 96 hours later. Ventricular tissue homogenates were pre-incubated with 10 μM *iso*-OMPA at 37°C for 15 minutes prior to measuring the residual ChE activity as described previously. PS produced a dose-dependent inhibition of AChE activity in the ventricles of adult and aged rats. Data (mean ± standard error) represent AChE activity in terms of percent of control. The asterisk and pound signs represent values that are significantly different from the control and low (adult: 9 mg/kg; aged: 3 mg/kg) dose groups, respectively.

Figure 132: The effects of PS on butyrylcholinesterase activity in ventricles from adult and aged rats. Rats (n=4-5/dose group) were treated with PS (sc) at the doses indicated and sacrificed 96 hours later. Ventricular tissue homogenates were pre-incubated with 10 μM BW284C51 at 37°C for 15 minutes prior to measuring the residual ChE activity as described previously. PS produced a dose-dependent inhibition of BChE activity in the ventricles of adult and aged rats. Data (mean ± standard error) represent BChE activity in terms of percent of control. The asterisk, pound and dollar signs represent values that are significantly different from control, low (adult: 9 mg/kg; aged: 3 mg/kg) and medium (adult: 13.5 mg/kg; aged: 4.5 mg/kg) dose groups, respectively.

Figure 133: The effects of PS on carboxylesterase activity in ventricles from adult and aged rats. Rats (n=4-5/dose group) were treated with PS (sc) at the doses indicated and sacrificed 96 hours later. Ventricular tissue homogenates were incubated at 37°C in the presence of the substrate p-nitrophenyl acetate to assess CarbE activity. All three doses of PS inhibited ~60% of CarbE activity in the ventricles of adult and aged rats. Data (mean ± standard error) represent CarbE activity in terms of percent of control. Asterisks represent values that are significantly different from control.
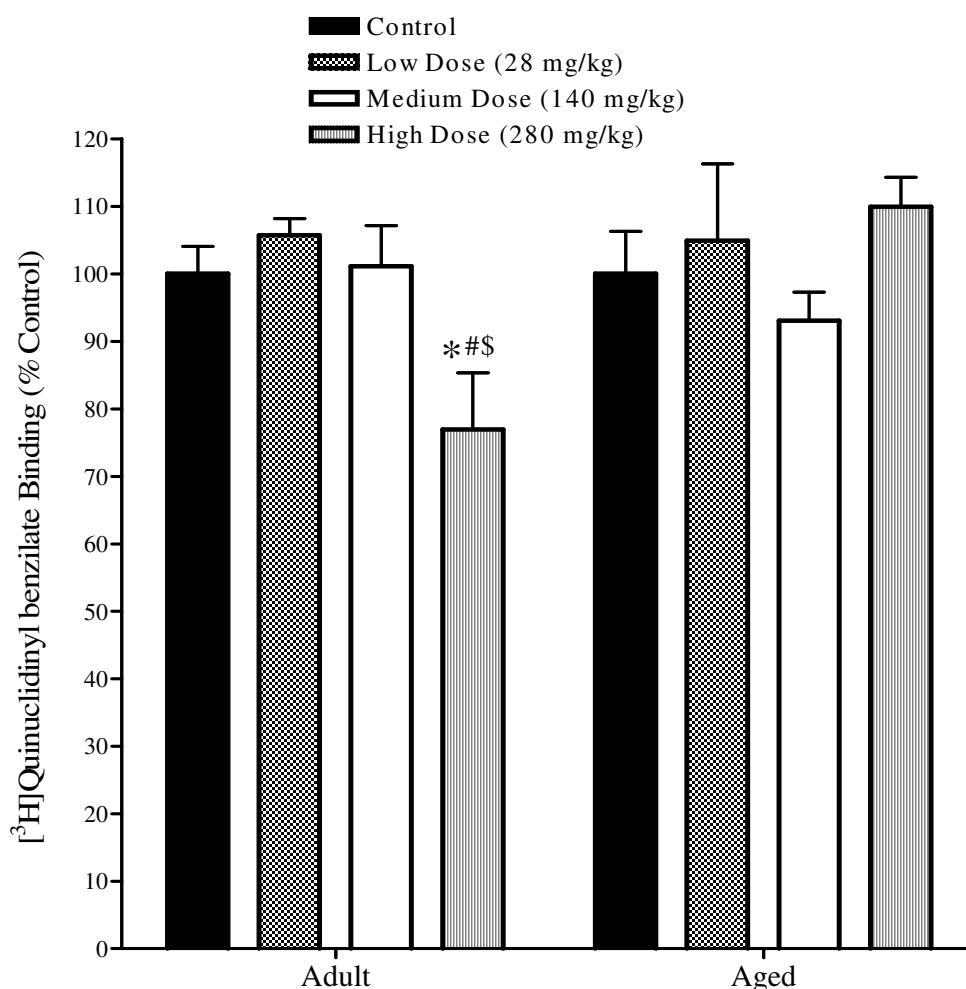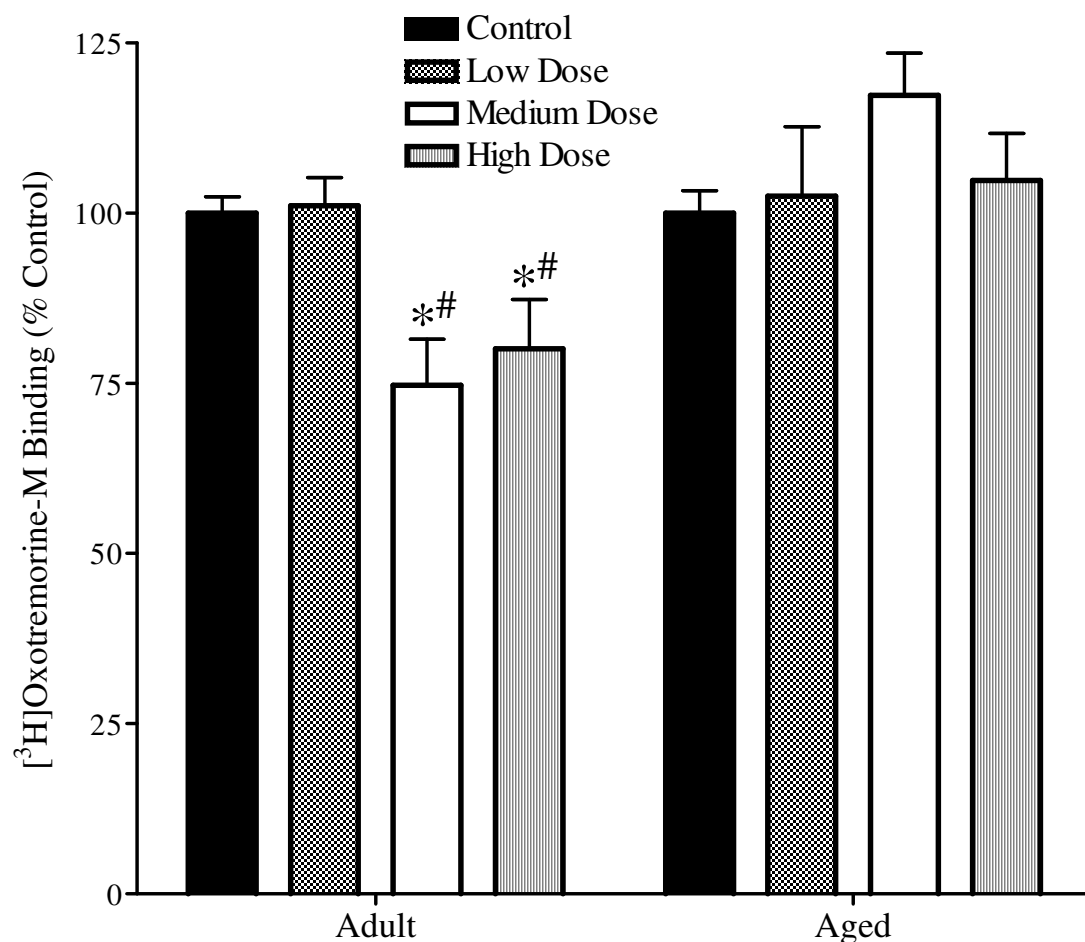
Figure 134: The effects of PS on muscarinic agonist binding in ventricles from adult and aged rats. Rats (n=4-5/dose group) were treated with PS (sc) at the doses indicated and sacrificed 96 hours later. Ventricular membranes were incubated at 21°C for 90 minutes in the presence of 1 nM [³H]Oxotremorine-M, with or without 10 μM atropine (to determine specific binding). PS produced a significant downregulation of muscarinic receptors in the medium and high dose groups of adult, but not aged rats. Data (mean ± standard error) represent specific binding in terms of percent of control. The asterisk and pound signs represent values that are significantly different from the control and low (adult: 9 mg/kg; aged: 3 mg/kg) dose groups, respectively.
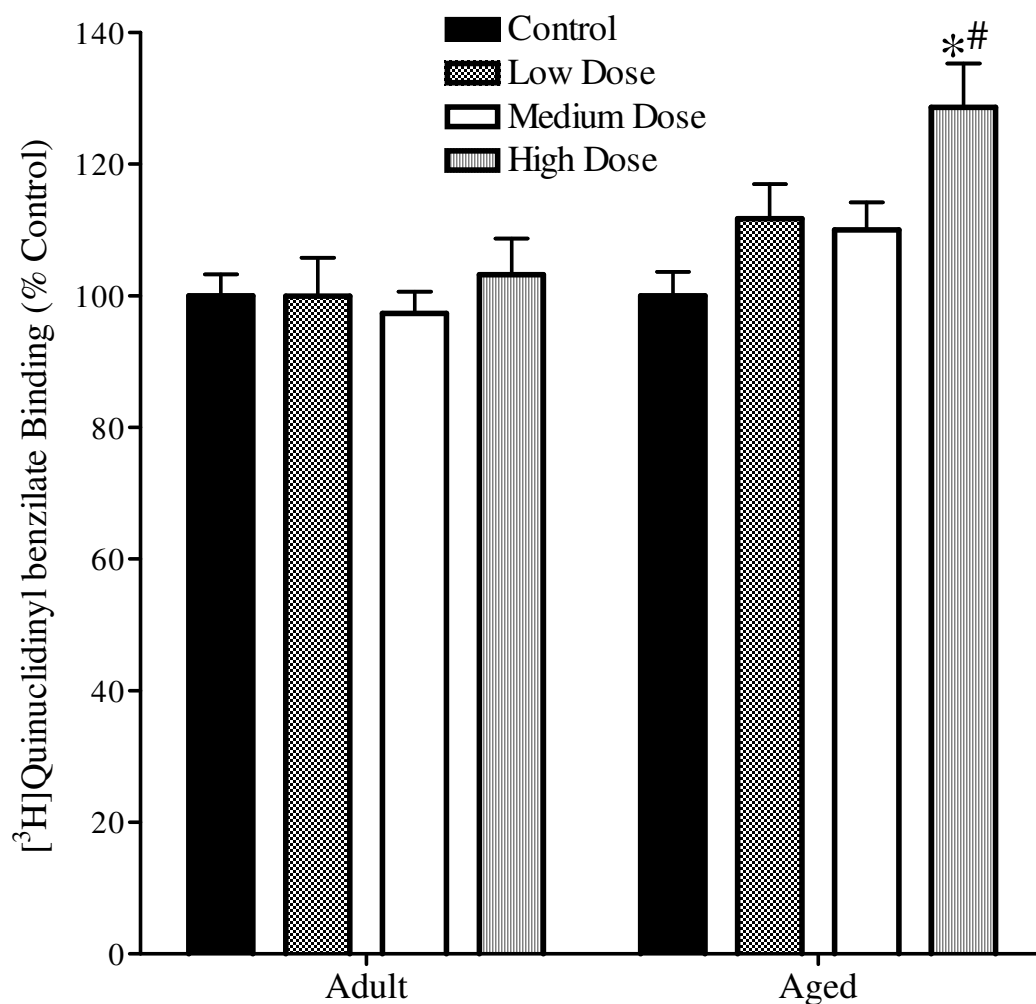
Figure 135: The effects of PS on muscarinic antagonist binding in ventricles from adult and aged rats. Rats (n=4-5/dose group) were treated with PS (sc) at the doses indicated and sacrificed 96 hours later. Ventricular membranes were incubated at 21°C for 90 minutes in the presence of 1 nM [^{3}H]Quinuclidinyl benzilate, with or without 10 μM atropine (to determine specific binding). PS caused a significant (30%) upregulation of muscarinic receptors in the high dose group of aged rats. Data (mean ± standard error) represent specific binding in terms of percent of control. The asterisk and pound signs represent values that are significantly different from the control and low (adult: 9 mg/kg; aged: 3 mg/kg) dose groups, respectively.
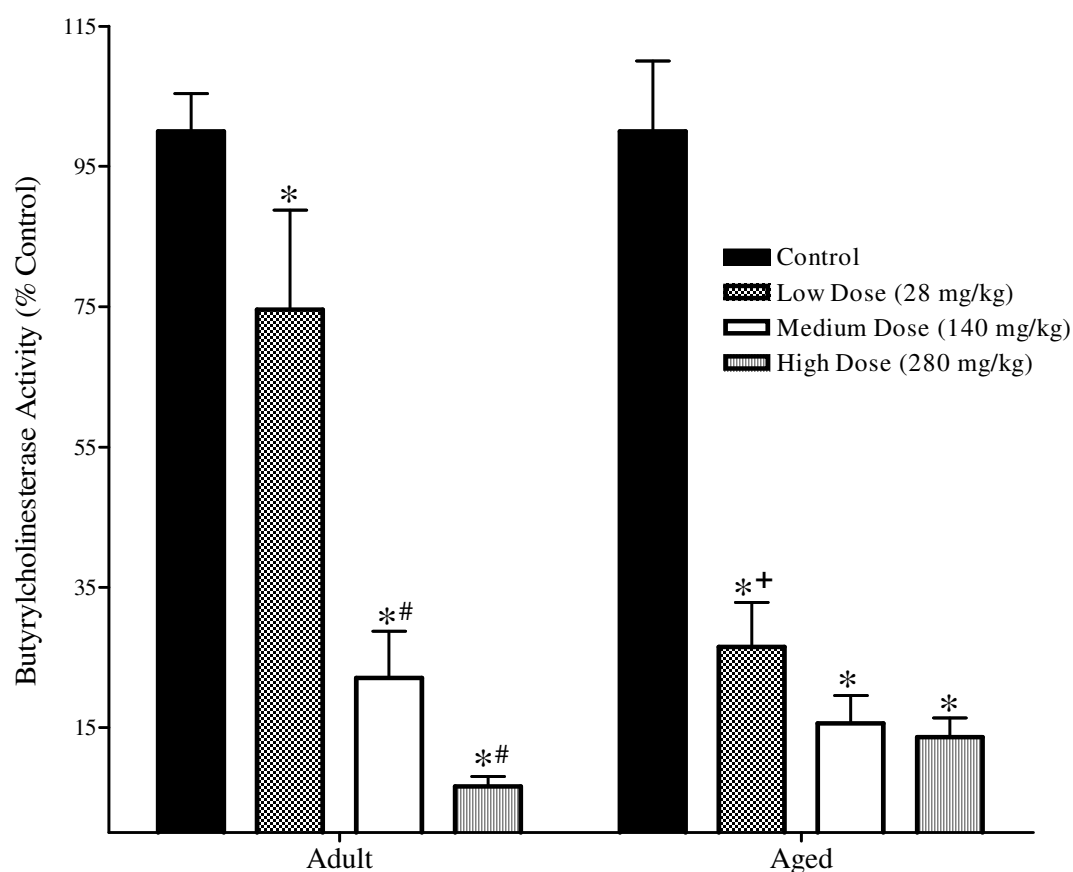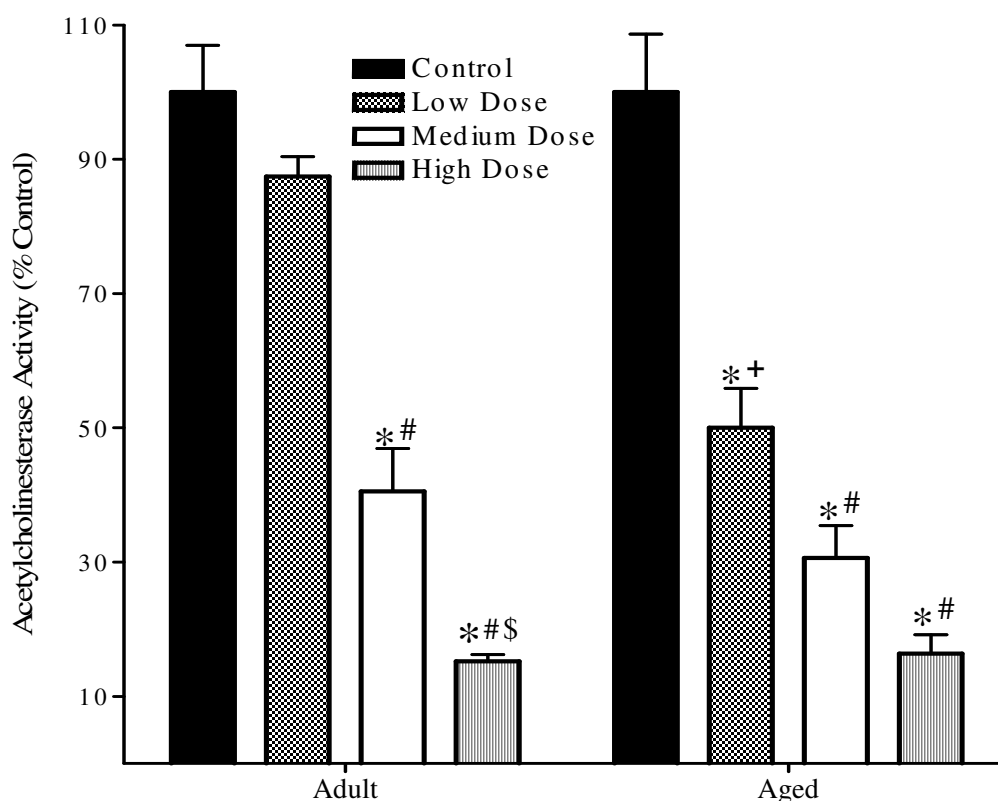
Figure 136: The effects of PS on acetylcholinesterase activity in atria from adult and aged rats. Rats (n=4-5/dose group) were treated with PS (sc) at the doses indicated and sacrificed 96 hours later. Atrial tissue homogenates were pre-incubated with 10 μM *iso*-OMPA at 37°C for 15 minutes prior to measuring the residual ChE activity as described previously. PS produced a dose-dependent inhibition of AChE activity in the atria of adult and aged rats. AChE in aged rats was inhibited to a significantly greater extent by the low dose of PS than AChE in adults. Data (mean ± standard error) represent AChE activity in terms of percent of control. The asterisk, pound and dollar signs represent values that are significantly different from control, low (adult: 9 mg/kg; aged: 3 mg/kg) and medium (adult: 13.5 mg/kg; aged: 4.5 mg/kg) dose groups, respectively, while the plus sign represents values that are significantly different from the same dose group in adults.
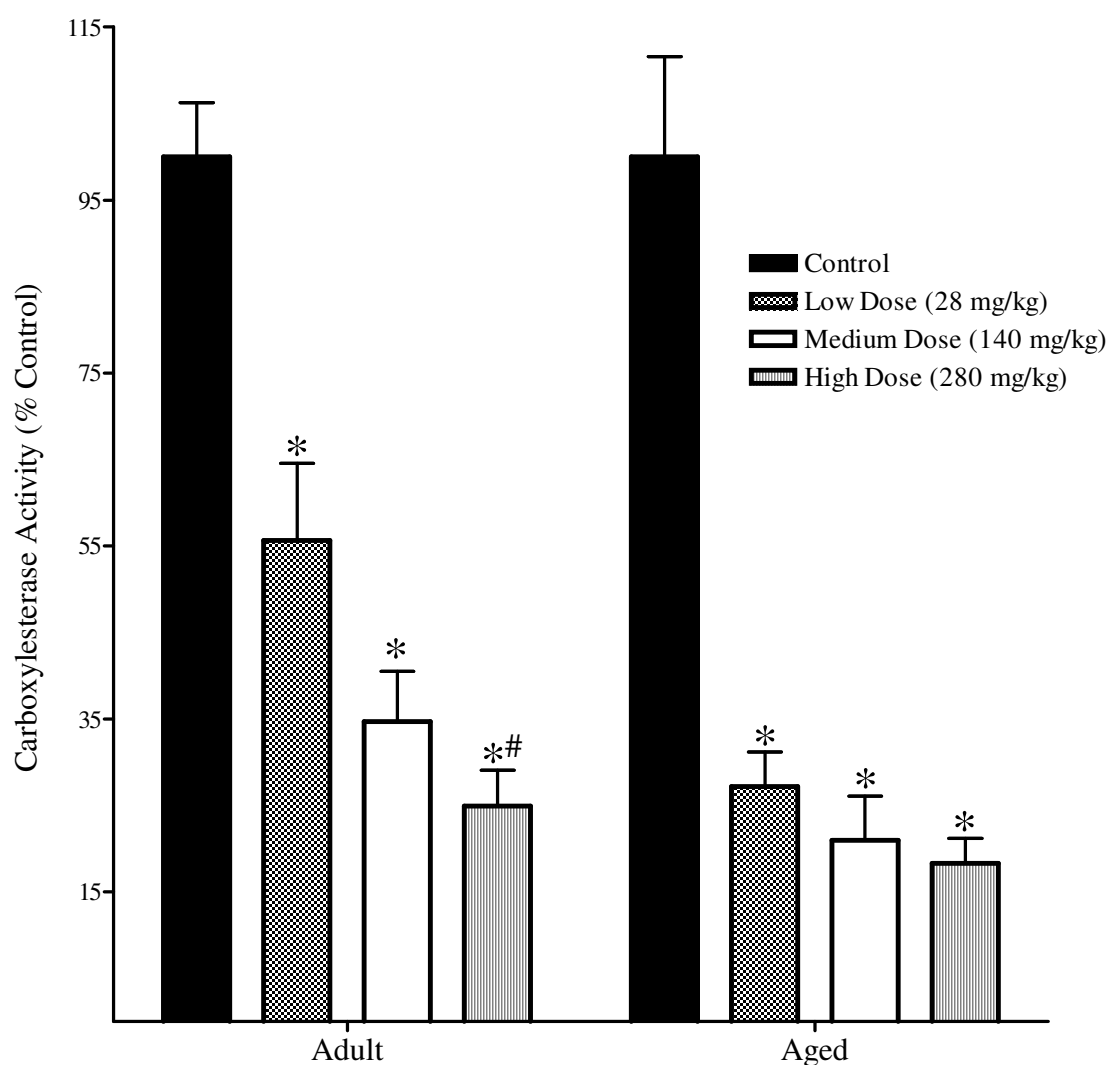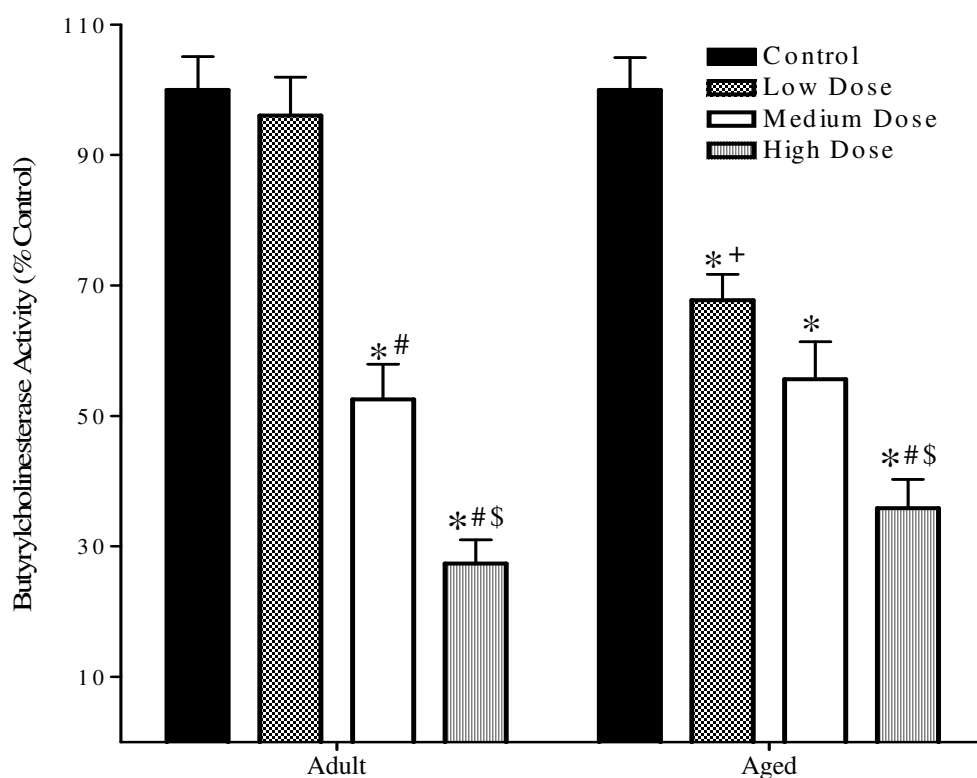
Figure 137: The effects of PS on butyrylcholinesterase activity in atria from adult and aged rats. Rats (n=4-5/dose group) were treated with PS (sc) at the doses indicated and sacrificed 96 hours later. Atrial tissue homogenates were pre-incubated with 10 µM BW284C51 at 37°C for 15 minutes prior to measuring the residual ChE activity as described previously. PS produced a dose-dependent inhibition of BChE activity in the atria of adult and aged rats. BChE in aged rats was inhibited to a significantly greater extent by the low dose of PS than BChE in adults. Data (mean ± standard error) represent BChE activity in terms of percent of control. The asterisk, pound and dollar signs represent values that are significantly different from control, low (adult: 9 mg/kg; aged: 3 mg/kg) and medium (adult: 13.5 mg/kg; aged: 4.5 mg/kg) dose groups, respectively, while the plus sign represents values that are significantly different from the same dose group in adults.
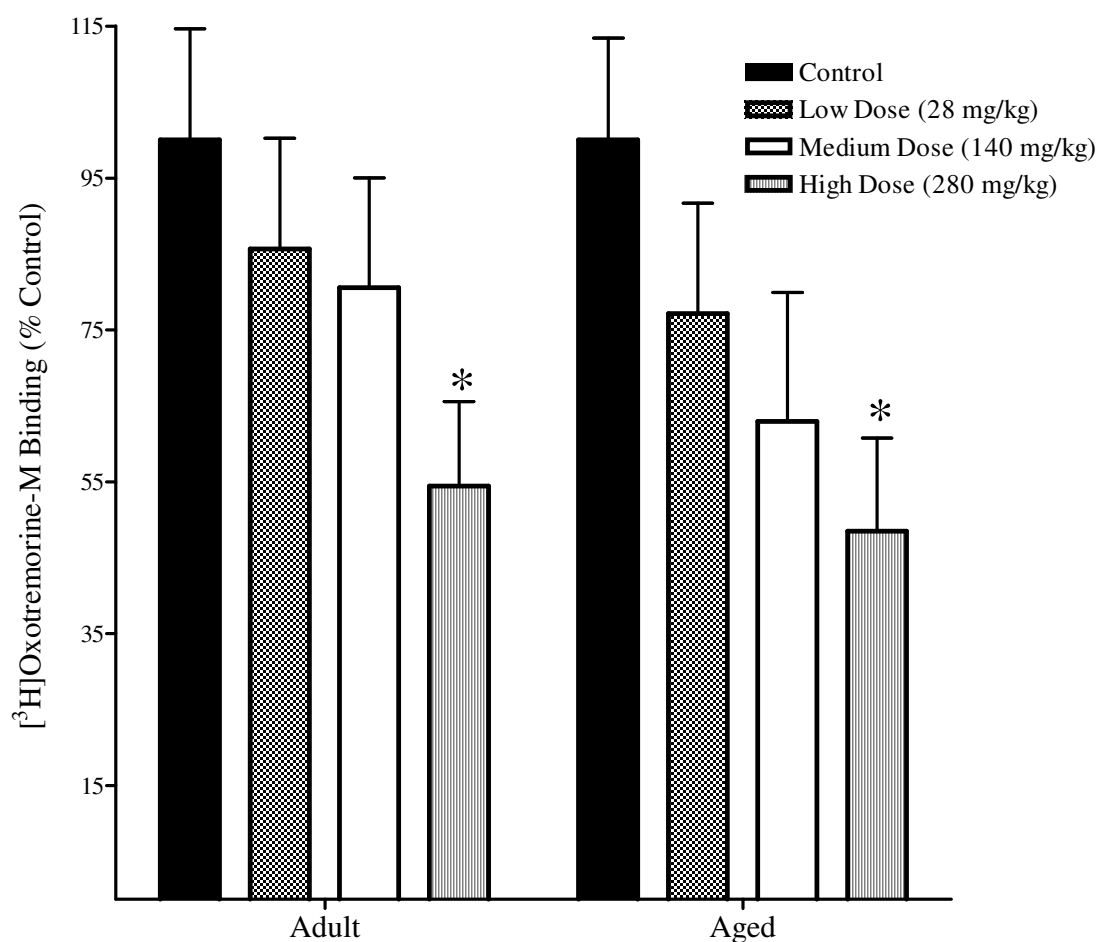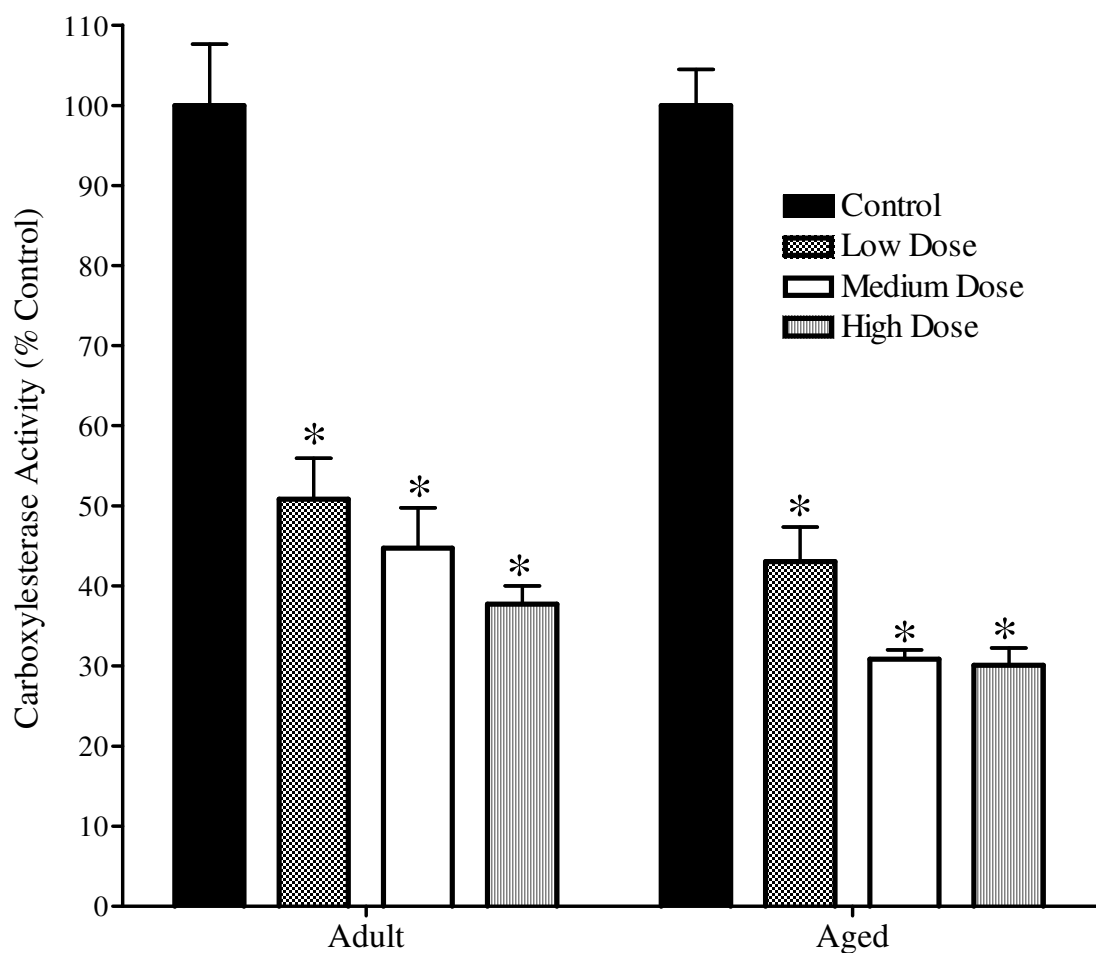
Figure 138: The effects of PS on carboxylesterase activity in atria from adult and aged rats. Rats (n=4-5/dose group) were treated with PS (sc) at the doses indicated and sacrificed 96 hours later. Atrial tissue homogenates were incubated at 37°C in the presence of the substrate p-nitrophenyl acetate to assess CarbE activity. PS produced a dose-dependent inhibition of CarbE activity in the atria of adult and aged rats. Data (mean ± standard error) represent CarbE activity in terms of percent of control. Asterisks represent values that are significantly different from control.
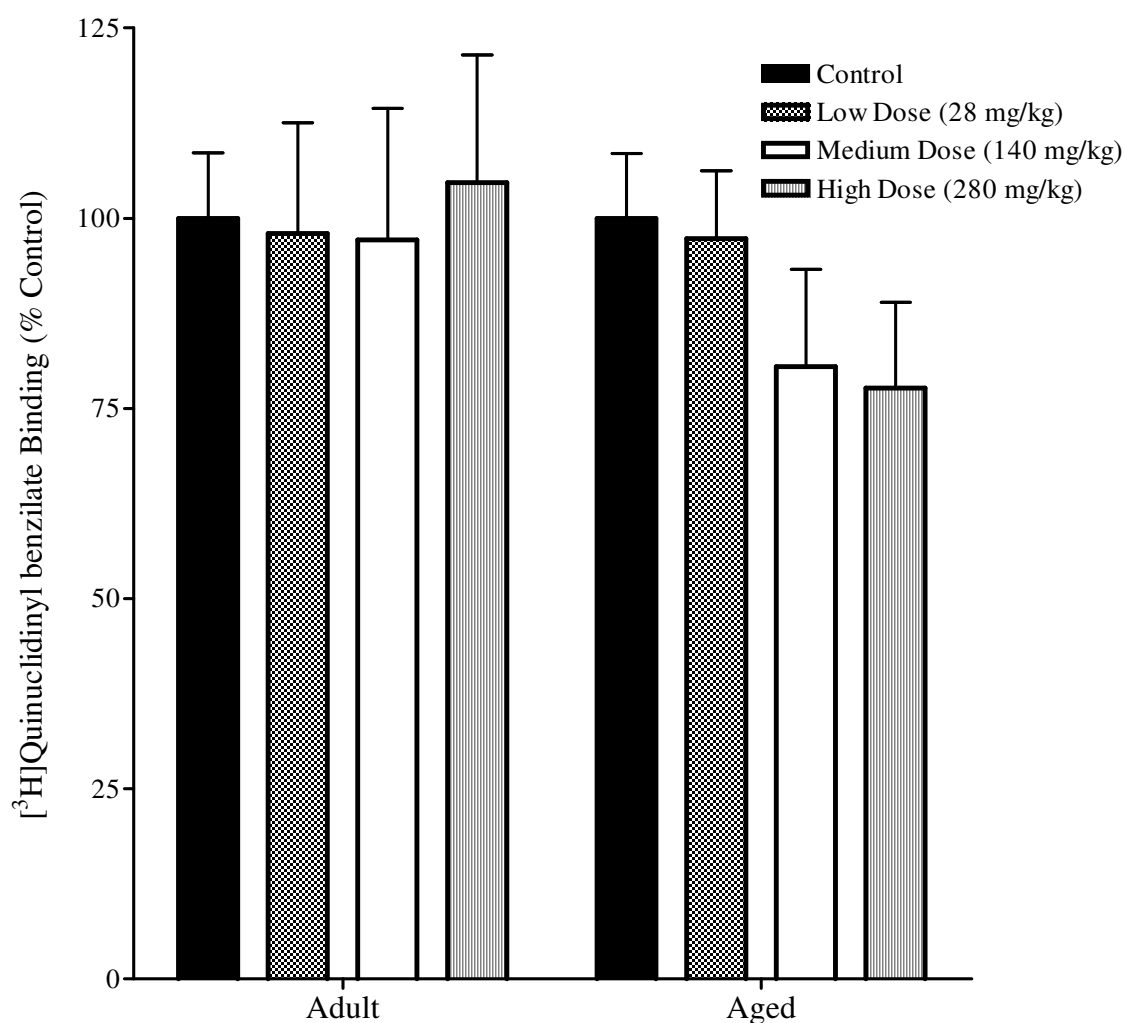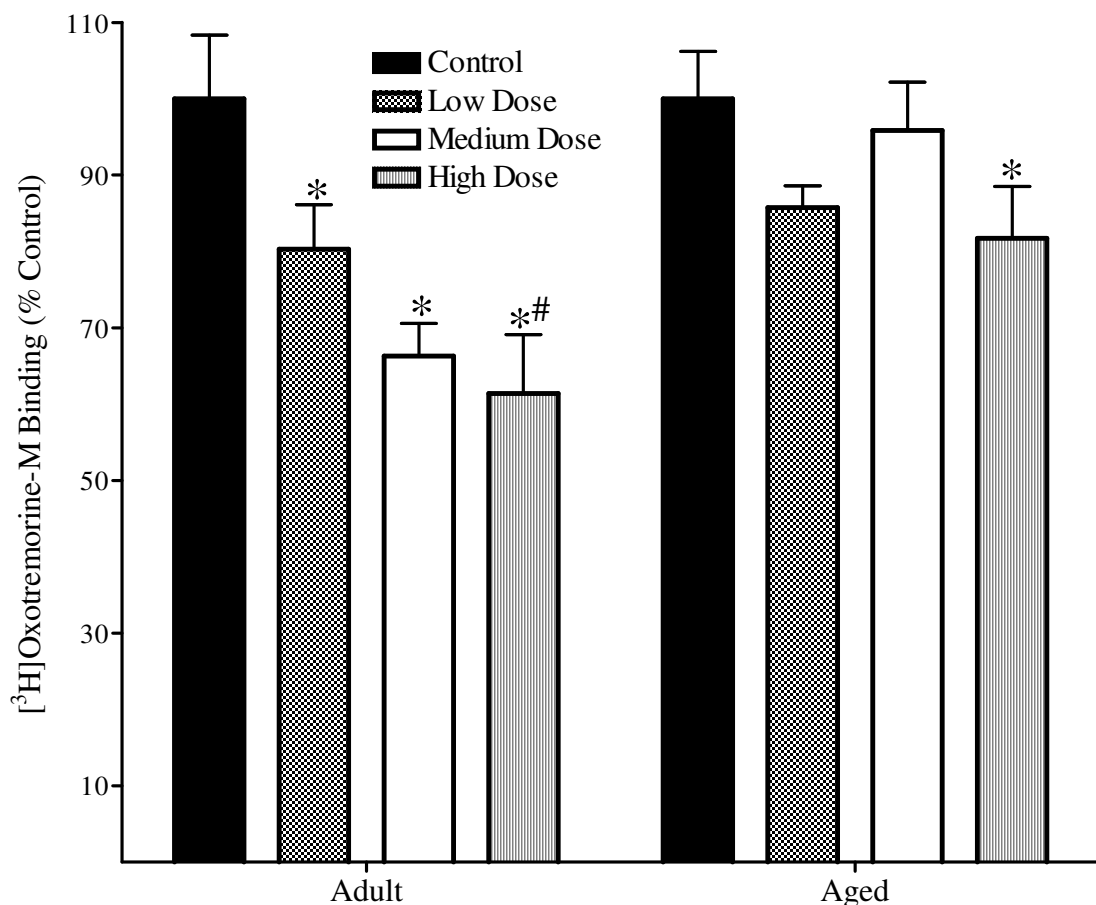
Figure 139: The effects of PS on muscarinic agonist binding in atria from adult and aged rats. Rats (n=4-5/dose group) were treated with PS (sc) at the doses indicated and sacrificed 96 hours later. Atrial membranes were incubated at 21°C for 90 minutes in the presence of 1 nM [^{3}H]Oxotremorine-M, with or without 10 μM atropine (to determine specific binding). The high dose of PS produced a significant downregulation of muscarinic receptors in adult and aged rats. Data (mean ± standard error) represent specific binding in terms of percent of control. The asterisk and pound signs represent values that are significantly different from the control and low (adult: 9 mg/kg; aged: 3 mg/kg) dose groups, respectively.

Figure 140: The effects of PS on muscarinic antagonist binding in atria from adult and aged rats. Rats (n=4-5/dose group) were treated with PS (sc) at the doses indicated and sacrificed 96 hours later. Atrial membranes were incubated at 21°C for 90 minutes in the presence of 1 nM [^{3}H]Quinuclidinyl benzilate, with or without 10 µM atropine (to determine specific binding). PS produced a slight upregulation of mucarinic receptors in the medium and high dose groups of aged, but not adult rats. Data (mean ± standard error) represent specific binding in terms of percent of control. The pound sign represent values that are significantly different from the low (adult: 9 mg/kg; aged: 3 mg/kg) dose group, while the plus sign represents values that are significantly different from the same dose group in adults.
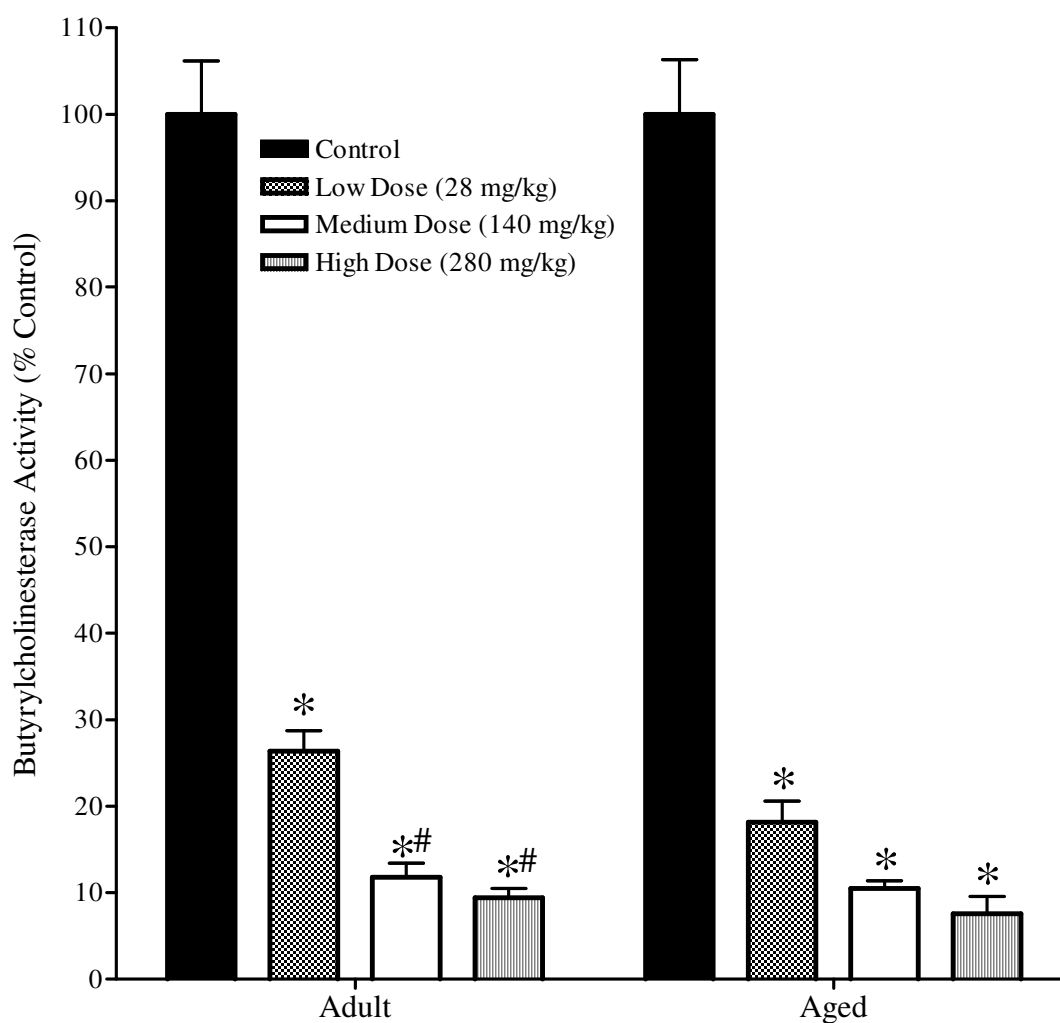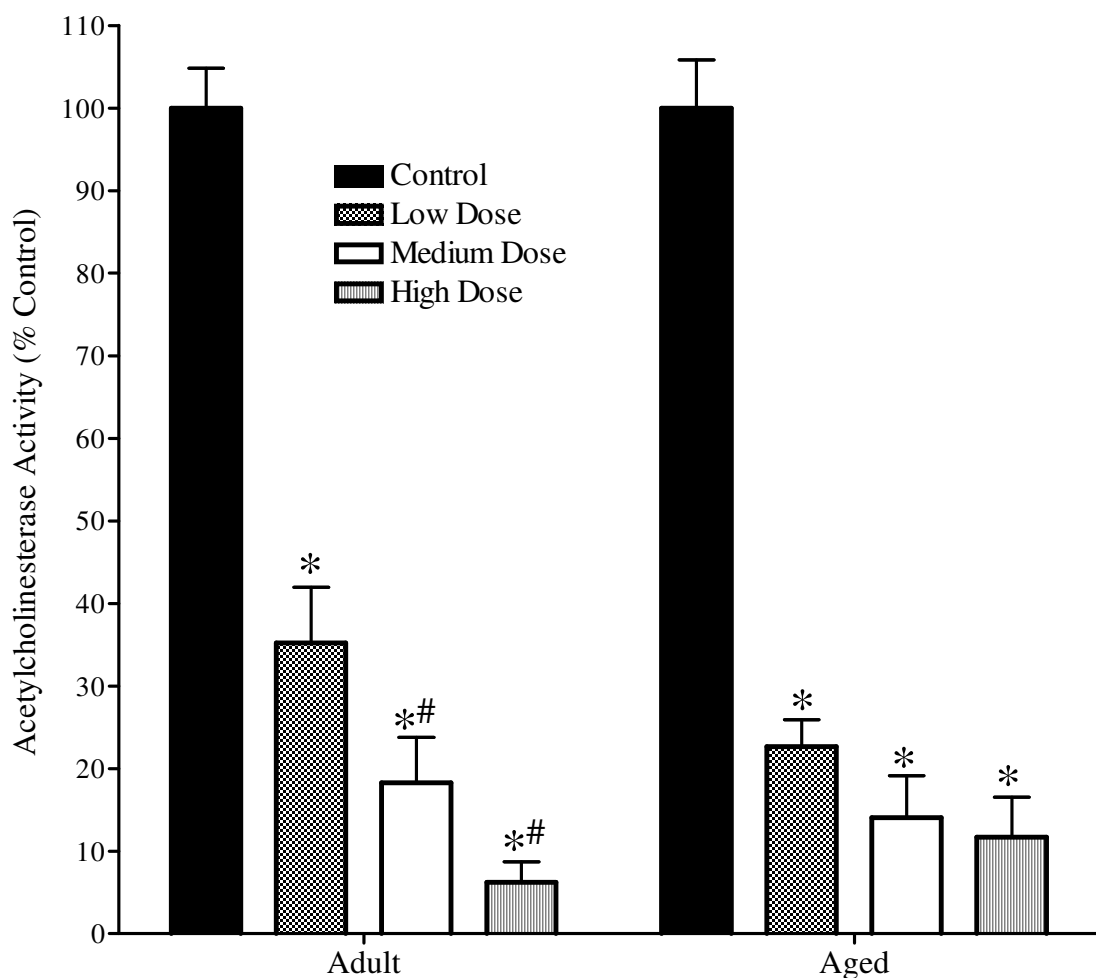
Figure 141: The effects of PS on acetylcholinesterase activity in cortex from adult and aged rats. Rats (n=4-5/dose group) were treated with PS (sc) at the doses indicated and sacrificed 96 hours later. Cortical tissue homogenates were pre-incubated with 10 μM *iso*-OMPA at 37°C for 15 minutes prior to measuring the residual ChE activity as described previously. PS produced a dose-dependent inhibition of AChE activity in the cortex of adult and aged rats. Data (mean ± standard error) represent AChE activity in terms of percent of control. The asterisk and pound signs represent values that are significantly different from the control and low (adult: 9 mg/kg; aged: 3 mg/kg) dose groups, respectively.
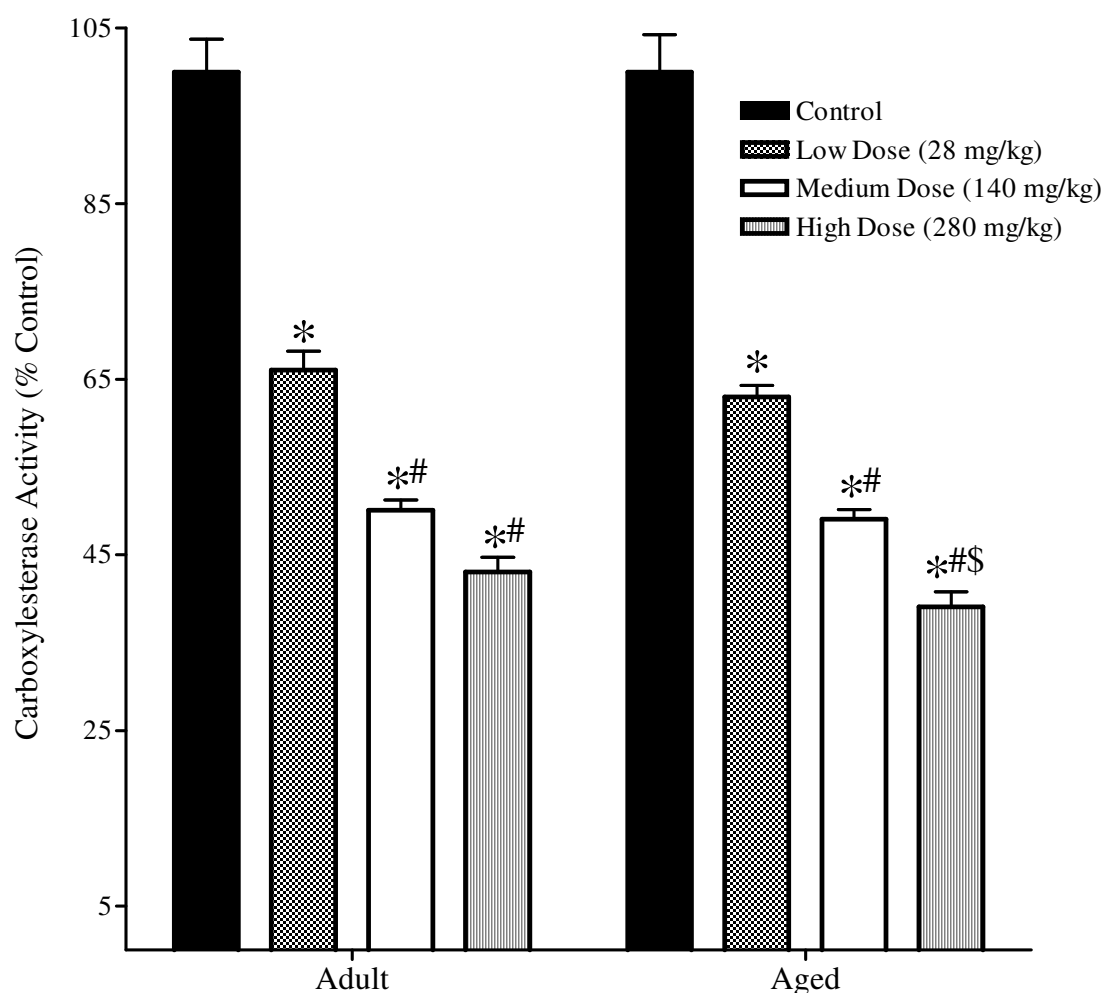
Figure 142: The effects of PS on butyrylcholinesterase activity in cortex from adult and aged rats. Rats (n=4-5/dose group) were treated with PS (sc) at the doses indicated and sacrificed 96 hours later. Cortical tissue homogenates were pre-incubated with 10 μM BW284C51 at 37°C for 15 minutes prior to measuring the residual ChE activity as described previously. PS produced a dose-dependent inhibition of BChE activity in the cortex of adult and aged rats. Data (mean ± standard error) represent BChE activity in terms of percent of control. The asterisk, pound and dollar signs represent values that are significantly different from control, low (adult: 9 mg/kg; aged: 3 mg/kg) and medium (adult: 13.5 mg/kg; aged: 4.5 mg/kg) dose groups, respectively.
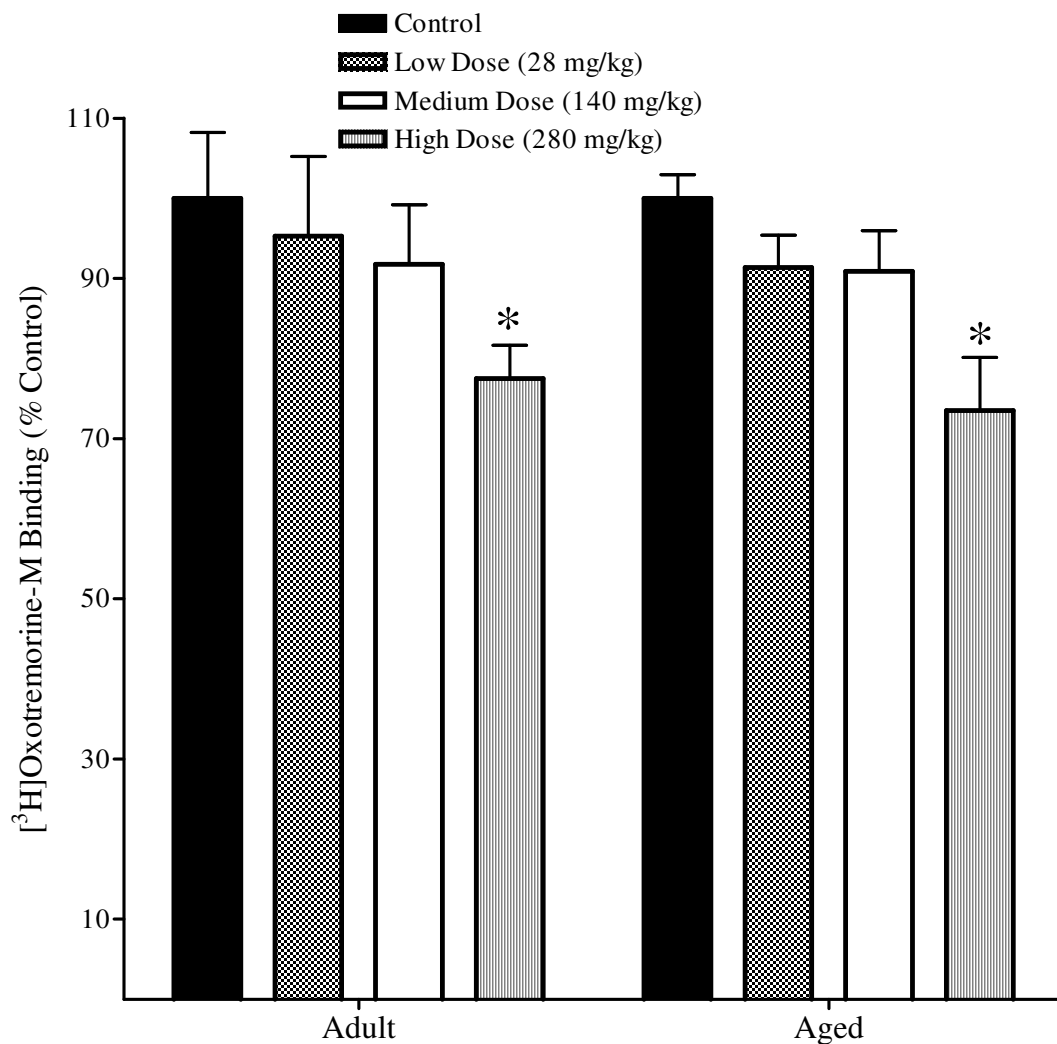
Figure 143: The effects of PS on carboxylesterase activity in cortex from adult and aged rats. Rats (n=4-5/dose group) were treated with PS (sc) at the doses indicated and sacrificed 96 hours later. Cortical tissue homogenates were incubated at 37°C in the presence of the substrate p-nitrophenyl acetate to assess CarbE activity. PS produced a dose-dependent inhibition of CarbE activity in the cortex of adult and aged rats. Data (mean ± standard error) represent CarbE activity in terms of percent of control. The asterisk and pound signs represent values that are significantly different from the control and low (adult: 9 mg/kg; aged: 3 mg/kg) dose groups, respectively.
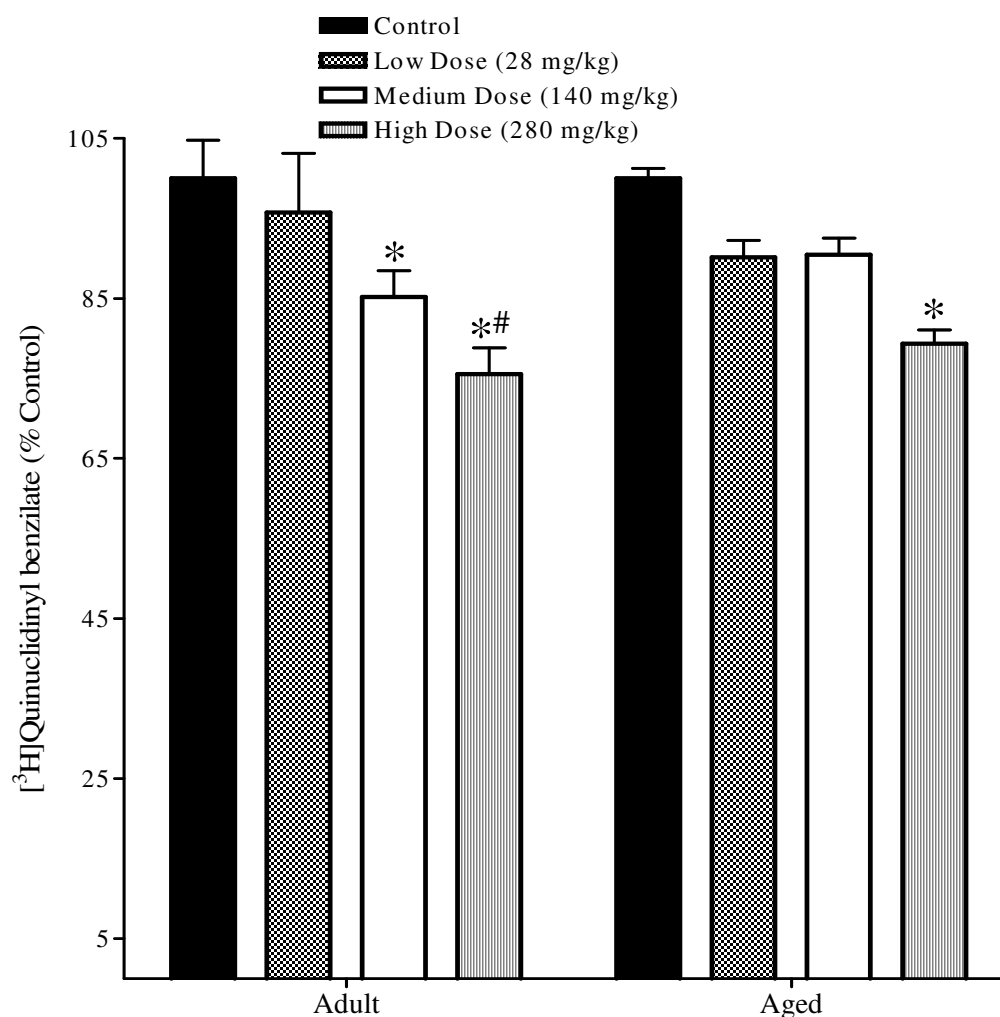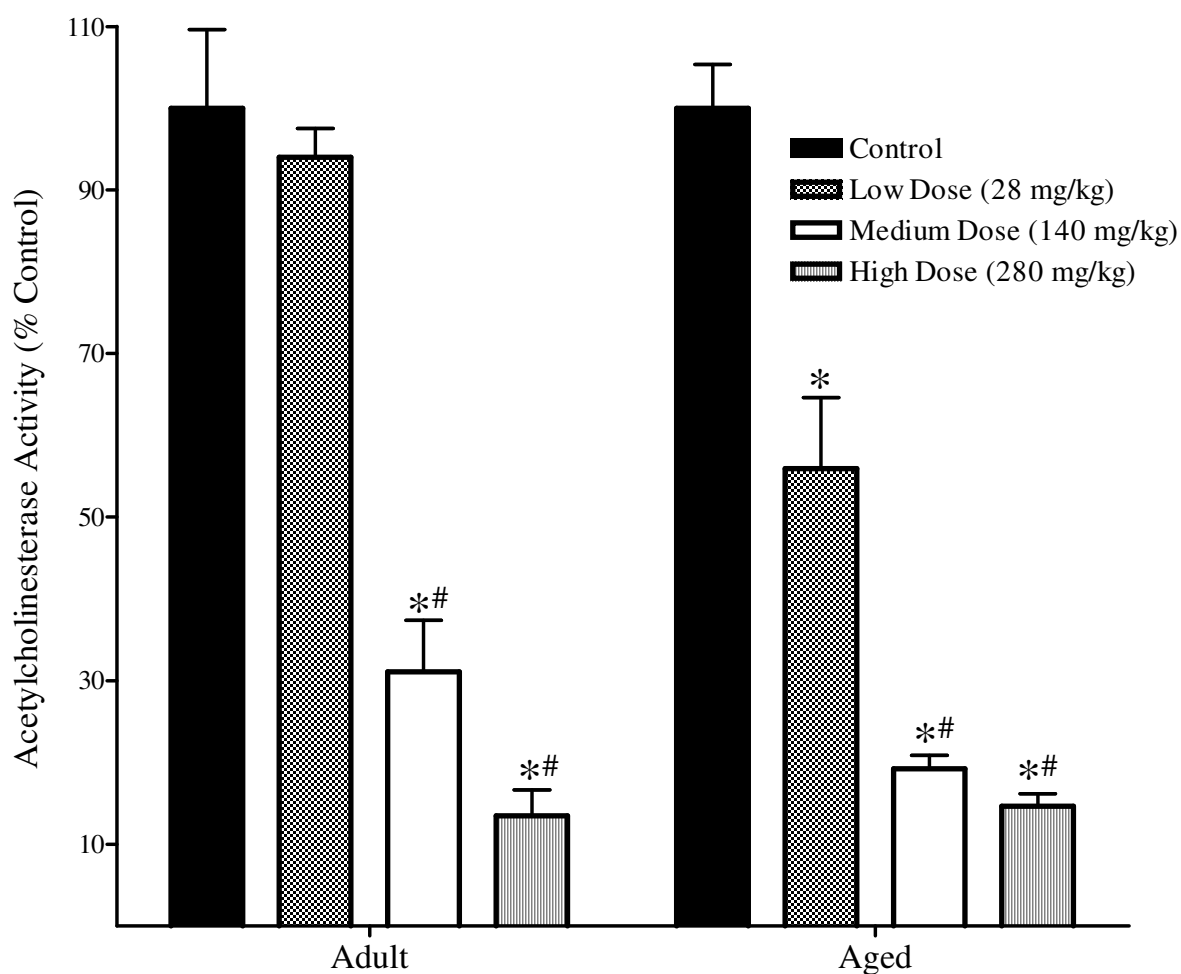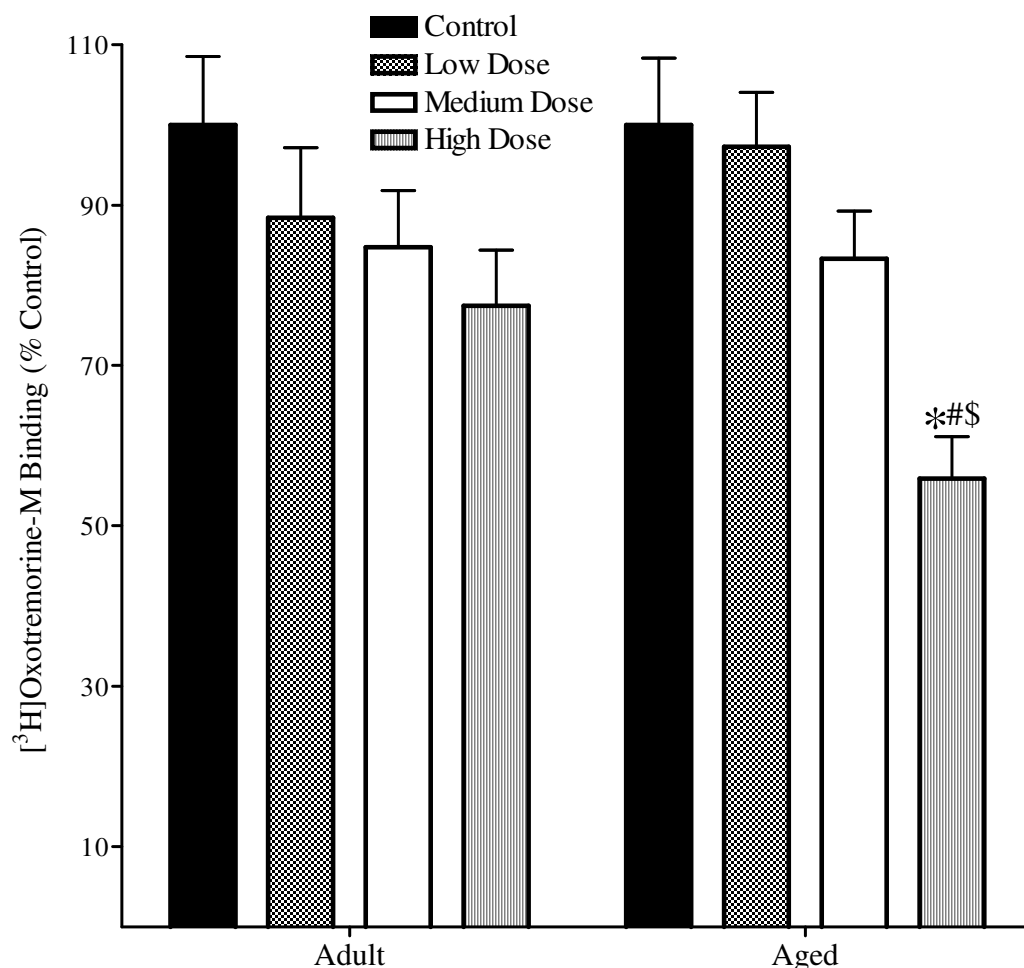
Figure 144: The effects of PS on muscarinic agonist binding in cortex from adult and aged rats. Rats (n=4-5/dose group) were treated with PS (sc) at the doses indicated and sacrificed 96 hours later. Cortical membranes were incubated at 21°C for 90 minutes in the presence of 1 nM [^{3}H]Oxotremorine-M, with or without 10 μM atropine (to determine specific binding). The high dose of PS produced a significant downregulation of muscarinic receptors in aged, but not adult rats. Data (mean ± standard error) represent specific binding in terms of percent of control. The asterisk, pound and dollar signs represent values that are significantly different from control, low (adult: 9 mg/kg; aged: 3 mg/kg) and medium (adult: 13.5 mg/kg; aged: 4.5 mg/kg) dose groups, respectively.
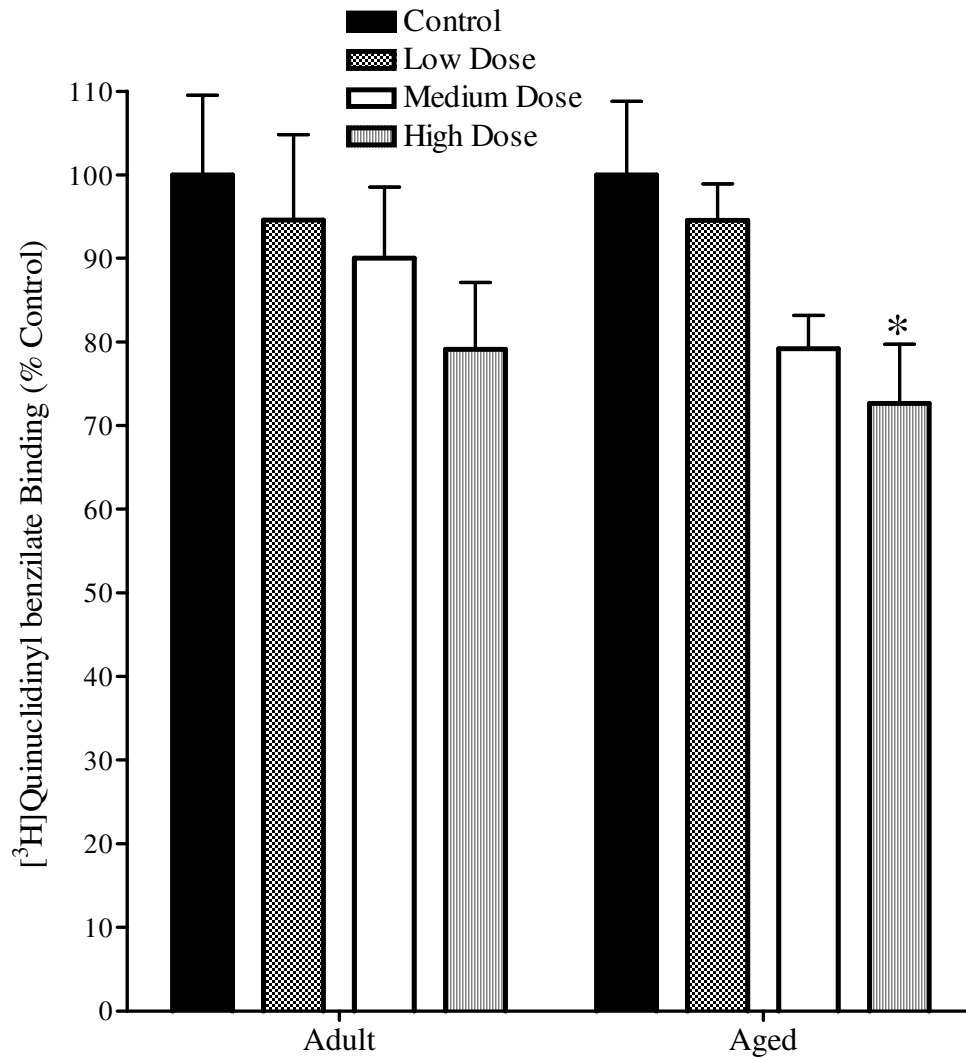
Figure 145: The effects of PS on muscarinic antagonist binding in cortex from adult and aged rats. Rats (n=4-5/dose group) were treated with PS (sc) at the doses indicated and sacrificed 96 hours later. Cortical membranes were incubated at 21°C for 90 minutes in the presence of 1 nM [³H]Quinuclidinyl benzilate, with or without 10 µM atropine (to determine specific binding). PS produced a significant downregulation of muscarinic receptors in the high dose-group of aged, but not adult rats. Data (mean ± standard error) represent specific binding in terms of percent of control. Asterisk represents values that are significantly different from control.
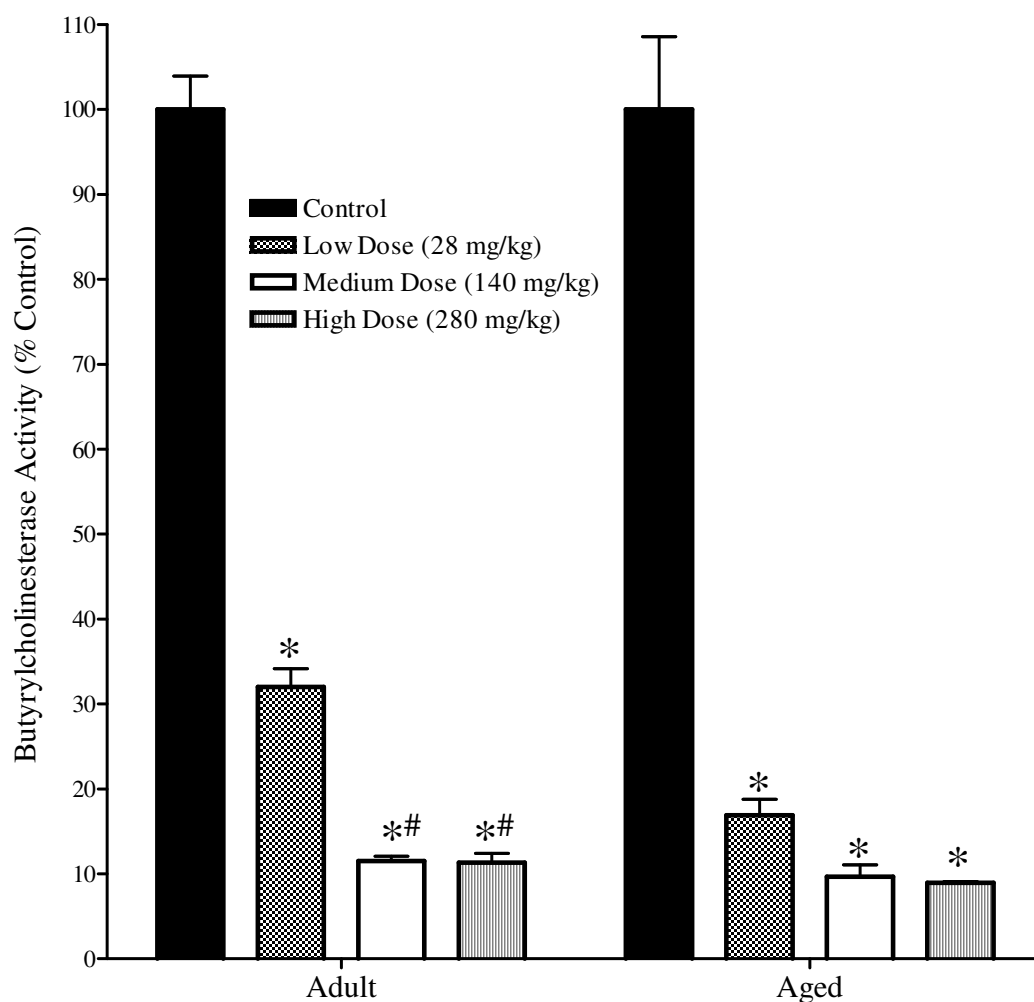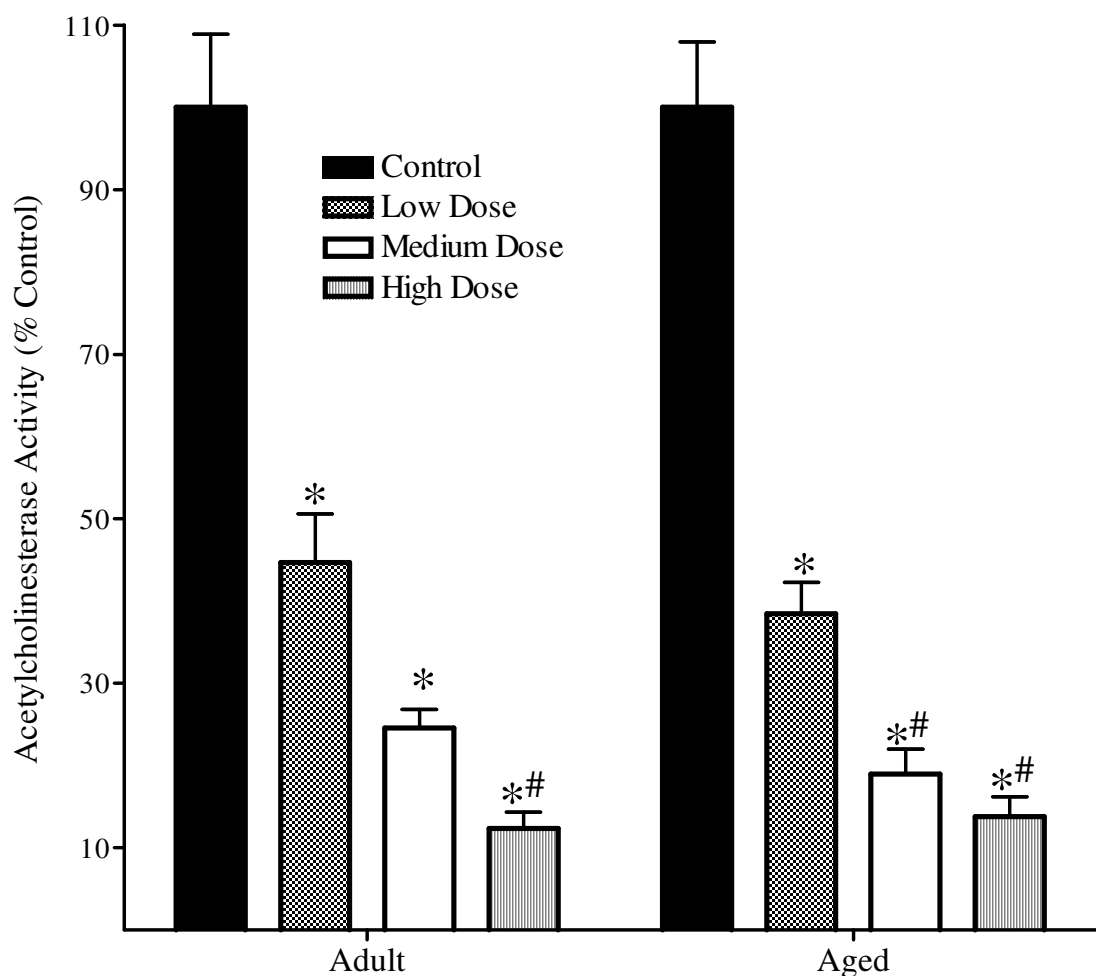
Figure 146: The effects of PS on acetylcholinesterase activity in plasma from adult and aged rats. Rats (n=4-5/dose group) were treated with PS (sc) at the doses indicated and sacrificed 96 hours later. Diluted plasma samples were pre-incubated with 10 μM *iso-OMPA* at 37°C for 15 minutes prior to measuring the residual ChE activity as described previously. PS produced a dose-dependent inhibition of AChE activity in the plasma of adult and aged rats. Data (mean ± standard error) represent AChE activity in terms of percent of control. The asterisk and pound signs represent values that are significantly different from control and low (adult: 9 mg/kg; aged: 3 mg/kg) dose groups, respectively.
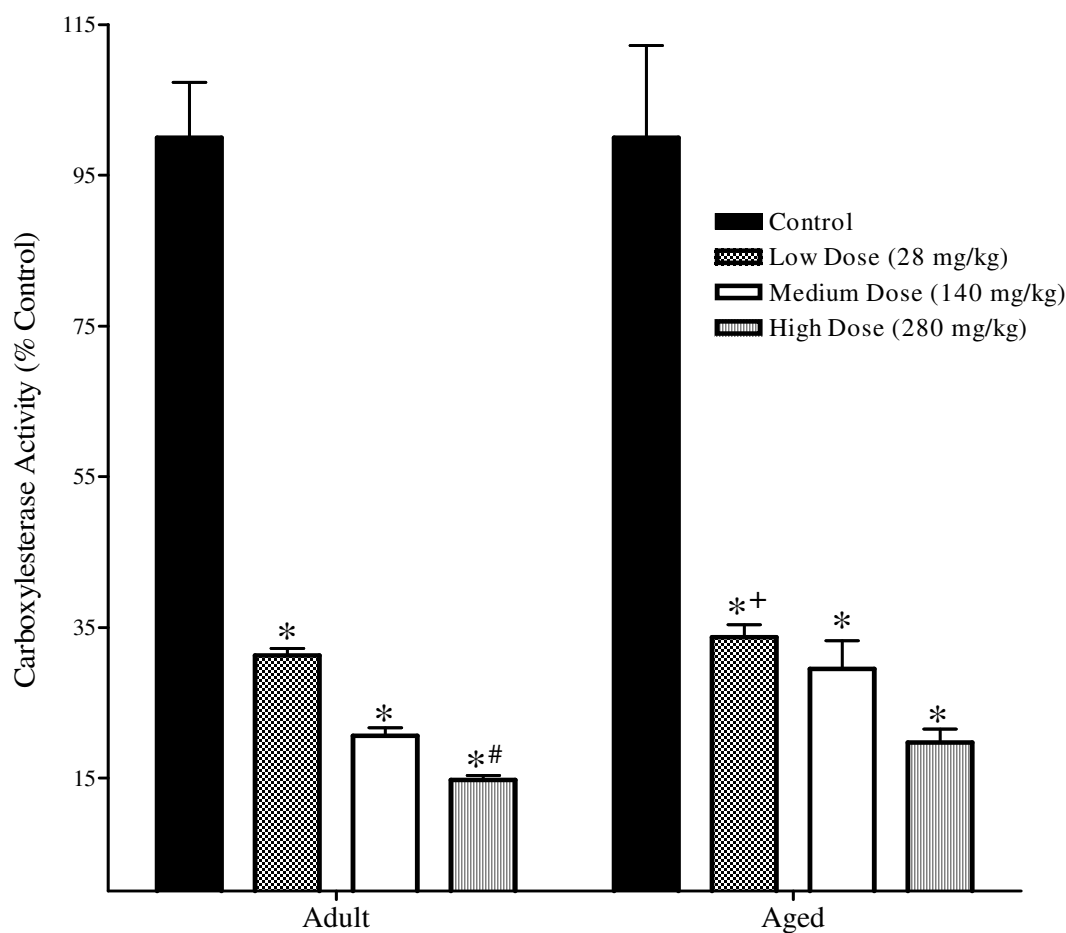
Figure 147: The effects of PS on butyrylcholinesterase activity in plasma from adult and aged rats. Rats (n=4-5/dose group) were treated with PS (sc) at the doses indicated and sacrificed 96 hours later. Diluted plasma samples were pre-incubated with 10 μM BW284C51 at 37°C for 15 minutes prior to measuring the residual ChE activity as described previously. PS produced a dose-dependent inhibition of BChE activity in the plasma of adult and aged rats. Data (mean ± standard error) represent BChE activity in terms of percent of control. The asterisk and pound signs represent values that are significantly different from control and low (adult: 9 mg/kg; aged: 3 mg/kg) dose groups, respectively.

Figure 148: The effects of PS on carboxylesterase activity in plasma from adult and aged rats. Rats (n=4-5/dose group) were treated with PS (sc) at the doses indicated and sacrificed 96 hours later. Diluted plasma samples were incubated at 37°C in the presence of the substrate p-nitrophenyl acetate to assess CarbE activity. PS produced a dose-dependent inhibition of CarbE activity in the plasma of adult and aged rats. Data (mean ± standard error) represent CarbE activity in terms of percent of control. The asterisk, pound and dollar signs represent values that are significantly different from control, low (adult: 9 mg/kg; aged: 3 mg/kg) and medium (adult: 13.5 mg/kg; aged: 4.5 mg/kg) dose groups, respectively.
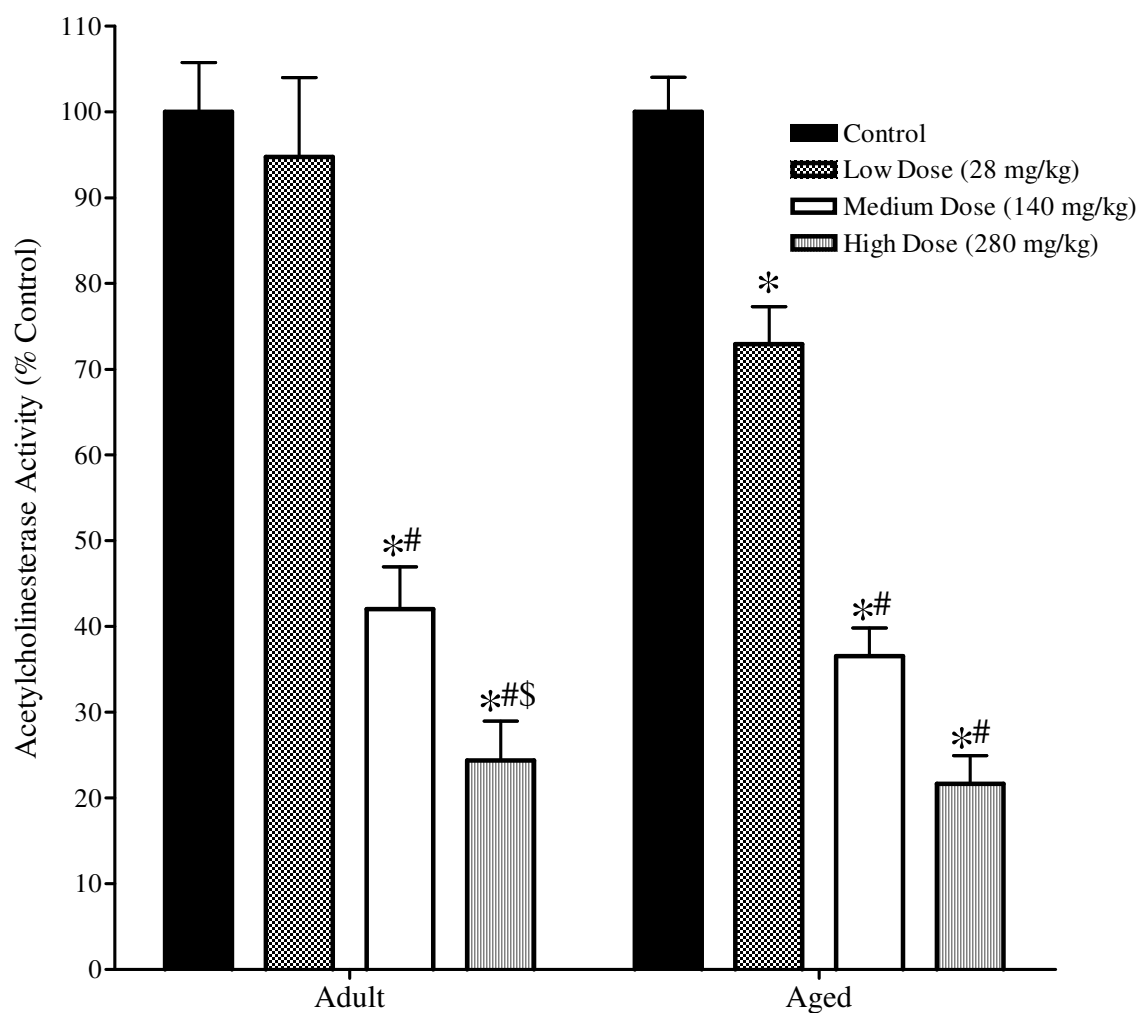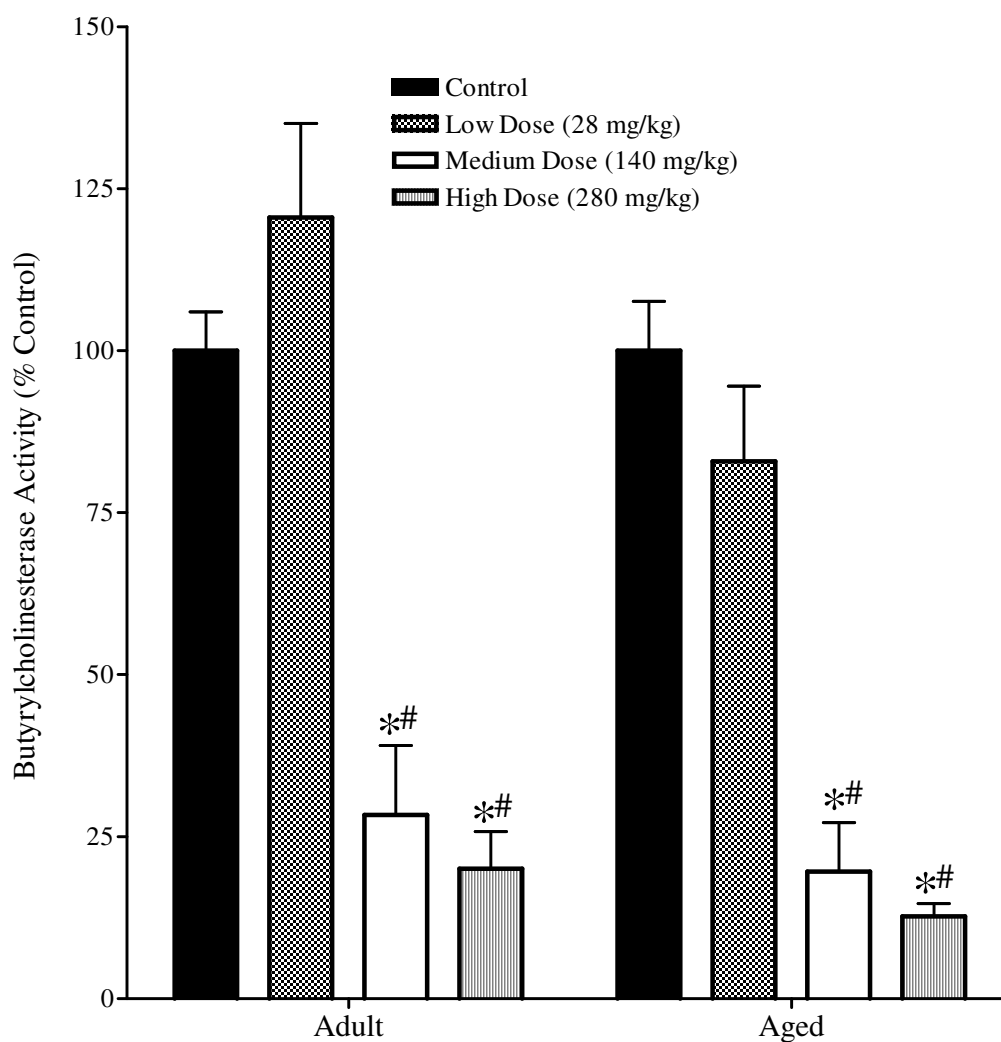
Figure 149: The effects of PS on acetylcholinesterase activity in diaphragm from adult and aged rats. Rats (n=4-5/dose group) were treated with PS (sc) at the doses indicated and sacrificed 96 hours later. Diaphragm tissue homogenates were pre-incubated with 10 μM *iso*-OMPA at 37°C for 15 minutes prior to measuring the residual ChE activity as described previously. PS produced a dose-dependent inhibition of AChE activity in the diaphragm of adult and aged rats. Data (mean ± standard error) represent AChE activity in terms of percent of control. The asterisk, pound and dollar signs represent values that are significantly different from control, low (adult: 9 mg/kg; aged: 3 mg/kg) and medium (adult: 13.5 mg/kg; aged: 4.5 mg/kg) dose groups, respectively.

Figure 150: The effects of PS on butyrylcholinesterase activity in diaphragm from adult and aged rats. Rats (n=4-5/dose group) were treated with PS (sc) at the doses indicated and sacrificed 96 hours later. Diaphragm tissue homogenates were pre-incubated with 10 μM BW284C51 at 37°C for 15 minutes prior to measuring the residual ChE activity as described previously. PS produced a dose-dependent inhibition of BChE activity in the diaphragm of adult and aged rats. Data (mean ± standard error) represent BChE activity in terms of percent of control. The asterisk, pound and dollar signs represent values that are significantly different from control, low (adult: 9 mg/kg; aged: 3 mg/kg) and medium (adult: 13.5 mg/kg; aged: 4.5 mg/kg) dose groups, respectively.

CHAPTER 4

DISCUSSION

Distribution of Acetylcholinesterase, Butyrylcholinesterase and Carboxylesterase Activities in Atria, Ventricles, Cortex and Plasma of Adult and Aged Rats

The distributions of acetylcholinesterase (AChE) and butyrylcholinesterase (BChE) were found to vary depending on the tissue examined (Tables 1 and 5). The total cholinesterase activity in the cortex of both adult and aged rats is comprised of ~90-95% AChE and 5-10% BChE. In both age-groups, the total ChE in the ventricles is made up of ~90% BChE and 10% AChE, while in the atria, ~80% BChE and 20% AChE make up the total ChE. In general, the atria contain ~2.5-fold more cholinesterase activity (4 times more AChE activity and 2 times more BChE activity), and 1.5-fold more carboxylesterase activity than the ventricles. In both adult and aged rats, plasma was comprised of ~70% AChE and ~30% BChE.

These findings generally agreed with work done by others in the field. Jbilo et al (1994a) reported that the liver and heart generally contain a high concentration of BChE, while the brain and skeletal muscles predominantly express AChE. Previous reports indicate that the adult rat brain contains ~80% AChE and 20% BChE, whereas in humans, ~95% of the total ChE in the brain is AChE, with only 5% BChE (Ballard et al, 2005; Giacobini, 2004). Chatonnet and Lockridge (1989) reported that the total ChE of adult

240

hearts of higher vertebrates is made up of around 85% BChE and around 15% AChE. Li et al (2000) estimated the AChE and BChE levels in various tissues from adult rats and found that AChE levels were higher than BChE in the brain, diaphragm and serum, whereas BChE predominated in the heart, liver, intestine and lung. In general, the ratios of AChE to BChE in the brain, heart, serum and diaphragm were very similar to the values obtained in the current studies.

Levels of AChE, BChE and CarbE were evaluated in aged rats to determine the effect of aging on the activity of these enzymes (Figures 106-110). While the levels of all three enzymes seemed to decrease slightly in aged (compared to adult) ventricles and cortex, this difference was not significant. However, in the plasma, AChE and BChE levels were significantly higher, while CarbE activity was significantly lower (~35%) in aged compared to adult rats. As both AChE and BChE increased proportionately in aged rats, their ratio in the plasma remained the same in aged and adult rats.

Atterberry and coworkers (1997) investigated the developmental changes in brain acetylcholinesterase and liver aliesterase (CarbE) in male Sprague-Dawley rats of different ages (1, 3, 12, 33 and 80 days). The specific activities of acetylcholinesterase in the cerebral cortex (but not in the medulla oblongata) and liver CarbE increased with maturation. This indicated that adult rats had higher levels of both target enzyme (AChE) as well as protective enzyme (CarbE) compared to juvenile rats. Similar results were obtained by Moser et al (1998), who measured the CarbE activity in the plasma and liver of pre-weanling (1, 4, 7, 12, 17 and 21 days old) and adult (82-92 days old) rats of both sexes. Pre-weanling rats were found to have considerably less CarbE than adults, and adult females had less liver CarbE than adult males. Pope and colleagues (2005b)

241

evaluated the human liver carboxylesterase activities in tissues from human infants (2-24 months) and adults (20-36 years). There was no significant difference between mean infant and adult CarbE activities, and the authors concluded that in contrast to rodents, human liver CarbE activity did not change extensively during postnatal maturation.

Karanth and Pope (2000) evaluated the activity of CarbE in the liver, plasma and lung of neonatal (7 days), juvenile (21 days), adult (3 months) and aged (24 months) male Sprague-Dawley rats. Neonatal and juvenile rats had significantly lower levels of CarbE than adults in all tissues examined. While CarbE levels were similar between adult and aged rats in the liver and lung, plasma CarbE levels in aged rats were 50% lower than in adults. In our current study, we found that plasma CarbE was 35%, (but not 50%) lower in aged rats than in adults. However, the aged rats used in these studies were 18 months-old as opposed to the 24 months-old rats used by Karanth and Pope (2000). Thus, plasma CarbE may decrease further with advanced aging in this strain of rat, potentially contributing to higher sensitivity to some organophosphorus insecticides.

Several researchers have reported an age-related decrease in cholinesterase in the whole brain (Sastry et al, 1983), as well as in different brain regions (Michalek et al, 1989; Sirvio et al, 1989; Pintor et al, 1990; Meneguz et al, 1992). This age-related change was suggested to be due to a selective loss of enzymatic activity of the G4 globular tetrameric isoform, but not the G1 isoform of AChE (Meneguz et al, 1992). Kosasa et al (1999) reported a decrease in cholinesterase activity in the heart, small intestine and pectoral muscle, and an increased cholinesterase activity in the liver and plasma of aged as compared to adult rats. The increased cholinesterase activity in the plasma of aged rats agreed with our findings.

Age-related differences in acetylcholinesterase and butyrylcholinesterase activities have been reported in a variety of species. Several reports indicate that basal parasympathetic tone decreases during aging. Meyer et al (1985), using a rat atrial mince preparation, reported that choline uptake, acetylcholine synthesis and acetylcholine release were all decreased in aged rats. Kelliher and Conahan (1980) found that the positive inotropic response that is normally observed following vagotomy in adult rats was abolished in aged rats. These authors also reported that the heart rate response to the muscarinic agonist methacholine was reduced in aged compared to adult rats. Kennedy and Seifen (1990) reported that right atrial preparations from aged rats were more sensitive to the negative chronotropic action of acetylcholine compared to adult rats. However, no age-related difference in sensitivity was observed with carbachol, a muscarinic agonist that is resistant to degradation by cholinesterases. When the right atrial preparations were pre-treated with diisopropylfluorophosphate (DFP), an irreversible OP cholinesterase inhibitor, age-related differences in responsiveness to acetylcholine were abolished. The authors concluded that the increased sensitivity of atria from aged rats to acetylcholine as compared to adults occurred as a result of decreased acetylcholinesterase activity. Su and Narayanan (1992), using isolated, perfused, spontaneously-beating rat hearts, arrived at a similar conclusion. They found that the greater sensitivity of aged rats to the negative chronotropic effects of acetylcholine as compared to adults, was diminished in the presence of a maximally effective concentration of eserine, a cholinesterase inhibitor. The negative chronotropic and inotropic response to carbachol was also greater in aged than in adult rats. Moreover, acetylcholinesterase activities were found to be decreased by 50-60% in aged atria and

ventricles; however, no age-related differences were observed in binding of the muscarinic antagonist [3H]QNB in either the atria or ventricles. These authors concluded that the enhanced responsiveness of the aging heart to cholinergic agonists was at least partly due to an age-related reduction in cardiac acetylcholinesterase activity.

Age-related changes in AChE and/or BChE activities and molecular isoforms have been reported in brain of several species including man. Skau and Triplett (1998) reported a significant reduction (20-50%) of AChE activity in different brain regions of aged (24 months) as compared to adult (6 months) Fischer 344 rats. When the ratio of G4/G1 isoforms was evaluated in different brain regions, it was found to be unaltered in aged rats, thus indicating that although aged rats exhibit decreased brain AChE levels, there did not appear to be any selective reduction of a particular isoform. In contrast, Das et al (2001) evaluating AChE activity in different brain regions of adult (3 months) and aged (18-22 months) male and female Sprague-Dawley rats found a significant decrease (40-55%) in G4 but not G1 AChE in brain regions of aged male rats. Relatively similar differences were observed in adult and aged female rats. Interestingly, higher levels of the G4 isoform were observed in female compared to male rats in both age-groups. From these studies, the authors concluded that age-related differences in AChE were predominantly due to changes in the G4 isoform, and gender-dependent differences occur. Atack et al (1986) compared the activities and molecular forms of AChE and BChE in different regions of the aged human CNS. AChE activity varied extensively (~50-fold) while BChE activity varied only slightly (3-fold) among the different regions studied. Although G4 was the predominant isoform, G1 and G2 isoforms were also detected in various brain regions. In contrast, the only molecular forms of BChE were G4

and G1, and both isoforms were evenly distributed between membrane bound and soluble types. The ratio of G4 to G1 isoforms of AChE varied widely between different regions, while the G4 to G1 ratio of BChE showed considerably less variation.

Sensitivity of Adult and Aged Cardiac and Cortical Acetylcholinesterase and Butyrylcholinesterase to Chlorpyrifos Oxon and Paraoxon

The *in vitro* potencies of chlorpyrifos oxon (CPO) (Figures 16-19) and paraoxon (PO) (Figures 20-23) on acetylcholinesterase (AChE) and butyrylcholinesterase (BChE) were evaluated in adult and aged heart and cortex. BChE in the cortex and heart was significantly more sensitive (4 to 11-fold) than AChE *in vitro* to inhibition by chlorpyrifos oxon. Furthermore, while there was no age-related difference in sensitivity of AChE to CPO, BChE in the heart from aged rats was significantly more sensitive to CPO than BChE in heart of adult rats (~ 2.5 fold). Although BChE in the cortex of aged rats was 2-fold more sensitive to the effect of CPO than BChE in the cortex of adult rats, this difference was not statistically significant. In contrast, AChE was more sensitive than BChE to paraoxon in both heart and brain, but no age-related difference was noted for either enzyme in either the cortex or the heart. The IC50 values obtained for CPO (Table 2) ranged from 6-35 nm for AChE and 0.6-8 nm for BChE. On the other hand, the IC50 values of PO (Table 3) ranged between 18-25 nm for AChE and 28-43 nm for BChE.

Amitai and coworkers (1998) examined the kinetics of inhibition of AChE and BChE by PO and CPO using various mammalian sources of AChE and BChE. The bimolecular rate constants (k_i) for the inhibition by PO of recombinant human (rH)

AChE, recombinant mouse (rM) AChE and fetal bovine serum (FBS) AChE were ~10-fold smaller than that obtained for the inhibition of these enzymes using CPO, even though both compounds form the same diethylphosphoryl-AChE conjugate. The k_i values obtained for inhibition of rM BChE, human serum BChE and rH BChE by PO were ~10-fold larger than those of AChE by PO in the same species. Significantly, the k_i values obtained for BChE from various species were 160-750-fold larger than those obtained by CPO for AChE from the same species. These results suggest that BChE is preferentially inhibited by CPO as compared to AChE, which is similar to the findings from our current study.

Most of the studies evaluating age-related differences in sensitivity to OP insecticides have focused on maturational differences, and less is known regarding possible sensitivity differences with aging. Benke and Murphy (1975) evaluated the effects of parathion and methyl parathion in male and female rats of different ages (ranging from newborn to adult). Cholinesterase sensitivity in vitro to inhibition by methyl paraoxon or paraoxon did not change with age, suggesting that differences in target enzyme sensitivity did not explain the increase in LD_{50} values with increasing age. Further investigation of various metabolic pathways revealed high correlations between cytochrome P450-mediated dearylation, A-esterase-mediated hydrolysis and CarbE-mediated hydrolysis, and LD_{50} changes. The authors concluded that these detoxification pathways were important in conferring differential sensitivity to methyl parathion and parathion with age. Similar results were obtained by Mortensen et al (1998), who found that the in vitro IC_{50} of CPO (along with other OP and carbamate compounds) for brain AChE remained the same (4.9 nM) in neonatal (postnatal day 4) and adult rats, thereby

supporting the hypothesis that the greater sensitivity of young animals is not due to greater sensitivity of target enzyme.

Atterberry and colleagues (1997) investigated age-related changes in the sensitivity of target and non-target esterase activities and bioactivation enzymes towards parathion and chlorpyrifos. Using several ages of rats ranging from 1-80 days of age, the authors measured the developmental patterns of AChE in the cortex and pons/medulla, and aliesterase (CarbE) activity in liver. The IC_{50} values towards the target enzyme AChE remained constant irrespective of age, for both PO and CPO. However, there were striking differences noted for IC_{50} values of PO and CPO towards aliesterases between young ($\leq$ 12 days old) and adult rats (80 days old). Moreover, no age-related changes were noted in the bioactivation of either PS or CPF. From this study, the authors concluded that neither the target enzyme inhibition, nor bioactivation of these two OPs were important in age-related differences in sensitivity to these compounds. Rather, the detoxification pathway *via* aliesterase in the liver appeared the most likely contributor to the higher sensitivity of the younger rats to these OPs. Padilla et al (2000) arrived at a similar conclusion when they observed that chlorpyrifos elicited a toxic response at a 5-fold lower dose in the pre-weanling rat than in the adult rat, whereas methamidophos had the same toxicity (oral maximum tolerated dose) in both age-groups of rats. Since CPF is detoxified by both CarbE and AE, while methamidophos is not significantly detoxified by either enzyme, the authors hypothesized that OP pesticides like CPF, which require CarbE or AE for detoxification, are more likely to exhibit age-related differences in toxicity than OPs that are not detoxified by these routes.

247

All of these studies have reported that the *in vitro* sensitivity of AChE to OPs does not change markedly during maturation. However, we found no studies evaluating the *in vitro* sensitivity of AChE and BChE to OPs during aging. Our studies indicate that BChE in the aged rat heart was about 2.5-fold more sensitive than adult heart BChE to inhibition by CPO. While AChE appeared to be ~ 1.5-fold more sensitive to the effect of PO as compared to BChE, no age-related difference in sensitivity was noted with this inhibitor for either enzyme. A possible explanation for the greater *in vitro* sensitivity of aged heart BChE than adult heart BChE to CPO could be that the molecular isoform of the enzyme changes during aging. However, in this study, *in vitro* sensitivity was assessed in a crude tissue homogenate (rather than by using the purified enzyme). Due to this, it was not known whether the difference in IC_{50}'s observed was due to expression of different isoforms during aging.

As mentioned above, age-related differences in sensitivity to OPs could arise from differences in CarbE and A-esterase enzymes in the different age-groups. Carboxylesterase and A-esterases are important enzymes that play a role in the detoxification of many OPs. Karanth and Pope (2000) found that while aged (24-month) Sprague Dawley rats exhibited relatively similar acute sensitivity to CPF as compared to adults (3-month) based on lethality, they were about 3-fold more sensitive to the acute effects of parathion. In the same study, they also evaluated the activity of carboxylesterases (CarbE) and A-esterases (AE) in the liver, plasma and lung, as well as the *in vitro* sensitivity of CarbE to CPO and PO. While aged rats demonstrated similar levels of AE in all tissues examined compared to adults, CarbE levels were similar between adult and aged rats in the liver and lung; however, plasma CarbE levels in aged

248

rats were 50% lower than in adults. Moreover, no significant age-related differences were observed in the *in vitro* sensitivity of CarbE to either CPO or PO in any tissue. The acute sensitivity with CPF was highly correlated with age-related differences in CarbE and AE activities across all three tissues, whereas, only plasma CarbE activity was highly correlated with acute sensitivity to PS. Thus, the authors concluded that although both CarbE and AE activities were correlated with acute sensitivity to CPF and PS, age-related differences in CarbE activity were likely more important in differential toxicity, and that plasma CarbE played a crucial role in differential sensitivity to PS between adult and aged rats. In the present study, we found relatively similar reductions in plasma CarbE in the aged rats, but found no difference in the levels of carboxylesterase in the cerebral cortex or heart of adult and aged rats (Figures 106-108). Moreover, the former study suggests that there are very few tissue-related differences between amounts of A-esterases in adult and aged rats.

In Vitro Effects of Chlorpyrifos oxon and Paraoxon on Cardiac and Cortical Muscarinic Receptor Binding in Adult and Aged Rats

Some organophosphorus anticholinesterases have been previously reported to displace agonists from binding to cardiac muscarinic receptors (Silveira et al., 1990; Howard and Pope, 2002), and these direct OP-receptor interactions may be important in selective toxicity. The relative potencies of chlorpyrifos oxon (CPO) and paraoxon to displace the agonist [^{3}H]Oxotremorine-M ([^{3}H]OXO) binding to muscarinic receptors were compared in adult and aged cardiac and cortical membranes. Both CPO and PO

displaced [³H]OXO binding in a concentration-dependent manner in the heart and cortex of adult and aged rats. Of the two oxons, CPO was the more potent displacer of [³H]OXO in the heart and cortex of both age-groups (Figures 24 and 25). Similarly, PO also displaced [³H]OXO from adult and aged cardiac and cortical membranes (Figures 26 and 27). Both OPs appeared to have similar efficacies in displacing [³H]OXO binding in heart and cortex of the two age-groups. However, no age-related difference was observed in displacement of [³H]OXO binding in either tissue (Table 4).

As noted above, several studies have evaluated the ability of OP compounds (mainly oxons) to alter radioligand binding in muscarinic receptors. Howard and Pope (2002) evaluated the *in vitro* effects of certain OPs (chlorpyrifos, parathion and methyl parathion, as well as their oxons) on cardiac muscarinic receptor binding in neonatal and adult rats. Although all three oxons displaced [³H]OXO binding from neonatal and adult cardiac muscarinic receptors in a concentration dependent manner, CPO was found to be the most potent and efficacious of the three. Surprisingly, methyl parathion (MePS) displaced [³H]OXO from adult but not neonatal cardiac muscarinic receptors. While the interaction between CPO and cardiac muscarinic receptors appeared to be irreversible, that between MePS and adult cardiac muscarinic receptors appeared reversible. This finding was similar to the studies by Bomser and Casida, who found that CPO bound covalently and irreversibly to the rat cardiac M2 receptor, as evidenced by the diethylphosphorylation of the receptors *in vitro*. Chlopyrifos oxon was a potent displacer of tritiated *cis*-dioxolane (CD, a high affinity M2-selective agonist) binding and inhibited adenylyl cyclase in the rat striatum (Huff et al, 1994). The abilities of paraoxon, malaoxon and chlorpyrifos oxon to alter muscarinic receptor-mediated phosphoinositide

turnover and cAMP formation in rat cortex were examined by Ward and Mundy (1996). All three oxons displaced CD binding and inhibited cAMP formation in a concentration-dependent manner, with chlorpyrifos oxon and malaoxon being most and least potent, respectively. All of the above studies suggest that CPO binds covalently and irreversibly to muscarinic receptors in a relatively potent manner.

Some studies have also investigated the in vitro effects of PO on muscarinic receptor binding. Volpe et al (1985) found that paraoxon, dichlorvos and tetraethylpyrophosphate inhibited QNB binding in bovine caudate membranes at low nanomolar concentrations. Subsequently, Katz and Marquis (1989) reported that paraoxon, at concentrations as low as 10^{-15} M, was capable of blocking radioligand binding to M_2 and M_3 receptors. As noted above, Silveira et al (1990) reported that paraoxon, echothiophate and the nerve agents VX, soman and tabun blocked the *in vitro* binding of CD to rat cardiac tissues at high nanomolar concentrations. Jett and colleagues (1991) reported that in rat striatal cells, paraoxon displaced CD binding and inhibited the formation of cAMP in an atropine-sensitive manner, while the parent insecticide parathion was 180-fold less potent. Ward et al (1993) reported that paraoxon and malaoxon were more potent at blocking CD binding to rat hippocampal and cortical membranes that their parent compounds, parathion and malathion.

All these studies, including the results from our studies, indicate that certain OPs are capable of binding directly to muscarinic M_2 receptors, and in some cases, acting as agonists (Silveira et al, 1990; Huff et al, 1994; Ward and Mundy, 1996). M_2 receptors are linked to the cAMP second messenger system *via* G proteins. If CPO competes directly for the agonist binding site and acts as an agonist, second messenger signaling could be

affected. Any alterations in the levels of cAMP could potentially induce changes in the long-term regulation of cardiac function or could affect neuronal function, separately from AChE inhibition.

Since the *in vitro* potencies of CPO and PO at displacing agonist binding (IC_{50}: CPO = 6-17 nm; PO = 18-44 nm) are very similar to their potencies towards AChE (IC_{50}: CPO = 6-35 nm; PO = 18-25 nm) and BChE (IC_{50}: CPO = 0.6-8 nm; PO = 28-43 nm) in the brain and heart of adult and aged rats, direct interaction with muscarinic receptors in these tissues could occur at toxicologically-relevant exposure levels and contribute to the expression of toxicity.

Effects of *iso*-OMPA on Heart Rate, Body Temperature and Physical Activity in Adult Male Sprague-Dawley Rats

The effects of *iso*-OMPA on heart rate, body temperature and physical activity were evaluated up to 96 hours post-treatment. From the dose-determination studies, 1.25 and 5 mg/kg were selected as the low and high dose groups, respectively. These doses were selected since they produced a dose-related inhibition of BChE, with no AChE inhibition, thus ensuring only cardiac ChE inhibition occurred in the absence of central ChE inhibition. Since there was no cholinesterase inhibition in the CNS, neither of the two doses of *iso*-OMPA produced any effect on body weight or functional signs of toxicity (data not shown).

As the heart contains a high density of BChE relative to AChE, and *iso*-OMPA is a BChE-selective inhibitor, we hypothesized that *iso*-OMPA could affect heart rate in the

absence of other physiological effects related to AChE inhibition. The low and high doses of *iso*-OMPA produced a decrease in heart rate (Figures 37, 38, 39 and 40) at 24 hours post-treatment, with subsequent recovery. Surprisingly, the magnitude of heart rate reduction was greater in the low-dose than in the high-dose group. Since most of the effects of *iso*-OMPA on heart rate seemed to occur up to 48 hours post-treatment, heart rate was grouped into 4 hourly intervals and viewed up to 48 hours post-treatment (Figure 40). The low and high doses of *iso*-OMPA produced a decrease in heart rate 16-20 hours post-treatment, with recovery occuring thereafter. Although there was a trend towards reduced heart rate at 36-40 hours post-treatment in both *iso*-OMPA dosing groups, it was not statistically significant.

Neither dose of *iso*-OMPA produced any effect on body temperature (Figures 41, 42 and 43) at any of the time points examined. Physical activity (Figures 44, 45 and 46) was only significantly reduced in the low-dose group 72 hours post-treatment (in the nocturnal phase), with subsequent recovery occurring to pre-treatment values.

As mentioned previously, the total ChE of adult hearts of higher vertebrates consists of around 85% BChE and 15% AChE (Chatonnet and Lockridge, 1989). Although present in small amounts, AChE is concentrated in the conducting system of the heart (sinus node, atrio-ventricular node and the ventricular conduction tissues), while BChE is concentrated in the contractile portions of the atria and ventricles (Chow et al, 2001). Moreover, the relative proportions of cardiac AChE and BChE vary during post-natal development. Slavikova and Tucek reported that the ratio of AChE in the rat heart atrium increased from 6% on postnatal day 1 to 12-15 % in the adult (Slavikova and Tucek, 1986). Additionally, it has been observed that in the human heart, the cardiac

conduction system predominantly contained BChE in the infant, and mainly AChE in the adult (Chow et al, 2001).

Chemnitius et al (1999), used the OP inhibitor mipafox to characterize the cholinesterases of human cardiac muscle with respect to substrate specificity and kinetics of enzyme inhibition. Cardiac cholinesterases were characterized as acetylcholinesterase, butyrylcholinesterase and an enzyme they classified as atypical cholinesterase, since it demonstrated some amount of ChE substrate specificity as well as minimal sensitivity to inhibition by mipafox.

Butyrylcholinesterase has long been considered to be a vestigial enzyme with no known physiological function, and until recently, has commonly been referred to as "pseudocholinesterase". More recently, however, it was found that BChE may, in fact, play a role in the hydrolysis of ACh. Perfusion of a selective BChE inhibitor into the rat brain was found to increase extracellular ACh by around 15-fold (Giacobini, 2004). Norel et al (1993) reported that BChE was present in human bronchial muscle, and possibly co-regulated the degradation of ACh in that tissue.

The role of BChE was evaluated by Oksana Lockridge and coworkers through the generation of the AChE-knockout (-/-, -/+) mouse model. AChE-knockout (-/-) mice expressing normal levels of BChE were found to live to adulthood, even though they had weak muscles, could not eat solid food and died prematurely from seizures. Three mechanisms were indentified that ensured the survival of AChE-knockouts, including a reduction in muscarinic and nicotinic receptors, morphological remodeling of the motor endplate, and hydrolysis of ACh by BChE (Li et al, 2003; Adler et al, 2004). These mice demonstrated a heightened sensitivity to BChE-specific inhibitors such as *iso*-OMPA and

bambuterol, suggesting that it was the BChE activity in the knockout mice that facilitated their survival, and that the role of BChE was to compensate for the function of AChE (i.e., hydrolysis of ACh) (Xie et al, 2000; Li et al, 2000). BChE was present in all parts of the brain receiving cholinergic signaling in wild types and knockouts. Moreover, it was suggested that BChE plays a constitutive rather than a back-up role in the hydrolysis of acetylcholine in the normal brain (Mesulam et al, 2002a). Further support for this hypothesis came from the fact that in the absence of AChE, BChE controls the levels of extracellular ACh, as evidenced by the fact that excessive hippocampal ACh levels in AChE-knock-out mice were regulated by BChE (Hartmann et al, 2007a).

Measurements of contractility on phrenic nerve-hemidiaphragm preparations from AChE (-/-) mice further support the conclusion that BChE functions to hydrolyze acetylcholine in these mice (Adler et al, 2004). In a separate study evaluating evoked quantal transmitter release in a nerve-muscle preparation from the AChE-knockout (-/-) mouse, however, researchers found that BChE was not involved in hydrolysis of ACh in the AChE-knockout (-/-) mice, since BChE inhibitors did not affect the time course of synaptic potentials (Minic et al, 2003). These inhibitors did however, decrease evoked-quantal transmitter release, suggesting that BChE might be involved in a presynaptic modulation of synaptic transmission at mature neuromuscular junctions (Minic et al, 2003). These investigators hypothesized that BChE inhibition leads to diminished rather than excessive acetylcholine in the neuromuscular junction (Girard et al, 2005; Girard et al, 2007), and measurements of respiratory activity in AChE (-/-) mice agreed with this hypothesis (Chatonnet et al, 2003).

Recently, BChE homozygous (-/-) and heterozygous (-/+) knockout mice have been generated (Li et al, 2006a). BChE (-/-, -/+) knockout, AChE (-/-) knockout and wild type mice were treated with the AChE-specific inihibitors huperzine A and donepezil, as well as with organophosphorus inhibitors, ecothiophate and chlorpyrifos oxon. After treatment with huperzine A and donepezil, the BChE homozygous knockout mice exhibited severe signs of toxicity and subsequently died. The BChE heterozygous knockouts exhibited intermediate signs of toxicity and survived for a longer time, while the wild type mice showed very minor signs of toxicity and recovered after 24 hours. Plasma AChE activity was inhibited to the same extent in all three groups, whereas plasma BChE activity was unaffected. This confirmed that the protective effect of BChE was not a result of inhibitor "scavenging". AChE (-/-) mice were unaffected by huperzine A and donepezil, thereby confirming their specificity for this enzyme. When AChE (-/-) mice were treated with chlorpryifos oxon, they lost all BChE activity, developed severe signs of cholinergic toxicity and died of seizures/convulsions, thus demonstrating again that BChE activity was essential for the survival of the AChE (-/-) mouse. From this study, Duysen et al (2007) concluded that BChE exerted its protective effect by hydrolyzing excess ACh in physiologically relevant regions such as the diaphragm, cardiac muscle and the brain, and that BChE normally participates in cholinergic neurotransmission. All of the above studies suggest a physiological role for butyrylcholinesterase in cholinergic neurotransmission.

Previous studies suggest discreet association of acetylcholinesterase and butyrylcholinesterase with separate populations of intrinsic cardiac neurons, and their possible selective involvement in neurotransmission in the intrinsic cardiac ganglia

(Darvesh et al, 1998). In the canine right atrial neurons, four neuronal populations were present: those containing a) only AChE, b) only BChE, c) both AChE and BChE and d) those containing neither enzyme. The local application of acetylcholine was found to increase the activity of intrinsic cardiac neurons, with an even greater increase being observed by local application of butyrylcholine. These two enzyme substrates were found to preferentially affect different populations of intrinsic cardiac neurons, which agreed with enzyme kinetic studies showing that canine AChE preferentially hydrolyzed ACh, while canine BChE preferentially hydrolyzed BCh. Using AChE-specific and BChE-specific inhibitors, as well as inhibitors targeting both enzymes, the activity of neurons in the intrinsic cardiac ganglia were only affected when both cholinesterases were inhibited, leading to the conclusion that AChE- and BChE-containing intrinsic cardiac neurons act synergistically to influence the overall tonic activity of the intrinsic cardiac ganglia. In a subsequent study using porcine intrinsic cardiac neurons, which contained AChE and/or BChE, acetylcholine and butyrylcholine increased or decreased the spontaneous activity of the intrinsic cardiac neurons. It was concluded from these studies that inhibition of AChE and BChE by cholinesterase inhibitors directly affects the porcine intrinsic cardiac nervous system (Darvesh et al, 2004).

In an earlier study, Burn and Walker (1954) reported that the BChE-specific inhibitor Nu 683 reduced heart rate while the AChE-specific inhibitor BW 284C51 had no effect using the Starling heart-lung preparation of the dog. They concluded BChE regulated parasympathetic control of heart rate. This finding agreed with results from our studies wherein, *iso*-OMPA-induced cardiac BChE inhibition decreased heart rate. The

lack of other physiological effects (such as effects on body temperature or motor activity) may be due to lack of AChE inhibition in the central and/or peripheral nervous system.

In the present study, both doses of *iso*-OMPA decreased heart rate. This was in direct contrast to Knuepfer and Gan (1999), who did not observe any difference in heart rate after treatment of rats with this compound. The authors reported that ten minutes after intravenous treatment of rats with 0.5 mg/kg *iso*-OMPA, no difference was observed in heart rate compared to baseline values. The experimental design of Knuepfer and Gan (1999) was very different from ours (intravenous vs. subcutaneous administration, 0.5 vs. 1.25 and 5 mg/kg doses, measurement of heart rate until 10 minutes post-treatment vs. until 96 hours post-treatment), which could possibly explain the differences in the observed outcome.

In the current study, a decrease in heart rate by *iso*-OMPA was observed between 16-20 hours post-treatment. Subsequent to that, heart rate in both dose-groups appeared to recover. This might be explained by the fact that *iso*-OMPA-induced BChE inhibition recovered between 24 and 96 hours post-treatment in the heart (Figures 48 and 52). Interestingly, the magnitude of heart rate decrease was greater in the low dose than the high dose group. Since the inhibition of BChE in the atria and ventricles was greater with the high dose than the low dose, we were surprised by this inverse dose-related effect. One possible explanation for this could be that *iso*-OMPA, in addition to inhibiting cardiac BChE, also bound directly to cardiac muscarinic receptors. If this were the case, *iso*-OMPA could antagonistically block the effects of accumulated ACh (which would presumably result from *iso*-OMPA-induced BChE inhibition) and thereby prevent ACh-induced slowing of heart rate. As mentioned previously, several OP compounds have

been shown to bind directly to muscarinic receptors. However, no studies have reported the effects of *iso*-OMPA binding on to muscarinic receptors. To test this hypothesis, we evaluated the relative *in vitro* inhibition of [³H]OXO binding and BChE activity by *iso*-OMPA in heart (Figure 47). These data suggested that in addition to inhibiting BChE, *iso*-OMPA can directly bind to [³H]OXO binding sites in the heart. *Iso*-OMPA was approximately three orders of magnitude more potent at inhibiting BChE (IC$_{50}$: 188 nM), however, than at displacing [³H]OXO binding (IC$_{50}$: 116 µM). At low concentrations, *iso*-OMPA may inhibit BChE with less effect on muscarinic receptors, and as the concentration of *iso*-OMPA increases, direct effects on muscarinic receptors may become more relevant. If so, this could explain the greater effect of the low dose of *iso*-OMPA in reducing heart rate than the high dose.

Effects of *iso*-OMPA on Acetylcholinesterase, Butyrylcholinesterase, Carboxylesterase and Muscarinic Receptor Binding in Ventricles, Atria, Cortex and Plasma 24 and 96 Hours Post-Treatment

The effects of *iso*-OMPA on AChE, BChE, CarbE and muscarinic receptor binding were evaluated 24 and 96 hours post-treatment. *Iso*-OMPA produced a dose-related inhibition of BChE (Figures 48, 52, 56 and 59) and CarbE (Figures 50, 54, 58 and 61) in all of the tissues investigated. *Iso*-OMPA inhibited ~60% (low dose) to 80% (high dose) BChE activity in the atria, ventricles and plasma at the 24 hour time point, with enzyme recovery occurring by the 96 hour time point. In the cortex, only the high dose produced a significant inhibition of BChE at the 24 hour time point, with enzyme

recovery occuring by the 96 hour time point. The amount of CarbE inhibited by *iso*-OMPA at the 24 hour time point ranged from ~10-30% for the low dose, and 10-40% for the high dose. The amount of CarbE inhibited remained approximately the same by 96 hours post-treatment for all tissues, except in the ventricles, wherein the high dose of *iso*-OMPA caused further inhibition of CarbE. Neither of the two doses of *iso*-OMPA used in the study produced any inhibition of AChE (Figures 49, 53, 57 and 60) at the 24 and 96 hour time points, thereby confirming their selectivity for BChE. Interestingly, significantly higher levels of AChE were noted in some tissues following treatment with *iso*-OMPA.

Muscarinic receptor binding (Figures 51 and 55) was evaluated using the agonist [^{3}H]oxotremorine-M. Muscarinic receptor binding was significantly reduced (~25%) by the high dose of *iso*-OMPA in the ventricles at 24 hours, with recovery occurring by 96 hours post-treatment. Approximately 20% down-regulation of muscarinic receptors occurred in the low and high dose groups of *iso*-OMPA in the atria at 24 hours post-treatment, which persisted until 96 hours. Thus, these data argue against a selective effect of high-dose *iso*-OMPA on cardiac muscarinic receptors as suggested above for dose-related differences in heart rate.

Iso-OMPA is an organophosphorus compound that has mainly been used for experimental purposes due to its highly selective inhibition of BChE relative to AChE (Girard et al, 2005; Minic et al, 2003). *Iso*-OMPA is a direct-acting esterase inhibitor, i.e., it does not require metabolic activation, and hence can elicit rapid cholinesterase inhibition. In addition to inhibiting BChE, the carboxylesterase inhibiting properties of *iso*-OMPA have also been recognized (Gupta et al, 1985; Gupta and Dettbarn, 1987;

Gupta and Kadel, 1989). Due to this fact, in addition to evaluating the effects of *iso*-OMPA on BChE and AChE, CarbE activity was also evaluated after treatment with this compound.

Gupta et al (1985) evaluated the effects of *iso*-OMPA (3 mg/kg, administered subcutaneously for 5 consecutive days) on acetylcholinesterase and butyrylcholinesterase activities in the diaphragm and cortex of adult rats. At this dose, *iso*-OMPA inhibited ~18% AChE in the cortex and 96% and 70% BChE in the diaphragm and cortex, respectively. In a subsequent study, *iso*-OMPA (1 mg/kg, sc) inhibited ~78% and 73% BChE activity in the plasma and liver, respectively 1 hour after treatment (Gupta and Dettbarn, 1987). Twenty-four hours after treatment (1 mg/kg), BChE was inhibited by 20% and 0% in the cortex and hemi-diaphragm, respectively.

Gupta and Kadel (1989) reported that 1 mg/kg *iso*-OMPA (sc) inhibited ~85%, 50% and 25% CarbE activity in the plasma, liver and cortex, respectively. In our study, we did not observe any CarbE inhibition in the cortex with the 1.25 mg/kg dose group and ~30% CarbE inhibition in the plasma with this dose. The discrepancy obtained between these studies may be explained by the different times of sacrifice and tissue collection. Gupta and Kadel (1989) reported that *iso*-OMPA produced maximal CarbE inhibition within 1 hour after treatment, whereas the earliest sacrifice time point we used was 24 hours post-treatment. Another explanation might be experiment to experiment variation, since, in a separate study, Gupta and Dettbarn (1987) reported that the same dose of *iso*-OMPA (1 mg/kg, sc) inhibited 100%, 70% and 30% CarbE activity in the plasma, liver and cerebral cortex 1 hour after treatment, which differed from the CarbE inhibition obtained in their previous study (Gupta and Kadel, 1989).

In our study, *iso*-OMPA exposure was associated with significantly higher AChE activity (compared to control) in the atria and cortex. Although increased levels of AChE might seem surprising following exposure to a BChE inhibitor, similar findings have been previously reported. Friedman et al (1996) reported that mice that were stressed (by forced swimming) and treated with pyridostigmine (which is a peripherally-acting cholinesterase inhibitor) had early and immediate increased levels of c-fos oncogene and AChE mRNAs in the brain. Further, they suggested that under conditions of stress, peripherally-acting drugs could reach the brain and affect centrally controlled functions. A subsequent study from the same laboratory (Kaufer et al, 1998) found that following stress exposure, there was a transient increase in acetylcholine release, accompanied by a phase of enhanced electrical brain activity. These authors found that this led to a similar bi-directional modulation of genes that regulated the availability of acetylcholine by either stress or AChE inhibition. Excessive cholinergic stimulation triggered rapid induction of the gene encoding the transcription factor c-Fos. Since c-Fos binding sites are present in the promoter regions of the genes encoding AChE, ChAT and VAChT, elevated c-Fos levels could lead to long-lasting changes in cholinergic gene expression *via* increased AChE mRNA levels and decreased ChAT and VAChT mRNA levels. Kaufer and colleagues (1999), using perfused mouse sagittal brain slices that were exposed to either an organophosphate (DFP) or carbamate (pyridostigmine) anticholinesterase reported overexpression of the mRNA encoding the immediate early response transcription factor, c-Fos within 10 minutes. Twenty minutes later, an 8-fold increase in AChE mRNA and a 3-fold decrease in ChAT mRNA and VAChT mRNA were noted. They concluded that low-level exposures to anticholinesterases could lead to

elevated levels of brain AChE *via* feedback induction, leading to possible long-term deleterious changes in cholinergic signaling and functions such as cognition. All of these studies suggest that in the presence of stress or an anticholinesterase, there may be rapid induction of AChE mRNA. These findings agree with our studies wherein we observed elevated levels of AChE in the atria and cortex of *iso*-OMPA treated rats as early as 24 hours post-treatment. Further studies should evaluate these possible changes in AChE gene induction by *iso*-OMPA.

Muscarinic receptors in the atria were down-regulated by ~20% in both *iso*-OMPA dose groups at both time points, in spite of the significant difference in BChE inhibition. BChE activity appeared to recover from 45% and 20% (low and high dose groups) at 24 hours to 75% and 80% (low and high dose groups) at 96 hours. Yet, muscarinic receptors remained down-regulated to the same extent at both time points with the two doses. Down-regulation of muscarinic receptors is typically regarded a tolerance mechanism in reponse to the effects of synaptic ACh accumulation and activation of the muscarinic receptors, and has been described by a number of researchers (Cioffi and El-Fakahany, 1988; Zhu et al, 1991; Howard et al, 2007; Karanth et al, 2007). It may be that after a degree of cholinesterase inhibition and resulting ACh accumulation, muscarinic receptors on the cell surface are reduced by approximately the same level. Similar results were observed with Howard et al (2007), when adult rats gavaged with 68 and 136 mg/kg CPF produced ~70% and ~90% cardiac cholinesterase inhibition at 4 and 24 hours post-treatment, respectively, along with ~25% down-regulation of cardiac muscarinic receptors at both time points.

Effects of Acute Chlorpryifos or Parathion Exposure on Heart Rate, Body Temperature and Physical Activity in Adult and Aged Rats

The effects of acute equitoxic doses of chlorpyrifos and parathion on heart rate, body temperature and motor (physical) activity were evaluated in adult and aged rats using radiotelemetry. Radiotelemetry is considered to be a humane and efficient method for observing physiological parameters in conscious, unrestrained animals (Kramer et al, 2001; Kramer et al, 2003). By using radiotelemetric devices, it is possible to monitor several physiological parameters in conscious, freely moving animals. Since no restraints are required, there is reduced handling stress to the animal. Moreover, it is possible to obtain data almost continuously from the animal, with minimal handling, which can also reduce variability among animals (Kramer et al, 2003). Continuous monitoring of data reduces the possibility of missing subtle changes that might otherwise be overlooked.

Both chlorpyrifos and parathion produced a dose-related decrease in heart rate in the medium and high dose groups of adult and aged rats. Both OPs caused a dose-related decrease in heart rate which persisted throughout the study. In general, the bradycardia induced by CPF and PS was preceded by a brief elevation in heart rate in the diurnal phase. Heart rate responded differently in aged rats (compared to adults) treated with PS (Figures 91-93). A brief period of tachycardia in the medium-dose group was followed by a decrease and a subsequent trend towards recovery by the end of the study. In the high-dose group, an initial decrease in heart rate was followed by a brief period of increase, after which the heart rate continued to decrease significantly until the end of the study.

Chlorpryifos and parathion produced a dose-related decrease in body temperature in the medium- and high dose-groups of both adult and aged rats. The decrease in body temperature in the medium- and high dose-groups of both OPs predominantly occurred during the nocturnal phase and peaked ~24 hours post-treatment. In general, body temperature either recovered to pre-treatment levels or remained suppressed until the end of the observation period in both adult and aged rats.

CPF and PS both produced a dose-dependent decrease in motor activity which peaked 24 hours after treatment in adult rats. Subsequently, CPF produced a diurnal increase in motor activity in the medium- and high-dose groups, which recovered to baseline values by the end of the study. With PS, motor activity remained depressed in the medium- and high dose-groups. In aged rats, both CPF and PS produced a dose-dependent decrease in motor activity that peaked by 24 hours following exposure. Thereafter, both OPs induced a diurnal increase in physical activity in the aged rats, which persisted until the end of the study. The basis for these directional changes in motor activity are unclear.

Numerous investigators have reported varying degrees of cardiotoxicity following exposure to organophosphorus insecticides. Electrocardiographical (ECG) abnormalities have been found to occur in humans with severe OP intoxication, the most common of which are prolongation of the Q-Tc interval and ST/T changes (elevated ST segment and inverted T waves) (Karki et al, 2004). Another common ECG abnormality that occurs in OP poisoning is the *torsade de pointes* type of polymorphic ventricular tachycardia, which has been attributed to the prolonged Q-Tc interval (Saadeh et al, 1997; Ludomirsky et al, 1982). In a 2007 review, Bar-Meir and coworkers proposed several

hypotheses to explain the phenomenon of OP-induced QT prolongation (considered an unfavorable prognostic indicator of survival): 1) vagal overstimulation 2) muscarinic receptor involvement leading to an abnormal regulation of potassium channels 3) effect on central or peripheral nervous system 4) direct effect on cardiac autonomic innervation, and 5) excessive cholinergic stimulation. Although the exact mechanism of cardiotoxicity is still unknown, there have been some proposed mechanisms. Saadeh et al (1997) suggested possible mechanisms of cadiotoxicity included sympathetic and parasympathetic over-activity, hypoxemia, acidosis, electrolyte imbalance and a direct toxic effect of the OP compounds on the myocardium. Peter and Cherian (2000) suggested that OP-induced cardiotoxicity may be due to 1) a direct toxic effect on the myocardium, 2) overactivity of muscarinic or nicotinic receptors leading to haemodynamic alterations, and/or 3) complications that might arise as a result of high dose atropine therapy. Abraham et al (2001) implicated several factors in OP-induced cardiotoxicity, including catecholamine overflow, neurogenic effects and direct myocardial damage. Allon et al (2005) reported a decrease in the threshold for epinephrine-induced arrhythmias in rats exposed to sarin vapors, which lasted up to 6 months after exposure. The authors concluded that this increase in vulnerability to developing arrhythmias long after OP exposure, especially under conditions like stress or physical exercise, may explain delayed mortality associated with severe OP intoxications.

In the present study, most doses of CPF and PS elicited a brief diurnal period of tachycardia, which was followed by prolonged bradycardia. While the initial elevation in heart rate might seem surprising, there have been reports of OP-induced tachycardia. Petroianu and Rufer (1992) found that high-dose intravenous administration of paraoxon

in mini pigs led to extreme hypertension, tachycardia and a hematocrit increase, with death occurring as a result of sympathetic overstimulation and hypovolemia. Petroianu and coworkers (1998) recommended antihypertensive therapy in such cases, due to what they called a "phaeochromocytoma-like pattern" which is caused by an excessive release of catecholamines from the adrenal medulla after activation by acetylcholine. Ludomirsky et al (1982) described three phases of organophosphate-induced cardiotoxicity: 1) a brief period of sympathetic tone, characterized by sinus tachycardia and hypertension 2) a prolonged period of parasympathetic tone characterized by sinus bradycardia and hypotension, ST-T wave abnormalities and AV conduction disturbances of varying degrees and 3) a prolonged Q-T interval with *torsades de pointes*, and sudden cardiac death. Hence, the current study agreed with the observations of Ludomirsky and coworkers, wherein bradycardia was generally preceded by a brief phase of tachycardia.

Several investigators have reported a decrease in heart rate following exposure to various OP insecticides in different animal models. Naidu et al (1986) reported that dichlorvos induced ECG abnormalities, bradycardia and cardiac arrest in Wistar rats. The degree of bradycardia was correlated with the degree of cholinesterase inhibition in the heart and brain. Bataillard and colleagues (1990) reported a marked, sustained increase in blood pressure accompanied by bradycardia following an intravenous administration of paraoxon and soman. Cetin et al (2007) observed chlorpyrifos-induced cardiac dysfunction in rabbits, which was manifested by significant decreases in heart rate, cardiac output, left ventricular fractional shortening, left ventricular ejection fraction, thickening of left ventricle posterior wall, and significant increases in left atrial diameter,

left ventricular internal diameter in end diastole, left ventricular end diastolic volume and end systolic volume.

Radiotelemetry has been previously used by Dr. Chris Gordon's laboratory to evaluate the effects of various OP insecticides on physiological parameters such as heart rate, body temperature and motor activity in the rat model. Gordon (1993) evaluated the acute and delayed effects of diisopropylfluorophosphate (DFP) on the above-mentioned parameters using radiotelemetry. In this study, physiological parameters were continuously monitored for 96 hour after subcutaneous treatment of Long-Evans rats with DFP (0, 0.1 or 1 mg/kg). The reduction in core body temperature in rats treated with 1 mg/kg DFP peaked by 5 hours post-treatment and recovered to control values by 17 hours after treatment. Although motor activity and heart rate were affected during the first 24 hours (motor activity decreased; heart rate initially increased, then decreased), core body temperature was significantly elevated during the 24-96 hour recovery phase. The 0.1 mg/kg DFP group displayed a hyperthermic response throughout. It has long been known that OP toxicity is associated with hypothermia in rats. However, this was the first report of a delayed hyperthermic response (preceded by hypothermia) following OP exposure. Rapid blockade of this hyperthermic response was achieved by administration of sodium salicylate, an antipyretic drug that acts through inhibition of cyclooxygenase activity (Gordon, 1996). This finding corroborated many observations of fever in humans acutely exposed to OP pesticides (Namba et al, 1971; Hirshberg and Lerman, 1984; Hantson et al, 1996).

Gordon and Padnos (2000b) assessed systolic, diastolic and mean blood pressure, pulse pressure (systolic-diastolic), heart rate, core body temperature and motor activity in

rats treated with various doses of orally administered chlorpyrifos (CPF). The highest dose of CPF increased blood pressure within 2 hours of treatment, which persisted throughout the night and into the next day, slightly decreased heart rate, and led to hypothermia followed by hyperthermia, elevated pulse pressure and decreased motor activity. The authors concluded that the increase in blood pressure without a corresponding increase in heart rate could be due to a CPF-induced increase in total peripheral resistance and an alteration of the baroreflex control of blood pressure. They concluded that although the initial effects of CPF on blood pressure could be explained by cholinergic stimulation of the central nervous system, the persistent pressor response probably involved neurohumoral pathways.

In the current study, the medium and high doses of CPF and PS elicited a decrease in body temperature, which either recovered to pre-treatment levels or remained suppressed until the end of the observation period. However, in most studies by Gordon and colleagues, CPF initially elicited a hypothermic response followed by a delayed fever. Gordon et al (1997b) evaluated the thermoregulatory effects of orally administered chlorpyrifos (0, 10, 50 or 80 mg/kg) in male and female Long-Evans rats using radiotelemetry. Following treatment with CPF, both male and female rats exhibited a significant hypothermic response that lasted ~16 hours and a delayed hyperthermia which persisted during the diurnal phase for 1-2 days after CPF exposure. Female rats were significantly more sensitive to CPF, exhibiting a significant hypothermic response at doses which did not produce hypothermia in male rats. Similar to DFP, the CPF-induced hyperthermia was blocked by administration of sodium salicylate. Castrated male rats were significantly more sensitive to the hypothermic and hyperthermic effects of CPF

compared to sham operated controls, whereas, ovariectomized female rats displayed similar sensitivity to CPF compared to sham operated controls. Hence, the authors concluded that testicular function plays an important role in gender-dependent differences in sensitivity to CPF. In a subsequent study, Gordon and Yang (2000a) reported that vasodilatation of the tail skin is an important mechanism by which core body temperature decreases during the acute hypothermic stage of CPF exposure, and that these hypothermic and vasodilatory responses to CPF are mediated *via* a cholinergic muscarinic pathway in the CNS. A radiotelemetric probe was used to non-invasively monitor the tail skin temperature of rats (Gordon et al, 2002).

Using the peripheral and central muscarinic antagonists methyl scopolamine and scopolamine, respectively, Gordon and Grantham (1999) concluded that cholinergic stimulation of heat loss pathways in the thermoregulatory centers of the CNS were responsible for CPF-induced hypothermia. While peripheral cholinergic pathways did not appear to play a role in CPF-induced hypothermia, they appeared to participate in CPF-induced fever. Gordon and Mack (2001) assessed the effect of time of exposure on the ability of CPF to alter core body temperature and motor activity in rats, by dosing at either 0900 or 1500 hours. While the maximum decrease in core temperature (T_c) was found to be similar with both dosing times, the temperature index (area under curve of ΔT_c with time) was significantly greater when CPF was administered in the afternoon as compared to the morning. Motor activity was depressed to a similar extent by CPF administered at both times. Hence, the authors concluded that time of day affected the thermoregulatory effects of CPF. Rowsey and Gordon (1999) reported the involvement of

endogenously produced tumor necrosis factor in the etiology of CPF-induced hypothermia and fever.

Gordon (1997a) studied the link between CPF-induced hypothermia and delayed hyperthermia to ascertain whether these two thermic responses were regulated by the thermoregulatory centers of the CNS. Core temperature and motor activity were monitored in rats housed in a temperature gradient. While non-heated rats underwent hypothermia followed by hyperthermia 48 hours after CPF exposure, rats maintained at high temperatures did not show a hypothermic response, but did demonstrate a hyperthermic response 48 hours after treatment with CPF. Motor activity was suppressed during the first nocturnal period post-treatment with CPF in both groups of rats. Hence, Gordon concluded that the delayed fever associated with CPF was not dependent on the development of hypothermia, and that both of these responses were regulated by the thermoregulatory centers in the CNS.

Ahdaya and coworkers (1976) examined the ability of mice held at 1°C, 27°C (room temperature) and 38°C to thermoregulate subsequent to treatment with parathion. While mice maintained at 1°C showed a slight decrease in rectal temperature, those kept at 27°C and 38°C did not vary from controls. Moreover, mice that were held at 1°C and 38°C showed greater mortality than those held at room temperature (27°C).

In general, work from Gordon's lab found that CPF leads to an initial period of hypothermia lasting for ~24 hours, followed by an elevation in diurnal core body temperature (delayed fever) lasting for 48-72 hours. While we observed a decrease in body temperature following exposure to both CPF and PS in adult and aged rats, we did not find any evidence of a hyperthermic response. Several factors could be responsible

for the differential responses noted between the two laboratories, such as strain differences of rats (Sprague-Dawley vs. Long-Evans), route of administration of OP insecticide (subcutaneous vs. oral), and (more likely) the relative site of placement of the transmitter within the rat (subcutaneous vs. intraperitoneal). It seems plausible that while subcutaneous placement of the transmitter can detect changes in body temperature, it might not be as accurate as intraperitoneal implantation. With subcutaneous implantation, changes in ambient temperature are more likely to influence the temperature sensor, whereas intraperitoneal implantation would be better at detecting core body temperature changes.

Gordon and Watkinson (1995) evaluated the intraspecies variation in the responses of heart rate, core body temperature and motor activity to DFP using Sprague-Dawley, Long-Evans, Fischer 344 and Wistar rats. The Fischer 344 rats, which had the lowest degree of brain and serum cholinesterase inhibition (as compared to the other strains) showed the least susceptibility to the hypothermic response to DFP. Sprague-Dawley rats differed from the other strains in that heart rate was elevated after DFP, in spite of a significant decrease in core body temperature and motor activity. Of all four strains, Long-Evans rats demonstrated the largest decrease in core body temperature and heart rate following DFP exposure.

Most of the studies involving CPF by Gordon's lab involved CPF administered *via* the oral route. In 1994, however, Gordon evaluated the effects of subcutaneously administered CPF (280 mg/kg) on core temperature, heart rate and motor activity. In contrast to the other reports from this laboratory, other than a significant reduction in nocturnal body temperature within the first 24 hours no other effects were observed on

272

core temperature. While motor activity was unaffected by CPF, heart rate was significantly elevated for up to 72 hours following treatment. Therefore, it appears that the route of administration of OPs can markedly influence the qualitiative outcome and the time course of effects on these physiological parameters.

In our studies, motor activity was initially reduced by both CPF and PS in adult and aged rats. However, towards the end of the observation period, there was a diurnal increase in activity with both OPs. A number of studies have reported changes in motor activity (predominantly a decrease) following exposure to common OP anticholinesterases including CPF, PS and DFP (Pope et al, 1992b; Gordon 1993; Gordon and Mack, 2001; Karanth et al, 2006, 2007). Pope et al (1992b) observed a reduction in motor activity for 2 days following exposure to 279 mg/kg CPF, administered subcutaneously. Subsequently, motor activity recovered to control levels. Karanth et al (2006) evaluated the effects of various doses of CPF on motor activity in adult, male Sprague-Dawley rats. While diurnal motor activity was unaffected by all doses of CPF, nocturnal motor activity (in particular, rearing) was significantly reduced in all CPF-treated rats from one to four days after exposure. Gordon and Mack (2001) also reported that CPF decreased nocturnal motor activity, with no significant effect on diurnal activity. Timofeeva and Gordon (2001, 2002) evaluated changes in EEG power spectra and behavioral states in rats exposed to CPF. Changes in EEG and behavior following CPF included cortical arousal, increased quiet waking and decreased sleep, occurring independently from a decrease in motor activity. These responses were concluded to be due to CPF-induced hyperactivity in brain cholinergic neuronal networks.

Karanth et al (2007) evaluated the effects of equitoxic doses of parathion on motor activity in adult (3 months, 27 mg/kg, sc) and aged (18 months, 9 mg/kg, sc) rats. Nocturnal motor activity (both ambulation and rearing) was reduced in both age-groups. In spite of similar reductions in striatal and diaphragm cholinesterase activities in the two age-groups, more prominent effects were observed (especially in nocturnal rearing) in adults. The highest dose of PS led to a significant reduction in rearing activity in adults until 7 days post-treatment, and only at 2 days following exposure in aged rats.

Lopez-Crespo and coworkers (2007) evaluated the time-course of effects of a single high dose (250 mg/kg, sc) of CPF on rat locomotor activity for 30 days after exposure. AChE inhibition in the whole brain recovered partially from 72% inhibition on day 2 to 55% inhibition on day 30. CPF had a biphasic effect on motor activity (similar to the results from the present study), wherein there was a reduction on day 2 followed by an increase over control by day 30. To explain this delayed increase in motor activity, the authors concluded that adaptive changes occurred in the cholinergic system to balance the effects of excessive acetylcholine accumulation, leading to this long-term alteration. Subsequently, due to the possibility of interactions with the dopaminergic system, the authors tested motor activity following challenge with amphetamine at 11 and 30 days following CPF exposure. Whereas amphetamine increased motor activity at both time points in the vehicle and CPF groups, rats treated with CPF exhibited less of an increase (relative to the vehicle-treated control). From these findings, the authors concluded that CPF affects the dopaminergic system, leading to subtle, long-lasting effects that are independent of its cholinergic effects.

Other studies have reported an interaction between CPF and the dopaminergic system. Karen et al (2001) examined the effects of CPF on striatal dopaminergic pathways in mice. CPF decreased dopamine uptake and increased dopamine turnover in striatal synaptosomes. Moreover, the highest dose of CPF also decreased open field behavior, providing additional information that dopaminergic neurotransmission is disrupted by exposure to CPF. Bloomquist et al (2002) evaluated the effects of CPF on the nigrostriatal dopaminergic nerve pathways in mice. They observed that CPF decreased dopamine uptake in striatal synaptosomes.

Moreno and colleagues (2008) investigated the time-course (up to 30 days post-treatment) of acute CPF (250 mg/kg, sc) on monoamine and cholinergic systems in the striatum and nucleus accumbens of adult rats. CPF elicited long-term inhibition of AChE in the striatum and nucleus accumbens, and significant decreases in dopamine, norepinephrine and serotonin content (along with their metabolites) in the nucleus accumbens for 30 days after exposure. Moreover, changes in dopamine metabolism and serotonin turnover were also observed in the striatum at various time-points following intoxication by CPF. The authors concluded that acute exposure to CPF leads to long-term changes in the monoamine systems (norepinephrine, dopamine and serotonin), that are independent of cholinergic dysfunction . All of the above studies suggest that the interaction of CPF and other organophosphorus insecticides with the dopaminergic system could elicit motor effects which are independent of OP-induced cholinergic dysfunction. Subsequent changes in dopaminergic neurotransmission may form the basis of expression of increased motor activity at later time points noted in our studies.

Effects of Acute Chlorpryifos or Parathion Exposure on Functional Signs of Toxicity, Acetylcholinesterase, Butyrlcholinesterase, Carboxylesterase and Muscarinic Receptor Binding in Adult and Aged Rats

In this study, equitoxic doses of CPF and PS were administered to adult and aged rats. Maximum tolerated doses or fractions thereof, of these two OPs were administered subcutaneously to adult and aged rats. Rats were sacrificed at 96 hours following CPF or PS exposure since previous studies had shown peak cholinesterase inhibition at this time point in adult rats (Pope et al, 1991; Karanth and Pope, 2003; Karanth et al, 2006). The effects of acute equitoxic doses of CPF and PS exposure on body weight and functional signs of toxicity [involuntary movements and SLUD (i.e., salivation, lacrimation, urination and defecation)] were evaluated in adult and aged rats. For CPF, adult and aged rats were treated with vehicle (peanut oil), 0.1 x MTD (low dose: 28 mg/kg), 0.5 x MTD (medium dose: 140 mg/kg) and 1 x MTD (high dose: 280 mg/kg), while for PS, rats of the two age-groups were treated with vehicle (peanut oil), 0.5 x MTD (low dose: adult = 9 mg/kg; aged = 3 mg/kg), 0.75 x MTD (medium dose: adult = 13.5 mg/kg; aged = 4.5 mg/kg) and 1 x MTD (high dose: adult = 18 mg/kg; aged = 6 mg/kg).

CPF (Figure 62 and 63) and PS (Figure 64 and 65) elicited a dose-related decrease in body weight, which persisted until the end of the study in the medium and high dose groups of adult and aged rats. The reduction in body weight peaked earlier in adult rats (48 hours post-treatment) than in aged rats (72 hours post-treatment) with both CPF and PS. In terms of percent body weight lost, the body weight decrease appeared to be greater in adults than in aged rats. The implication for this relative "toxicity", considering that

276

the aged rats were markedly higher in body weight to at the start of the study, is unclear..

Although CPF produced some evidence of toxicity (mainly IM) in the high dose group of adult and aged rats (Tables 6, 7, 8 and 9), these changes were not significantly different. Figures 66, 67, 68 and 69 show the functional signs of toxicity (IM and SLUD) in adult and aged rats after acute exposure to PS. In adult rats, the high dose of PS produced IM and SLUD signs 24 hours after treatment, which peaked by 72 hours, and these effects persisted until the end of the study. Involuntary movements had a slightly delayed onset (48 hours post-treatment) in the high dose group of aged rats, after which it peaked by 72 hours. SLUD signs were observed in the high dose group of adult rats 24 hours after treatment, and these effects diminished by 72 hours post-treatment. Karanth et al (2006) using various doses of (84, 156 and 279 mg/kg) CPF in adult male Sprague-Dawley rats, observed a significant reduction in body weight gain in the high dose group (as compared to the control). Similar to results from the present study, very few functional signs of cholinergic toxicity were observed in any of the treatment groups. This phenomenon of minimal signs of cholinergic toxicity following doses of CPF that produce extensive AChE inhibition in the brain has been observed in the past (Won et al, 2001; Zhang et al, 2002; Karanth and Pope, 2003a). In a subsequent study, Karanth and colleagues (2007) evaluated the effects of a range of doses of parathion in adult and aged rats. In both age-groups, the highest dose of PS (adult: 27 mg/kg; aged: 9 mg/kg) led to a time-dependent decrease in body weight, and marked signs of cholinergic toxicity, manifested as involuntary movements and SLUD signs peaking 3-4 days following exposure, similar to results reported herein.

The effects of CPF and PS on AChE, BChE, CarbE, and muscarinic receptor agonist and antagonist binding were evaluated in adult and aged rats. CPF and PS inhibited AChE and BChE in all of the tissues examined in a dose-related manner, in both adult and aged rats. In general, the same dose of CPF inhibited BChE (Figures 112, 117, 122, 127 and 130) to a greater extent (~2 to 2.5 fold) than AChE (Figures 111, 116, 121, 126 and 129), while the same dose of PS inhibited AChE (Figures 131, 136, 141, 146 and 149) to a greater extent (~1.5 fold) than BChE (Figures 132, 137, 142, 147 and 150). This was especially apparent in the low and medium dose groups. In *vitro*, there was greater selectivity of CPO for BChE, while PO was a more selective AChE inhibitor. In this respect, these *in vivo* results seem to agree with the *in vitro* studies. AChE and BChE in the ventricles were inhibited to a greater extent than in the atria, with all doses of CPF and PS. In the atria, the low dose of CPF and PS elicited a significantly greater inhibition of both AChE and BChE in aged than in adult rats. Similarly, AChE and BChE in the plasma and diaphragm of aged rats showed a trend towards greater inhibition in aged compared to adult rats. Although not significant, BChE in the plasma of aged rats appeared to be inhibited to a greater degree than in adult rats by the same dose of PS; however, no such age-related difference was observed for plasma AChE activity.

In general, very few studies have assessed the effects of acute exposure to anticholinesterases including OPs on cholinesterase activity in aged rats (Overstreet, 2000). Scali and coworkers (1997) evaluated the effects of the Alzheimer's drug metrifonate (which is an organophosphate AChE inhibitor), in adult and aged rats. Although the same doses of metrifonate produced slightly greater levels of brain regional cholinesterase inhibition in aged rats compared to adults, these differences were not

statistically significant. Kosasa et al (1999) evaluated the effects of donepezil and tacrine on cholinesterase activity in the brain and peripheral tissues (brain, plasma, erythrocytes, heart, small intestine, liver and pectoral muscle) of adult and aged rats. Tacrine, which is a non-selective cholinesterase inhibitor, produced more extensive cholinesterase inhibition in all tissues examined in aged as compared to adult rats. On the other hand, donepezil, which displays more selectivity towards AChE, elicited greater cholinesterase inhibition in the brain, erythrocyte and pectoral muscle of aged rats, relative to adults. The brain and plasma concentrations of the parent compound were higher in aged than in adult rats, due to which, the authors concluded that toxicokinetic factors could be responsible for the greater cholinesterase inhibition observed in aged rats. Similarly, Karanth and Pope (2000) reported significantly lower levels of plasma carboxylesterase in aged compared to adult rats. Moreover, age-related reductions in the levels of certain isoforms of cytochrome P450 have been reported (Warringtom et al, 2004; Wauthier et al, 2006). In the Karanth et al (2006) study, cholinesterase activities in the diaphragm and striatum were extensively inhibited in a time-dependent, but not dose-dependent manner. Peak cholinesterase inhibition occurred by day 4 in both tissues, with apparent recovery occurring by day 7 only in the diaphragm. The cholinesterase inhibition obtained by the highest dose (280 mg/kg) at 4 days in the diaphragm and striatum agreed closely with the data we obtained in adult rats. In a subsequent study, Karanth and colleagues (2007) evaluated the effects of a range of doses of parathion in adult and aged rats. Cholinesterase activities in the diaphragm and striatum were inhibited in a dose and time-dependent manner, with significantly greater inhibition in aged animals treated with the same dose of PS.

The atria of aged rats showed greater inhibition of both AChE and BChE by CPF and PS. In our *in vitro* studies, we BChE (but not AChE) in the heart from aged rats was significantly more sensitive to the effect of CPO than BChE from adult rat heart. In contrast, neither enzyme displayed an age-related difference in sensitivity to the effects of PO. We observed that both CPF and PS produced significantly greater inhibition of both cholinesterases in the atria from aged compared to adult rats. One reason for higher sensitivity in aged rats could be less detoxifying enzyme, carboxylesterase, in the plasma of this age-group. However, if this were the case, this age-related difference in enzyme inhibition should extend to other tissues as well. This was not the case, however, since similar levels of both enzymes were inhibited in all other tissues. Another reason for greater cholinesterase inhibition in the atria of aged rats compared to adults could be that lower levels of both enzymes exist in the atria of aged rats as compared to adults. In this case, the same dose of OP would lead to a more extensive inhibition in this age-group. We did not, however, observe any age-related decrease in atrial AChE or BChE. It is possible that the isoforms of the two enzymes might change during aging, such that the total cholinesterase activity remains the same. As noted previously, the molecular isoforms of AChE and BChE in the brain change as a function of age. Hence, it is possible that such changes might occur in the atria as well, which might account for the differential sensitivity.

Carboxylesterase was also inhibited in a dose-related manner by CPF (Figures 113, 118, 123 and 128) and PS (Figures 133, 138, 143 and 148) in adult and aged rats. Other than the ventricles (for CPF), there did not appear to be any age-related difference in the degree of CarbE inhibition by any dose of CPF or PS. The highest dose of CPF and

PS inhibited a maximum of ~80% and ~70%, respectively, of the total CarbE activity in a tissue, with the exception of the cortex, which had ~40-50% residual enzyme after treatment with the highest dose of CPF or PS.

Age-related differences in sensitivity to OPs could arise from tissue differences in carboxylesterase and A-esterase enzymes in the different age-groups. As noted above, our laboratory evaluated carboxylesterase and A-esterase activities in the liver, lung and plasma of rats during maturation and aging, and compared it to the toxicity of CPF and PS in rats (Karanth and Pope, 2000). Plasma of aged rats had 50% less carboxylesterase compared to adult rats. In the present study, we did not find any difference in the levels of carboxylesterase in the cerebral cortex or heart of adult and aged rats.

Muscarinic receptor binding was also evaluated using radioligand binding of a muscarinic agonist ([^{3}H]OXO) and antagonist ([^{3}H]QNB). In general, [^{3}H]QNB binding was reduced by ~20-25% in adult and aged rats treated with medium and/or high dose groups of CPF (Figures 115, 120, 125 and 130) or PS (Figures 135, 140, 145 and 150), with the exception of aged rats treated with the high dose of PS, wherein there was ~30% increase in binding. Muscarinic agonist binding in cortex was reduced by ~25% in adult and aged rats treated with the high dose of CPF, and by ~45% in aged rats treated with the high dose of PS. Muscarinic agonist binding in the ventricles was unaffected by CPF, and was reduced by ~25% in the medium and high dose groups of adults. A more robust decrease in [^{3}H]OXO binding was observed in the atria, where ~50% of the receptors were down-regulated in adult and aged rats treated with the high dose of CPF. Similarly, PS decreased [^{3}H]OXO binding (20%) in the atria with the low dose in adult rats and high dose in aged rats, with a more substantial decrease being observed in the medium

and high dose groups of adult rats (~35-40%). In general, more extensive changes were noted in muscarinic agonist (OXO) binding than muscarinic antagonist (QNB) binding with both CPF and PS. Karanth et al (2007) reported somewhat similar findings following PS exposure. Muscarinic antagonist (QNB) binding was significantly lower in the striatum of aged as compared to adult rats. QNB binding was significantly reduced (~46%) in the striatum of adult rats at the highest dose (27 mg/kg) up to 7 days after treatment, and in aged rats by ~33% in the two highest doses (6 and 9 mg/kg). PS produced an extensive (~78%) reduction in OXO binding in adult rat striatum and with somewhat lesser effect (54% reduction) in aged rats.

Several studies demonstrated that prolonged and extensive AChE inhibition leads to an adaptive down-regulation of muscarinic receptors in rats of different ages (Costa et al, 1982; Russell and Overstreet, 1987; Pintor et al, 1988; Jett et al, 1993; Zhang et al, 2002; Karanth et al, 2007). Both CPF and PS have been shown to affect different subtypes of muscarinic receptors in the brain (Chaudhuri et al, 1993; Chakraborti et al, 1993; Zhang et al, 2002). Numerous studies have suggested that the ability of muscarinic receptors to adapt to prolonged AChE inhibition is less efficient in the senescent rather than adult nervous system. Pedigo and coworkers (1984) compared the effects of cholinergic drugs and muscarinic receptor binding in the brain of adult and aged rats. Although muscarinic receptor density decreased with age, no age-related changes in receptor affinity were observed. Aged rats were markedly more sensitive to the effects of the cholinergic agonist, oxotremorine, and were less sensitive to the cholinergic antagonist, scopolamine, than adult rats. These researchers concluded that the observed age-related differences in sensitivity between adult and aged rats to the effects of

cholinergic drugs represented a decreased ability on the part of the aged rats to adapt to changes in its environment. Pintor and colleagues (1988) evaluated the plasticity of muscarinic receptors in the brain of adult and aged rats, by observing the response of these animals to repeated administration of the OP anticholinesterase, DFP. Aged rats were more sensitive than adults to the effects of the same dose of DFP. The authors concluded that increased sensitivity of aged rats resulted from a failure of adaptive mechanisms.

In the present study, we did not observe significant differences between adult and aged rats in the apparent adaptive down-regulation of muscarinic receptors following exposure to either CPF or PS. We did note, however, a trend towards up-regulation (which was significant in some cases) in muscarinic antagonist binding in aged rats but not in adults following PS exposure. It is possible that age-related differences in the membrane composition or muscarinic receptor density could explain this differential response of aged rats to the effects of PS. There are several conflicting reports on aging-related changes in the functionality and density of muscarinic receptors in rats (Dhein et al, 2001). Narayanan and Derby (1983) reported that while muscarinic receptor density was higher in the atria of aged rats compared to adults, ventricles from both age-groups had similar densities of muscarinic receptors. Baker et al (1985) reported that with increasing age, the ability of the cardiac muscarinic receptor to form a high affinity agonist binding state was reduced. Chevalier et al (1991) reported a reduction in cardiac muscarinic receptor density in aged rats. Several investigators have reported a reduction in cardiac parasympathetic activity with increasing age in humans. This reduced activity has been ascribed to a decrease in the density (Brodde et al, 1998) as well as functionality

(Brodde et al, 1998; Oberhauser et al, 2001; Poller et al, 1997) of cardiac muscarinic receptors in the heart of older individuals.

A decrease in the densities of muscarinic receptors in the brain of aged as compared to adult animals has been reported by several investigators (Tayebati et al, 2006; Yufu et al, 1994; Araujo et al, 1990; Kadar et al, 1990) using a variety of experimental approaches, including radioligand binding methods (Yufu et al, 1994; Araujo et al, 1990; Schwarz et al, 1990; Amenta et al, 2006; Amenta et al, 1995), in vitro quantitative receptor autoradiography (Tayebati et al, 2006; Kadar et al, 1990) and assessing subtype specific mRNA expression (Lee et al, 1994; Blake et al, 1991). Using the radial arm maze, Kadar et al (1990) correlated working memory deficits in 3, 12, 17 and 24 month-old Wistar rats with an age-related decrease in muscarinic receptor density in various brain regions.

The results obtained from the current study suggest that selective cardiac BChE inhibition by *iso*-OMPA (in the absence of AChE inhibition) leads to altered heart rate. BChE is more sensitive to inhibition by CPF than AChE, both *in vitro* and *in vivo*. The reverse was true for PS, wherein this compound showed greater selectivity for AChE than BChE *in vitro* and *in vivo*. In general, age-related differences were only noted for both compounds in the atria, wherein both AChE and BChE were inhibited to a greater extent in aged than in adult animals. However, the higher sensitivity of atrial cholinesterases to CPF and PS in aged rats did not appear correlated with more extensive dysregulation of heart rate in this age-group. Equitoxic doses of CPF and PS produced disparate functional signs of toxicity, with PS demonstrating greater toxicity than CPF in both adult and aged

rats. Yet, relatively similar changes in cardiac function and other physiological parameters were observed with both CPF and PS.

According to the World Health Organization, around 3 million people worldwide suffer from acute pesticide poisoning each year. Organophosphates are the most commonly used class of insecticides. While their use is somewhat lower in the US now than in the recent past, they will continue to be used in substantial quantities, and their use worldwide is expected to increase in the future due to a variety of reasons (Walker and Nidiry, 2002). Recent studies reported that exposure to OP insecticides, especially CPF, has occurred, or is occurring in essentially everyone in the US, either in minute amounts through the diet, or in the home or work place (Barr et al, 2004; 2005). Approximately 2.5 million people, primarily agricultural workers and pesticide applicators, are directly exposed to pesticides, and hence, are the most predisposed to the ill-effects of pesticide exposure (Walker and Nidiry, 2002). Although organophosphates are one of the most extensively studied classes of insecticides, the main focus of research has been on neurotoxicity produced by AChE inhibition, and effects on cardiac function have received considerably less attention. This study evaluated the role of BChE in cardiac function, and the cardiotoxic consequences of parathion and chlorpyrifos in adult and aged rats.

In elderly people suffering from Alzheimer's disease, cholinesterase inhibitors with selective affinities for either AChE alone, BChE alone, or both AChE and BChE, are being currently used or evaluated for therapy (Giacobini, 2003b; Masuda, 2004). Although ChE inhibitors have been demonstrated to improve cognitive function, possibly by increasing ACh levels in the brain, concomitant inhibition of ChE in the heart may

produce selective effects in this organ, especially in compromised patients (Masuda, 2004). Hence, a thorough understanding of the effects of ChE inhibitors on cardiac function is critical. Moreover, due to the continuing wide-spread use of OPs, knowledge of the cardiotoxic consequences of these toxicants, in particular during aging, is essential. In the current study we evaluated the cardiotoxic potential of the OP insecticides, CPF and PS during aging, which could have implications in formulating regulatory policies governing the usage of these pesticides, especially for the protection of the elderly subpopulation.

CHAPTER 5

SUMMARY

Acetylcholinesterase (AChE) makes up most of the cholinesterase activity in the cortex, diaphragm and plasma, while butyrylcholinesterase (BChE) predominates in the atria and ventricles. The ratio of AChE to BChE in the cortex, atria, ventricles and plasma of adult and aged rats is approximately 9:1, 1:9, 2:8 and 7:3, respectively. In both adult and aged rats, the relative amounts of both enzymes remained roughly the same for each tissue. In general, the atria contained ~2.5-fold more cholinesterase activity, and 1.5-fold more carboxylesterase activity than the ventricles (specific activity relative to protein content). While the levels of these enzymes decreased slightly in aged (compared to adult) ventricles and cortex, this difference was not statistically significant. However, in the plasma, AChE and BChE levels were significantly higher, while CarbE activity was significantly lower in aged than adult rats.

BChE in the cortex and heart was significantly more sensitive (4- to 11-fold) than AChE *in vitro* to inhibition by chlorpyrifos oxon (CPO) in both adult and aged rats. Furthermore, cardiac BChE from aged rats was significantly more sensitive to CPO than cardiac BChE in adult rats (~ 2.5 fold). Relatively similar differences in sensitivity were noted in the cortex BChE. Age-related differences in potency did not appear to be due to differences in endogenous detoxification *via* CarbE or A-esterase. AChE was more sensitive than BChE to paraoxon (PO) in both heart and cortex. No age-related

differences were noted for either enzyme, however. CPO and PO displaced muscarinic agonist ([^{3}H]oxotremorine-M) binding in a concentration-dependent manner in the heart and cortex of adult and aged rats. Of the two oxons, CPO was the more potent displacer of [^{3}H]oxotremorine-M binding in the heart and cortex of both age-groups. However, no age-related difference was observed in displacement of [^{3}H]oxotremorine-M binding in either tissue with either oxon.

The low (1.25 mg/kg) and high (5 mg/kg) doses of *iso*-OMPA decreased heart rate at 24 hours post-treatment, with recovery occuring thereafter. The magnitude of heart rate reduction was greater in the low-dose than in the high-dose group. Additional non-cholinesterase actions of *iso*-OMPA may be important in this dose-related difference in response. Neither dose of *iso*-OMPA produced any effect on body temperature or motor activity at any of the time points examined. Selective reduction of heart rate by *iso*-OMPA in the absence of other physiological effects appeared due to specific inhibition of cardiac BChE, in the absence of AChE inhibition. BChE and CarbE were inhibited by *iso*-OMPA at 24 hours, with enzyme recovery generally occuring by 96 hours. Recovery of cardiac BChE activity after 24 hours could be responsible for return of heart rate to baseline conditions at later time points. In some tissues, increased levels of AChE were noted at later time points following *iso*-OMPA exposure. Muscarinic receptors were significantly down-regulated in the atria and ventricles by both doses of *iso*-OMPA used in the study.

Chlorpyrifos (CPF) and parathion (PS) generally elicited a brief period of tachycardia during the initial diurnal phase, which was followed by prolonged dose-related bradycardia in both adult and aged rats. Heart rate remained depressed until the

end of the observation period. Heart rate responded somewhat differently in aged rats compared to adults following PS exposure. A brief period of tachycardia in the medium dose group was followed by a decrease in rate and a subsequent trend towards recovery by the end of the study. In the high dose group, an initial decrease in heart rate was followed by a brief period of increase, after which the heart rate continued to decrease significantly until the end of the study. The reason for this time-dependent difference in response to PS in aged rats is unclear. The medium and high doses of CPF and PS elicited a dose-related decrease in body temperature, which either recovered to pre-treatment levels or remained suppressed until the end of the observation period in adult and aged rats. Motor activity was initially reduced by both CPF and PS in adult and aged rats. However, towards the end of the observation period, there was an increase in activity during the diurnal phase, most prominently in aged rats.

CPF and PS decreased body weight in a dose-related manner, persisting until the end of the study in the medium and high dose groups of adult and aged rats. In terms of percent body weight lost, the body weight reduction appeared greater in adults than in aged rats. The relative impact of such body weight reductions needs to be considered based on pre-treatment body weights, however. In spite of extensive cholinesterase inhibition, CPF did not produce any significant signs of cholinergic toxicity in either adult or aged rats. PS produced signs of cholinergic toxicity (involuntary movements and SLUD), in both adult and aged rats, peaking at around 72 hours after exposure. Both CPF and PS inhibited AChE, BChE and CarbE activity in a dose-related manner in all of the tissues examined in adult and aged rats. In general, BChE was inhibited to a greater extent than AChE by CPF, while the reverse was true for PS. The only evidence of an

age-related biochemical difference was in the atria, wherein the low doses of CPF and PS elicted a significantly greater inhibition of both AChE and BChE in aged than in adult rats. However, the higher sensitivity of atrial cholinesterases to CPF and PS in aged rats did not appear to be correlated with more extensive dysregulation of heart rate in this age-group. *In vivo*, CPF and PS reduced muscarinic receptor binding (QNB and OXO binding) in both adult and aged rats. In general, more extensive changes were noted in muscarinic agonist (OXO) binding than with muscarinic antagonist (QNB) binding with both CPF and PS.

These studies suggest that butyrylcholinesterase plays a role in the normal functioning of the heart. Thus, OP toxicants that selectively target this enzyme may have cardiotoxic potential. Moreover, some OP insecticides bind directly to muscarinic receptors at low concentrations, indicating that direct interaction with muscarinic receptors in these tissues could occur at toxicologically relevant exposure levels. Both adult and aged rats are susceptible to the effects of CPF and PS, as evidenced by changes in heart rate, body temperature and motor activity.

Equitoxic doses of CPF and PS have been found to produce very different degrees of functional toxicity, with PS eliciting more extensive cholinergic signs than CPF in both adult and aged rats. We observed similar differences in the expression of functional signs of toxicity between these two insecticides. Interestingly, in our studies we found that while PS elicited more extensive cholinergic signs, relatively similar degrees of cardiac dysfunction and disruption of other physiological parameters were noted following exposure to either CPF or PS.

CHAPTER 6

CONCLUSIONS

Previous studies have suggested that butyrylcholinesterase plays a role in the modulation of cholinergic neurotransmission. Since the heart of several species has been found to contain disproportionately more butyrylcholinesterase than acetylcholinesterase, in this study we evaluated the role of BChE in the regulation of cardiac function. The effects of tetraisopropylpyrophosphoramide (*iso*-OMPA), an OP with high selectivity towards BChE, on cardiac function were evaluated using radiotelemetry. We also compared cardiac function in adult and aged rats following exposure to the common OPs chlorpyrifos (CPF) and parathion (PS). Our studies also evaluated *in vitro* tissue- and age-related differences in sensitivity of cholinesterases and muscarinic receptors to chlorpyrifos oxon (CPO) and paraoxon (PO) in heart and brain of adult and aged rats.

BChE was significantly more sensitive than AChE to inhibition by CPF both *in vitro* and *in vivo*, in adult and aged rats. Furthermore, BChE in the heart from aged rats was significantly more sensitive to CPO than BChE in heart of adult rats *in vitro*. In contrast, PS preferentially targeted AChE as compared to BChE. However, no age-related difference in sensitivity was observed with this OP for either enzyme. Both CPO and PO were found to bind directly to muscarinic receptors at low concentrations, indicating that direct interaction with muscarinic receptors in these tissues could occur at toxicologically relevant exposure levels.

Selective BChE inhibition in the heart by *iso*-OMPA, in the absence of AChE inhibition, significantly reduced heart rate, suggesting BChE does play a role in the regulation of cholinergic neurotransmission in the heart. Thus, OP toxicants that selectively target this enzyme may have cardiotoxic potential. Since CPF was observed to preferentially target BChE as compared to PS, the former OP was expected to have a differential expression of cardiotoxicity as compared to PS.

Effective dosages of CPF and PS initially decreased heart rate, temperature and motor activity in both adult and aged rats. Heart rate remained depressed for four days in both age-groups, while temperature either recovered to pre-treatment levels or remained suppressed until the end of the observation period in adult and aged rats. Towards the end of the observation period, there was an increase in motor activity during the diurnal phase, most prominently in aged rats. This delayed increase in motor activity predominantly in aged rats, could be due to a differential effect of OPs on the dopaminergic system in this age-group, or an age-related difference in the interaction between the cholinergic and dopaminergic systems.

Both CPF and PS elicited dose-dependent AChE and BChE inhibition in atria, ventricles, cortex, plasma and diaphragm in adult and aged rats. In spite of extensive cholinesterase inhibition, CPF did not produce any significant signs of cholinergic toxicity in either adult or aged rats. On the other hand, PS produced signs of cholinergic toxicity in both adult and aged rats. Atrial cholinesterases in aged rats appeared more sensitive to the low doses of both, CPF and PS as compared to adults. Toxicokinetic differences might be responsible for the age-related difference in sensitivity of aged AChE and BChE to CPF and PS *in vivo*, since no such difference was observed *in vitro*.

However, the higher sensitivity of atrial cholinesterases to CPF and PS in aged rats did not appear to be correlated with more extensive dysregulation of heart rate in this age-group.

It has been a common finding that equitoxic doses (operationally defined as doses that produce similar levels of AChE inhibition) of chlorpyrifos and parathion elicit very different degrees of toxicity (IM and SLUD), with PS being more toxic. We observed similar differences in the expression of functional signs of toxicity between these two insecticides. Interestingly, in our studies we found that while PS elicited more extensive cholinergic signs, relatively similar degrees of cardiac dysfunction and disruption of other physiological parameters were noted following exposure to either CPF or PS.

In summary, radiotelemetry was successfully optimized for obtaining physiological data including heart rate, electrocardiogram, body temperature and motor activity in both adult and aged rats. These studies suggest that BChE plays a role in the normal functioning of the heart. Thus, OP toxicants that selectively target this enzyme may have cardiotoxic potential. Moreover, some OP insecticides bind directly to muscarinic receptors at low concentrations, suggesting that direct interaction with muscarinic receptors could occur at toxicologically relevant exposure levels. Equitoxic doses of CPF and PS produce very different degrees of functional toxicity, with PS eliciting more extensive cholinergic signs than CPF in both adult and aged rats. In contrast, relatively similar changes in heart rate, body temperature, and motor activity were observed following exposure to CPF or PS.

Future studies should further investigate the role of CPF and PS on cardiac function, *via* assessment of the Q-T cycle length in electrocardiograms. Moreover, the

use of cardiac biomarkers (such as cardiac Troponin I and T) would also aid in assessment of the time course of possible cardiac damage. Histopathological analysis of the hearts of adult and aged rats could reveal possible differential effects of these OP insecticides on the myocardium.

BIBLIOGRAPHY

Abdallah, E. A., D. A. Jett, et al. (1992). "Differential effects of paraoxon on the M3 muscarinic receptor and its effector system in rat submaxillary gland cells." Journal of biochemical toxicology **7**(2): 125-32.

Abraham, S., N. Oz, et al. (2001). "QTc prolongation and cardiac lesions following acute organophosphate poisoning in rats." Proceedings of the Western Pharmacology Society **44**: 185-6.

Adler, M., H. A. Manley, et al. (2004). "Reduced acetylcholine receptor density, morphological remodeling, and butyrylcholinesterase activity can sustain muscle function in acetylcholinesterase knockout mice." Muscle & nerve **30**(3): 317-27.

Ahdaya, S. M., P. V. Shah, et al. (1976). "Thermoregulation in mice treated with parathion, carbaryl, or DDT." Toxicology and applied pharmacology **35**(3): 575-80.

Alberts, B., Bray, D., Lewis, J., Raff, M., Roberts, K.,Watson, J.D., 1994 Cell signaling. In Robertson, M. (Ed.), *Molecular Biology of the Cell.* Garland Publishing, New York, pp. 721-785.

Aldridge, W. N., Reiner, E. (1972). Enzyme inhibitors as substrates. Amsterdam and New York, North-Holland/American Elsevier.

Allon, N., I. Rabinovitz, et al. (2005). "Acute and long-lasting cardiac changes following a single whole-body exposure to sarin vapor in rats." Toxicological sciences **87**(2): 385-90.

Amenta, F., A. Liu, et al. (1995). "Age-related changes in the density of muscarinic cholinergic M1 and M2 receptor subtypes in pyramidal neurons of the rat hippocampus." European journal of histochemistry **39**(2): 107-16.

Amenta, F., A. Ricci, et al. (2002). "The peripheral dopaminergic system: morphological analysis, functional and clinical applications." Italian journal of anatomy and embryology = Archivio italiano di anatomia ed embriologia **107**(3): 145-67.

Amenta, F., S. K. Tayebati, et al. (2006). "Association with the cholinergic precursor choline alphoscerate and the cholinesterase inhibitor rivastigmine: an approach for enhancing cholinergic neurotransmission." Mechanisms of ageing and development **127**(2): 173-9.

Amitai, G., D. Moorad, et al. (1998). "Inhibition of acetylcholinesterase and butyrylcholinesterase by chlorpyrifos-oxon." Biochemical pharmacology **56**(3): 293-9.

Andrus, A. K., B. R. Marable, et al. (2007). "Effects of intensity and type of prepulse stimulus on prepulse inhibition in scopolamine treated rats." Pharmacology, biochemistry, and behavior **87**(4): 481-8.

Araujo, D. M., P. A. Lapchak, et al. (1990). "Effects of aging on nicotinic and muscarinic autoreceptor function in the rat brain: relationship to presynaptic cholinergic markers and binding sites." The Journal of neuroscience **10**(9): 3069-78.

Arpagaus, M., A. Chatonnet, et al. (1991). "Use of the polymerase chain reaction for homology probing of butyrylcholinesterase from several vertebrates." J Biol Chem **266**(11): 6966-74.

Atack, J. R., E. K. Perry, et al. (1986). "Molecular forms of acetylcholinesterase and butyrylcholinesterase in the aged human central nervous system." Journal of neurochemistry **47**(1): 263-77.

Atkinson, B. (1976). "Organophosphate insecticide poisoning." Journal of the Mississippi State Medical Association **17**(4): 91-4.

Atterberry, T. T., W. T. Burnett, et al. (1997). "Age-related differences in parathion and chlorpyrifos toxicity in male rats: target and nontarget esterase sensitivity and cytochrome P450-mediated metabolism." Toxicology and applied pharmacology **147**(2): 411-8.

Avola, R., M. A. Di Tullio, et al. (2004). "Glial fibrillary acidic protein and vimentin expression is regulated by glucocorticoids and neurotrophic factors in primary rat astroglial cultures." Clinical and experimental hypertension (New York, N.Y. **26**(4): 323-33.

Ayyagari, P. V., M. Gerber, et al. (1998). "Uncoupling of muscarinic cholinergic phosphoinositide signals in senescent cerebral cortical and hippocampal membranes." Neurochemistry international **32**(1): 107-15.

Baker, S. P., S. Marchand, et al. (1985). "Age-related changes in cardiac muscarinic receptors: decreased ability of the receptor to form a high affinity agonist binding state." Journal of gerontology **40**(2): 141-6.

Bakry, N. M., A. H. el-Rashidy, et al. (1988). "Direct actions of organophosphate anticholinesterases on nicotinic and muscarinic acetylcholine receptors." Journal of biochemical toxicology **3**: 235-59.

Bakry, N. M., A. T. Eldefrawi, et al. (1982). "Interactions of quaternary ammonium drugs with acetylcholinesterase and acetylcholine receptor of Torpedo electric organ." Molecular pharmacology **22**(1): 63-71.

Bakry, N. M., S. M. Sherby, et al. (1986). "Oxadiazolidinones: irreversible inhibition of cholinesterases and effects on acetylcholine receptors." Neurotoxicology **7**(3): 1-10.

Ballard, C. G., N. H. Greig, et al. (2005). "Cholinesterases: roles in the brain during health and disease." Current Alzheimer research **2**(3): 307-18.

Bar-Meir, E., O. Schein, et al. (2007). "Guidelines for treating cardiac manifestations of organophosphates poisoning with special emphasis on long QT and Torsades De Pointes." Critical reviews in toxicology **37**(3): 279-85.

Barr, D. B., R. Allen, et al. (2005). "Concentrations of selective metabolites of organophosphorus pesticides in the United States population." Environmental research **99**(3): 314-26.

Barr, D. B., R. Bravo, et al. (2004). "Concentrations of dialkyl phosphate metabolites of organophosphorus pesticides in the U.S. population." Environmental health perspectives **112**(2): 186-200.

Bataillard, A., F. Sannajust, et al. (1990). "Cardiovascular consequences of organophosphorus poisoning and of antidotes in conscious unrestrained rats." Pharmacology & toxicology **67**(1): 27-35.

Batulevicius, D., N. Pauziene, et al. (2003). "Topographic morphology and age-related analysis of the neuronal number of the rat intracardiac nerve plexus." <u>Ann Anat</u> **185**(5): 449-59.

Batulevicius, D., N. Pauziene, et al. (2004). "Key anatomic data for the use of rat heart in electrophysiological studies of the intracardiac nervous system." <u>Medicina (Kaunas)</u> **40**(3): 253-9.

Batulevicius, D., N. Pauziene, et al. (2005). "Architecture and age-related analysis of the neuronal number of the guinea pig intrinsic cardiac nerve plexus." <u>Ann Anat</u> **187**(3): 225-43.

Batulevicius, D., V. Skripka, et al. (2008). "Topography of the porcine epicardiac nerve plexus as revealed by histochemistry for acetylcholinesterase." <u>Auton Neurosci</u> **138**(1-2): 64-75.

Beinert, H., R. W. Shaw, et al. (1980). "Studies on the origin of the near-infrared (800-900 nm) absorption of cytochrome c oxidase." <u>Biochimica et biophysica acta</u> **591**(2): 458-70.

Benke, G. M. and S. D. Murphy (1975). "The influence of age on the toxicity and metabolism of methyl parathion and parathion in male and female rats." <u>Toxicology and applied pharmacology</u> **31**(2): 254-69.

Berrie, C. P., N. J. Birdsall, et al. (1979). "Guanine nucleotides modulate muscarinic receptor binding in the heart." <u>Biochemical and biophysical research communications</u> **87**(4): 1000-5.

Biegon, A., M. Hanau, et al. (1989). "Aging and brain cholinergic muscarinic receptor subtypes: an autoradiographic study in the rat." Neurobiology of aging **10**(4): 305-10.

Blake, M. J., N. M. Appel, et al. (1991). "Muscarinic acetylcholine receptor subtype mRNA expression and ligand binding in the aged rat forebrain." Neurobiology of aging **12**(3): 193-9.

Bloomquist, J. R., R. L. Barlow, et al. (2002). "Selective effects of insecticides on nigrostriatal dopaminergic nerve pathways." Neurotoxicology **23**(4-5): 537-44.

Bognar, I. T., B. Beinhauer, et al. (1990). "Different muscarinic receptors mediate autoinhibition of acetylcholine release and vagally-induced vasoconstriction in the rat isolated perfused heart." Naunyn-Schmiedeberg's archives of pharmacology **341**(4): 279-87.

Bomser, J. A. and J. E. Casida (2001). "Diethylphosphorylation of rat cardiac M2 muscarinic receptor by chlorpyrifos oxon in vitro." Toxicology letters **119**(1): 21-6.

Boudinot, E., M. J. Emery, et al. (2004). "Increased ventilation and CO2 chemosensitivity in acetylcholinesterase knockout mice." Respiratory physiology & neurobiology **140**(3): 231-41.

Boudinot, E., L. Taysse, et al. (2005). "Effects of acetylcholinesterase and butyrylcholinesterase inhibition on breathing in mice adapted or not to reduced acetylcholinesterase." Pharmacology, biochemistry, and behavior **80**(1): 53-61.

Bourne, H. R., Roberts, J.M. 1995. Drug receptors and pharmacodynamics. In *Basic and Clinical Pharmacology*, ed. Katzung, B.G., 6th ed., 9-32. Norwalk, CT, Appleton and Lange.

Brimijoin, S. and C. Koenigsberger (1999). "Cholinesterases in neural development: new findings and toxicologic implications." Environmental health perspectives **107 Suppl 1**: 59-64.

Brodde, O. E., U. Konschak, et al. (1998). "Cardiac muscarinic receptors decrease with age. In vitro and in vivo studies." The Journal of clinical investigation **101**(2): 471-8.

Brody, T. M. 1994. Sites of action: Receptors. In *Human Pharmacology: Molecular to Clinical*, eds. Brody, T.M., Larner, J., Minneman, K.P., and Neu, H.C., 2nd ed., 9-23. St. Louis, Mosby.

Brown, J. H., Taylor, P (1996). "Muscarinic receptor agonists and antagonists. In: Hardman, J.G., Limbird, L.E. (Eds.), Goodman and Gilman's The Pharmacological Basis of Therapeutics. McGraw-Hill, New York, pp. 141–160."

Burn, J. H. and J. M. Walker (1954). "Anticholinesterases in the heart-lung preparation." The Journal of physiology **124**(3): 489-501.

Bytyqi, A. H., O. Lockridge, et al. (2004). "Impaired formation of the inner retina in an AChE knockout mouse results in degeneration of all photoreceptors." The European journal of neuroscience **20**(11): 2953-62.

Candell, L. M., S. H. Yun, et al. (1990). "Differential coupling of subtypes of the muscarinic receptor to adenylate cyclase and phosphoinositide hydrolysis in the longitudinal muscle of the rat ileum." Molecular pharmacology **38**(5): 689-97.

Casida, J. E. and G. B. Quistad (2005). "Serine hydrolase targets of organophosphorus toxicants." Chemico-biological interactions **157-158**: 277-83.

Caulfield, M. P. (1993). "Muscarinic receptors--characterization, coupling and function." Pharmacology & therapeutics **58**(3): 319-79.

Caulfield, M. P. and N. J. Birdsall (1998). "International Union of Pharmacology. XVII. Classification of muscarinic acetylcholine receptors." Pharmacological reviews **50**(2): 279-90.

Caulfield, M. P. and D. A. Brown (1991). "Pharmacology of the putative M4 muscarinic receptor mediating Ca-current inhibition in neuroblastoma x glioma hybrid (NG 108-15) cells." British journal of pharmacology **104**(1): 39-44.

Cetin, N., E. Cetin, et al. (2007). "Chlorpyrifos induces cardiac dysfunction in rabbits." Research in veterinary science **82**(3): 405-8.

Chakraborti, T. K., J. D. Farrar, et al. (1993). "Comparative neurochemical and neurobehavioral effects of repeated chlorpyrifos exposures in young and adult rats." Pharmacology, biochemistry, and behavior **46**(1): 219-24.

Chambers, H. W. (1992). Organophosphorus compounds: An overview. In *Organophsophates. Chemistry, Fate, and Effects*. San Diego, CA, Academic Press, Inc**:** 3-17.

Chambers, H. W., Brown, B., Chambers, J.E. (1990). "Noncatalytic detoxification of six organophosphorus compounds by rat liver homogenates." Pest. Biochem. Physiol. **36**: 308-15.

Chanda, A., D. L. Popescu, et al. (2006). "High-valent iron complexes with tetraamido macrocyclic ligands: structures, Mossbauer spectroscopy, and DFT calculations." Journal of inorganic biochemistry **100**(4): 606-19.

Chanda, S. M., P. Harp, et al. (1995). "Comparative developmental and maternal neurotoxicity following acute gestational exposure to chlorpyrifos in rats." Journal of toxicology and environmental health **44**(2): 189-202.

Chanda, S. M. and C. N. Pope (1996). "Neurochemical and neurobehavioral effects of repeated gestational exposure to chlorpyrifos in maternal and developing rats." Pharmacology, biochemistry, and behavior **53**(4): 771-6.

Chatonnet, A. and O. Lockridge (1989). "Comparison of butyrylcholinesterase and acetylcholinesterase." Biochem J **260**(3): 625-34.

Chatonnet, F., E. Boudinot, et al. (2004). "Breathing without acetylcholinesterase." Advances in experimental medicine and biology **551**: 165-70.

Chatonnet, F., E. Boudinot, et al. (2003). "Respiratory survival mechanisms in acetylcholinesterase knockout mouse." The European journal of neuroscience **18**(6): 1419-27.

Chaudhuri, J., T. K. Chakraborti, et al. (1993). "Differential modulation of organophosphate-sensitive muscarinic receptors in rat brain by parathion and chlorpyrifos." Journal of biochemical toxicology **8**(4): 207-16.

Chemnitius, J. M., R. Sadowski, et al. (1999). "Organophosphate inhibition of human heart muscle cholinesterase isoenzymes." Chemico-biological interactions **119-120**: 183-92.

Chevalier, B., P. Mansier, et al. (1991). "Alterations in beta adrenergic and muscarinic receptors in aged rat heart. Effects of chronic administration of propranolol and atropine." Mechanisms of ageing and development **60**(2): 215-24.

Chow, L. T., S. S. Chow, et al. (2001). "Autonomic innervation of the human cardiac conduction system: changes from infancy to senility--an immunohistochemical and histochemical analysis." The Anatomical record **264**(2): 169-82.

Cioffi, C. L. and E. E. el-Fakahany (1988). "Lack of alterations in muscarinic receptor subtypes and phosphoinositide hydrolysis upon acute DFP treatment." European journal of pharmacology **156**(1): 35-45.

Cooper, J. R. (1994). "Unsolved problems in the cholinergic nervous system." Journal of neurochemistry **63**(2): 395-9.

Costa, L. G. (2006). "Current issues in organophosphate toxicology." Clinica chimica acta; international journal of clinical chemistry **366**(1-2): 1-13.

Costa, L. G., B. W. Schwab, et al. (1982). "Differential alterations of cholinergic muscarinic receptors during chronic and acute tolerance to organophosphorus insecticides." Biochemical pharmacology **31**(21): 3407-13.

Craig, T. J., S. P. Lin, et al. (1985). "Clinical correlates of readmission in a schizophrenic cohort." The Psychiatric quarterly **57**(1): 5-10.

Darvesh, S., R. C. Arora, et al. (2004). "Cholinesterase inhibitors modify the activity of intrinsic cardiac neurons." Experimental neurology **188**(2): 461-70.

Darvesh, S., D. A. Hopkins, et al. (2003). "Neurobiology of butyrylcholinesterase." Nature reviews **4**(2): 131-8.

Darvesh, S., S. E. MacDonald, et al. (1998). "Cholinesterases in cardiac ganglia and modulation of canine intrinsic cardiac neuronal activity." Journal of the autonomic nervous system **71**(2-3): 75-84.

Das, A., M. Dikshit, et al. (2001). "Profile of acetylcholinesterase in brain areas of male and female rats of adult and old age." Life sciences **68**(13): 1545-55.

Dave, K. R. and S. S. Katyare (2002). "Effect of alloxan-induced diabetes on serum and cardiac butyrylcholinesterases in the rat." The Journal of endocrinology **175**(1): 241-50.

Deighton, N. M., S. Motomura, et al. (1990). "Muscarinic cholinoceptors in the human heart: demonstration, subclassification, and distribution." Naunyn-Schmiedeberg's archives of pharmacology **341**(1-2): 14-21.

Demirag, K., I. Cankayali, et al. (2005). "The comparison of therapeutic effects of atropine and pralidoxime on cardiac signs in rats with experimental organophosphate poisoning." Advances in therapy **22**(2): 79-86.

Denisova, N. A., S. A. Erat, et al. (1998). "Differential effect of aging on cholesterol modulation of carbachol-stimulated low-K(m) GTPase in striatal synaptosomes." Experimental gerontology **33**(3): 249-65.

Dhein, S., C. J. van Koppen, et al. (2001). "Muscarinic receptors in the mammalian heart." Pharmacological research **44**(3): 161-82.

Di Tullio, M. A., S. K. Tayebati, et al. (2004). "Identification of adenosine A1 and A3 receptor subtypes in rat pial and intracerebral arteries." Neuroscience letters **366**(1): 48-52.

Duysen, E. G., D. L. Fry, et al. (2002). "Early weaning and culling eradicated Helicobacter hepaticus from an acetylcholinesterase knockout 129S6/SvEvTac mouse colony." Comparative medicine **52**(5): 461-6.

Duysen, E. G., B. Li, et al. (2007). "Sensitivity of butyrylcholinesterase knockout mice to (--)-huperzine A and donepezil suggests humans with butyrylcholinesterase deficiency may not tolerate these Alzheimer's disease drugs and indicates butyrylcholinesterase function in neurotransmission." Toxicology **233**(1-3): 60-9.

Duysen, E. G., B. Li, et al. (2001). "Evidence for nonacetylcholinesterase targets of organophosphorus nerve agent: supersensitivity of acetylcholinesterase knockout mouse to VX lethality." The Journal of pharmacology and experimental therapeutics **299**(2): 528-35.

Duysen, E. G. and O. Lockridge (2006). "Phenotype comparison of three acetylcholinesterase knockout strains." Journal of molecular neuroscience **30**(1-2): 91-2.

Duysen, E. G., J. A. Stribley, et al. (2002). "Rescue of the acetylcholinesterase knockout mouse by feeding a liquid diet; phenotype of the adult acetylcholinesterase deficient mouse." Brain research **137**(1): 43-54.

Ecobichon, D. J. (1996). Toxic effects of Pesticides. New York, McGraw-Hill.

Ecobichon, D. J. (2001). Toxic effects of pesticides. In *Casarett and Doull's Toxicology: The Basic Science of Posions*, ed. C.D. Klaassen. New York, McGraw-Hill. **5th ed:** 643-89.

Eglen, R. M., H. Reddy, et al. (1994). "Selective inactivation of muscarinic receptor subtypes." The International journal of biochemistry **26**(12): 1357-68.

Ehlert, F. J. and L. P. Tran (1990). "Regional distribution of M1, M2 and non-M1, non-M2 subtypes of muscarinic binding sites in rat brain." <u>The Journal of pharmacology and experimental therapeutics</u> **255**(3): 1148-57.

Ehrich, M. (1998). "Organophosphates. In *Encyclopedia of Toxicology*, ed. P. Wexler." <u>San Diego, CA: Academic Press</u> pp. 467-471.

Eldefrawi, M. E., G. Schweizer, et al. (1988). "Desensitization of the nicotinic acetylcholine receptor by diisopropylfluorophosphate." <u>Journal of biochemical toxicology</u> **3**: 21-32.

Fields, J. Z., W. R. Roeske, et al. (1978). "Cardiac muscarinic cholinergic receptors. Biochemical identification and characterization." <u>The Journal of biological chemistry</u> **253**(9): 3251-8.

Fonarow, G. C. (2008). "Comprehensive adrenergic blockade post myocardial infarction left ventricular dysfunction." <u>Cardiology clinics</u> **26**(1): 79-89.

Fonarow, G. C. (2008). "Epidemiology and risk stratification in acute heart failure." <u>American heart journal</u> **155**(2): 200-7.

Fonarow, G. C., W. F. Peacock, et al. (2008). "Usefulness of B-type natriuretic peptide and cardiac troponin levels to predict in-hospital mortality from ADHERE." <u>The American journal of cardiology</u> **101**(2): 231-7.

FQPA (1996). "Food Quality Protection Act, Public Law 104-170."

Friedman, A., D. Kaufer, et al. (1996). "Pyridostigmine brain penetration under stress enhances neuronal excitability and induces early immediate transcriptional response." <u>Nature medicine</u> **2**(12): 1382-5.

Fuortes, L. (2000). "Overview of insecticide toxicity." <u>Central European journal of public health</u> **8 Suppl**: 56-8.

Furlong, C. E., R. J. Richter, et al. (1989). "Spectrophotometric assays for the enzymatic hydrolysis of the active metabolites of chlorpyrifos and parathion by plasma paraoxonase/arylesterase." <u>Analytical biochemistry</u> **180**(2): 242-7.

Gaines, T. B. (1969). "Acute toxicity of pesticides." <u>Toxicology and applied pharmacology</u> **14**(3): 515-34.

Gallo, M. P., G. Alloatti, et al. (1993). "M1 muscarinic receptors increase calcium current and phosphoinositide turnover in guinea-pig ventricular cardiocytes." <u>The Journal of physiology</u> **471**: 41-60.

Galper, J. B. and T. W. Smith (1978). "Properties of muscarinic acetylcholine receptors in heart cell cultures." <u>Proceedings of the National Academy of Sciences of the United States of America</u> **75**(12): 5831-5.

Giacobini, E. (2000). "Cholinesterase inhibitors stabilize Alzheimer disease." <u>Neurochemical research</u> **25**(9-10): 1185-90.

Giacobini, E. (2001). "Selective inhibitors of butyrylcholinesterase: a valid alternative for therapy of Alzheimer's disease?" <u>Drugs & aging</u> **18**(12): 891-8.

Giacobini, E. (2003a). "Cholinergic function and Alzheimer's disease." <u>International journal of geriatric psychiatry</u> **18**(Suppl 1): S1-5.

Giacobini, E. (2003b). "Cholinesterases: new roles in brain function and in Alzheimer's disease." <u>Neurochemical research</u> **28**(3-4): 515-22.

Giacobini, E. (2004). "Cholinesterase inhibitors: new roles and therapeutic alternatives." <u>Pharmacological research</u> **50**(4): 433-40.

Giessler, C., S. Dhein, et al. (1999). "Muscarinic receptors in the failing human heart." European journal of pharmacology **375**(1-3): 197-202.

Giles, K. (1997). "Interactions underlying subunit association in cholinesterases." Protein engineering **10**(6): 677-85.

Girard, E., J. Barbier, et al. (2005). "Synaptic remodeling at the skeletal neuromuscular junction of acetylcholinesterase knockout mice and its physiological relevance." Chemico-biological interactions **157-158**: 87-96.

Girard, E., V. Bernard, et al. (2007). "Butyrylcholinesterase and the control of synaptic responses in acetylcholinesterase knockout mice." Life sciences **80**(24-25): 2380-5.

Glowinski, J. and L. Iversen (1966). "Regional studies of catecholamines in the rat brain. 3. Subcellullar distribution of endogenous and exogenous catecholamines in various brain regions." Biochemical pharmacology **15**(7): 977-87.

Gordon, C. J. (1993). "Acute and delayed effects of diisopropyl fluorophosphate on body temperature, heart rate, and motor activity in the awake, unrestrained rat." Journal of toxicology and environmental health **39**(2): 247-60.

Gordon, C. J. (1994). "Thermoregulatory effects of chlorpyrifos in the rat: long-term changes in cholinergic and noradrenergic sensitivity." Neurotoxicology and teratology **16**(1): 1-9.

Gordon, C. J. (1996). "Pharmacological analysis of diisopropyl fluorophosphate: effects on core temperature, heart rate, and motor activity in the unrestrained rat." Pharmacology, biochemistry, and behavior **55**(2): 185-94.

Gordon, C. J. (1997a). "Behavioral thermoregulatory response to chlorpyrifos in the rat." Toxicology **124**(3): 165-71.

Gordon, C. J. and T. A. Grantham (1999). "Effect of central and peripheral cholinergic antagonists on chlorpyrifos-induced changes in body temperature in the rat." Toxicology **142**(1): 15-28.

Gordon, C. J., T. A. Grantham, et al. (1997b). "Hypothermia and delayed fever in the male and female rat exposed to chlorpyrifos." Toxicology **118**(2-3): 149-58.

Gordon, C. J. and C. M. Mack (2001). "Diurnal variation in thermoregulatory response to chlorpyrifos and carbaryl in the rat." Toxicology **169**(2): 93-105.

Gordon, C. J. and B. K. Padnos (2000b). "Prolonged elevation in blood pressure in the unrestrained rat exposed to chlorpyrifos." Toxicology **146**(1): 1-13.

Gordon, C. J., E. Puckett, et al. (2002). "Rat tail skin temperature monitored noninvasively by radiotelemetry: characterization by examination of vasomotor responses to thermomodulatory agents." Journal of pharmacological and toxicological methods **47**(2): 107-14.

Gordon, C. J. and Y. L. Yang (2000a). "Chlorpyrifos-induced hypothermia and vasodilation in the tail of the rat: blockade by scopolamine." Pharmacology & toxicology **87**(1): 6-10.

Greig, N. H., T. Giordano, et al. (2004). "Thalidomide-based TNF-alpha inhibitors for neurodegenerative diseases." Acta neurobiologiae experimentalis **64**(1): 1-9.

Greig, N. H., D. K. Lahiri, et al. (2002). "Butyrylcholinesterase: an important new target in Alzheimer's disease therapy." International psychogeriatrics / IPA **14 Suppl 1**: 77-91.

Greig, N. H., M. P. Mattson, et al. (2004). "New therapeutic strategies and drug candidates for neurodegenerative diseases: p53 and TNF-alpha inhibitors, and GLP-1 receptor agonists." Annals of the New York Academy of Sciences **1035**: 290-315.

Greig, N. H., K. Sambamurti, et al. (2005a). "An overview of phenserine tartrate, a novel acetylcholinesterase inhibitor for the treatment of Alzheimer's disease." Current Alzheimer research **2**(3): 281-90.

Greig, N. H., T. Utsuki, et al. (2005b). "Selective butyrylcholinesterase inhibition elevates brain acetylcholine, augments learning and lowers Alzheimer beta-amyloid peptide in rodent." Proceedings of the National Academy of Sciences of the United States of America **102**(47): 17213-8.

Gupta, R. C. (1998). Organophosphate poisoning, intermediate syndrome. In *Encyclopedia of Toxicology 2*. New York, Academic Press**:** 465-67.

Gupta, R. C. and W. D. Dettbarn (1987). "iso-OMPA-induced potentiation of soman toxicity in rat." Archives of toxicology **61**(1): 58-62.

Gupta, R. C. and W. L. Kadel (1989). "Concerted role of carboxylesterases in the potentiation of carbofuran toxicity by iso-OMPA pretreatment." Journal of toxicology and environmental health **26**(4): 447-57.

Gupta, R. C., G. T. Patterson, et al. (1985). "Mechanisms involved in the development of tolerance to DFP toxicity." Fundamental and applied toxicology **5**(6 Pt 2): S17-28.

Habermeier-Muth, A., U. Altes, et al. (1990). "A presynaptic excitatory M1 muscarine receptor at postganglionic cardiac noradrenergic nerve fibres that is activated by

endogenous acetylcholine." Naunyn-Schmiedeberg's archives of pharmacology **342**(5): 483-9.

Haddad el, B. and J. Rousell (1998). "Regulation of the expression and function of the M2 muscarinic receptor." Trends in pharmacological sciences **19**(8): 322-7.

Hamilton, S. E., M. L. Schlador, et al. (1998). "Molecular mechanisms for the regulation of the expression and function of muscarinic acetylcholine receptors." Journal of physiology, Paris **92**(3-4): 275-8.

Hancock, J. C., D. B. Hoover, et al. (1987). "Distribution of muscarinic receptors and acetylcholinesterase in the rat heart." Journal of the autonomic nervous system **19**(1): 59-66.

Hantson, P., P. Hainaut, et al. (1996). "Regulation of body temperature after acute organophosphate poisoning." Canadian journal of anaesthesia = Journal canadien d'anesthesie **43**(7): 755.

Happe, H. K. and L. C. Murrin (1993). "High-affinity choline transport sites: use of [3H]hemicholinium-3 as a quantitative marker." Journal of neurochemistry **60**(4): 1191-201.

Harel, M., J. L. Sussman, et al. (1992). "Conversion of acetylcholinesterase to butyrylcholinesterase: modeling and mutagenesis." Proceedings of the National Academy of Sciences of the United States of America **89**(22): 10827-31.

Hartmann, J., C. Kiewert, et al. (2007a). "Excessive hippocampal acetylcholine levels in acetylcholinesterase-deficient mice are moderated by butyrylcholinesterase activity." Journal of neurochemistry **100**(5): 1421-9.

Hartmann, J., C. Kiewert, et al. (2007b). "Choline availability and acetylcholine synthesis in the hippocampus of acetylcholinesterase-deficient mice."

Hartzell, H. C. (1980). "Distribution of muscarinic acetylcholine receptors and presynaptic nerve terminals in amphibian heart." The Journal of cell biology **86**(1): 6-20.

Heckman, G. A., C. J. Patterson, et al. (2007). "Heart failure and cognitive impairment: challenges and opportunities." Clinical interventions in aging **2**(2): 209-18.

Hirshberg, A. and Y. Lerman (1984). "Clinical problems in organophosphate insecticide poisoning: the use of a computerized information system." Fundamental and applied toxicology **4**(2 Pt 2): S209-14.

Holmstedt, B. (1963). Structure-activity relationships of the organophosphorus anticholinesterase agents. In *Cholinesterases and Anticholinesterase Agents*. Berlin, Springer-Verlag**:** 428-85.

Hoover, D. B. and J. C. Hancock (1987). "Autoradiographic localization of substance P binding sites in guinea-pig airways." Journal of the autonomic nervous system **19**(2): 171-4.

Hoskins, B., Ho, I.K. (1992). Tolerance to organophosphorus cholinesterase inhibitors. In *Organophosphates. Chemistry, Fate and Effects*. San Diego, CA, Academic Press, Inc**:** 285-97.

Howard, M. D., N. Mirajkar, et al. (2007). "Comparative effects of oral chlorpyrifos exposure on cholinesterase activity and muscarinic receptor binding in neonatal and adult rat heart." Toxicology **238**(2-3): 157-65.

Howard, M. D. and C. N. Pope (2002). "In vitro effects of chlorpyrifos, parathion, methyl parathion and their oxons on cardiac muscarinic receptor binding in neonatal and adult rats." Toxicology **170**(1-2): 1-10.

Hrabovska, A., E. G. Duysen, et al. (2005). "Delivery of human acetylcholinesterase by adeno-associated virus to the acetylcholinesterase knockout mouse." Chemico-biological interactions **157-158**: 71-8.

Huff, R. A. and M. B. Abou-Donia (1995). "In vitro effect of chlorpyrifos oxon on muscarinic receptors and adenylate cyclase." Neurotoxicology **16**(2): 281-90.

Huff, R. A., A. W. Abu-Qare, et al. (2001). "Effects of sub-chronic in vivo chlorpyrifos exposure on muscarinic receptors and adenylate cyclase of rat striatum." Archives of toxicology **75**(8): 480-6.

Huff, R. A., J. J. Corcoran, et al. (1994). "Chlorpyrifos oxon binds directly to muscarinic receptors and inhibits cAMP accumulation in rat striatum." The Journal of pharmacology and experimental therapeutics **269**(1): 329-35.

Jbilo, O., C. F. Bartels, et al. (1994b). "Tissue distribution of human acetylcholinesterase and butyrylcholinesterase messenger RNA." Toxicon **32**(11): 1445-57.

Jbilo, O., Y. L'Hermite, et al. (1994a). "Acetylcholinesterase and butyrylcholinesterase expression in adult rabbit tissues and during development." European journal of biochemistry / FEBS **225**(1): 115-24.

Jeck, D., R. Lindmar, et al. (1988). "Subtypes of muscarinic receptor on cholinergic nerves and atrial cells of chicken and guinea-pig hearts." British journal of pharmacology **93**(2): 357-66.

Jett, D. A., Abdallah, E.A.M., El-Fakahany, E.E., Eldefrawi, M.E., and Eldefrawi, A.T. (1991). "High-affinity activation by paraoxon of a muscarinic receptor subtype in rat brain striatum." Pest. Biochem. Physiol. **39**: 149-57.

Jett, D. A., J. C. Fernando, et al. (1994). "Differential regulation of muscarinic receptor subtypes in rat brain regions by repeated injections of parathion." Toxicology letters **73**(1): 33-41.

Jett, D. A., E. F. Hill, et al. (1993). "Down-regulation of muscarinic receptors and the m3 subtype in white-footed mice by dietary exposure to parathion." Journal of toxicology and environmental health **39**(3): 395-415.

Johnson, C. D. and R. L. Russell (1975). "A rapid, simple radiometric assay for cholinesterase, suitable for multiple determinations." Analytical biochemistry **64**(1): 229-38.

Joseph, J. A., R. Cutler, et al. (1993). "Changes in G protein-mediated signal transduction in aging and Alzheimer's disease." Annals of the New York Academy of Sciences **695**: 42-5.

Joseph, J. A. and G. S. Roth (1993). "Hormonal regulation of motor behavior in senescence." Journal of gerontology **48 Spec No**: 51-5.

Kacham, R., S. Karanth, et al. (2006). "Interactive toxicity of chlorpyrifos and parathion in neonatal rats: role of esterases in exposure sequence-dependent toxicity." Toxicology and applied pharmacology **210**(1-2): 142-9.

Kadar, T., M. Silbermann, et al. (1990). "Age-related changes in the cholinergic components within the central nervous system. II. Working memory impairment

and its relation to hippocampal muscarinic receptors." <u>Mechanisms of ageing and development</u> **55**(2): 139-49.

Karanth, S., T. Holbrook, et al. (2008). "Selective inhibition of butyrylcholinesterase in vivo in horses by the feed-through larvacide Equitrol((R))." <u>Regul Toxicol Pharmacol</u> **50**(2): 200-5.

Karanth, S., J. Liu, et al. (2006). "Effects of acute chlorpyrifos exposure on in vivo acetylcholine accumulation in rat striatum." <u>Toxicology and applied pharmacology</u> **216**(1): 150-6.

Karanth, S., J. Liu, et al. (2004). "Interactive toxicity of the organophosphorus insecticides chlorpyrifos and methyl parathion in adult rats." <u>Toxicol Appl Pharmacol</u> **196**(2): 183-90.

Karanth, S., J. Liu, et al. (2007). "Comparative in vivo effects of parathion on striatal acetylcholine accumulation in adult and aged rats." <u>Toxicology</u> **239**(3): 167-79.

Karanth, S., K. Olivier, Jr., et al. (2001). "In vivo interaction between chlorpyrifos and parathion in adult rats: sequence of administration can markedly influence toxic outcome." <u>Toxicology and applied pharmacology</u> **177**(3): 247-55.

Karanth, S. and C. Pope (2000). "Carboxylesterase and A-esterase activities during maturation and aging: relationship to the toxicity of chlorpyrifos and parathion in rats." <u>Toxicological sciences</u> **58**(2): 282-9.

Karanth, S. and C. Pope (2003a). "Age-related effects of chlorpyrifos and parathion on acetylcholine synthesis in rat striatum." <u>Neurotoxicology and teratology</u> **25**(5): 599-606.

Karanth, S. and C. Pope (2003b). "In vitro inhibition of blood cholinesterase activities from horse, cow, and rat by tetrachlorvinphos." Int J Toxicol **22**(6): 429-33.

Karen, D. J., W. Li, et al. (2001). "Striatal dopaminergic pathways as a target for the insecticides permethrin and chlorpyrifos." Neurotoxicology **22**(6): 811-7.

Karki, P., J. A. Ansari, et al. (2004). "Cardiac and electrocardiographical manifestations of acute organophosphate poisoning." Singapore medical journal **45**(8): 385-9.

Katz, L. S. and J. K. Marquis (1989). "Modulation of central muscarinic receptor binding in vitro by ultralow levels of the organophosphate paraoxon." Toxicology and applied pharmacology **101**(1): 114-23.

Kaufer, D., A. Friedman, et al. (1998). "Acute stress facilitates long-lasting changes in cholinergic gene expression." Nature **393**(6683): 373-7.

Kaufer, D., A. Friedman, et al. (1999). "Anticholinesterases induce multigenic transcriptional feedback response suppressing cholinergic neurotransmission." Chemico-biological interactions **119-120**: 349-60.

Kayyali, U. S., T. B. Moore, et al. (1991). "Neurotoxic esterase (NTE) assay: optimized conditions based on detergent-induced shifts in the phenol/4-aminoantipyrine chromophore spectrum." Journal of analytical toxicology **15**(2): 86-9.

Kecik, Y., D. Yorukoglu, et al. (1993). "A case of acute poisoning due to organophosphate insecticide." Anaesthesia **48**(2): 141-3.

Kelliher, G. J. and S. T. Conahan (1980). "Changes in vagal activity and response to muscarinic receptor agonists with age." Journal of gerontology **35**(6): 842-9.

Kelly, J. F., J. A. Joseph, et al. (1995). "Dissociation of striatal GTPase and dopamine release responses to muscarinic cholinergic agonists in F344 rats: influence of age and dietary manipulation." Journal of neurochemistry **64**(6): 2755-64.

Kelly, J. F., R. P. Mason, et al. (1995). "Age-related impairment in striatal muscarinic cholinergic signal transduction is associated with reduced membrane bilayer width measured by small angle X-ray diffraction." Biochemical and biophysical research communications **213**(3): 869-74.

Kennedy, R. H. and E. Seifen (1990). "Aging: effects on chronotropic actions of muscarinic agonists in isolated rat atria." Mechanisms of ageing and development **51**(1): 81-7.

Kiely T, D. D., Grube A. (The U.S.EPA publication Pesticide Industry Sales and Usage,2000 and 2001 Market Estimates. U.S. Pesticide Sales and Usage 2005; 18(2).).

Knuepfer, M. M. and Q. Gan (1999). "Role of cholinergic receptors and cholinesterase activity in hemodynamic responses to cocaine in conscious rats." The American journal of physiology **276**(1 Pt 2): R103-12.

Kosasa, T., Y. Kuriya, et al. (1999). "Inhibitory effects of donepezil hydrochloride (E2020) on cholinesterase activity in brain and peripheral tissues of young and aged rats." European journal of pharmacology **386**(1): 7-13.

Kramer, K., L. Kinter, et al. (2001). "The use of radiotelemetry in small laboratory animals: recent advances." Contemporary topics in laboratory animal science / American Association for Laboratory Animal Science **40**(1): 8-16.

Kramer, K. and L. B. Kinter (2003). "Evaluation and applications of radiotelemetry in small laboratory animals." Physiological genomics **13**(3): 197-205.

Lahiri, D. K., D. Chen, et al. (2007). "The experimental Alzheimer's disease drug posiphen [(+)-phenserine] lowers amyloid-beta peptide levels in cell culture and mice." The Journal of pharmacology and experimental therapeutics **320**(1): 386-96.

Lahiri, D. K., M. R. Farlow, et al. (2003). "A critical analysis of new molecular targets and strategies for drug developments in Alzheimer's disease." Current drug targets **4**(2): 97-112.

Lahiri, D. K., Y. W. Ge, et al. (2006). "Taking down the unindicted co-conspirators of amyloid beta-peptide-mediated neuronal death: shared gene regulation of BACE1 and APP genes interacting with CREB, Fe65 and YY1 transcription factors." Current Alzheimer research **3**(5): 475-83.

Lahiri, D. K., J. T. Rogers, et al. (2004). "Rationale for the development of cholinesterase inhibitors as anti-Alzheimer agents." Current pharmaceutical design **10**(25): 3111-9.

Lapchak, P. A., D. M. Araujo, et al. (1990). "Opiate receptor-mediated inhibition of acetylcholine release from mammalian brain: tissue- and species-dependence." Progress in clinical and biological research **328**: 347-50.

Lassiter, T. L., S. Barone, Jr., et al. (1999). "Gestational exposure to chlorpyrifos: dose response profiles for cholinesterase and carboxylesterase activity." Toxicological sciences **52**(1): 92-100.

Lazareno, S., N. J. Buckley, et al. (1990). "Characterization of muscarinic M4 binding sites in rabbit lung, chicken heart, and NG108-15 cells." Molecular pharmacology **38**(6): 805-15.

Lee, H. J., M. Clagett-Dame, et al. (1994). "The effect of age on muscarinic receptor transcripts in rat brain." Neuroscience letters **174**(2): 205-8.

Lee, K. B., J. A. Ptasienski, et al. (2000). "Arrestin binding to the M(2) muscarinic acetylcholine receptor is precluded by an inhibitory element in the third intracellular loop of the receptor." The Journal of biological chemistry **275**(13): 9284-9.

Lefkowitz, R. J., Hoffman, B.B. and Taylor, P. (1996). Neurotransmission: The autonomic and somatic motor nervous systems. In Goodman and Gilman's The Pharmacological Basis of Therapeutics, 9th ed. New York, McGraw-Hill**:** 105-39.

Li, B., E. G. Duysen, et al. (2008). "The butyrylcholinesterase knockout mouse as a model for human butyrylcholinesterase deficiency." The Journal of pharmacology and experimental therapeutics **324**(3): 1146-54.

Li, B., E. G. Duysen, et al. (2006b). "Gene transfer of acetylcholinesterase protects the knockout mouse from the toxicity of DFP." Journal of molecular neuroscience **30**(1-2): 79-80.

Li, B., E. G. Duysen, et al. (2006c). "Protection from the toxicity of diisopropylfluorophosphate by adeno-associated virus expressing acetylcholinesterase." Toxicology and applied pharmacology **214**(2): 152-65.

Li, B., E. G. Duysen, et al. (2006a). "Production of the butyrylcholinesterase knockout mouse." Journal of molecular neuroscience **30**(1-2): 193-5.

Li, B., E. G. Duysen, et al. (2003). "Regulation of muscarinic acetylcholine receptor function in acetylcholinesterase knockout mice." <u>Pharmacology, biochemistry, and behavior</u> **74**(4): 977-86.

Li, B., M. Sedlacek, et al. (2005). "Butyrylcholinesterase, paraoxonase, and albumin esterase, but not carboxylesterase, are present in human plasma." <u>Biochemical pharmacology</u> **70**(11): 1673-84.

Li, B., J. A. Stribley, et al. (2000). "Abundant tissue butyrylcholinesterase and its possible function in the acetylcholinesterase knockout mouse." <u>Journal of neurochemistry</u> **75**(3): 1320-31.

Litovitz, T. L., M. Smilkstein, et al. (1997). "1996 annual report of the American Association of Poison Control Centers Toxic Exposure Surveillance System." <u>The American journal of emergency medicine</u> **15**(5): 447-500.

Liu, J., T. Chakraborti, et al. (2002). "In vitro effects of organophosphorus anticholinesterases on muscarinic receptor-mediated inhibition of acetylcholine release in rat striatum." <u>Toxicology and applied pharmacology</u> **178**(2): 102-8.

Liu, J., R. C. Gupta, et al. (2007). "Modulation of parathion toxicity by glucose feeding: Is nitric oxide involved?" <u>Toxicology and applied pharmacology</u> **219**(2-3): 106-13.

Liu, J., S. Karanth, et al. (2005). "Dietary modulation of parathion-induced neurotoxicity in adult and juvenile rats." <u>Toxicology</u> **210**(2-3): 135-45.

Liu, J., K. Olivier, et al. (1999). "Comparative neurochemical effects of repeated methyl parathion or chlorpyrifos exposures in neonatal and adult rats." <u>Toxicology and applied pharmacology</u> **158**(2): 186-96.

Liu, J. and C. N. Pope (1996). "Effects of chlorpyrifos on high-affinity choline uptake and [3H]hemicholinium-3 binding in rat brain." <u>Fundamental and applied toxicology</u> **34**(1): 84-90.

Liu, J. and C. N. Pope (1998). "Comparative presynaptic neurochemical changes in rat striatum following exposure to chlorpyrifos or parathion." <u>Journal of toxicology and environmental health</u> **53**(7): 531-44.

Lockridge, O. and B. N. La Du (1986). "Amino acid sequence of the active site of human serum cholinesterase from usual, atypical, and atypical-silent genotypes." <u>Biochemical genetics</u> **24**(5-6): 485-98.

Logsdon, C. D. (1999). "The influence of the cellular context on receptor function: a necessary consideration for physiologic interpretations of receptor expression studies." <u>Life sciences</u> **64**(6-7): 369-74.

Lopez-Crespo, G. A., F. Carvajal, et al. (2007). "Time course of biochemical and behavioural effects of a single high dose of chlorpyrifos." <u>Neurotoxicology</u> **28**(3): 541-7.

Lowry, O. H., N. J. Rosebrough, et al. (1951). "Protein measurement with the Folin phenol reagent." <u>The Journal of biological chemistry</u> **193**(1): 265-75.

Ludomirsky, A., H. O. Klein, et al. (1982). "Q-T prolongation and polymorphous ("torsade de pointes") ventricular arrhythmias associated with organophosphorus insecticide poisoning." <u>The American journal of cardiology</u> **49**(7): 1654-8.

Mansier, P., B. Chevalier, et al. (1991). "Membrane proteins of the myocytes in cardiac overload." <u>Acta cardiologica</u> **46**(3): 299-307.

Marable, B. R., J. P. Maurissen, et al. (2007). "Differential sensitivity of blood, peripheral, and central cholinesterases in beagle dogs following dietary exposure to chlorpyrifos." Regulatory toxicology and pharmacology **47**(3): 240-8.

Mason, G. F., R. Gruetter, et al. (1995). "Simultaneous determination of the rates of the TCA cycle, glucose utilization, alpha-ketoglutarate/glutamate exchange, and glutamine synthesis in human brain by NMR." Journal of cerebral blood flow and metabolism **15**(1): 12-25.

Masson, P., A. Chatonnet, et al. (1990). "Evidence for a single butyrylcholinesterase gene in individuals carrying the C5 plasma cholinesterase variant (CHE2)." FEBS Lett **262**(1): 115-8.

Masuda, Y. (2004). "Cardiac effect of cholinesterase inhibitors used in Alzheimer's disease--from basic research to bedside." Current Alzheimer research **1**(4): 315-21.

Mattsson, J. L., J. W. Wilmer, et al. (1996). "Single-dose and 13-week repeated-dose neurotoxicity screening studies of chlorpyrifos insecticide." Food and chemical toxicology **34**(4): 393-405.

McArdle, J. R., T. K. Trow, et al. (2007). "Pulmonary hypertension in older adults." Clinics in chest medicine **28**(4): 717-33, vi.

McTiernan, C., S. Adkins, et al. (1987). "Brain cDNA clone for human cholinesterase." Proc Natl Acad Sci U S A **84**(19): 6682-6.

Meneguz, A., G. M. Bisso, et al. (1992). "Age-related changes in acetylcholinesterase and its molecular forms in various brain areas of rats." Neurochemical research **17**(8): 785-90.

Mesco, E. R., S. G. Carlson, et al. (1993). "Decreased striatal D2 dopamine receptor mRNA synthesis during aging." Brain research **17**(1-2): 160-2.

Mesco, E. R., J. A. Joseph, et al. (1991). "Loss of D2 receptors during aging is partially due to decreased levels of mRNA." Brain research **545**(1-2): 355-7.

Mesulam, M., A. Guillozet, et al. (2002b). "Widely spread butyrylcholinesterase can hydrolyze acetylcholine in the normal and Alzheimer brain." Neurobiology of disease **9**(1): 88-93.

Mesulam, M. M., A. Guillozet, et al. (2002a). "Acetylcholinesterase knockouts establish central cholinergic pathways and can use butyrylcholinesterase to hydrolyze acetylcholine." Neuroscience **110**(4): 627-39.

Meyer, E. M., A. Esen Momol, et al. (1985). "Age-related reductions in rat atrial high affinity choline uptake, ACh synthesis, and ACh release. A brief note." Mechanisms of ageing and development **30**(2): 221-5.

Michalek, H., S. Fortuna, et al. (1989). "Age-related differences in brain choline acetyltransferase, cholinesterases and muscarinic receptor sites in two strains of rats." Neurobiology of aging **10**(2): 143-8.

Minic, J., A. Chatonnet, et al. (2003). "Butyrylcholinesterase and acetylcholinesterase activity and quantal transmitter release at normal and acetylcholinesterase knockout mouse neuromuscular junctions." British journal of pharmacology **138**(1): 177-87.

Moffett, D. F., Moffett, S.B. and Schauf, C.L. (1993). Somatic and autonomic motor systems. In *Human Physiology: Foundations and Frontiers*, 2nd ed. St. Louis, MO, Mosby**:** 324-53.

Moreno, M., F. Canadas, et al. (2008). "Long-term monoamine changes in the striatum and nucleus accumbens after acute chlorpyrifos exposure." Toxicology letters **176**(2): 162-7.

Mortensen, S. R., S. Brimijoin, et al. (1998a). "Comparison of the in vitro sensitivity of rat acetylcholinesterase to chlorpyrifos-oxon: what do tissue IC50 values represent?" Toxicology and applied pharmacology **148**(1): 46-9.

Mortensen, S. R., S. M. Chanda, et al. (1996). "Maturational differences in chlorpyrifos-oxonase activity may contribute to age-related sensitivity to chlorpyrifos." Journal of biochemical toxicology **11**(6): 279-87.

Mortensen, S. R., M. J. Hooper, et al. (1998b). "Rat brain acetylcholinesterase activity: developmental profile and maturational sensitivity to carbamate and organophosphorus inhibitors." Toxicology **125**(1): 13-9.

Moser, V. C., S. M. Chanda, et al. (1998). "Age- and gender-related differences in sensitivity to chlorpyrifos in the rat reflect developmental profiles of esterase activities." Toxicological sciences **46**(2): 211-22.

Moser, V. C., P. M. Phillips, et al. (2005). "Neurobehavioral effects of chronic dietary and repeated high-level spike exposure to chlorpyrifos in rats." Toxicological sciences **86**(2): 375-86.

Motomura, S., N. M. Deighton, et al. (1990a). "Chronic beta 1-adrenoceptor antagonist treatment sensitizes beta 2-adrenoceptors, but desensitizes M2-muscarinic receptors in the human right atrium." British journal of pharmacology **101**(2): 363-9.

Motomura, S., N. M. Deighton, et al. (1990b). "Differential regulation of human cardiac beta-adrenergic and muscarinic receptors by chronic beta-adrenoceptor antagonist treatment." British journal of clinical pharmacology **30 Suppl 1**: 112S-114S.

Myslivecek, J., E. G. Duysen, et al. (2007). "Adaptation to excess acetylcholine by downregulation of adrenoceptors and muscarinic receptors in lungs of acetylcholinesterase knockout mice." Naunyn-Schmiedeberg's archives of pharmacology **376**(1-2): 83-92.

Naidu, K. A., S. Viswanatha, et al. (1987). "Cardiotoxic effects of dichlorvos (DDVP) in albino rats." Indian journal of physiology and pharmacology **31**(1): 19-24.

Namba, T., C. T. Nolte, et al. (1971). "Poisoning due to organophosphate insecticides. Acute and chronic manifestations." The American journal of medicine **50**(4): 475-92.

Narang, N., J. A. Joseph, et al. (1996). "Age-related loss of cholinergic-muscarinic coupling to PLC: comparison with changes in brain regional PLC subtypes mRNA distribution." Brain research **708**(1-2): 143-52.

Narayanan, N. and J. A. Derby (1983). "Effects of age on muscarinic cholinergic receptors in rat myocardium." Canadian journal of physiology and pharmacology **61**(8): 822-9.

Nestler, E. J., Duman, R.S. 1999. G Proteins. In *Basic Neurochemistry: Molecular, Cellular and Medical Aspects*, eds. Siegel, G.J., Agranoff, B.W., Albers, R.W., Fisher, S.K., and Uhler, M.D., 6th ed., 401-14. Philadelphia, PA, Lippincott-Raven.

Nicoll, R. A. (1995). Introduction to the pharmacology of CNS drugs. In *Basic and Clinical Pharmacology*, 6th ed. Norwalk, CT, Appleton and Lange**:** 323-32.

Nishimaru, K., Y. Tanaka, et al. (2000). "Positive and negative inotropic effects of muscarinic receptor stimulation in mouse left atria." Life sciences **66**(7): 607-15.

Nomura, D. K., D. Leung, et al. (2005). "A brain detoxifying enzyme for organophosphorus nerve poisons." Proceedings of the National Academy of Sciences of the United States of America **102**(17): 6195-200.

Norel, X., M. Angrisani, et al. (1993). "Degradation of acetylcholine in human airways: role of butyrylcholinesterase." British journal of pharmacology **108**(4): 914-9.

Nyquist-Battie, C., C. Hodges-Savola, et al. (1987). "Acetylcholinesterase molecular forms in rat heart." Journal of molecular and cellular cardiology **19**(9): 935-43.

O'Neill, J. J., Doukas, P.H. 1994. Drugs affecting the parasympathetic nervous system and autonomic ganglia. In *Human Pharmacology: Molecular to Clinical*, eds. Brody, T.M., Larner, J., Minneman, K.P., and Neu, H.C., 2nd ed., 97-111. St. Louis, Mosby.

Oberhauser, V., E. Schwertfeger, et al. (2001). "Acetylcholine release in human heart atrium: influence of muscarinic autoreceptors, diabetes, and age." Circulation **103**(12): 1638-43.

Olivier, K., Jr., J. Liu, et al. (2001). "Inhibition of forskolin-stimulated cAMP formation in vitro by paraoxon and chlorpyrifos oxon in cortical slices from neonatal, juvenile, and adult rats." Journal of biochemical and molecular toxicology **15**(5): 263-9.

Oortgiesen, M., R. G. van Kleef, et al. (1997). "Dual, non-competitive interaction of lead with neuronal nicotinic acetylcholine receptors in N1E-115 neuroblastoma cells." Brain research **747**(1): 1-8.

Padilla, S., J. Buzzard, et al. (2000). "Comparison of the role of esterases in the differential age-related sensitivity to chlorpyrifos and methamidophos." Neurotoxicology **21**(1-2): 49-56.

Padilla, S., R. S. Marshall, et al. (2005). "Neurochemical effects of chronic dietary and repeated high-level acute exposure to chlorpyrifos in rats." Toxicological sciences **88**(1): 161-71.

Parnetti, L., V. Caso, et al. (2006). "Stroke prevention and statin treatment." Clinical and experimental hypertension (New York, N.Y. **28**(3-4): 335-44.

Patocka, J., K. Kuca, et al. (2004). "Acetylcholinesterase and butyrylcholinesterase-- important enzymes of human body." Acta medica (Hradec Kralove) / Universitas Carolina, Facultas Medica Hradec Kralove **47**(4): 215-28.

Pedigo, N. W., Jr., L. D. Minor, et al. (1984). "Cholinergic drug effects and brain muscarinic receptor binding in aged rats." Neurobiology of aging **5**(3): 227-33.

Peeples, E. S., L. M. Schopfer, et al. (2005). "Albumin, a new biomarker of organophosphorus toxicant exposure, identified by mass spectrometry." Toxicological sciences **83**(2): 303-12.

Perry, E. K., R. H. Perry, et al. (1978). "Changes in brain cholinesterases in senile dementia of Alzheimer type." Neuropathology and applied neurobiology **4**(4): 273-7.

Peter, J. V. and A. M. Cherian (2000). "Organic insecticides." <u>Anaesthesia and intensive care</u> **28**(1): 11-21.

Pintor, A., S. Fortuna, et al. (1990). "Impaired recovery of brain muscarinic receptor sites following an adaptive down-regulation induced by repeated administration of diisopropyl fluorophosphate in aged rats." <u>Life sciences</u> **46**(14): 1027-36.

Pintor, A., S. Fortuna, et al. (1988). "Muscarinic receptor plasticity in the brain of senescent rats: down-regulation after repeated administration of diisopropyl fluorophosphate." <u>Life sciences</u> **42**(21): 2113-21.

Poller, U., G. Nedelka, et al. (1997). "Age-dependent changes in cardiac muscarinic receptor function in healthy volunteers." <u>Journal of the American College of Cardiology</u> **29**(1): 187-93.

Pond, A. L., C. P. Coyne, et al. (1996). "Identification and isolation of two rat serum proteins with A-esterase activity toward paraoxon and chlorpyrifos-oxon." <u>Biochemical pharmacology</u> **52**(2): 363-9.

Pope, C., S. Karanth, et al. (2005a). "Pharmacology and toxicology of cholinesterase inhibitors: uses and misuses of a common mechanism of action." <u>Environmental Toxicology and Pharmacology</u> **19**: 433-446.

Pope, C. E., B. L. Dresser, et al. (1997). "Birth of a western lowland gorilla (Gorilla gorilla gorilla) following in vitro fertilization and embryo transfer." <u>American journal of primatology</u> **41**(3): 247-60.

Pope, C. N. (1999). "Organophosphorus pesticides: do they all have the same mechanism of toxicity?" <u>Journal of toxicology and environmental health</u> **2**(2): 161-81.

Pope, C. N. (2001). The influence of age on pesticide toxicology. In *The Handbook of Pesticide Toxicology* Volume I. Principles, eds. Krieger, R.I., Doull, J., Ecobichon, D., Gammon, D., Hodgson, E., Reiter, L., and Ross, J., 2nd ed.,. San Diego, CA, Academic Press**:** 873-85.

Pope, C. N. and T. K. Chakraborti (1992a). "Dose-related inhibition of brain and plasma cholinesterase in neonatal and adult rats following sublethal organophosphate exposures." Toxicology **73**(1): 35-43.

Pope, C. N., T. K. Chakraborti, et al. (1992b). "Long-term neurochemical and behavioral effects induced by acute chlorpyrifos treatment." Pharmacology, biochemistry, and behavior **42**(2): 251-6.

Pope, C. N., T. K. Chakraborti, et al. (1991). "Comparison of in vivo cholinesterase inhibition in neonatal and adult rats by three organophosphorothioate insecticides." Toxicology **68**(1): 51-61.

Pope, C. N., S. Karanth, et al. (2005b). "Comparative carboxylesterase activities in infant and adult liver and their in vitro sensitivity to chlorpyrifos oxon." Regulatory toxicology and pharmacology **42**(1): 64-9.

Rice, S. G., L. Nowak, et al. (2007). "Neuropathological and immunochemical studies of brain parenchyma in acetylcholinesterase knockout mice: implications in Alzheimer's disease." Journal of Alzheimer's disease **11**(4): 481-9.

Richardson, R. J., T. B. Moore, et al. (1993). "Chlorpyrifos: assessment of potential for delayed neurotoxicity by repeated dosing in adult hens with monitoring of brain acetylcholinesterase, brain and lymphocyte neurotoxic esterase, and plasma

butyrylcholinesterase activities." <u>Fundamental and applied toxicology</u> **21**(1): 89-96.

Roberts, C. M. and J. Konjovic (1969). "Differences in the chronotropic and inotropic response of the rat atrium to choline esters, cholinesterase inhibitors and certain blocking agents." <u>The Journal of pharmacology and experimental therapeutics</u> **169**(1): 109-19.

Roskoski, R., Jr., R. R. Reinhardt, et al. (1985). "Cardiac cholinergic muscarinic receptors: changes in multiple affinity forms with down-regulation." <u>The Journal of pharmacology and experimental therapeutics</u> **232**(3): 754-9.

Roth, G. S., J. A. Joseph, et al. (1995). "Membrane alterations as causes of impaired signal transduction in Alzheimer's disease and aging." <u>Trends in neurosciences</u> **18**(5): 203-6.

Rother, R. P., S. P. Squinto, et al. (1995). "Protection of retroviral vector particles in human blood through complement inhibition." <u>Human gene therapy</u> **6**(4): 429-35.

Rowsey, P. J. and C. J. Gordon (1999). "Tumor necrosis factor is involved in chlorpyrifos--induced changes in core temperature in the female rat." <u>Toxicology letters</u> **109**(1-2): 51-9.

Russell, R. W. and D. H. Overstreet (1987). "Mechanisms underlying sensitivity to organophosphorus anticholinesterase compounds." <u>Progress in neurobiology</u> **28**(2): 97-129.

Saadeh, A. M., N. A. Farsakh, et al. (1997). "Cardiac manifestations of acute carbamate and organophosphate poisoning." <u>Heart (British Cardiac Society)</u> **77**(5): 461-4.

Sambamurti, K., A. C. Granholm, et al. (2004). "Cholesterol and Alzheimer's disease: clinical and experimental models suggest interactions of different genetic, dietary and environmental risk factors." Current drug targets **5**(6): 517-28.

Sambamurti, K., N. H. Greig, et al. (2002). "Advances in the cellular and molecular biology of the beta-amyloid protein in Alzheimer's disease." Neuromolecular medicine **1**(1): 1-31.

Sambamurti, K., A. Suram, et al. (2006). "A partial failure of membrane protein turnover may cause Alzheimer's disease: a new hypothesis." Current Alzheimer research **3**(1): 81-90.

Sastry, B. V., V. E. Janson, et al. (1983). "Changes in enzymes of the cholinergic system and acetylcholine release in the cerebra of aging male Fischer rats." Pharmacology **26**(2): 61-72.

Saunders, D. S., Harper, C. (1994). Pesticides. In *Principles and Methods of Toxicology, 3rd ed.* New York, Raven Press**:** 389-415.

Sauviat, M. P. (1999). "[Muscarinic modulation of cardiac activity]." Journal de la Societe de biologie **193**(6): 469-80.

Scali, C., M. G. Giovannini, et al. (1997). "Effect of metrifonate on extracellular brain acetylcholine and object recognition in aged rats." European journal of pharmacology **325**(2-3): 173-80.

Schlador, M. L. and N. M. Nathanson (1997). "Synergistic regulation of m2 muscarinic acetylcholine receptor desensitization and sequestration by G protein-coupled receptor kinase-2 and beta-arrestin-1." The Journal of biological chemistry **272**(30): 18882-90.

Schwarz, R. D., A. A. Bernabei, et al. (1990). "Loss of muscarinic M1 receptors with aging in the cerebral cortex of Fisher 344 rats." Pharmacology, biochemistry, and behavior **35**(3): 589-93.

Sharma, V. K., H. M. Colecraft, et al. (1996). "Molecular and functional identification of m1 muscarinic acetylcholine receptors in rat ventricular myocytes." Circulation research **79**(1): 86-93.

Shi, H., H. Wang, et al. (1999). "Choline modulates cardiac membrane repolarization by activating an M3 muscarinic receptor and its coupled K+ channel." The Journal of membrane biology **169**(1): 55-64.

Silman, I. and J. L. Sussman (2005). "Acetylcholinesterase: 'classical' and 'non-classical' functions and pharmacology." Current opinion in pharmacology **5**(3): 293-302.

Silveira, C. L., A. T. Eldefrawi, et al. (1990). "Putative M2 muscarinic receptors of rat heart have high affinity for organophosphorus anticholinesterases." Toxicology and applied pharmacology **103**(3): 474-81.

Silver, A. (1974). The biology of cholinesterases / Ann Silver. Amsterdam New York, North-Holland Pub. Co. ; American Elsevier Pub. Co.

Sirvio, J., A. Pitkanen, et al. (1989). "Brain cholinergic enzymes and cortical EEG activity in young and old rats." Comparative biochemistry and physiology **94**(1): 277-83.

Skau, K. A. and C. G. Triplett (1998). "Age-related changes in activity of Fischer 344 rat brain acetylcholinesterase molecular forms." Molecular and chemical neuropathology / sponsored by the International Society for Neurochemistry and

the World Federation of Neurology and research groups on neurochemistry and cerebrospinal fluid **35**(1-3): 13-21.

Slavikova, J. and S. Tucek (1986). "Postnatal changes in the activities of acetylcholinesterase and butyrylcholinesterase in rat heart atria." Physiologia Bohemoslovaca **35**(1): 11-6.

Slavikova, J., J. Vlk, et al. (1982). "Acetylcholinesterase and butyrylcholinesterase activity in the atria of the heart of adult albino rats." Physiologia Bohemoslovaca **31**(5): 407-14.

Sparks, S. E., G. B. Quistad, et al. (1999). "Organophosphorus pesticide-induced butyrylcholinesterase inhibition and potentiation of succinylcholine toxicity in mice." Journal of biochemical and molecular toxicology **13**(2): 113-8.

Stillman, M. J., B. Shukitt-Hale, et al. (1996). "Effects of M2 antagonists on in vivo hippocampal acetylcholine levels." Brain research bulletin **41**(4): 221-6.

Su, N. and N. Narayanan (1992). "Enhanced chronotropic and inotropic responses of rat myocardium to cholinergic stimulus with aging." Canadian journal of physiology and pharmacology **70**(12): 1618-24.

Sulakhe, P. V., G. Jagadeesh, et al. (1990). "Two distinct, divalent cation-sensitive, antagonist binding states of heart muscarinic receptors: differential modulation by guanine nucleotide." General pharmacology **21**(2): 211-8.

Sultatos, L. G. (1994). "Mammalian toxicology of organophosphorus pesticides." Journal of toxicology and environmental health **43**(3): 271-89.

Sun, T., H. Takatsuki, et al. (1994). "Detection of minimal residual disease in a patient with acute promyelocytic leukemia by RT-PCR: necessity of chemotherapy

following ATRA therapy." <u>Fukuoka igaku zasshi = Hukuoka acta medica</u> **85**(2): 52-6.

Tayebati, S. K., F. Amenta, et al. (2002). "Muscarinic cholinergic receptor subtypes in the hippocampus of aged rats." <u>Mechanisms of ageing and development</u> **123**(5): 521-8.

Tayebati, S. K., M. A. Di Tullio, et al. (2004). "Age-related changes of muscarinic cholinergic receptor subtypes in the striatum of Fisher 344 rats." <u>Experimental gerontology</u> **39**(2): 217-23.

Tayebati, S. K., M. A. Di Tullio, et al. (2006). "Muscarinic cholinergic receptor subtypes in cerebral cortex of Fisher 344 rats: a light microscope autoradiography study of age-related changes." <u>Mechanisms of ageing and development</u> **127**(2): 115-22.

Thiermann, H., K. Kehe, et al. (2007). "Red blood cell acetylcholinesterase and plasma butyrylcholinesterase status: important indicators for the treatment of patients poisoned by organophosphorus compounds." <u>Arhiv za higijenu rada i toksikologiju</u> **58**(3): 359-66.

Tice, M. A., T. Hashemi, et al. (1996). "Distribution of muscarinic receptor subtypes in rat brain from postnatal to old age." <u>Brain research</u> **92**(1): 70-6.

Tiedt, T. N., E. X. Albuquerque, et al. (1979). "Voltage- and time-dependent actions of piperocaine on the ion channel of the acetylcholine receptor." <u>Molecular pharmacology</u> **16**(3): 909-21.

Timofeeva, O. A. and C. J. Gordon (2001). "Changes in EEG power spectra and behavioral states in rats exposed to the acetylcholinesterase inhibitor chlorpyrifos and muscarinic agonist oxotremorine." <u>Brain research</u> **893**(1-2): 165-77.

Timofeeva, O. A. and C. J. Gordon (2002). "EEG spectra, behavioral states and motor activity in rats exposed to acetylcholinesterase inhibitor chlorpyrifos." Pharmacology, biochemistry, and behavior **72**(3): 669-79.

Van Den Beukel, I., F. A. Dijcks, et al. (1997). "Differential muscarinic receptor binding of acetylcholinesterase inhibitors in rat brain, human brain and Chinese hamster ovary cells expressing human receptors." The Journal of pharmacology and experimental therapeutics **281**(3): 1113-9.

Veronesi, B., M. Ehrich, et al. (1997). "Cell culture models of interspecies selectivity to organophosphorous insecticides." Neurotoxicology **18**(1): 283-97.

Vickroy, T. W., M. Watson, et al. (1984). "Agonist binding to multiple muscarinic receptors." Federation proceedings **43**(13): 2785-90.

Volpe, L. S., T. M. Biagioni, et al. (1985). "In vitro modulation of bovine caudate muscarinic receptor number by organophosphates and carbamates." Toxicology and applied pharmacology **78**(2): 226-34.

Volpicelli-Daley, L. A., E. G. Duysen, et al. (2003a). "Altered hippocampal muscarinic receptors in acetylcholinesterase-deficient mice." Annals of neurology **53**(6): 788-96.

Volpicelli-Daley, L. A., A. Hrabovska, et al. (2003b). "Altered striatal function and muscarinic cholinergic receptors in acetylcholinesterase knockout mice." Molecular pharmacology **64**(6): 1309-16.

Walker, B., Jr. and J. Nidiry (2002). "Current concepts: organophosphate toxicity." Inhalation toxicology **14**(9): 975-90.

Wang, H., H. Shi, et al. (1999). "Pilocarpine modulates the cellular electrical properties of mammalian hearts by activating a cardiac M3 receptor and a K+ current." British journal of pharmacology **126**(8): 1725-34.

Ward, T. R., D. J. Ferris, et al. (1993). "Correlation of the anticholinesterase activity of a series of organophosphates with their ability to compete with agonist binding to muscarinic receptors." Toxicology and applied pharmacology **122**(2): 300-7.

Ward, T. R. and W. R. Mundy (1996). "Organophosphorus compounds preferentially affect second messenger systems coupled to M2/M4 receptors in rat frontal cortex." Brain research bulletin **39**(1): 49-55.

Warnick, J. E., M. A. Maleque, et al. (1982). "Structure-activity relationships of amantadine. I. Interaction of the N-alkyl analogues with the ionic channels of the nicotinic acetylcholine receptor and electrically excitable membrane." Molecular pharmacology **22**(1): 82-93.

Warrington, J. S., D. J. Greenblatt, et al. (2004). "Age-related differences in CYP3A expression and activity in the rat liver, intestine, and kidney." The Journal of pharmacology and experimental therapeutics **309**(2): 720-9.

Watson, M., H. I. Yamamura, et al. (1986). "[3H]pirenzepine and (-)-[3H]quinuclidinyl benzilate binding to rat cerebral cortical and cardiac muscarinic cholinergic sites. I. Characterization and regulation of agonist binding to putative muscarinic subtypes." The Journal of pharmacology and experimental therapeutics **237**(2): 411-8.

Wauthier, V., V. Schenten, et al. (2006). "Ageing is associated with increased expression but decreased activity of CYP2E1 in male Wistar rats." Life sciences **79**(20): 1913-20.

Wei, J. W. and P. V. Sulakhe (1978). "Regional and subcellular distribution of myocardial muscarinic cholinergic receptors." European journal of pharmacology **52**(2): 235-8.

Wei, J. W. and P. V. Sulakhe (1980). "Cardiac muscarinic cholinergic receptor sites: opposing regulation by divalent cations and guanine nucleotides of receptor-agonist interaction." European journal of pharmacology **62**(4): 345-7.

Wessler, I. (1992). "Acetylcholine at motor nerves: storage, release, and presynaptic modulation by autoreceptors and adrenoceptors." International review of neurobiology **34**: 283-384.

WHO (1986). Properties and analytical methods. In *Organophosphorus insecticides:A general introduction.* Environmental Health Criteria. Geneva, World Health Organization**:** 63:23-9.

Won, Y. K., J. Liu, et al. (2001). "Age-related effects of chlorpyrifos on acetylcholine release in rat brain." Neurotoxicology **22**(1): 39-48.

Xie, W., J. A. Stribley, et al. (2000). "Postnatal developmental delay and supersensitivity to organophosphate in gene-targeted mice lacking acetylcholinesterase." J Pharmacol Exp Ther **293**(3): 896-902.

Xie, W., P. J. Wilder, et al. (1999). "Knockout of one acetylcholinesterase allele in the mouse." Chem Biol Interact **119-120**: 289-99.

Yasuda, R. P., W. Ciesla, et al. (1993). "Development of antisera selective for m4 and m5 muscarinic cholinergic receptors: distribution of m4 and m5 receptors in rat brain." Molecular pharmacology **43**(2): 149-57.

Yufu, F., T. Egashira, et al. (1994). "Age-related changes of cholinergic markers in the rat brain." Japanese journal of pharmacology **66**(2): 247-55.

Zhang, H., J. Liu, et al. (2002). "Age-related effects of chlorpyrifos on muscarinic receptor-mediated signaling in rat cortex." Archives of toxicology **75**(11-12): 676-84.

Zhu, S. Z., S. Z. Wang, et al. (1991). "DFP-induced regulation of cardiac muscarinic receptor mRNA in vivo measured by DNA-excess solution hybridization." Life sciences **48**(26): 2579-84.

Zurich, M. G., P. Honegger, et al. (2004). "Involvement of glial cells in the neurotoxicity of parathion and chlorpyrifos." Toxicology and applied pharmacology **201**(2): 97-104.

Zwart, R., R. G. van Kleef, et al. (1997). "Cellular aspects of persistent neurotoxicants: effects of Pb2+ on neuronal nicotinic acetylcholine receptors." Neurotoxicology **18**(3):709-17.

VITA

Nikita Shriram Mirajkar

Candidate for the Degree of

Doctor of Philosophy

Thesis: CHOLINERGIC MODULATION OF CARDIAC FUNCTION: SELECTIVE
          DISRUPTION BY ORGANOPHOSPHORUS ANTICHOLINESTERASES

Major Field: Veterinary Biomedical Sciences (Neurotoxicology)

Biographical:

    EDUCATION:
              Graduated with a Bachelor of Veterinary Sciences and Animal
              Husbandry, BVSc & AH (DVM equivalent) from Bombay Veterinary
              College, Maharashtra Animal and Fishery Sciences University,
              Seminary Hills, Nagpur, India in 2002.

              Completed the requirements for the Doctor of Philosophy in Veterinary
              Biomedical Sciences, with an emphasis in Neurotoxicology at Oklahoma
              State University, Stillwater, Oklahoma in July, 2008.

    EXPERIENCE:
              Underwent an internship (with disease diagnostic laboratories,
              veterinary dispensaries, animal hospitals, poultry and cattle farms) in
              Maharashtra; served as an adjunct veterinarian in a small animal clinic in
              Mumbai; employed as a Graduate teaching assistant by Oklahoma State
              University; performed research in the capacity of a graduate student in
              the Neurotoxicology lab at Oklahoma State University.

    PROFESSIONAL MEMBERSHIPS:
              Society of Toxicology
              National Honors Society
              American Association for Advancement of Science

Name: Nikita Shriram Mirajkar   Date of Degree: July, 2008

Institution: Oklahoma State University   Location: OKC or Stillwater, Oklahoma

Title of Study: CHOLINERGIC MODULATION OF CARDIAC FUNCTION:
               SELECTIVE DISRUPTION BY ORGANOPHOSPHORUS
               ANTICHOLINESTERASES

Pages in Study: 339   Candidate for the Degree of Doctor of Philosophy

Major Field: Veterinary Biomedical Sciences (Neurotoxicology)

Scope and Method of Study: Organophosphorus insecticides (OPs) elicit toxicity by inhibiting acetylcholinesterase (AChE). Most OPs also inhibit a related enzyme, butyrylcholinesterase (BChE), which is highly expressed in cardiac tissues. However, little is known regarding the function of BChE or its possible role in OP toxicity. While aging is associated with higher sensitivity to neurotoxicity of some OPs, little is known about age-related sensitivity of the cardiac system. The present study was undertaken to evaluate the *in vitro* and *in vivo* sensitivity of AChE and BChE in the heart and cortex of adult (3 months) and aged (18 months) rats to the common OPs, chlorpyrifos (CPF) and parathion (PS). Tetraisopropylpyrophosphoramide (*iso*-OMPA), a BChE-selective OP inhibitor, was used to probe the possible role of BChE in the regulation of heart rate in adult rats. We also compared the *in vivo* effects of CPF and PS on AChE and BChE inhibition and heart rate, temperature and physical activity in adult and aged rats. In all cases, we evaluated the effects of OP-induced BChE and/or AChE inhibition on heart rate, body temperature and physical activity using radiotelemetry.

Findings and Conclusions: BChE was significantly more sensitive than AChE to inhibition by CPF both *in vitro* and *in vivo*, while the reverse was true for PS. Furthermore, BChE in the heart from aged rats was significantly more sensitive to CPO than BChE in heart of adult rats *in vitro*. Selective BChE inhibition in the heart by *iso*-OMPA, in the absence of AChE inhibition, significantly reduced heart rate, suggesting BChE does play a role in the regulation of cholinergic neurotransmission in the heart. Both CPF and PS elicited dose-dependent AChE and BChE inhibition in atria, ventricles and other tissues in both age-groups. Effective dosages initially decreased heart rate, temperature and motor activity in both adult and aged rats. Heart rate remained depressed for four days, while temperature recovered to baseline and activity increased above baseline in both age groups, with both OPs. Atrial cholinesterases in aged rats appeared more sensitive to both CPF and PS, but this difference was not correlated with higher sensitivity to cardiac dysregulation. Equitoxic doses of CPF and PS produce very different degrees of functional toxicity, with PS eliciting more extensive cholinergic signs than CPF in both adult and aged rats. In contrast, relatively similar changes in heart rate, body temperature, and motor activity were observed following exposure to CPF or PS.

ADVISER'S APPROVAL: Dr. Carey N. Pope